



Norwegian University of
Science and Technology

Wave Runup and Wave Rundown on Shorelines and Coastal Structures Based on Long-Term Variation of Wind and Wave Conditions

Tonje Sunde

Marine Technology

Submission date: June 2017

Supervisor: Dag Myrhaug, IMT

Norwegian University of Science and Technology
Department of Marine Technology



NTNU Trondheim

Norwegian University of Science and Technology

Department of Marine Technology – Group of Marine Structures

MASTER THESIS IN MARINE TECHNOLOGY

SPRING 2017

FOR

STUD. TECHN. TONJE SUNDE

WAVE RUNUP AND WAVE RUNDOWN ON SHORELINES AND COASTAL STRUCTURES BASED ON LONG-TERM VARIATION OF WIND AND WAVE CONDITIONS

The surf parameter, also often referred to as the surf similarity parameter or the Iribarren number, is used to characterize surf zone processes. Shallow water regions where waves break are referred to as the surf zone, and the different breakers on slopes are defined and classified in terms of the surf parameter. It also appears that the surf parameter enters in many empirical and theoretical models for wave-induced phenomena in the surf zone, e.g. such as wave runup and wave rundown on shorelines and coastal structures. Long-term assessment of wave runup and wave rundown are appropriate in formulating risks of e.g. damage of shorelines, breakwaters, seawalls and artificial reefs.

The thesis will focus on using some available empirical formulae for wave runup and wave rundown together with some available long-term wind and wave statistics to obtain characteristic statistical values of wave runup and wave rundown.

The student shall:

1. Give a general background of wave runup and wave rundown on shorelines and coastal structures.
2. Give a description of the empirical wave runup and wave rundown formulae used in this thesis.
3. Describe the long-term wind and wave statistics used in this thesis.
4. Calculate characteristic statistical values of wave runup and wave rundown by using the information given in 2) and 3). Results corresponding to n-years return period values for both wind and waves shall be included.
5. Present and discuss the results.

The work scope may prove to be larger than initially anticipated. Subject to approval from the supervisor, topics may be deleted from the list above or reduced in extent.

In the thesis the candidate shall present her personal contribution to the resolution of problem within the scope of the thesis work.

Theories and conclusions should be based on mathematical derivations and/or logic reasoning identifying the various steps in the deduction.

The candidate should utilize the existing possibilities for obtaining relevant literature.



The thesis should be organized in a rational manner to give a clear exposition of results, assessments, and conclusions. The text should be brief and to the point, with a clear language. Telegraphic language should be avoided.

The thesis shall contain the following elements: A text defining the scope, preface, list of contents, summary, main body of thesis, conclusions with recommendations for further work, list of symbols and acronyms, reference and (optional) appendices. All figures, tables and equations shall be numerated.

The supervisor may require that the candidate, in an early stage of the work, present a written plan for the completion of the work. The plan should include a budget for the use of computer and laboratory resources that will be charged to the department. Overruns shall be reported to the supervisor.

The original contribution of the candidate and material taken from other sources shall be clearly defined. Work from other sources shall be properly referenced using an acknowledged referencing system.

Deadline: 11.06.2017

Dag Myrhaug
Supervisor

Summary

In the recent years the fear of violent storms occurring more often, and with increasing violence, has drawn new attention to research on wave runup and wave rundown. Severe storm conditions could cause great damage on coastal infrastructure, buildings, and the land itself; both due to flooding and direct impact from waves.

Since wave runup is an important design parameter for coastal protection work, it is important to have reliable methods to predict this parameter. This thesis presents a method for estimating wave runup and wave rundown based on wind and wave statistics, and is based on published methods. Both wind and wave statistics were applied to the method, and several empirical wave runup and wave rundown equations were used to provide results.

Based on general equations representing the empirical equations, a formulae was obtained for wave runup and wave rundown as a function of wave period, significant wave height, and bottom slope. Through a Phillips spectrum this formulae was further modified to be a function of mean wind speed. Both wind and wave distributions were applied to the associated version of the formulae to generate results. Also, extreme values were found based on the probability of exceeding once every n -year for the wind distributions, and from environmental contour lines for the wave distributions.

Results obtained by the different empirical equations showed that some of the equations generated estimates significantly different from the others. However, these equations are developed from different conditions, and deviations in results are therefore expected. The extreme value estimates, which are important in design, did in general lie outside the range of validity of the empirical equations, and they were therefore based on extrapolation with associated uncertainty.

This method could be convenient to use due to its simplicity, but because of large uncertainties it should only be used in early estimates followed by more accurate analysis.

Sammendrag

Bølgeopp skyl ling og bølge ned skyl ling har i de siste årene fått økende oppmerksomhet som følge av frykt for at klimaendringer skal føre til hyppigere og mer voldsomme stormer. Kraftige stormer kan forårsake stor skade på infrastruktur, bygninger og jordmasser langs kysten; enten som følge av bølgeslag eller oversvømmelse.

Bølgeopp skyl ling er en viktig designparameter i prosjektering av konstruksjoner langs kysten, og det er derfor viktig å ha pålitelige metoder for å beregne opp skyl lingshøyden. Her blir det presentert en metode for estimering av opp skyl lingshøyden basert på vind- og bølge statistikk. Metoden er et resultat av å kombinere flere forskjellige publiserte metoder, og tar utgangspunkt i empiriske formler for bølgeopp skyl ling og bølge ned skyl ling. Vind- og bølge statistikk fra flere områder er anvendt på metoden for å vise resultater som denne metoden kan gi.

To generelle formler representerer de empiriske formlene for bølgeopp skyl ling og bølge ned skyl ling. Ved å omformulere de generelle formlene blir de uttrykt ved bunnhellingen, signifikant bølge høyde og toppunktperioden. Formlene kan deretter bli uttrykt ved gjennomsnittlig vindhastighet ved å bruke et Phillipsspekter for å relatere vindhastigheten til bølge parameterne. På denne måten kan både vind- og bølge statistikk anvendes for å finne bølgeopp skyl lingen. I tillegg er ekstremverdier estimert basert på gjentaksintervall for vindstatistikk, og konturlinjer for et gitt gjentaksintervall for bølge statistikk. Både vind- og bølge statistikk fra forskjellige områder er anvendt på denne metoden både for å vise hvordan den kan bli brukt og for å sammenlikne de svarene den gir.

Resultatene viser at noen av de empiriske formlene gir en bølgeopp skyl ling som avviker betydelig fra de andre. De formlene som gir størst avvik er de som er basert på andre forhold og dette er derfor forventet. Ekstremverdiene ligger stort sett utenfor de parameterområdene som formlene er basert på, og ekstrapolering av formlene er derfor benyttet, noe som fører til

usikkerhet i deres pålitelighet.

Metoden er relativt enkel og kan derfor være nyttig å bruke for å gjøre overslag i tidligfase design. Den er imidlertid forbundet med nokså stor usikkerhet og det bør derfor gjøres mer nøyaktige beregninger i den videre prosessen.

Preface

This thesis is written as the completing part of a five years master's degree in Marine Technology at the Norwegian University of Science and Technology (NTNU) in Trondheim. The work with an analytical method for calculation of wave runup and wave rundown has been carried out during the spring 2017 under supervision by Professor Dag Myrhaug, and is a continuation of the work done in my project thesis. Preexisting methods, formulae, and wind and wave statistics were combined to establish the method.

I would like to express my gratitude towards Professor Dag Myrhaug for valuable guidance during the past year. The supervision meetings have been a good platform for technical discussions, and they have contributed to my professional development within this scientific field.

Tonje Sunde Trondheim 8/6-17

Tonje Sunde

Place and date

Contents

List of Figures	xiii
List of Tables	xv
Symbols and Abbreviations	xix
1 Introduction	1
2 Background	3
2.1 Surf Zone Theory	3
2.1.1 Terminology and Definitions	3
2.1.2 Swash Motion	6
2.1.3 Wave Setup	8
2.1.4 Tides	12
2.1.5 Storm Surge	13
2.2 Empirical Equations for Wave Runup and Wave Rundown	15
2.3 Statistical Modelling of Wind and Waves	20
2.3.1 Long-Term Wind Statistics	21
2.3.2 Mean Wind Distributions	22
2.3.3 Long-Term Wave Statistics	24
2.3.4 Joint Wave Distributions	25
2.4 Inversed First-Order-Reliability-Method	29
3 Method	31
3.1 General Equations for Wave Runup and Wave Rundown	31
3.2 Wave Runup and Wave Rundown Based on Wind Statistics	33
3.2.1 Stochastic Approach	34
3.2.2 Deterministic Approach	36

3.2.3	Extreme Values	37
3.3	Wave Runup and Rundown Based on Wave Statistics	37
3.3.1	Stochastic Approach	37
3.3.2	Expected Value of H_S	39
3.3.3	Contour Lines	40
3.3.4	Extreme Values	41
4	Individual Studies	43
5	Results	45
5.1	Wave Runup and Wave Rundown Based on Wind Statistics	45
5.1.1	Stochastic Approach	45
5.1.2	Deterministic Approach	52
5.2	Wave Runup and Wave Rundown Based on Wave Statistics	53
5.2.1	Stochastic Approach	53
5.2.2	Comparison of Results	64
5.3	Extreme Value Estimates	66
5.3.1	Based on Long-Term Wind Distributions	66
5.3.2	Based on Long-Term Wave Distributions	71
5.3.3	Comparison of Extreme Values	77
5.3.4	Range of Validity	78
6	Discussion	81
6.1	Wave Runup and Wave Rundown Based on Wind and Wave Statistics	81
6.2	Extreme Value Estimates	82
6.3	Error Sources and Uncertainties	83
6.4	Evaluation of Results	84
7	Conclusions and Recommendations	87
	References	88
	Appendices	I
A	Calculations	I

A.1	Expressing R_2 in Terms of U_{10}	I
A.2	Change of Variables from (H_S, T) to (H_S, R_2)	III
B	Results	VII
B.1	Based on Wind Distributions	VIII
B.2	Based on Wave Distributions	XII
B.3	Extreme Values from Wind Distributions	XXII
B.4	Contour Lines with Runup Models	XXXI
B.5	Extreme Values from Wave Distributions	LI
C	MATLAB Codes	LXXI
C.1	Wave Runup and Wave Rundown Based on Wind Statistics	LXXI
C.2	Wave Runup and Wave Rundown Based on Wave Statistics	LXXIV
C.3	Extreme Value Estimates Based on Wind Statistics	LXXVII
C.4	Extreme Value Estimates Based on Wave Statistics	LXXX

List of Figures

2.2	Swash zone on a beach with wave runup and wave rundown in the upper and lower limits	4
2.1	Definitions of components contributing to sea level rise at the shore	5
2.3	Amplitude of an oscillating motion along a slope, which is $H/2\sin\gamma$ for perfect reflection of wave energy	8
2.4	Deviation of the mean surface elevation from the still water level before and after breaking	11
2.5	Illustration of an Earth-Moon system	12
2.6	Wind probability density functions	24
2.7	Conditional wave probability density functions for $H_S = 3\text{m}$	29
3.1	Phillips spectrum	34
3.2	Contour lines for the MGAU05 distribution with runup model B11	42
5.1	Normalised expected value of wave runup and wave rundown	47
5.2	Expected value of wave runup with standard deviation from wind distributions .	48
5.3	Expected value of wave rundown with standard deviation from wind distributions	51
5.4	Normalised expected value of wave runup and wave rundown	54
5.5	Expected value of wave runup with standard deviation from wave distributions .	57
5.6	Expected value with standard deviation for wave rundown	62
5.7	Extreme values of wave runup and wave rundown normalised with significant wave height	78

List of Tables

2.1	Breaker types classified by the magnitude of the surf similarity parameter ξ_b . . .	7
2.2	Abbreviation for runup model equations	20
2.3	Parameters for the long-term Weibull wind distributions	23
2.4	Parameters for the conditional wave distributions for T given H_S	28
2.5	Weibull parameters for marginal distribution of H_S in (2.48)	28
3.1	Parameter values for the general equations for runup models	32
3.2	Overview of runup model range	33
5.1	Expected value of mean wind speed	46
5.2	Ratio between results from deterministic and stochastic approach	52
5.3	Expected value of the significant wave height for the wave distributions	53
5.4	Wave runup and wave rundown R_2 in metres for $H_S = 3\text{m}$	64
5.5	Mean wind speed for the JMH02 distribution for 1 hour and 10 minute averages	66
5.6	Extreme environmental parameters	67
5.7	Extreme wave runup and wave rundown from wind statistics	69
5.8	Extreme wave runup and wave rundown from wave statistics	72
5.9	Validity of runup models for 1 year extreme values for bottom slope 1/10	79

Symbols and Abbreviations

η	surface elevation
γ	angle between bottom slope and the horizontal
$\hat{\omega}$	latitude
\hat{m}	mass of body
κ	breaker index
ω	wave frequency
ω_S	Earth's angular velocity
$\bar{\eta}$	time averaged free surface elevation
$\bar{\eta}_b$	mean surface elevation at breaking point
\vec{r}_E	vector from the Moon to the Earth sentrum
Φ	standard Gaussian cdf
ϕ	velocity potential for propagating wave
ρ	water density
ρ_A	air density
ξ	surf similarity parameter
ξ_b	surf similarity parameter based on H_b
ξ_P	deep water surf similarity parameter
a	wave amplitude

A_g	acceleration due to gravity along a bottom slope
A_{max}	maximum acceleration along a bottom slope
c	phase speed of waves
C_D	drag coefficient
c_g	group velocity
cdf	cumulative distribution function
D_{50}	sediment size
E	time-averaged wave-induced energy per unit horizontal area
F	wind stress
f	Coriolis parameter
F_C	centrifugal force
F_G	gravitational force
G	gravitational constant
g	acceleration due to gravity
H	wave height
h	water depth
H_0	deep water wave height
H_b	breaker height
h_b	water depth at breaking point
H_S	significant wave height
$H_{S,max}$	extreme value of H_S
k	wave number
L_0	deep water wave length
M	mass of the Moon

m	bottom slope
m_d	number of sea states per year
MWL	mean water level
N	number of individual U_{10}
P_A	atmospheric pressure
pdf	probability density function
q	probability of exceedance
r	vector from the Moon to a point on Earth
R_2	wave runup or wave rundown exceed by 2%
$R_{2,max}$	extreme value of R_2
S_{XX}	radiation stress
SWL	still water level
T	wave period
t	time
T_P	spectral peak period
T_Z	zero-crossing wave period
$T_{P,max}$	extreme value of T_P
T_{return}	return period
u	current parallel to shore
$U_{10,max}$	extreme value of U_{10}
U_{10}	mean wind speed at 10m elevation above sea level
x_b	x-location of breaking point

Chapter 1

Introduction

When waves are approaching the coast, they usually break and run up on the coast, be it a structure or a beach. For low laying land or areas particularly exposed to the elements this can have critical consequences, such as flooding, coastal erosion, and damage on coastal infrastructure.

Research on wave runup has been in progress for many years. According to de la Pena et al. (2014) the first statistical studies on wave runup were done on structures exposed to regular waves by Iribarren and Nogales (1949), and Miche (1944), cited in de la Pena et al. (2014). Furthermore, Hunt (1959) linked the Iribarren number to the runup; and van Oorshot and D'Angremond (1968) conducted the first experiments with irregular waves, followed by Battjes (1974) who studied gentler slopes more suitable for beaches (de la Pena et al. 2014); all cited in de la Pena et al. (2014). Still, extensive research is published. In the recent years attention has increased driven by the focus on climate change and consequently possible sea level rise and more extreme weather.

It is especially the extreme situations that are critical, and extreme value estimates are hence important in design of coastal protection works. In the recent years, new attention has therefore been drawn towards finding reliable methods for predicting extreme wave runup events and new values for sea levels that reflect the changes in the environment in order to maintain safe and cost effective coastal protection and constructions. For that reason, experiments on wave runup and wave rundown have recently been performed, and empirical equations based on the experiments have been published.

Even though the sophistication of numerical methods is continuously increasing, experimental

methods are still highly relevant in wave runup and wave rundown analysis, both for determining empirical equations and for validation of numerical methods. In the surf zone area, where irregular waves are breaking, numerical analysis become complex, and experiments are therefore essential despite today's fast increasing computer power. Because detailed numerical analysis of wave runup and wave rundown is time consuming and resource demanding, it would be useful with a simple method for initial estimation of the phenomenon in for instance early feasibility studies, or for estimations in the field.

This thesis is based on research in Myrhaug (2015), Myrhaug & Leira (2017), and Myrhaug (2017) as a basis for further development of a method for calculating characteristic statistical values of wave runup and wave rundown, including extreme values. The objective of the thesis is to provide a method for estimating wave runup and wave rundown based on either long-term wind or wave distributions, and to compare the results that are generated by this method.

A selection of the empirical equations is included in this thesis with focus on choosing those with a relatively simple expression in order to be able to use these in analytical calculations. The equations are then combined with long-term wind and wave distributions to provide examples of estimates of wave runup and wave rundown. Also, extreme values for wave runup and wave rundown for n -years return periods are found based on these distributions.

The method could be convenient to use for initial estimations because it only requires analytical calculations, and it is therefore relatively simple to implement in a computer program such as MATLAB, which is used here. The thesis is limited to comparison of nine runup models, two rundown models, four long-term wind distributions, and ten long-term wave distributions.

This thesis starts out by giving a background on the theory behind relevant phenomena in the surf zone. The empirical wave runup and wave rundown equations that are used in the thesis are then presented along with the long-term wind and wave distributions that are applied to these equations. A brief background on statistical modelling of wind and waves is also included. Then, the method for calculating the characteristic statistical values is presented, including the method for calculating the extreme values. Moreover, the results found by applying the runup models and the distributions to the method is presented, compared, and discussed.

Chapter 2

Background

This chapter presents relevant theory for the wave runup and wave rundown phenomena. This includes the two main components, swash and setup; but also other phenomena that can contribute to change in sea level. Some empirical wave runup and wave rundown formulae that are used in the thesis are presented, and also a background on long-term wind and wave modelling. Finally, the Inversed First-Order-Reliability-Method is presented, which is used to find environmental contours for a given return period for the long-term wave distributions.

2.1 Surf Zone Theory

2.1.1 Terminology and Definitions

In this section some definitions and relevant terminology for the surf zone will be presented, mainly based on Nielsen (2009).

The surf zone is the shallow water region between the land and the sea where waves are breaking. This zone is bounded seawards by the point where the largest waves start to break, and landward by the highest point that the waves reach on the coast. The extent of the surf zone will change with tides and wave conditions.

The inner most part of the surf zone is called the swash zone, and this area alternates between being covered by water and not. The swash zone is limited by wave runup landwards and wave rundown seawards. Wave runup is defined as the vertical distance between the still water level

(SWL) and the highest point that the waves reach at a given location. Wave rundown is defined as the vertical distance between the SWL and the lowest point that the waves reach at a given location.

Wave runup can be described as a combination of two physical phenomena: the wave setup, which is the deviation of the mean water level (MWL) from SWL; and the swash motion, which is the oscillating motion around MWL. Other factors can also cause the sea level to rise, such as tides and storm surges. These two components combined are called storm tide. Figure 2.1 shows the different components causing the sea level to rise at the shore.

Figure 2.2 shows a swash zone on a beach, where wave runup and wave rundown are the upper and lower limit of the oscillating motion. The transition between the saturated and the unsaturated surface shows the extent of recent wave runup events.



Figure 2.2: Swash zone on a beach with wave runup and wave rundown in the upper and lower limits of the oscillating motion. The transition between the saturated and the unsaturated surface shows the extent of recent wave runup events. (Pedersen 2014)

Wave runup and wave rundown are often described in terms of the wave runup exceeded by 2% of the wave runup maxima, and the wave rundown exceeded by 2% of the wave rundown minima; due to the stochastic nature of the incoming waves, and consequently also the wave runup and wave rundown. This will be referred to as R_2 in the following for both wave runup and wave rundown.

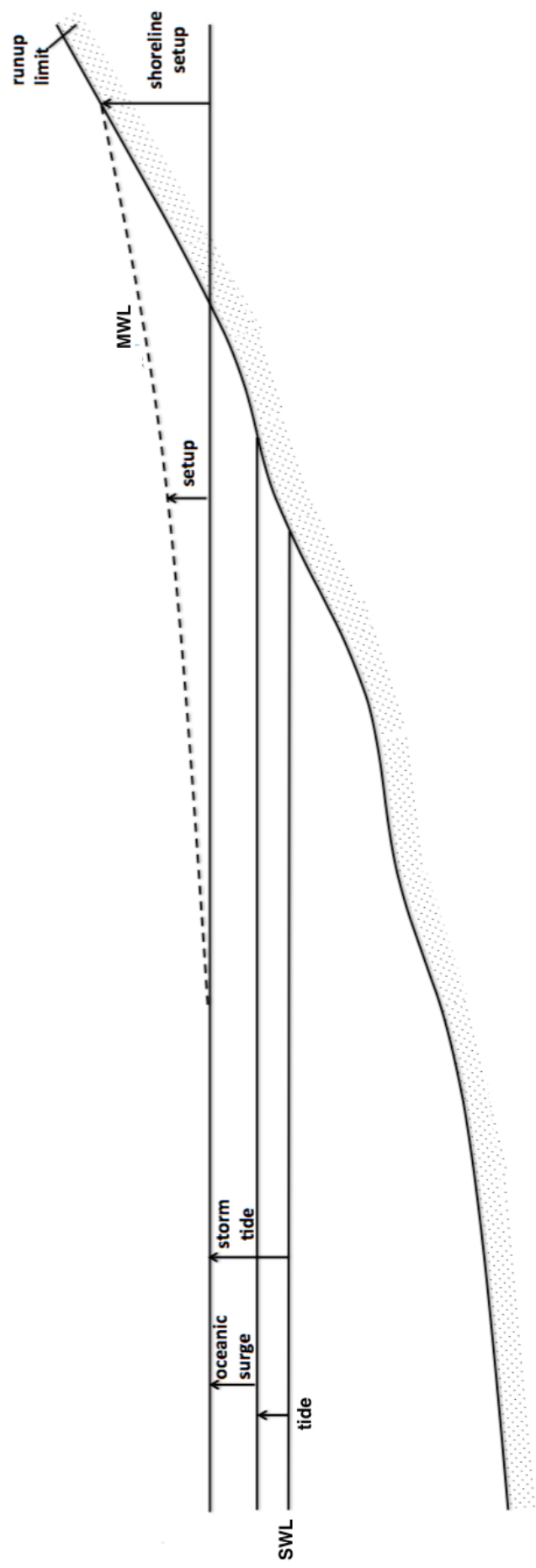


Figure 2.1: Definitions of components contributing to sea level rise at the shore

The bottom slope is an important parameter for calculation of wave runup and wave rundown. This parameter is often taken as the averaged bottom slope of the swash zone or the surf zone.

2.1.2 Swash Motion

Swash motion is the oscillating motion of the water around MWL on the shoreline. On very flat beaches, lots of wave energy is dissipated by breaking before they reach the shoreline. In this case, there will be very little swash motion. On steep beaches or structures, however, larger swash motion can take place.

Experiments have shown that the wave runup is proportional to the wave height and the surf similarity parameter for breaking waves (Nielsen 2009). The surf similarity parameter ξ , also called Iribarren number, is often used to characterise the surf zone. This quantity, defined in Eq. (2.1), gives a measure of the extent at which wave energy is being reflected when waves approach the shore contrary to being dissipated by breaking (Holthuijsen 2007).

$$\xi = \tan \gamma / \sqrt{H/L_0} \quad (2.1)$$

Here, L_0 is the deep water wave length, $\tan \gamma$ is the bottom slope, and H can be either the deep water wave height H_0 or the breaker height H_b , and the ratio H/L_0 is the wave steepness.

For steep waves and/ or gentle slopes the surf similarity parameter is small, which in terms means that the reflection is small; while for steep slopes and gentle wave steepness the surf similarity parameter is large and consequently also the reflection dissipation ratio. This is in line with the large amount of energy being dissipated at flat beaches.

The magnitude of the surf similarity parameter also describes different wave breaker types when the surf similarity parameter ξ_b is defined by the breaker height. Table 2.1 shows the approximate range for commonly classified breaker types on a straight slope (Nielsen 2009).

Table 2.1: Breaker types classified by the magnitude of the surf similarity parameter ξ_b

Surf similarity parameter range	Breaker types
$4 < \xi_b$	little or no breaking
$2 < \xi_b < 4$	surging breakers
$0.4 < \xi_b < 2$	plunging breakers
$\xi_b < 0.4$	spilling breakers

For irregular waves the surf similarity parameter can be expressed in terms of H_S and T_P , where H_S is the significant wave height, and T_P is the spectral peak period for the sea state. This is done by utilising the relation $L_0 = \frac{g}{2\pi} T_P^2$ between wave length L_0 and T_P from deep water linear wave theory, where g is the acceleration of gravity, see for instance Dean & Dalrymple (1984) for details on linear wave theory. The surf similarity parameter in deep water can then be expressed as in Eq. (2.2) by inserting this relation and naming the bottom slope $\tan \gamma = m$.

$$\xi_P = m \sqrt{\frac{\frac{g}{2\pi} T_P^2}{H_S}} = m \left(\frac{H_S}{\frac{g}{2\pi} T_P^2} \right)^{-1/2} \quad (2.2)$$

The background of the surf similarity parameter can be described by considering the oscillation up and down along a plane slope caused by an incoming wave. In the following, this description will be presented based on Nielsen (2009).

The amplitude of the oscillating motion that corresponds to perfect reflection is $\frac{1}{2} \frac{H}{\sin \gamma}$, see Figure 2.3. For an incoming wave with angular frequency ω the corresponding maximum acceleration along the slope is of the order given in Eq. (2.3).

$$A_{max} = \omega^2 \frac{H}{2} \frac{1}{\sin \gamma} \quad (2.3)$$

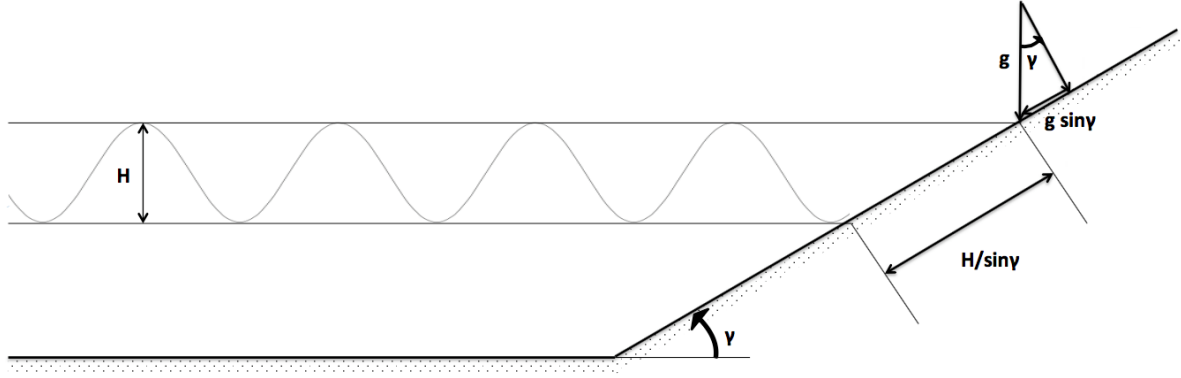


Figure 2.3: Amplitude of an oscillating motion along a slope, which is $H/2\sin\gamma$ for perfect reflection of wave energy

For the oscillatory motion to be possible, this acceleration must be smaller than the acceleration due to gravity along the slope given in Eq. (2.4).

$$A_g = g \sin \gamma \quad (2.4)$$

If not, then the waves must break, so a criterion for reflection contrary to breaking becomes $A_{max} < A_g$. By applying the formulations for A_{max} and A_g in Eq. (2.3) and Eq. (2.4), this criterion can be written as shown in Eq. (2.5), where the relation $\omega^2/g \propto 1/L_0$ has been utilised.

$$\frac{A_g}{A_{max}} = \frac{g \sin \gamma}{\omega^2 \frac{H}{2} \frac{1}{\sin \gamma}} \propto \frac{L_0}{H} \sin^2 \gamma > const. \quad (2.5)$$

For gentle bottom slopes the angle γ is small, so the actual slope $\tan \gamma$ can be approximated by $\sin \gamma$. The above criterion can then, for gentle slopes, be written as $L_0/H \tan \gamma > const.$, and this is recognised as the surf similarity parameter in Eq. (2.1).

2.1.3 Wave Setup

In the following a mathematical description of wave setup will be presented based on Dean & Dalrymple (1984).

By using Eulers formula on the free surface, Eq. (2.6), an expression for mean surface elevation can be derived by using linear theory of waves. Here, ϕ is the velocity potential for a propagat-

ing wave, and $C(t)$ is a constant, for an axis system where x points in the direction normal to the shore and z points in the vertical direction. Also, the velocity vector is $\vec{v} = -\nabla\phi$.

$$\frac{1}{2} \left[\left(\frac{\partial\phi}{\partial x} \right)^2 + \left(\frac{\partial\phi}{\partial z} \right)^2 \right] - \frac{\partial\phi}{\partial t} + gz = C(t) \quad (2.6)$$

From linear theory, the expressions for the surface elevation in Eq. (2.7) and the velocity potential in (2.8) are known, where a is the wave amplitude, k is the wave number, and h is the water depth.

$$\eta = a \cos(kx - \omega t) \quad (2.7)$$

$$\phi = -\frac{ga \cosh k(z+h)}{\omega \cosh kh} \quad (2.8)$$

By using Taylor expansion of Eq. (2.6) around the still water level ($z = 0$) to the first order of η , time-averaging over one wave period, and keeping terms of order a^2 , then Eq. (2.6) can be expressed as in Eq. (2.9). Due to time averaging, the second term is neglected.

$$\frac{1}{2} \left[\overline{\left(\frac{\partial\phi}{\partial x} \right)^2 + \left(\frac{\partial\phi}{\partial z} \right)^2} \right]_{z=0} - \overline{\frac{\partial\phi}{\partial t}} \Big|_{z=0} - \overline{\eta \frac{\partial^2\phi}{\partial t \partial z}} \Big|_{z=0} + g\bar{\eta} = \overline{C(t)} \quad (2.9)$$

After substituting (2.7) and Eq. (2.8) into Eq. (2.9), an expression for the time averaged free surface elevation $\bar{\eta}$ can be expressed as in Eq. (2.10).

$$\bar{\eta} = -\frac{a^2 k}{2 \sinh 2kh} + \frac{C(t)}{g} \quad (2.10)$$

At deep water ($kh \gg 1$), $\bar{\eta}$ is zero, which gives $\overline{C(t)} = 0$ because $\sinh 2kh$ goes to infinity when kh increases. The expression for $\bar{\eta}$ can then be expressed as in (2.11) as the waves approach shallow water because $\sinh 2kh$ goes to $2kh$ when kh decreases. In other words, $\bar{\eta}$ becomes more and more negative as kh decreases. This phenomenon is called wave setdown, and is valid until breaking occurs.

$$\bar{\eta} = -\frac{a^2 k}{2 \sinh 2kh} < 0 \quad (2.11)$$

At the point where the waves break, the wave amplitude can be expressed by the empirical breaker index κ as in Eq. (2.12), where h_b is the water depth at the breaking point, and $\bar{\eta}_b$ is the mean surface elevation from Eq. (2.11) at the breaking point.

$$a = \frac{\kappa(h_b + \bar{\eta}_b)}{2} \quad (2.12)$$

For shallow water, where $\sinh(2kh) \rightarrow 2kh$, Eq. (2.11) can be expressed as in Eq. (2.13), and combined with Eq. (2.12) the expression can be formulated as in Eq. (2.14) by assuming that $\bar{\eta}_b \ll h_b$.

$$\bar{\eta} = -\frac{a^2}{4h} \quad (2.13)$$

$$\bar{\eta}_b = -\frac{\kappa^2}{4h_b} \frac{1}{4} (h_b + \bar{\eta}_b)^2 \approx -\frac{\kappa^2}{16} h_b \quad (2.14)$$

Typical values for κ are $0.7 \leq \kappa \leq 1.3$, and for $\kappa = 0.8$ the mean surface elevation at breaking $\bar{\eta}_b$ becomes $\leq 5\%$ of h_b .

Radiation stress in the direction of the waves can be defined as in Eq. (2.15), see for instance Holthuijsen (2007). The radiation stress is the time-averaged transport of x-momentum in x-direction when the x-direction is defined normal to the shore. Here, E is the time-averaged, wave energy per unit horizontal area for linear waves, c_g is the group velocity and c is the phase speed of the waves. In shallow water $c_g = c$, and by substituting $E = \frac{1}{2}\rho g a^2$ and Eq. (2.12) into Eq. (2.15), the radiation stress can be expressed by Eq. (2.16), where ρ is the water density.

$$S_{xx} = \left(2\frac{c_g}{c} - \frac{1}{2}\right) E \quad (2.15)$$

$$S_{xx} = \frac{3}{16}\rho g \kappa^2 (h + \bar{\eta})^2 \quad (2.16)$$

The relation in Eq. (2.17) can be derived from the change in horizontal momentum flux for waves that are approaching a beach, see Dean & Dalrymple (1984) for details. By substituting Eq. (2.16) into Eq. (2.17), the expression in Eq. (2.18) can be obtained; and by integrating

Eq. (2.18) from x_b to x , an expression for the mean surface elevation after breaking can be formulated as in Eq. (2.19). Here, x_b is the location of the breaking point in the x-direction.

$$-\frac{1}{\rho g (h + \bar{\eta})} \frac{dS_{xx}}{dx} = \frac{d\bar{\eta}}{dx} \quad (2.17)$$

$$\frac{d\bar{\eta}}{dx} \left(1 + \frac{3\kappa^2}{8} \right) = -\frac{3\kappa^2}{8} \frac{dh}{dx} \quad (2.18)$$

$$\bar{\eta}(x) = \bar{\eta}_b + \frac{3\kappa^2/8}{1 + 3\kappa^2/8} (h_b - h(x)) \quad (2.19)$$

For waves approaching a shoreline or a coastal structure, the depth $h(x)$ after breaking is smaller than h_b , which means that $\bar{\eta}(x)$ increases with x . This phenomenon is called setup.

At the shoreline, where $h = 0$, the term Eq. (2.19) reduces to Eq. (2.20), and this term represents the contribution from the wave setup to the wave runup. For $\kappa = 0.8$, $\bar{\eta}(0)$ is approximately 15% of h_b .

$$\bar{\eta}(0) = \bar{\eta}_b + \frac{3\kappa^2/8}{1 + 3\kappa^2/8} h_b \quad (2.20)$$

Figure 2.4 illustrates the deviation of $\bar{\eta}$ from SWL, $z = 0$, that is the setdown and the setup. At deep water the deviation is zero, and $\bar{\eta}$ decreases before breaking and increases after breaking.

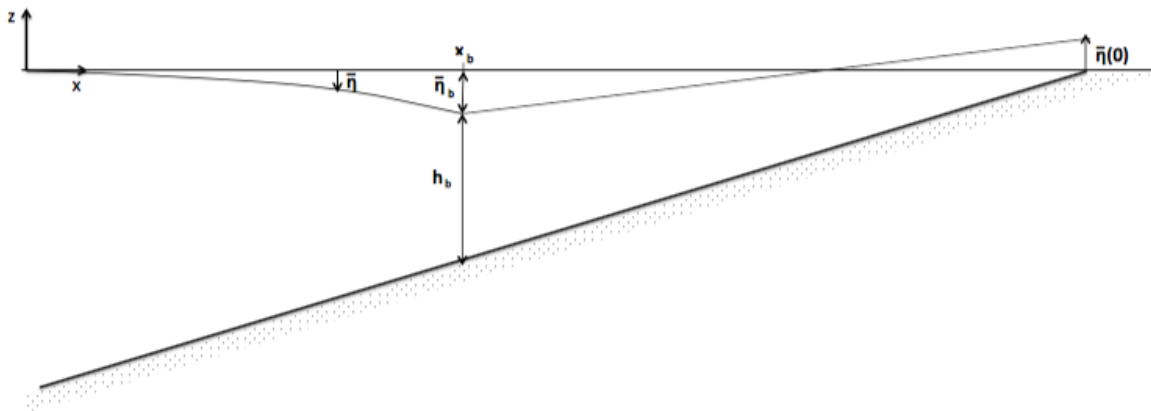


Figure 2.4: Deviation of the mean surface elevation from the still water level before and after breaking. $\bar{\eta}$ coincide with SWL at deep water (leftmost in the figure), decreases towards breaking, and increases after breaking

2.1.4 Tides

The theory on tides in this section is based on Myrhaug (2012). Tides are caused by the gravitational forces from the Moon and the Sun, and the centripetal acceleration caused by the Earths and Moons rotation around their common centre of mass.

The gravitational force from the Moon with mass M acting on a body with mass \hat{m} at a point on Earth can be written as in Eq. (2.21); where r is the vector from the Moon to the point on Earth, and G is the gravitational constant. This force will vary with the location on Earth. In addition, the centrifugal force will act on the body with mass \hat{m} with the force in Eq. (2.22), where \vec{r}_E is the vector from the Moon to the Earth's centre. Figure 2.5 shows an Earth-Moon system that illustrates the different components in these equations. Note that the axis of rotation for the Earth-Moon system in reality lies inside the Earth.

$$F_G = -G \frac{\hat{m}M}{r^2} \quad (2.21)$$

$$F_C = -\hat{m} \vec{\Omega} \times \vec{\Omega} \times \vec{r}_E \quad (2.22)$$

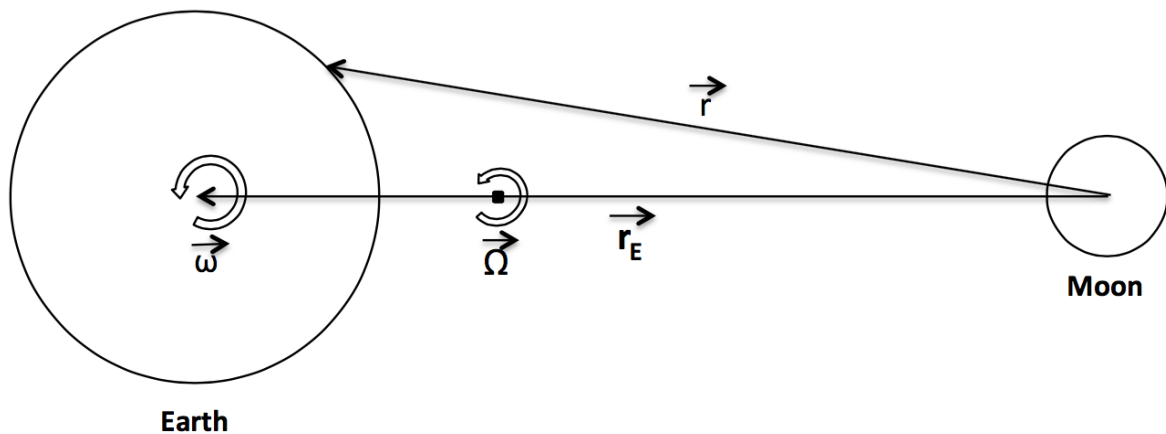


Figure 2.5: Illustration of an Earth-Moon system where gravitational and centrifugal forces act on a point on earth and causes a resulting tidal force

At the centre of the Earth, the gravitational and the centrifugal force is balanced. However, at positions closer and further away from the centre, these two forces are not balanced causing a resultant force that acts in the direction towards the Moon on the side that faces the Moon,

and away from the Moon on the opposite side. At the Earth's surface this causes the water to be drawn in the directions that these forces act, causing two tidal bulges at each side of the Earth. As the Earth rotates around itself once each day, two high tides and two low tides will be observed each day at one location at the Earth.

Similarly, a tidal force is caused by the Sun with a magnitude of approximately 50% of the tidal force generated by the Moon. When the Moon and Sun are aligned, such that the tidal forces from both the Moon and the Sun contribute in the same direction, a larger tidal range than usual will occur, called spring tide. When these forces counteract, a smaller tidal range will occur, and this is called neap tide. The former occurs when the Sun, the Moon and the Earth is aligned; and the latter occurs when the Moon and the Sun are separated by 90° when viewed from the Earth.

In reality the tides will deviate from this regularity because of several effects. These effects include the fact that the Earth's real axis of rotation is not perpendicular to the axis between the centres of the Earth and the Moon, and the fact that the time it takes for the Moon and the Earth to rotate around their common axis is 24h 50min and 47sec. This gives a daily variation in the tides.

In addition, the Moon's path around the Earth, and the Earth's path around the Sun are elliptic; thus, the tidal forces will be stronger when the separation is smaller with periods of approximately one month and one year respectively. The geometry of these paths changes every 8.85 year for the Moon and every 20 900 year for the Sun. Also, tidal forces have its maxima when the paths of the planets cross the Equator plan, which happens every 14th day for the Moon, and every half year for the Sun. Also, the tidal stream is influenced by land and other effects, giving local variations in the tidal range.

2.1.5 Storm Surge

The theory in this section is based on Pugh (2004). Storm surge is the excess sea level generated by a storm, and is produced by two contributions. Firstly, the change in barometric pressure associated with low pressure weather systems, and secondly the forces caused by wind drag at the sea surface.

The first contribution is often called the "inverted barometer effect", and is caused by the low

atmospheric pressure in the presence of a low pressure weather system. For a given change in atmospheric pressure ΔP_A , the corresponding change in sea level can be expressed as in Eq. (2.23) for equilibrium conditions of the sea, which is a condition where there are no currents caused by this pressure difference.

$$\Delta\eta = -\frac{\Delta P_A}{\rho g} \quad (2.23)$$

This equation indicates that for every millibar decrease in atmospheric pressure, an increase in sea level of one centimetre will occur. Typical values for atmospheric pressures in extra-tropical regions are in the range 980-1030 millibar. By comparing with a Standard Atmosphere of 1013 millibar, this will cause a change in sea level from +33cm to -17cm.

The second contribution is due to the drag from wind on the sea surface. This will move the water and can cause sea level rise. The drag is theoretically given as $C_D\rho_A U_{10}^2$, where C_D is the drag coefficient of the surface, and ρ_A is the air density, and U_{10} is the mean wind speed at 10 metre elevation above the sea level. At steady state the force from the wind stress will be balanced by the pressure gradient caused by this rise in sea level. By neglecting the bottom friction, the surface slope can be written as in Eq. (2.24).

$$\text{slope} = \frac{\text{Increase in sea level}}{\text{Horizontal distance}} = \frac{C_D\rho_A U_{10}}{\rho g h} \quad (2.24)$$

The time it takes to reach steady state is of the same order as the period of the Earth's rotation. Hence, rotational effects cannot be ignored. At the northern hemisphere the net transport of the water is shifted to the right of the wind stress direction in accordance with the Ekman transport. This results in a net transport per metre of section normal to the wind stress given in Eq. (2.25). Here, F is the wind stress; f is the Coriolis parameter $2\omega_S \sin \hat{\omega}$, where $\hat{\omega}$ is the latitude, and ω_S is the Earth's angular velocity.

$$\text{transport} = \frac{F}{f\rho} \quad (2.25)$$

An important effect of this phenomenon is observed for wind blowing along the coast. If the coast is on the right hand side of the wind stress direction, this will increase the sea level at

the coast in the northern hemisphere. The resulting sea surface slope can be written as in Eq. (2.26), where u is the generated current parallel to the shore given in Eq. (2.27).

$$\text{slope} = \frac{fu}{g} \quad (2.26)$$

$$u = \frac{Ft}{\rho h} \quad (2.27)$$

Here, t is the time, which from Eq. (2.27) indicates that the current is proportional to time and inversely proportional to the water depth. This current is, however, limited by the bottom friction.

2.2 Empirical Equations for Wave Runup and Wave Run-down

In this section the empirical wave runup and wave rundown formulae, called runup models, that will be used in the calculations are presented with a brief description of how they were obtained and the data that they were based on.

Blenkinsopp et al. (2016) have presented two wave runup and one wave rundown formulae given in Eq. (2.28), Eq. (2.29) and Eq. (2.30). The wave runup formulae are based on the formulations by Mase (1989) and Hedges & Mase (2004), with new empirical coefficients fitted to the equations. Regression analysis were performed in order to find the coefficients that most closely matched the data from the BARDEX II experiment. The wave rundown formula was found by linear regression through the wave rundown data when plotted as wave rundown normalised by the deep water significant wave height as a function of the deepwater Iribarren number.

$$R_2 = 1.165\xi_P^{0.77}H_S \quad (2.28)$$

$$R_2 = (0.39 + 0.795\xi_P)H_S \quad (2.29)$$

$$R_2 = (0.21 - 0.44\xi_p)H_S \quad (2.30)$$

This experiment was a large-scale laboratory experiment performed in 2012 in the Delta Flume in the Netherlands. A 4.5m high sand barrier was constructed in the flume with medium sized sand with sediment size $D_{50} = 0.42\text{mm}$. Shallow water irregular waves were generated by a wavemaker based on the JONSWAP spectrum, and the deepwater significant wave height was calculated according to linear wave theory. Different sensor techniques were used in this experiment; however, only the data obtained from an ultrasonic sensor array was used to calculate the new coefficients. The bottom slope was taken as the beach face gradient (swash zone gradient) and varied between 0.088 and 0.154 during the measurements leading to an Iribarren number in the range 0.99 to 2.87. For details on the BARDEX II experiment, see Masselink et al. (2016).

Schüttrumpf et al. (1994) performed a laboratory experiment in the Large Wave Flume of Hannover, Germany. The experiment was carried out using both uniform slopes with steepness 1:6 and 1:12, and composite slopes with steepness 1:3 for the lower slope and 1:6 for the upper slope. For the composite slopes an appropriate average slope was calculated. The slope surface was covered by an asphalt concrete layer imitating the surface of dikes and similar structures. The waves were generated based on Pierson-Moskowitz and JONSWAP wave spectra covering wave steepness H_S/L_0 in the range 0.001-0.031. For the range $0.5 < \xi < 2.5$ Schüttrumpf et al. (1994) suggested the formula in Eq. (2.31) for wave rundown.

$$R_2 = -0.1\xi^{2.21}H_S \quad (2.31)$$

de la Pena et al. (2014) have proposed a runup model for deep water Iribarren number $\xi_p < 0.6$. The formula is given in Eq. (2.32), where m is the average slope between the time-averaged water level at the shore and the depth of closure.

$$\frac{R_2}{H_S} = 4m^{0.3}\xi_p \quad (2.32)$$

This model is based on a model experiment performed at CEDEX Laboratory for Maritime Experimentation. The conditions tested, in which the runup model is based on, correspond to the following full scale values: $D_{50} = 0.7\text{mm}$, $\xi_p = 0.1-0.6$, $H_S = 0.5-4\text{m}$ and $T_p = 4-14\text{s}$. Three different slopes were tested: 1/50, 1/30 and 1/20 corresponding to dissipative, intermediate and

reflective beaches. Irregular waves were generated by a piston type wave paddle according to JONSWAP spectrum with a peakedness parameter of 3.3, and the wave height was measured by wave gauges close to the paddle. A runup wire parallel with the slope measured the swash motion and another gauge measured the setup. The geometric scale of the model was 1:20 and Froude similarity was used for scaling. Wave runup, R_2 , was obtained directly from the sample by the peak method. The proposed runup model was found by scaling the wave runup with ξ_P by least-squares regression forced through the origin. Application of the formula to storm conditions is within the range of the Iribarren numbers in this experiment for dissipative and intermediate beaches, but not for reflective beaches. Higher scatter in data were found for the results from the reflective beach compared to the dissipative and intermediate.

Based on a field experiment performed in 1982, Holman (1987) presented the runup model given in Eq. (2.33). This experiments was performed at CERC Field Research Facility at Duck, North Carolina. The beach used in the experiment is located at the Outer Banks with little disturbance of incoming waves.

$$R_2 = 0.83 \tan \beta \sqrt{H_S L_0} + 0.2 H_S = (0.2 + 0.83 \xi_P) H_S \quad (2.33)$$

The data used to determine the model was collected during a three-week period by Super-8 movie cameras in time-series of 35 minutes with a frame shot every second. Markers were placed at known locations at the beach to provide reference to the images. Profile data for the beach were collected once or twice a day by FRF Zeiss Elta-2 electronic total station system, and the beach slope was found as the mean slope over 5m width of the beach. Wave data were found a two locations: one at deep water by an offshore wave buoy 3km offshore at 20m depth; and another at intermediate water depth 560m offshore at approximately 6m depth. Tidal data were provided by a NOAA gauge at the latter offshore location, which was outside the surf zone other than during the largest storms.

Digitisation of the film data was performed resulting in 149 runup time series, where most of them were at two locations at the beach. All data were converted to the vertical component of wave runup and the tidal component was removed. Therefore, the wave runup represents the swash peaks relative to the still water level. Regression coefficients were found for wave runup normalised by the deep water significant wave height as a function of Iribarren number. The result is the regression line $0.83 \xi_P + 0.20$, which is the runup model in Eq. (2.33), with

coefficients ± 0.06 and ± 0.10 respectively.

The data obtained during the experiment contained measurements from a major storm, causing the conditions for when the data was obtained to vary significantly both in incoming waves and beach morphology. On the other hand, data were obtained at only one beach, hence the accuracy of the runup model applied on other locations is most likely poorer. Performance of application to other locations have been investigated by for instance Atkinson et al. (2017).

Another empirical runup model has been proposed by Vousdoukas & Wziatek (2012). This model is based on field experiments performed at Faro Beach at the southern coast of Portugal. The beach is characterised as reflective with a beach face slope decreasing eastward on the beach ending in a low tide terrace state at the far east of the beach. Sediments were classified as medium to very coarse, moderately well sorted with $D_{50} = 0.50\text{mm}$ and $D_{90} = 2\text{mm}$.

Offshore wave data were provided from an offshore wave buoy at 93m depth by the Portuguese Hydrographic Institute, and tidal data were measured at Huelva Harbor and provided by Spanish Port Authorities. Offshore wave conditions in terms of significant wave height and spectral peak period that were measured during the experiments were in the range $0.17\text{m} < H_S < 3.6\text{m}$ with a mean of 1.4m and mode of 0.4m, and $2.7\text{s} < T_P < 16.5\text{s}$ with a mean of 9.5s and mode of 4.2s. Topographic monitoring was performed by a real time kinematics differential GPS detecting beach face slopes in the range $4\% < m < 15\%$ with a mean of 10.3% and mode of 10%. Iribarren numbers varied from 0.3 to 2.8779.

Video cameras were used to detect the wave runup recording 10min every hour during daylight with an acquisition frequency of 1Hz. Time stack images for wave runup were generated hourly from the recordings. Then, lens distortion correction was applied and transformation from image to world coordinates was carried out. Linear regression was fitted to the profile section in the vertical range of tidal surface elevation \pm two times the standard deviation of the swash motion. This resulted in 426 wave runup measurements that were used to produce empirical runup models by fitting the results to different parameters. The runup model that showed the best performance with an RMS error equal 0.39m was the model in Eq. (2.34).

$$R_2 = 0.53\beta \sqrt{H_S L_P} + 0.58 \tan \beta H_S + 0.45 = (0.58m + 0.53\xi_P) H_S + 0.45 \quad (2.34)$$

Atkinson et al. (2017) have presented two new models that are based on nine existing and

commonly used runup models. Eight of the models are based on field-data and one is based on data from a large scale wave flume. Together they cover a wide range of beach types and sea states. Some of the models are, however, based on the same data sets. None of the experiments that the models are based on recorded significant wave heights larger than 4.6m or spectral peak periods above 17s, hence applying the Atkinson et al. (2017) models beyond these limits would be baseless. These models are on the form $C \tan \beta \sqrt{H_S L_P}$ proposed by Hunt (1958), where C is a coefficient found by least square analysis for the line of best fit to the predictions from the models. These models are given in Eq. (2.35) and Eq. (2.36), where the former is forced through the origin. The least square analysis gave a coefficient of variation R^2 for the line of values 0.71 and 0.72 respectively.

$$R_2 = 0.99 \tan \beta \sqrt{H_S L_P} = 0.99 \xi_P H_S \quad (2.35)$$

$$R_2 = 0.92 \tan \beta \sqrt{H_S L_P} + 0.16 H_S = (0.16 + 0.92 \xi_P) H_S \quad (2.36)$$

None of the empirical models that Eq. (2.35) and Eq. (2.36) are based on are valid for near vertical slopes, such as cliffs. Hence, these models are neither. Extreme wave runup events often occur when the wave runup strikes a near vertical structure, and consequently, these models are not valid for conditions resulting in such extreme wave runup events. However, the models dependence on H_S and L_P allow for extrapolation to extreme conditions, but their accuracy in such a case is uncertain.

According to Poate et al. (2016), the wave runup on gravel beaches are under-predicted by runup models developed using data from sandy beaches. Gravel beaches do usually have steeper profiles and they are able to maintain their profile characteristics even during highly energetic conditions; sandy beaches, however, are usually dominated by infragravity waves during extreme conditions while the incident storm waves are breaking and dissipating their energy further offshore. Poate et al. (2016) have therefore presented two new runup models intended for pure gravel beaches. These models are given in Eq. (2.37) and Eq. (2.38).

$$R_2 = 0.49 \tan \gamma^{0.5} T_Z H_S \quad (2.37)$$

$$R_2 = 0.33 \tan \gamma^{0.5} T_P H_S \quad (2.38)$$

These models are based on synthetic data from a numerical model of a gravel beach. This allows for generation of data runs over a large parameter space, which in this case is $m = 0.05-0.20$, $D_{50} = 2-50$, $H_S = 2.00\text{m}-7.02\text{m}$, $T_P = 5.11\text{s}-19.55\text{s}$. The runup models are validated by field data obtained at four gravel beaches in the southern England. Parameter range for the beaches were $m = 0.10-0.40$ and $D_{50} = 2-60\text{mm}$ during the measurements. Measurements were centred during high energy conditions causing large wave runup due to waves breaking directly at the shore and therefore also little dissipation of energy further offshore.

Each of the empirical equations are given an abbreviation for later reference, and these are given in Table 2.2.

Table 2.2: Abbreviation for runup model equations

Equation number	Abbreviation
2.28	B11
2.29	B12
2.30	B1d
2.31	Sc
2.32	Pe
2.33	Ho
2.34	Vo
2.35	At1
2.36	At2
2.37	Po1
2.38	Po2

2.3 Statistical Modelling of Wind and Waves

This section presents the theory behind long-term wind and wave modelling. Also, the long-term wind and wave distributions that are applied to the method herein are presented.

2.3.1 Long-Term Wind Statistics

DNV-RP-C205 (2014) recommends assuming a Weibull distribution for the mean wind speed in 10 minutes intervals at a given height above the sea level unless data indicates otherwise. The cumulative distribution function (cdf) for a two-parameter Weibull distribution is given in Eq. (2.39), where α and β are the shape and scale parameters. The n 'th moment for this distribution can be expressed as in (2.40), where Γ is the gamma function.

$$F_{U_{10}}(u_{10}) = 1 - \exp \left[- \left(\frac{u_{10}}{\beta} \right)^\alpha \right] \quad (2.39)$$

$$\mu_{U_{10}}^n = \beta^n \Gamma \left(1 + \frac{n}{\alpha} \right) \quad (2.40)$$

The distribution of the mean wind speed can also be expressed in terms of a joint probability density function (pdf) of H_S and U_{10} on the form given in Eq. (2.41). Such a joint pdf consists of a conditional distribution of U_{10} given H_S , and a marginal distribution of H_S . In DNV-RP-C205 (2014) a two-parameter Weibull distribution is suggested also for the conditional model like for the marginal distribution of U_{10} . For the marginal distribution of H_S , DNV-RP-C205 (2014) recommends a three-parameter Weibull distribution unless data indicates otherwise. The conditional and marginal distributions are expressed in Eq. (2.42), and Eq. (2.43) where s is the scale parameter, r is the shape parameter, and t is the location parameter for the distribution.

$$f_{U_{10}H_S}(h_s, u_{10}) = f_{U_{10}|H_S}(u_{10}|h_s) f_{H_S}(h_s) \quad (2.41)$$

$$f_{U_{10}|H_S}(u_{10}|h_s) = \frac{\alpha}{\beta} \left(\frac{u_{10}}{\beta} \right)^{\alpha-1} \exp \left[- \left(\frac{u_{10}}{\beta} \right)^\alpha \right] \quad (2.42)$$

$$f_{H_S}(h_s) = \frac{r}{s} \left(\frac{h_s - t}{s} \right)^{r-1} \exp \left[- \left(\frac{h_s - t}{s} \right)^r \right] \quad (2.43)$$

The probability of exceeding a certain value of the mean wind speed $u_{10,max}$ can be expressed in Eq. (2.44) as the probability of exceeding once every T_{return} years, where N is the number of individual U_{10} during T_{return} years (Myrhaug & Lian 2009), and N can be calculated by Eq. (2.45).

$$P(U_{10} > u_{10,max}) = 1 - F_{U_{10}}(u_{10}) = \frac{1}{N} \quad (2.44)$$

$$N = T_{return} \cdot 365 \cdot 24 \cdot \frac{60\text{min}}{10\text{min}} \quad (2.45)$$

A value for mean wind speed corresponding to this probability of exceedance can be found by inserting Eq. (2.39) into Eq. (2.44) and solve for $u_{10,max}$, resulting in the expression in Eq. (2.46).

$$u_{10,max} = \beta (\ln N)^{1/\alpha} \quad (2.46)$$

2.3.2 Mean Wind Distributions

Johannessen et al. (2002) have presented a cumulative two-parameter Weibull distribution for 1-hour mean wind speed at 10m above sea level, hereafter referred to as JMH02. Parameters for this distribution, $\alpha = 1.708$ and $\beta = 8.426$, were estimated by method of moments from data obtained in the Northern North Sea in the period 1973-1999. The data used for the estimation are based on measurements from the fields Brent, Troll, Statfjord, Gullfaks and from the weather ship Stevenson, and model data from the Norwegian hindcast archive (WINCH, gridpoint 1415) where data were missing, so that a continuous time-series of 20 years were obtained.

Mao & Rychlik (2016) have presented two two-parameter Weibull distributions for 10min average wind speed U_{10} , hereafter referred to MR15 (1) and MR15 (2). A spatio-temporal wind model was used to estimate Weibull parameters at fixed locations in the North Atlantic from hindcast data for the period 2003-2013. For the location $10^\circ\text{W } 40^\circ\text{N}$ just outside the west coast of Portugal these parameters were estimated to $\alpha = 2.30$ and $\beta = 7.11$, and at $20^\circ\text{W } 60^\circ\text{N}$ south of Iceland the estimated parameters are $\alpha = 2.46$ and $\beta = 10.99$.

Bitner-Gregersen (2015) has presented a joint model for wind, waves and current. This joint model contains a joint distribution for U_{10} and H_S that will be used here, hereafter referred to as BG15. The parameters for this distribution were estimated from hindcast data from the Northwest Shelf of Australia generated for the period 1994-2005. The joint model for U_{10} and H_S is given by the conditional two-parameter Weibull distribution for 10 minute mean

wind speed U_{10} given H_S in Eq. (2.42), and a three-parameter marginal Weibull distribution for H_S in Eq. (2.48). The estimated parameters for the two-parameter Weibull distribution are $\alpha = c_1 + c_2 h_s^{c_3}$ and $\beta = c_4 + c_5 h_s^{c_6}$, where $c_1 = 1.250$, $c_2 = 5.600$, $c_3 = 0.660$, $c_4 = 0.050$, $c_5 = 5.514$ and $c_6 = 0.280$ for the Northwest Shelf of Australia. The parameters for the three-parameter marginal distribution are $s = 0.605$, $r = 0.867$ and $t = 0.322$.

Table 2.3 shows the Weibull parameters for the distributions. The pdfs for the distributions are shown in Figure 2.6, where the conditional distribution is used for the BG15 distribution. Figure 2.6 shows that the conditional probability function is narrower and higher than the other three marginal distributions, indicating higher kurtosis for this distribution. The JMH02 and the MR15 (1) distributions are both skewed to the left, while the MR15 (2) distribution is more symmetric.

Table 2.3: Parameters for the long-term Weibull wind distributions

Distribution	α	β
JMH02	1.708	8.426
MR15 (1)	2.30	7.11
MR16 (2)	2.46	10.99
BG15	$1.250 + 5.600h_s^{0.660}$	$0.050 + 5.514h_s^{0.280}$

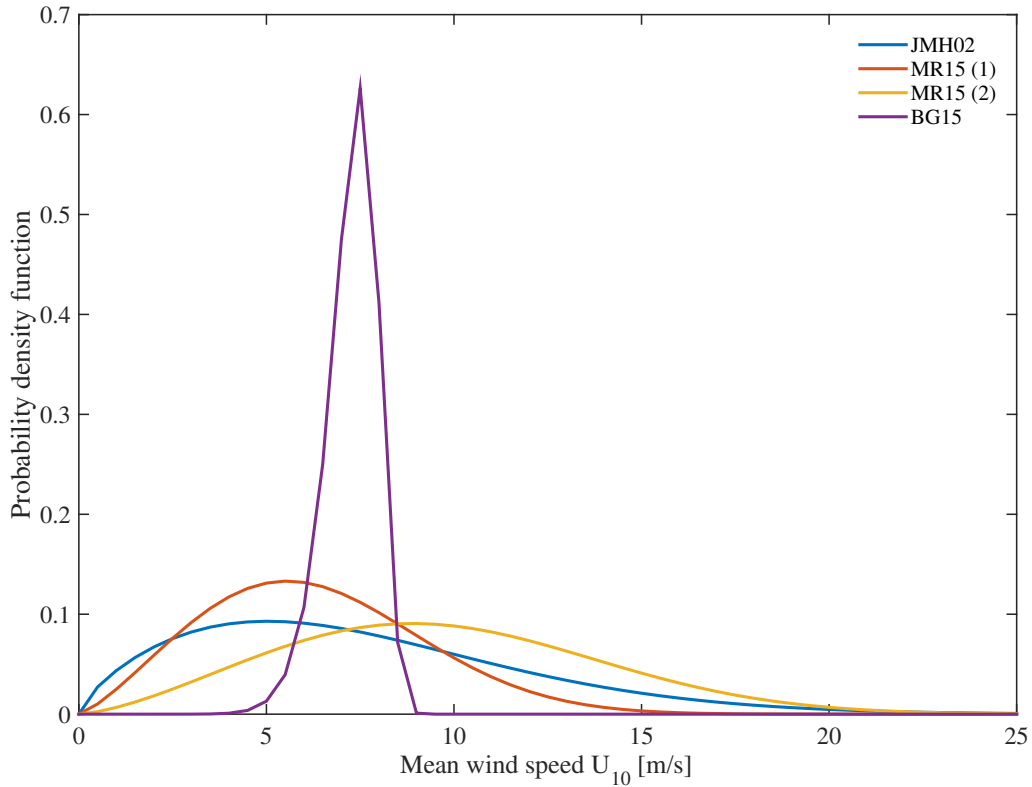


Figure 2.6: Wind probability density functions

2.3.3 Long-Term Wave Statistics

Long-term wave statistics is often expressed in terms of a joint pdf of H_S and T_P , or H_S and T_Z . Joint pdfs for H_S and T_P , or H_S and T_Z , are given on the form in Eq. (2.47), where T represents either T_P or T_Z . The relation between T and T_P is defined as $T_P = \hat{c}T$, where \hat{c} is a coefficient. Here, $f_{H_S|T}(t|h_s)$ is the conditional pdf of T given H_S , and $f_{H_S}(h_s)$ is the marginal pdf of H_S .

$$f_{H_S T}(h_s, t) = f_{H_S|T}(t|h_s) f_{H_S}(h_s) \quad (2.47)$$

DNV-RP-C205 (2014) suggests that a joint distribution of significant wave height and period is modelled by a three-parameter Weibull distribution for the marginal distribution of H_S and a lognormal distribution for the conditional distribution. The form of this marginal distribution is given in Eq. (2.48) where s is the scale parameter, r is the shape parameter, and t is the location parameter for the distribution.

$$f_{H_S}(h_s) = \frac{r}{s} \left(\frac{h_s - t}{s} \right)^{r-1} \exp \left[- \left(\frac{h_s - t}{s} \right)^r \right] \quad (2.48)$$

The conditional pdf $f_{T|H_S}(t|h_s)$ is given by Eq. (2.49), where μ_T and σ_T^2 are the mean value and the variance of $\ln T$. The mean value of $\ln T$ is on the form in Eq. (2.50), and the variance or standard deviation can either be on the form in Eq. (2.51), (2.53), or (2.52); where a_1, a_2, a_3, b_1, b_2 and b_3 are parameters determined by the distribution.

$$f_{T|H_S}(t|h_s) = \frac{1}{\sqrt{2\pi}\sigma_T t} \exp \left[- \frac{(\ln t - \mu_T)^2}{2\sigma_T^2} \right] \quad (2.49)$$

$$\mu_T = a_1 + a_2 H_S^{a_3} \quad (2.50)$$

$$\sigma_T^2 = b_1 + b_2 \exp(b_3 H_S) \quad (2.51)$$

$$\sigma_T = b_1 + b_2 \exp(b_3 H_S) \quad (2.52)$$

$$\sigma_T = b_1 + b_2 H_S^{b_3} \quad (2.53)$$

Another alternative for the marginal distribution of H_S is a combined log-normal and Weibull distribution given in Eq. (2.54) (Haver 1980), where h_s^* is the shifting point from the log-normal to the Weibull distribution. The parameters μ_H and σ_H^2 are the mean value and the variance of $\ln H_S$, and s and r are Weibull parameters.

$$f_{H_S}(h_s) = \begin{cases} \frac{1}{\sqrt{2\pi}\sigma_H h_s} \exp \left[- \frac{(\ln h_s - \mu_H)^2}{2\sigma_H^2} \right] & \text{for } h_s \leq h_s^* \\ r \frac{h_s^{r-1}}{s^r} \exp \left[- \left(\frac{h_s}{s} \right)^r \right] & \text{for } h_s > h_s^* \end{cases} \quad (2.54)$$

2.3.4 Joint Wave Distributions

Moan et al. (2005) have presented a joint pdf for H_S and T_P consisting of a log-normal conditional distribution of T_P given H_S in Eq. (2.49) with parameters in Eq. (2.50) and Eq. (2.51),

and a combined log-normal and two-parameter Weibull marginal distribution in Eq. (2.54); hereafter referred to as MGAU05. This distribution was fitted to data recorded by a wave buoy in the Northern North Sea during a 29-year period from 1974 to 2002. Measurements of the significant wave height ranged from 0.25m to 12.75m in this period, and spectral peak period from 0.5s to 29.5s.

The shifting point h_s^* between the two marginal distributions was determined by an iterative procedure based on chi-square testing, resulting in $h_s^* = 3.25\text{m}$ (Moan et al. 2005). Parameters for this joint distribution were provided by Gao (2007) cited in Myrhaug & Fouques (2010), where the values for the conditional distribution are presented in Table 2.4; and values for the parameters of the combined marginal distribution are $\mu_H = 0.801$ and $\sigma_H^2 = 0.371$ for the mean and the variance of $\ln H_S$, and the Weibull parameters are $s = 2.713$ and $r = 1.531$. The Weibull parameters are also given in Table 2.5.

Orimolade et al. (2016) have presented parameters for a long-term joint distribution of H_S and T_P , hereafter referred to as OHG16. This joint distribution consists of a three-parameter marginal Weibull distribution of H_S in Eq. (2.48); and a log-normal conditional distribution of T_P given H_S in Eq. (2.49), with parameters in Eq. (2.50) and Eq. (2.51). Estimation of the parameters for the joint distribution was based on hindcast data from the Norwegian Reanalysis 10km (NORA10) consisting of 3hourly wave fields at a resolution of 10km. This data was collected in the Barents Sea at 72.02°N 22.10°E during a period of 57 years from 1957 to 2014. In this area the significant wave height ranged from 0.2m to 17m during that period. Parameters for the marginal distribution of H_S were estimated by the method of moments resulting in the parameters presented in Table 2.5, and the estimated parameters for the conditional distribution for T_P given H_S are presented in Table 2.4.

Bitner-Gregersen & Guedes Soares (2007) have presented parameters for a joint distribution of H_S and T_Z based on five different data sets, hereafter referred to as BGG07. The joint distribution is given by Eq. (2.48), and (2.49) with parameters in Eq. (2.50) and Eq. (2.53). For estimation of the parameters the least square method is used on the datasets.

All the data were collected from the ocean region west of the British Isles and south of Iceland in the North Atlantic. Three datasets from global databases are among these. These datasets consist of data collected at three locations in the North Atlantic at the locations 59°N 19°W , 54°N 21°W and 59°N 18.45°W , west of the British Isles. The data were collected over a

period of 44, 19 and 12 years at the respective locations every third hour for all but the second location where data were sampled every sixth hour. Another dataset from the Global Wave Statistics is also used for estimation of parameters from data from the region. These data are based on visual observations collected from ships in service since 1949 in the selected ocean region. The fifth dataset is based on data collected over a 13-year period at the Ocean Weather Station Juliet stationed at 52 °N 20 °W in the mid-1900s. The parameter values are given in Table 2.4 where the number of the datasets are referred to in the parenthesis. Parameters for the marginal distribution in Eq. (2.48) are given in Table 2.5.

Mathisen & Bitner-Gregersen (1990) have presented three joint distributions with associated parameters. These distributions consist of three-parameter marginal Weibull distributions for H_S in Eq. (2.48), and conditional log-normal distributions for T_Z given H_S in Eq. (2.49) with parameters in Eq. (2.50) and Eq. (2.52).

Parameters for the joint distributions were estimated based on three data sets from the Norwegian Continental Shelf at Tromsøflaket (71°30'N 19°00'E), Utsira (59°18'N 4°48'E), and Haltenbanken (64°11'N 9°8'E). Data for Tromsøflaket were provided by the Environmental Data Centre of the Norwegian Meteorological Institute and is based on observations by Waverider buoys every three hour during the period 1977-1983, and data for Utsira and Haltenbanken were extracted from two reports of the ODAP - Oceanographic Data Acquisition Project. Weibull parameters were estimated by nonlinear least squares, and the log-normal parameters were found by first calculating μ_T and σ_T for each class of significant wave height and then fitting the a_1 , a_2 , a_3 , b_1 , b_2 and b_3 parameters to Eq. (2.50) and Eq. (2.52) by the nonlinear least squares technique.

The parameter values for the conditional log-normal distribution are given in Table 2.4, and parameter values for the marginal Weibull distribution are given in Table 2.5.

Table 2.4: Parameters for the conditional wave distributions for T given H_S

Distribution	Parameters					
	a_1	a_2	a_3	b_1	b_2	b_3
MGAU05	1.780	0.288	0.474	0.001	0.097	-0.255
OHG16	0.740	1.200	0.210	0.001	0.113	-0.275
BGGS07 (1)	1.350	0.366	0.392	0.020	0.165	-0.166
BGGS07 (2)	1.365	0.375	0.453	0.033	0.285	-0.752
BGGS07 (3)	0.790	0.805	0.292	0.055	0.195	-0.269
BGGS07 (4)	0.835	1.139	0.119	0.140	0.030	-0.958
BGGS07 (5)	1.952	0.168	0.499	0.070	0.066	-0.081
MBG90 (1)	1.240	0.337	0.538	0.0728	0.383	-0.665
MBG90 (2)	1.090	0.479	0.417	0.0407	0.221	-0.289
MBG90 (3)	0.933	0.578	0.395	0.0550	0.336	-0.585

Table 2.5: Weibull parameters for marginal distribution of H_S in (2.48)

Distribution	s	r	t
MGAU05	2.713	1.531	
OHG16	1.690	1.160	0.760
BGGS07 (1)	3.104	1.357	0.906
BGGS07 (2)	2.848	1.419	1.021
BGGS07 (3)	2.939	1.240	0.896
BGGS07 (4)	2.857	1.449	0.838
BGGS07 (5)	2.420	1.169	1.258
MBG90 (1)	1.410	1.120	0.987
MBG90 (2)	1.910	1.270	0.532
MBG90 (3)	1.500	1.150	0.679

Figure 2.7 shows the conditional pdfs of T given $H_S = 3\text{m}$. This figure shows that the BGGS07 distributions have significantly higher kurtosis than the MGAU05 and OHG16 distributions, and

the MBG90 distributions show even higher kurtosis. The MGAU05 and OHG16 distributions show very similar shape and peak wave period.

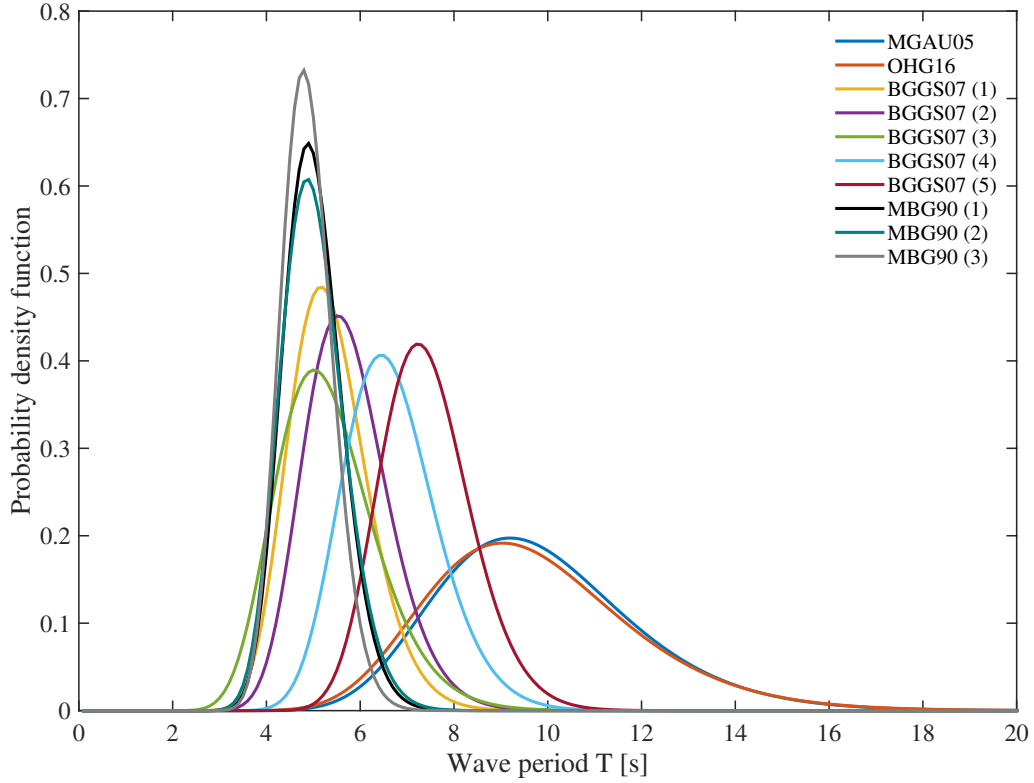


Figure 2.7: Conditional wave probability density functions for $H_S = 3\text{m}$

2.4 Inversed First-Order-Reliability-Method

This method is based on DNV-RP-C205 (2014). First, the joint distribution for the relevant sea state parameters are established. The form of a joint distribution for H_S and T_Z is given in Eq. (2.55).

$$f_{H_S T}(h_s, t) = f_{H_S|T}(t|h_s)f_{H_S}(h_s) \quad (2.55)$$

The joint distribution can then be transformed to standard normalised U-space, with axis u_1 and u_2 , by Eq. (2.56) and Eq. (2.57).

$$\Phi(u_1) = F_{H_S}(h) \quad (2.56)$$

$$\Phi(u_2) = F_{T_P|H_S}(t|h) \quad (2.57)$$

In the standard normalised U-space, points with constant probability density are located on a circle with a constant radius r . For a given return period this radius can be found from Eq. (2.58), where q is the probability of exceedance associated with the given return period.

$$r = \sqrt{u_1^2 + u_2^2} = -\Phi^{-1}(q) \quad (2.58)$$

The circle can then be transformed back to environmental parameter space defining the contour line for the given return period by Eq. (2.59) and Eq. (2.60).

$$h_s = F_{H_S}^{-1}(\Phi(u_1)) \quad (2.59)$$

$$t = F_{T|H_S}^{-1}(\Phi(u_2)) \quad (2.60)$$

Chapter 3

Method

This chapter presents the method that is used to calculate characteristic statistical values of wave runup and wave rundown by using the empirical formulae and the long-term wind and wave distributions presented in Chapter 2.

3.1 General Equations for Wave Runup and Wave Rundown

In this section two general formulae are presented. All the empirical formulae in Section 2.2 can be expressed through these two equations.

The first eight equations for R_2 , Eqs. (2.28) to (2.36), can be described by the general expression given in Eq. (3.1). Eq. (2.37) and Eq. (2.38) can both be described by Eq. (3.2). Here, T represents either T_P or T_Z , and the relation between T_P and T_Z is taken as $T_P = 1.28T_Z$ so that $\hat{c} = 1$ for $T = T_P$, and $\hat{c} = 1.28$ for $T = T_Z$, based on Figure 11 in Myrhaug & Kjeldsen (1987). This is valid for a JONSWAP spectrum with peakedness factor 3.3, and is not necessarily valid for the distributions used here.

$$\begin{aligned} R_2 &= (a + b\xi_p^c)H_S + d \\ &= aH_S + bm^c \hat{c}^c \left(\frac{g}{2\pi}\right)^{c/2} H_S^{1-c/2} T^c + d \end{aligned} \quad (3.1)$$

$$R_2 = Cm^{0.5} \hat{c} T H_S \quad (3.2)$$

Values for the different parameters in Eq. (3.1) and Eq. (3.2) are given in Table 3.1 for each runup model. Table 3.2 gives an overview of the range of the runup models. Note that some values in Table 3.2 have been read from figures in the original articles, and are not necessarily values specified explicitly by the authors of these articles.

Table 3.1: Parameter values for the general equations for runup models

Runup model	Values in general equations				
	a	b	c	d	C
B11	0	1.165	0.77	0	
B12	0.39	0.795	1	0	
B1d	0.21	-0.44	1	0	
Sc	0	-0.1	2.21	0	
Pe	0	$4m^{0.3}$	1	0	
Ho	0.2	0.83	1	0	
Vo	$0.58m$	0.53	1	0.45	
At1	0	0.99	1	0	
At2	0.16	0.92	1	0	
Po1					0.49/1.28
Po2					0.33

Table 3.2: Overview of runup model range. **Bold** indicates values that the authors have suggested as range for the formulae. Normal is values from the experiments that the formulae are based on.

Runup model	Range					
	m [-]	ξ [-]	D_{50} [mm]	H_S [m]	T_P [s]	H/L [-]
B11, B12, B1d	0.088- 0.154	0.99-2.87	0.42			
Sc		0.5-2.5	asphalt concrete			0.001- 0.031
Pe	1/50, 1/30, 1/20	< 0.6	0.7	0.5-4	4-14	
Ho	dissipative to reflective		beach	0.4-4.0	4-17	
Vo	0.04-0.15	0.3- 2.8779	0.50	0.17-3.6	2.7-16.5	
At1, At2	dissipative to reflective			-4.6	-17s	
Po1, Po2	0.05-0.20	0.20-1.94	2-50	2-7.02	5.11- 19.55	

3.2 Wave Runup and Wave Rundown Based on Wind Statistics

This section presents the method for calculating characteristic statistical values of wave runup and wave rundown based on wind statistics. Both a stochastic, and a simplified deterministic approach are presented. This stochastic method is based on Myrhaug (2017).

3.2.1 Stochastic Approach

An expression for R_2 can be derived from the single sided Phillips spectrum given in Eq. (3.3), where $\omega \rightarrow \infty$, $\omega \geq \omega_p = g/U_{10}$, where $\hat{\alpha}=0.0081$ is the Phillips constant.

$$S(\omega) = \hat{\alpha} \frac{g^2}{\omega^5} \quad (3.3)$$

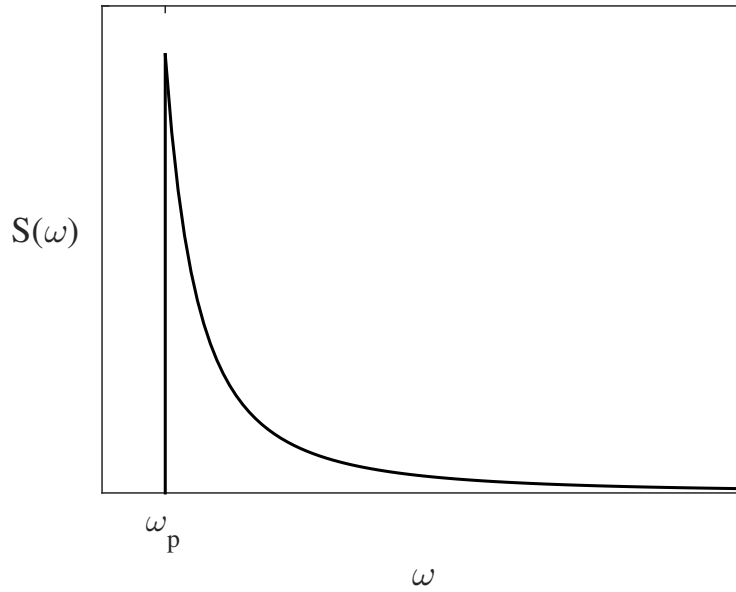


Figure 3.1: Phillips spectrum

From the restrictions of spectral peak frequency ω_p , an expression for the spectral peak period T_p can be defined by utilising the relation $T_p = 2\pi/\omega_p$. This gives an expression for T_p as a function of U_{10} defined in Eq. (3.4).

$$T_p = \frac{2\pi}{\omega_p} = \frac{2\pi}{g} U_{10} \quad (3.4)$$

The moments of the spectrum are defined as $m_n = \int_0^{\infty} \omega^n S(\omega) d\omega$. Based on the moments, an expression can be found for both the significant wave height H_S and the zero-crossing period T_Z . By estimating H_S from the spectrum, the expression is found from the relation $H_S = 4\sqrt{m_0}$. The expression for H_S as a function of U_{10} is given in Eq. (3.5).

$$H_S = 4\sqrt{m_0} = \frac{2\sqrt{\hat{\alpha}}}{g} U_{10}^2 \quad (3.5)$$

The zero-crossing period can be found from the spectrum by using the relation $T_Z = 2\pi\sqrt{m_0/m_2}$. The expression for T_Z as a function of U_{10} is given in Eq. (3.6).

$$T_Z = 2\pi\sqrt{\frac{m_0}{m_2}} = \frac{\sqrt{2}\pi}{g}U_{10} \quad (3.6)$$

In order to write the general expression for R_2 in Eq. (3.1) as a function of U_{10} , the expression for ξ_P in Eq. (2.2) in Section 2.1.2. and the expressions for T_P and H_S are inserted into the original expression. The result is given in Eq. (3.7), where C_1 is given in Eq. (3.8), and the details in the calculation can be found in Appendix A.1.

$$\begin{aligned} R_2 &= (a + b\xi_P^c)H_S + d \\ &= aH_S + b\left(m\sqrt{\frac{g}{2\pi}}\frac{T_P}{\sqrt{H_S}}\right)^c H_S + d \\ &= \left[a\frac{2\sqrt{\hat{\alpha}}}{g} + bm^c\left(\frac{2\pi}{g}\right)^{\frac{c}{2}}\left(\frac{2\sqrt{\hat{\alpha}}}{g}\right)^{1-\frac{c}{2}} \right] U_{10}^2 + d \\ &= C_1 U_{10}^2 + d \end{aligned} \quad (3.7)$$

$$C_1 = a\frac{2\sqrt{\hat{\alpha}}}{g} + bm^c\left(\frac{2\pi}{g}\right)^{\frac{c}{2}}\left(\frac{2\sqrt{\hat{\alpha}}}{g}\right)^{1-\frac{c}{2}} \quad (3.8)$$

Expressions for the expected value and the variance of R_2 can be found by utilising the relation between R_2 and U_{10} in Eq. (3.7). These expressions are given in Eq. (3.9) and Eq. (3.10), where $\mu_{U_{10}}^n$ is the n'th moment of U_{10} in Eq. (2.40).

$$\begin{aligned} E[R_2] &= E[C_1 U_{10}^2 + d] = C_1 E[U_{10}^2] + d \\ &= C_2 \mu_{U_{10}}^2 + d \end{aligned} \quad (3.9)$$

$$\begin{aligned} \text{Var}[R_2] &= \text{Var}[C_1 U_{10}^2 + d] = \text{Var}[C_1 U_{10}^2] \\ &= E[(C_1 U_{10}^2)^2] - (E[C_1 U_{10}^2])^2 \\ &= C_1^2 E[U_{10}^4] - C_1^2 (E[U_{10}^2])^2 \\ &= C_1^2 (\mu_{U_{10}}^4 - (\mu_{U_{10}}^2)^2) \end{aligned} \quad (3.10)$$

For the general expression in Eq. (3.2), R_2 can be expressed in terms of U_{10} as shown in Eq. (3.11), where C_2 is given in Eq. (3.12), and the details in the calculation can be found in Appendix A.1.

$$R_2 = Cm^{0.5}TH_S = C_2U_{10}^3 \quad (3.11)$$

$$C_2 = \begin{cases} 0.49m^{0.5} \frac{2\pi\sqrt{2\hat{\alpha}}}{g^2} & \text{for Po1} \\ 0.33m^{0.5} \frac{4\pi\sqrt{\hat{\alpha}}}{g^2} & \text{for Po2} \end{cases} \quad (3.12)$$

The expected value and variance of R_2 in Eq. 3.2 can be written as in Eq. (3.13) and Eq. (3.14).

$$E[R_2] = E [C_2U_{10}^3] = C_2E [U_{10}^3] = C_2\mu_{U_{10}}^3 \quad (3.13)$$

$$\begin{aligned} Var[R_2] &= E [R_2^2] - (E [R_2])^2 \\ &= E [(C_2U_{10}^3)^2] - (E [C_2U_{10}^3])^2 \\ &= C_2^2E [U_{10}^6] - C_2^2(E [U_{10}^3])^2 \\ &= C_2^2 (\mu_{U_{10}}^6 - (\mu_{U_{10}}^3)^2) \end{aligned} \quad (3.14)$$

3.2.2 Deterministic Approach

When information is limited, a deterministic approach can be used. For this approach, only the expected value of the mean wind speed is needed, in contrast to the 0th to 6th moment of the distribution in the stochastic approach. The expected value of the wave runup and wave rundown can in this case be calculated by Eq. (3.15) for the general equation in Eq. (3.1), and by Eq. (3.16) for the general equation in Eq. (3.2). The standard deviation becomes zero for the deterministic approach.

$$E[R_2] = C_1E [U_{10}^2] + d = C_1(\mu_{U_{10}})^2 + d \quad (3.15)$$

$$E[R_2] = CE [U_{10}^3] = C(\mu_{U_{10}})^3 \quad (3.16)$$

3.2.3 Extreme Values

Extreme values for R_2 , $R_{2,max}$, can be found by utilising the relation between R_2 and U_{10} in Eq. (3.7) and Eq. (3.11). By inserting the extreme values for the mean wind speed found by Eq. (2.46) into this relation, values of $R_{2,max}$ can be obtained by Eq. (3.17) and Eq. (3.18).

$$R_{2,max} = C_1 (u_{10,max})^2 + d \quad (3.17)$$

$$R_{2,max} = C_2 (u_{10,max})^3 \quad (3.18)$$

3.3 Wave Runup and Rundown Based on Wave Statistics

This section presents the method for calculating characteristic statistical values of wave runup and wave rundown based on wave statistics.

3.3.1 Stochastic Approach

The method in this section is based on methods presented by Myrhaug (2015) and Myrhaug & Leira (2017), and is used for calculating wave runup and wave rundown based on joint distributions of H_S and T_p , or H_S and T_Z .

Based on the general equation for R_2 in Eq. (3.1), a joint pdf for H_S and R can be found by change of variables from the joint pdf for H_S and T in Eq. (2.47). Here, R is defined as $R = R_2 - aH_S - d$ to simplify the calculations. This joint pdf will be on the form in Eq. (3.19), and the change of variables will only affect the conditional pdf for R given H_S , leaving $f(H_S)$ unchanged.

$$f(H_S, R) = f(R|H_S)f(H_S) \quad (3.19)$$

The conditional pdf for R given H_S can be found by change of variables from the conditional pdf for T given H_S in Eq. (2.49), and the result is given in Eq. (3.20). The mean value and

variance of $\ln R$ are given in Eq. (3.21) and Eq. (3.22), and μ_T and σ_T are found in Eq. (2.50), and Eq. (2.51), (2.52) or (2.53). For further details on the calculation, see Appendix A.2.

$$f(R|H_S) = \frac{1}{\sqrt{2\pi}\sigma_R R} \exp\left[-\frac{(\ln R - \mu_R)^2}{2\sigma_R^2}\right] \quad (3.20)$$

$$\mu_R = c\mu_T + \ln\left(bm^c \hat{c}^c \left(\frac{g}{2\pi}\right)^{c/2} H_S^{1-c/2}\right) \quad (3.21)$$

$$\sigma_R^2 = c^2 \sigma_T^2 \quad (3.22)$$

The conditional cdf for R given H_S can be found from Eq. (3.23), where Φ is the standard Gaussian cdf. From this expression the conditional expected value and standard deviation of R given H_S can be described as in Eq. (3.24) and Eq. (3.25) (Bury 1975).

$$F(R|H_S) = \Phi\left[\frac{\ln R - \mu_R}{\sigma_R}\right] \quad (3.23)$$

$$E[R|H_S] = \exp\left(\mu_R + \frac{1}{2}\sigma_R^2\right) \quad (3.24)$$

$$\sigma[R|H_S] = \left[\left(e^{\sigma_R^2} - 1\right) \exp(2\mu_R + \sigma_R^2)\right]^{1/2} \quad (3.25)$$

The conditional expected value and standard deviation of R_2 can then be found by utilising the relationship $R = R_2 - aH_S - d$, and the expressions are given in Eq. (3.26) and Eq. (3.27).

$$E[R_2|H_S] = E[R|H_S] + aH_S + d \quad (3.26)$$

$$\sigma[R_2|H_S] = \sigma[R|H_S] \quad (3.27)$$

Similarly, change of variables can be performed by considering the general expression in Eq. (3.2). This change of variables results in the conditional pdf given in Eq. (3.28) with the mean and variance of $\ln R_2$ in Eq. (3.29) and Eq. (3.30), see Appendix A.2 for details on the calculation.

$$f(R_2|H_S) = \frac{1}{\sqrt{2\pi}\sigma_{R_2}R_2} \cdot \exp\left[-\frac{(\ln R_2 - \mu_{R_2})^2}{2\sigma_{R_2}^2}\right] \quad (3.28)$$

$$\mu_{R_2} = \mu_T + \ln\left(Cm^{0.5}\hat{c}H_S\right) \quad (3.29)$$

$$\sigma_{R_2} = \sigma_T \quad (3.30)$$

The expected value and standard deviation of R_2 can then be found from Eq. (3.31) and Eq. (3.32).

$$E[R_2|H_S] = \exp\left(\mu_{R_2} + \frac{1}{2}\sigma_{R_2}^2\right) \quad (3.31)$$

$$\sigma[R_2|H_S] = \left[\left(e^{\sigma_{R_2}^2} - 1\right) \exp\left(2\mu_{R_2} + \sigma_{R_2}^2\right)\right]^{1/2} \quad (3.32)$$

3.3.2 Expected Value of H_S

The expected value of the marginal distribution of H_S can be calculated from Eq. (3.33) by calculating the first moment of the respective distributions.

$$E[H_S] = \mu_{H_S} = \int_{-\infty}^{\infty} h_s f(h_s) dh_s \quad (3.33)$$

By performing this calculation for the marginal distributions $f_{H_S}(h_s)$ in Eq. (2.48) and Eq. (2.54), the resulting expected values can be written as in Eq. (3.34) and Eq. (3.35).

$$E[H_S] = t + s\Gamma\left(1 + \frac{1}{r}\right) \quad (3.34)$$

$$E[H_S] = e^{\mu_H + \frac{1}{2}\sigma_H} \Phi\left[\frac{\ln h_s^* - (\mu_H + \sigma_H^2)}{\sigma_H}\right] + \beta\Gamma\left(1 + \frac{1}{\alpha}, \left(\frac{h_s^*}{\beta}\right)^\alpha\right) \quad (3.35)$$

3.3.3 Contour Lines

Contour lines for H_S and T_P can be found from the Inversed First-Order-Reliability-Method presented in Section 2.4. For a given return period T_{return} , the probability of exceedance is calculated by Eq. (3.36), where m_d is the number of sea states per year.

$$q = \frac{1}{T_{return}m_d} \quad (3.36)$$

For each return period, combinations of u_1 and u_2 in the standard normalised U-space are found through the relations $u_1 = r \cos \theta$ and $u_2 = r \sin \theta$ based on Eq. (2.58) for θ between 0 and 2π . For every combination of u_1 and u_2 , a pair of H_S and T_P values are calculated by Eq. (2.59) and Eq. (2.60).

The cumulative distribution function for the marginal distributions presented in Eq. (2.48) and Eq. (2.54) and the conditional distribution in Eq. (2.49) are given in the following along with expressions for h_s and t found from Eq. (2.59) and Eq. (2.60).

For the combined log-normal and Weibull distribution in Eq. (2.54) the corresponding cumulative distribution is given in Eq. (3.37), and the expression for h_s is given in Eq. (3.38).

$$F(H_S) = \begin{cases} \Phi \left[\frac{\ln h_s - \theta}{\kappa} \right] & \text{for } H_S \leq 3.25 \text{ m} \\ 1 - \exp \left[- \left(\frac{h_s}{s} \right)^r \right] & \text{for } H_S > 3.25 \text{ m} \end{cases} \quad (3.37)$$

$$h_s = \begin{cases} \exp(s + u_1 k) & \text{for } H_S \leq 3.25 \text{ m} \\ s [-\ln(1 - F(h_s))]^{1/r} & \text{for } H_S > 3.25 \text{ m} \end{cases} \quad (3.38)$$

For the three-parameter marginal Weibull distribution in Eq. (2.48) the corresponding cumulative distribution is given in Eq. (3.39), and the expression for h_s is given in Eq. (3.40).

$$F(h_s) = 1 - \exp \left[- \left(\frac{h_s - t}{s} \right)^r \right] \quad (3.39)$$

$$h_s = t + s [-\ln(1 - F(h_s))]^{1/r} \quad (3.40)$$

For the conditional log-normal distribution of T given H_S the corresponding cumulative distribution is given in Eq. (3.41), and an expression for t is given in Eq. (3.42).

$$F(t|h_s) = \Phi \left[\frac{\ln t - \mu_T}{\sigma_T} \right] \quad (3.41)$$

$$t = \exp(u_2\sigma + \mu) \quad (3.42)$$

The combinations of t and h_s values are then plotted giving the contour lines of the probability determined by q .

3.3.4 Extreme Values

When the contour lines for the distributions are established, extreme wave runup and wave rundown can be found on the contour lines for each of the runup models.

In order to do so, first the wave runup and wave rundown values are calculated by each runup model for every combination of H_S and T_P , or H_S and T_Z along the contours. Then, the largest wave runup or wave rundown value is located, along with the sea state combination that produces this value. This wave runup or wave rundown is identified as the extreme runup/ rundown $R_{2,max}$.

By plotting each of the runup models with their $R_{2,max}$ in the contour line plots, the models appears as a tangent to the associated contour line. An example is shown in Figure 3.2 where the B11 runup model appears as a tangent to the MGAU05 contour lines for five different return periods. Here the B11 runup model is plotted with the $R_{2,max}$ that were found for this combination of distribution and runup model. Similar plots for other combinations of runup models and wave distributions can be found in Appendix B.4.

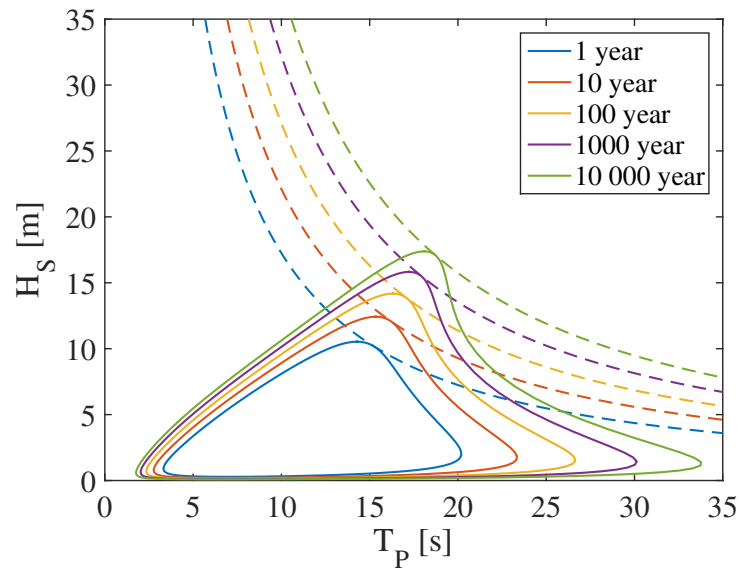


Figure 3.2: Contour lines for the MGAU05 distribution (solid lines) with runup model B11 (dashed lines) for extreme wave runup

Chapter 4

Individual Studies

The analytical method for estimating characteristic statistical values is exemplified through application of several empirical wave runup and wave rundown equations, along with both wind and wave distributions. Eleven runup models, four wind distributions, and ten wave distributions were applied. This selection of models and distributions are all available in the literature and they were chosen because of their relevance and relatively simple expression. The latter criterion was relevant in order to be able to do analytical calculations without unnecessary difficulties. The method is explained in Chapter 3, and the runup models and distributions that were applied are presented in Section 2.2, 2.3.2, and 2.3.4.

For the wind distributions to be used, the Phillips spectrum was chosen for establishing a relation between wind and waves. This particular spectrum was chosen due to its simplicity in its expression allowing the formulae to continue to be relatively simple and possible to handle analytically. This resulted in an expression for wave runup and wave rundown based on wind statistics, and it is this expression that was used in the calculations, presented in Section 3.2. Both a stochastic and a deterministic approach was used. Calculating the ratio between the expected values from both approaches allowed for comparison of the results from these two approaches. A deterministic approach could be convenient when information is limited because only the expected value of the wind distribution is required for the calculations. For the conditional BG15 distribution, a significant wave height of 3m was used.

For the wave distribution to be applied, transformation of variables was performed generating an expression for wave runup and wave rundown based a joint pdf for H_S and T , as described

in Section 3.3. The wave runup and wave rundown are described in terms of the expected value and the standard deviation. In order to generate results for the conditional wave distributions, a significant wave height of 3m was also here chosen for the calculations.

Most of the results are presented on dimensionless form, where R_2 is normalised by the significant wave height. Results with dimensions can be found in Appendix B.1 and B.2. For the wind distributions the significant wave height used in the normalisation was found through the Phillips spectrum by inserting the expected mean wind speed for the distribution in Eq. (3.5). For the wave distribution, the R_2 values are normalised by the expected value of the significant wave height found from the respective marginal distributions calculated by the procedure in Section 3.3.2. Results from wind and wave distributions have been compared for a significant wave height of 3m and a bottom slope of 1/10.

The wave rundown is defined such that positive values indicate wave rundown above SWL and negative values indicate wave rundown below SWL. Due to complications in the calculations by applying this definition, the wave rundown was calculated with opposite sign, and then the sign was changed back in the presentation of the results.

Extreme values of R_2 have been found from both wind and wave distributions for return periods of 1, 10, 100, 1000 and 10 000 years for a bottom slope of 1/10. For the wind distributions the method in Section 3.2.3 was used. When applying the JMH02 distribution averages of 1 hour were used, while for the other distributions 10min averages were used, so that 8760 and 52 560 averages were assumed respectively.

Extreme values based on the wave distributions were found from the contour lines for a given return period according to the procedure in Section 3.3.4. It was assumed 2920 sea states per year in the calculations of the contour lines. Furthermore, 1 year return period extreme values for bottom slope 1/10 from both wind and wave distributions were compared. Finally, the extreme values for the distributions were compared with the range of validity for the empirical equations.

All calculations were performed in MATLAB. The codes can be found in Appendix C.

Chapter 5

Results

This chapter presents the results that were found through the method in Chapter 3, which was further explained in Chapter 4. First, the results based on long-term wind statistics will be presented; secondly, the results based on long-term wave statistics; and finally, extreme values for given return periods.

5.1 Wave Runup and Wave Rundown Based on Wind Statistics

5.1.1 Stochastic Approach

The expected value of the mean wind speed $E[U_{10}]$ for the long-term wind distributions, and the significant wave height, calculated by inserting $E[U_{10}]$ into (3.5), are shown in Table 5.1. This table shows that the significant wave height calculated from the four different wind distributions are not the same, and varies with $E[U_{10}]$.

Table 5.1: Expected value of mean wind speed and corresponding significant wave height calculated from the expected mean wind speed

Distribution	$E[U_{10}]$ [m/s]	H_S [m]
JMH01	7.52	1.04
MR15 (1)	6.30	0.73
MR15 (2)	9.75	1.74
BG15	7.25	0.97

Figure 5.1 shows the expected value of the wave runup and wave rundown normalised by the significant wave height in Table 5.1 as a function of bottom slope for different runup models. This figure shows that the normalised wave runup increases with increasing bottom slope; and that wave rundown decreases, meaning the rundown becomes more negative with increasing bottom slope. In other words, the ratio between wave runup or wave rundown, and significant wave height increases for steeper slopes. For gentle slopes, the difference between wave runup and wave rundown is small, indicating little swash motion compared to steep slopes. At steep slopes, it is observed that the results from runup model Pe differs significantly from results from the other runup models. Figure 5.1 does not show the results from the Pe model at very steep slopes because this model is based on experiments with a maximum slope of 0.05, hence its reliability at steeper slopes is limited.

Varying runup models predict the largest wave runup depending on the bottom slope. For the MR15 (1) and BG15 distributions, it is the Po1 and Po2 models that estimate significantly lower wave runup than the other models. Recall that wave runup and wave rundown are defined relative to SWL. At gentle slopes the Bld model predicts wave rundown above SWL, and at steep slopes it predicts more negative wave rundown than the Sc model, which predicts less diversified estimates.

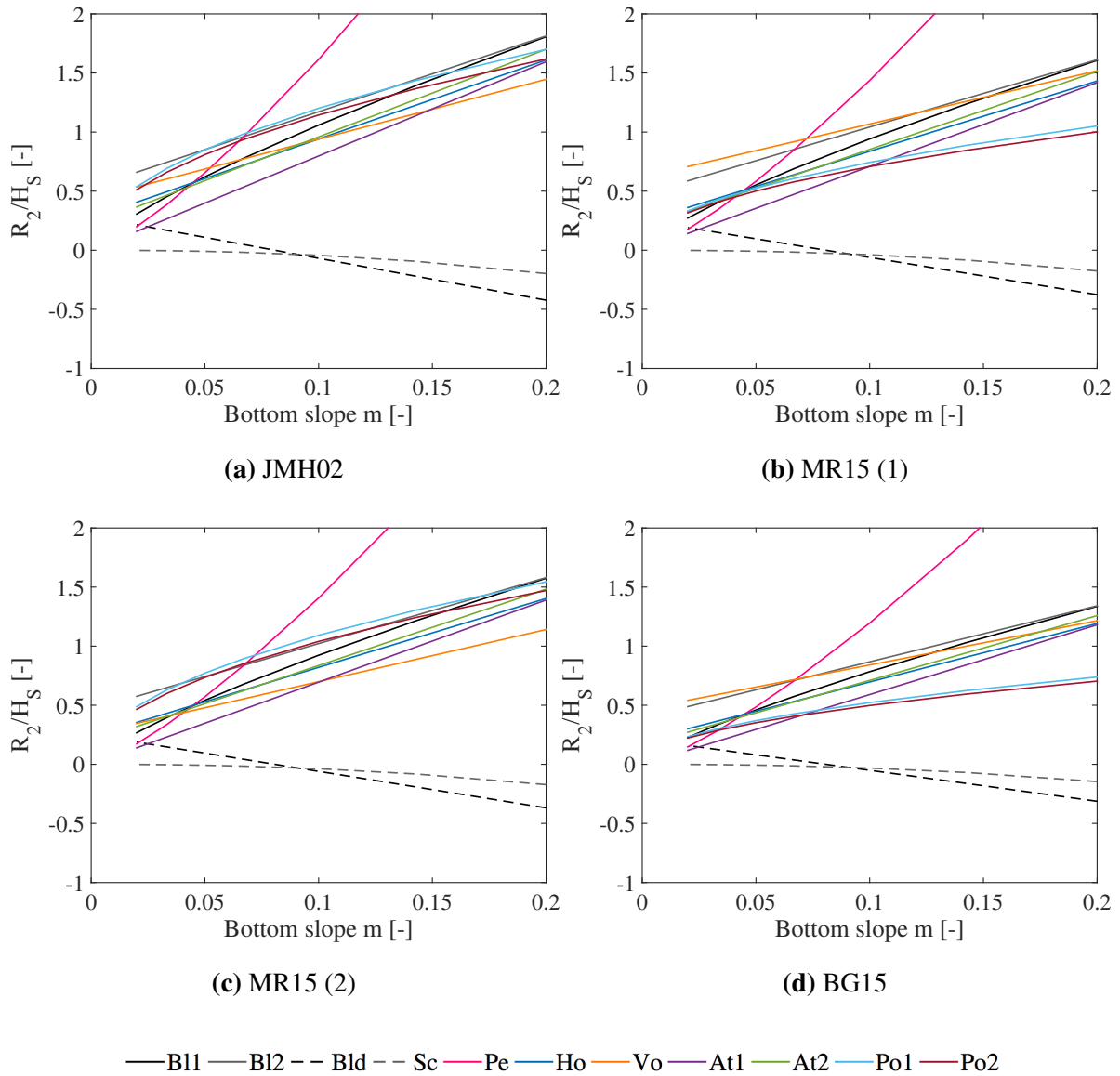
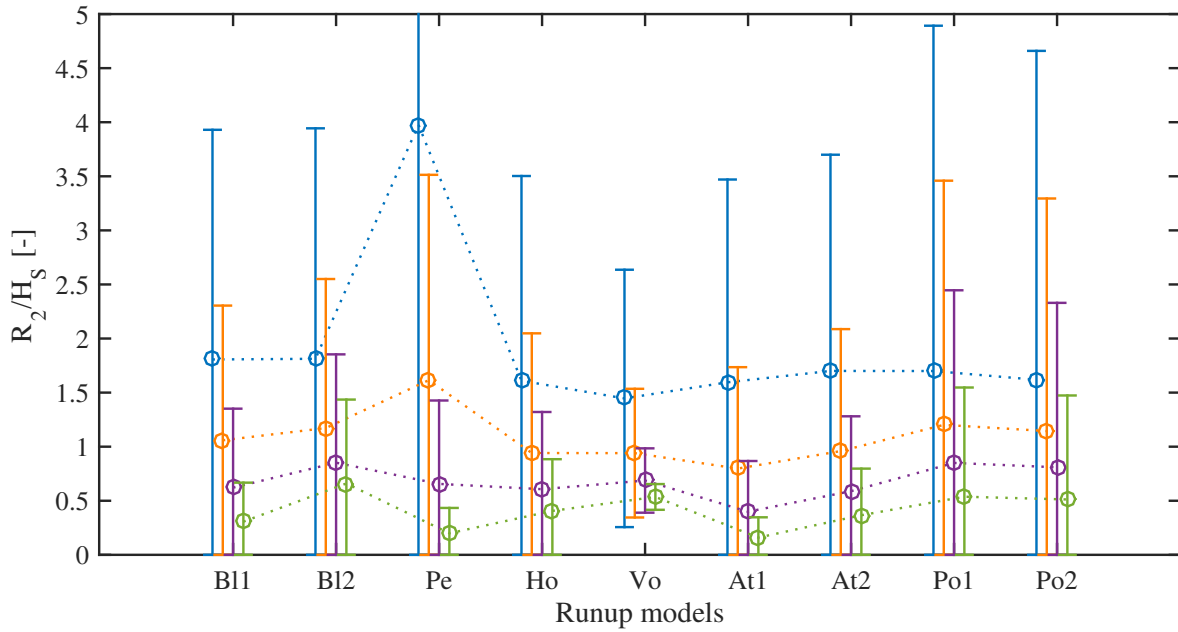


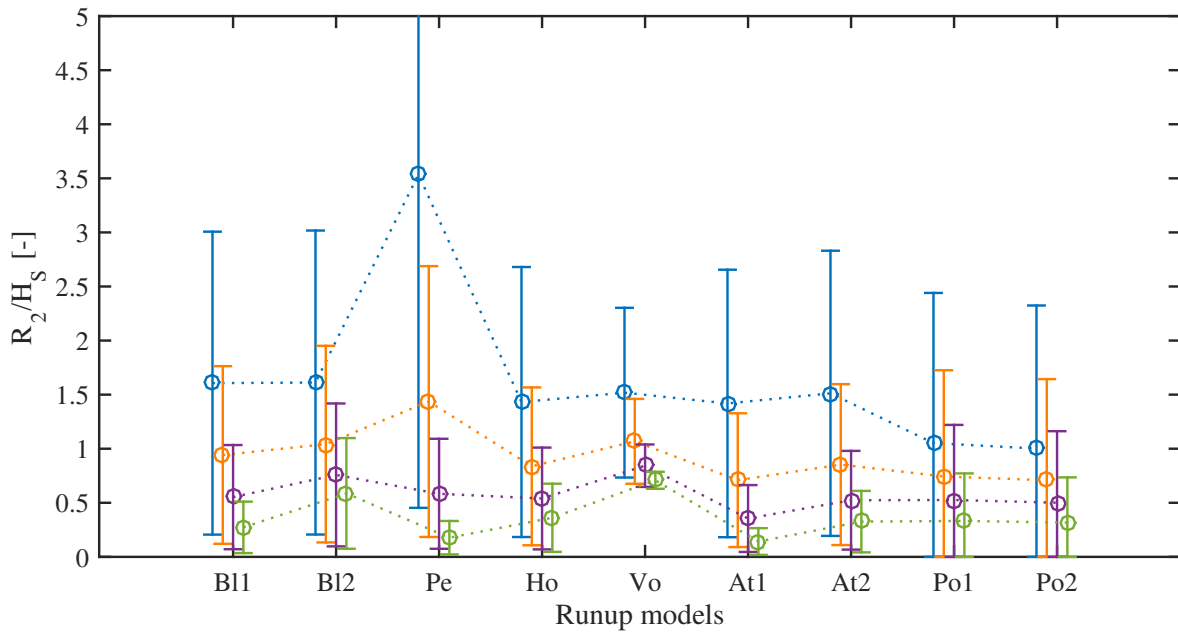
Figure 5.1: Expected value of wave runup and wave rundown normalised by the significant wave height as a function of bottom slope. Solid lines are used for wave runup, and dashed lines for wave rundown

Figure 5.2 shows the expected value (circles) and the standard deviation (bars) of the wave runup calculated by the different runup models for the four wind distributions and for four different bottom slopes. The bottom slopes are identified by different colours. Also here, the wave runup is normalised by the significant wave height in Table 5.1.

It is observed from Figure 5.2 that the difference between the runup models has the same trend for all four distributions. This figure also shows that results from runup model Pe differs significantly from the other runup models at steep bottom slopes. In addition it is observed that the



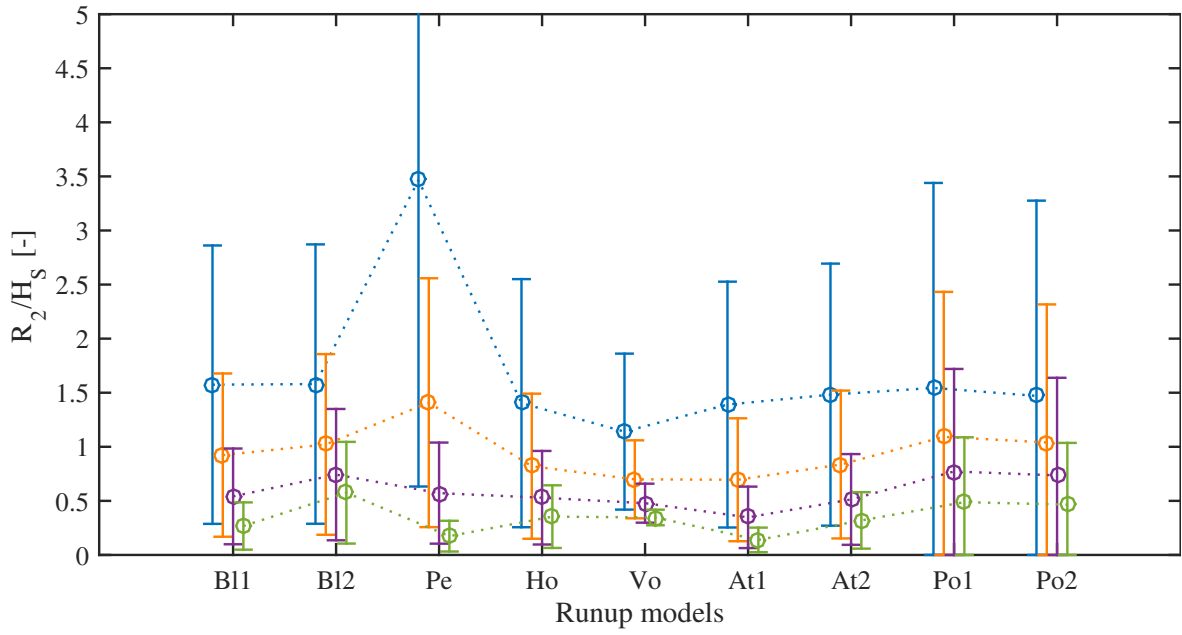
(a) JMH02



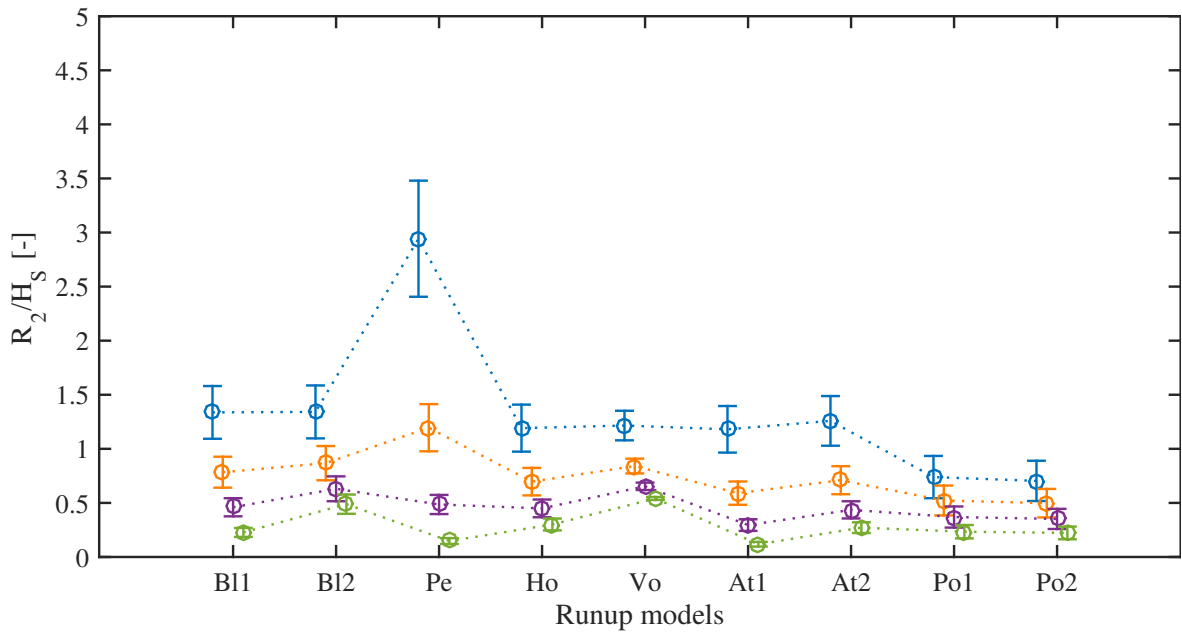
(b) MR15 (1)

⋯○⋯ 1/5
 ⋯○⋯ 1/10
 ⋯○⋯ 1/20
 ⋯○⋯ 1/50

Figure 5.2: Expected value (circle) with standard deviation (bars) for wave runup normalised by significant wave height at four different bottom slopes



(c) MR15 (2)



(d) BG15

⋯○⋯ 1/5
 ⋯○⋯ 1/10
 ⋯○⋯ 1/20
 ⋯○⋯ 1/50

Figure 5.2: (Continued)

MR15 (1) and the BG15 distributions predict smaller wave runup with the Po1 and Po2 models at steep bottom slopes compared to the other two distributions. At more gentle bottom slopes the B12 and Vo models predict slightly larger wave runup than the other models, and for the JMH02 and the MR15 (2) distributions, also the Po1 and Po2 models predict slightly larger values. The standard deviation in Figure 5.2 increases with increasing bottom slope. Furthermore, the expected values of the normalised wave runup are quite similar for the four distributions, while the standard deviation differs more. The BG15 distribution stands out from the other distributions by its significantly lower standard deviation and slightly lower expected value. Recall that BG15 is a conditional distribution, while the other three are marginal distributions.

Figure 5.3 shows the expected value (circles) and the standard deviation (bars) of the wave rundown calculated by the different runup models for the four wind distributions and at four different bottom slopes. The estimates are also here normalised by the significant wave height in Table 5.1.

Figure 5.3 shows that the trend between the distributions are in general the same. Slightly different expected value is observed between the distributions, and the Sc model gives less variation in the expected value compared to B1d. The BG15 distribution does also here stand out from the others by its significantly lower standard deviation. It is observed that the wave rundown decreases, with increasing bottom slope for both runup models, meaning that it gets further below SWL. Some of the estimates are larger than zero for the B1d model, indicating wave rundown above SWL.

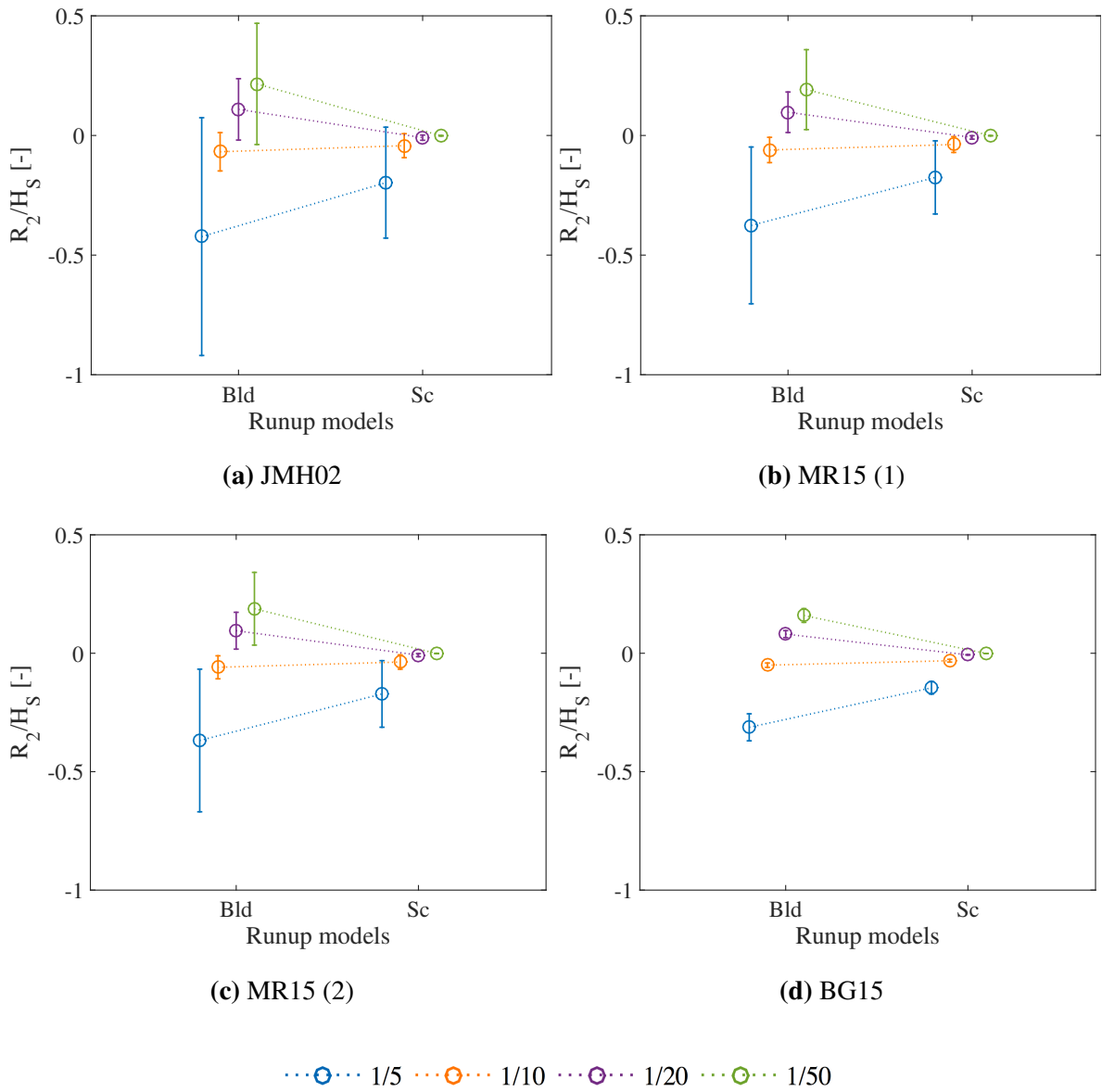


Figure 5.3: Expected value (circle) with standard deviation (bars) for wave rundown normalised by significant wave height

5.1.2 Deterministic Approach

Table 5.2 shows the ratio between the expected value from the deterministic and the stochastic approach presented in Section 3.2.2. This ratio is equal for all the runup models with $d=0$ in Table 3.1, and the Po1 and Po2 runup models do also generate results similar to each other. All the ratios are less than one, meaning that the stochastic approach generates higher absolute wave runup and wave rundown values. The difference in the results between the deterministic and the stochastic approach is at its smallest for the BG15 distribution. The MR15 (1) and MR15 (2) distributions do also give large ratios, and the ratio is at its smallest for the JMH02 distribution.

Table 5.2: Ratio between expected value of wave runup and wave rundown calculated by the deterministic and the stochastic approach

Runup model	Ratio			
	JMH02	MR15 (1)	MR15 (2)	BG15
B11	0.733	0.825	0.841	0.991
B12	0.733	0.825	0.841	0.991
B1d	0.733	0.825	0.841	0.991
Sc	0.733	0.825	0.841	0.991
Pe	0.733	0.825	0.841	0.991
Ho	0.733	0.825	0.841	0.991
Vo	0.857	0.926	0.900	0.996
At1	0.733	0.825	0.841	0.991
At2	0.733	0.825	0.841	0.991
Po1	0.439	0.594	0.626	0.974
Po2	0.439	0.594	0.626	0.974

5.2 Wave Runup and Wave Rundown Based on Wave Statistics

5.2.1 Stochastic Approach

The expected value of the significant wave height calculated from the marginal distributions of H_S for the long-term wave statistics are presented in Table 5.3.

Table 5.3: Expected value of the significant wave height for the wave distributions

Distribution	$E[H_S]$ [m]
MGAU05	2.1
OHG16	2.4
BGGS07 (1)	3.7
BGGS07 (2)	3.6
BGGS07 (3)	3.6
BGGS07 (4)	3.4
BGGS07 (5)	3.6
MBG90 (1)	2.3
MBG90 (2)	2.3
MBG90 (3)	2.1

Figure 5.4 shows the expected value of the wave runup and wave rundown normalised by the expected value of the significant wave height in Table 5.3 as a function of bottom slope for the different runup models. A quite similar trend with increasing wave runup and wave rundown for increasing bottom slope is observed as from the results generated from wind distributions in Figure 5.1. However, it is not the same runup models that generate the largest estimates. Still, the Pe model predicts significantly larger estimates at steep bottom slopes, but the Po1 and Po2 models generate some of the highest estimates as opposed to what was observed from the wind distributions. With exception of the Pe model it is in general the Po1 model that predicts the largest wave runup, and the Vo model that predicts the smallest. The wave rundown estimates are not significantly different from the estimates based on the wind distributions.

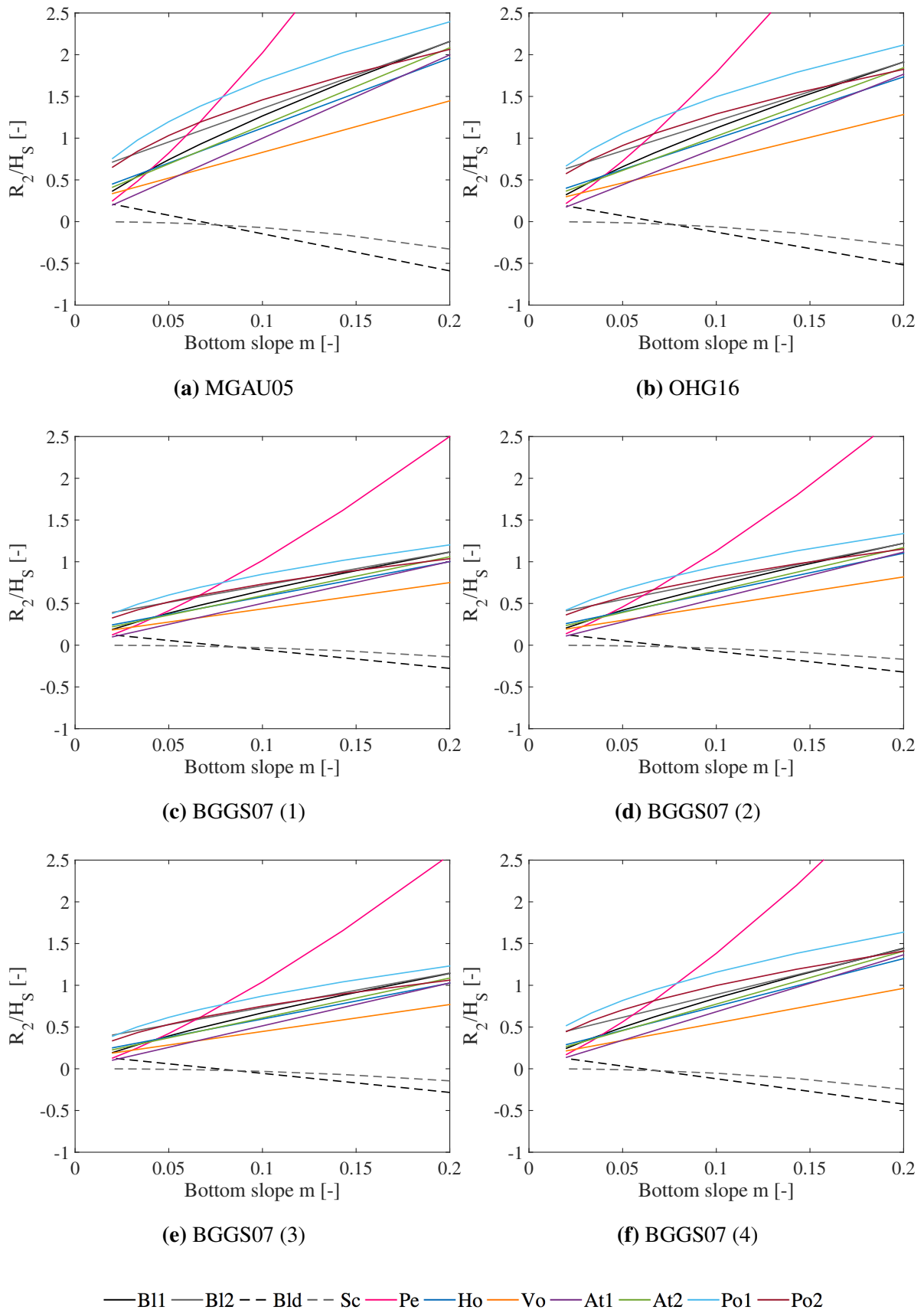


Figure 5.4: Expected value of wave runup and wave rundown normalised by the expected value of significant wave height over varying bottom slope for different runup models

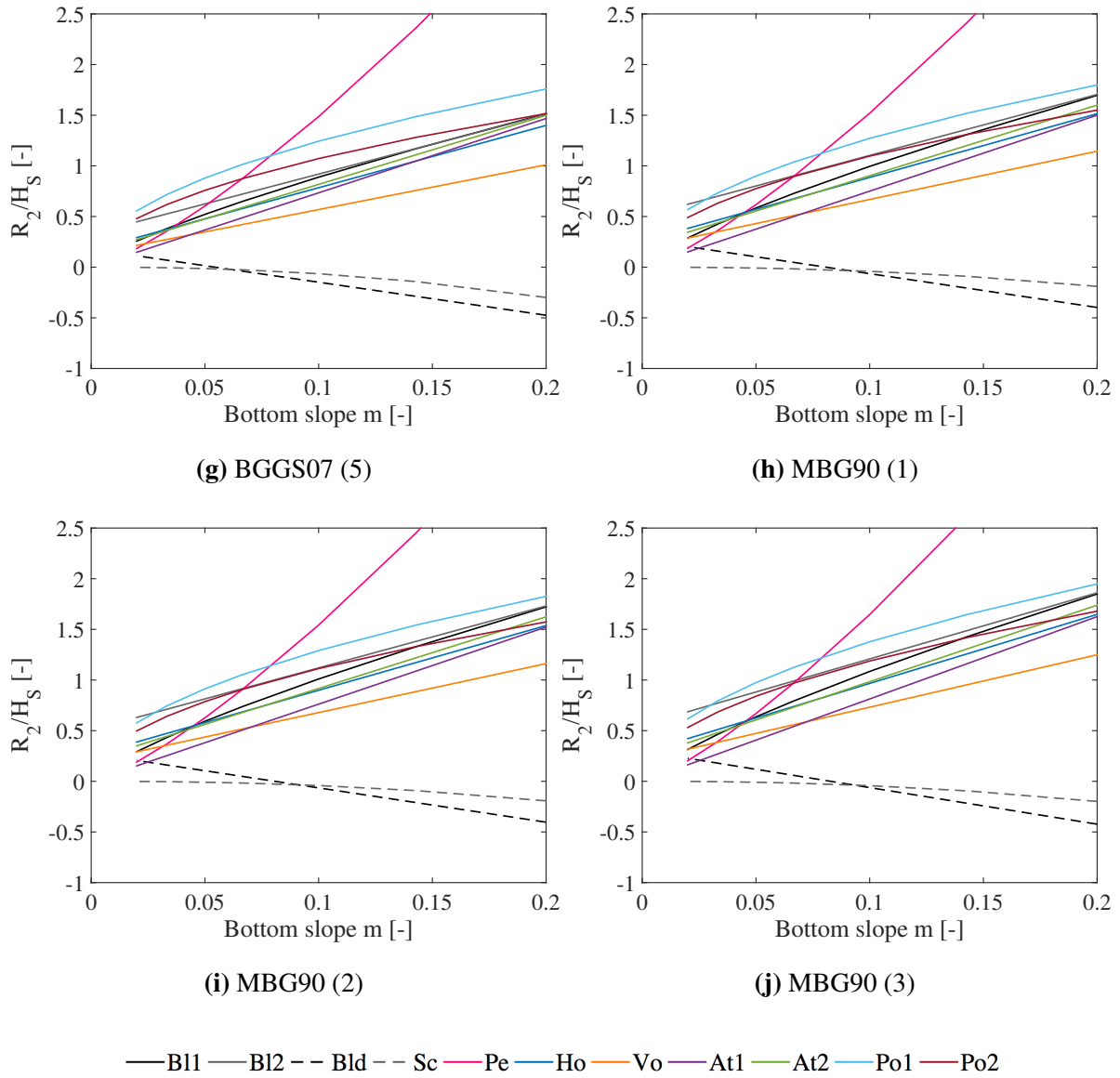


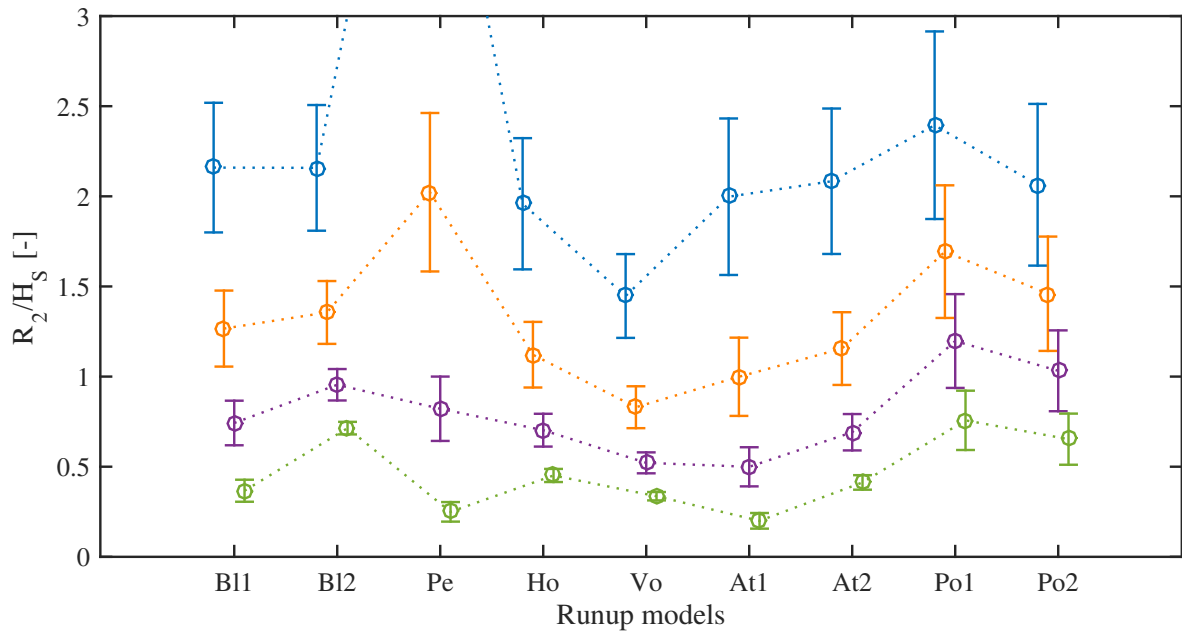
Figure 5.4: (Continued)

Figure 5.5 shows the expected values (circles) and standard deviation (bars) for the wave runup calculated from the long-term wave distributions for each runup model at four different bottom slopes. The values are normalised by the expected value of the significant wave height in Table 5.3. Like for the wind distributions, the runup models show the same trend for all the wave distributions. However, the expected value is significantly larger in value for the MGAU05 distribution, followed by the OHG16 and the three MBG90 distributions. Also here, the Pe model predicts significantly larger wave runup than the other models, and this model is not included when the estimates are very different because it is strictly not valid.

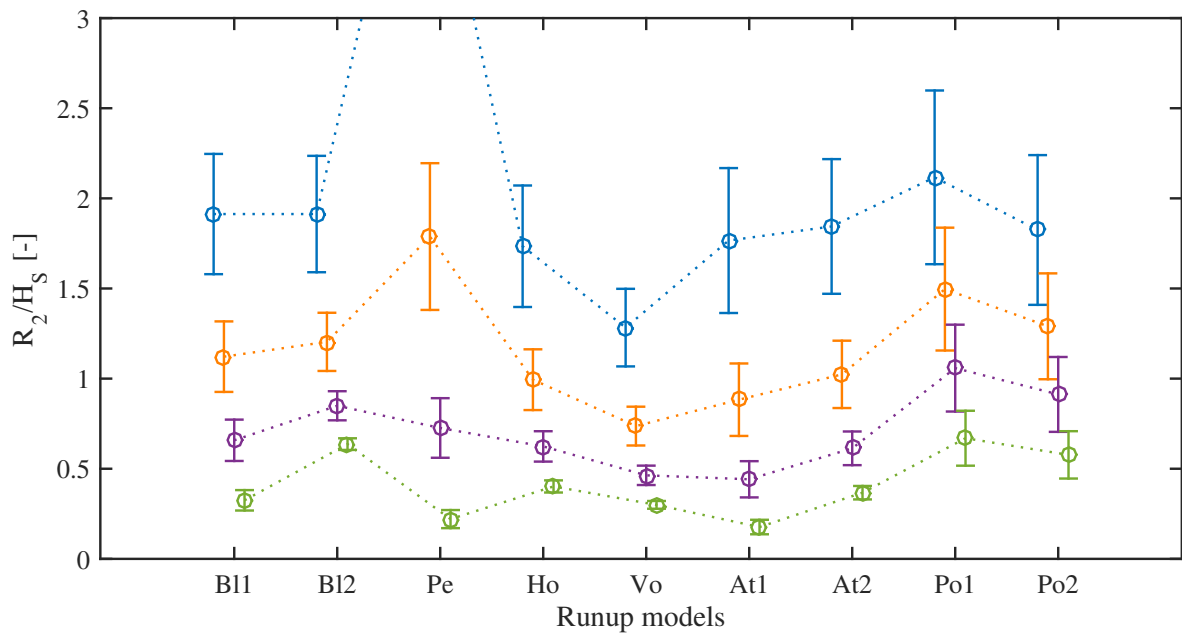
At gentle bottom slopes it is the B12, Po1 and Po2 models that predict the largest wave runup,

while Pe and At1 predicts the smallest values. At steeper bottom slopes, however, it is the Vo model that stands out with smaller estimates than the others, and the Pe model with very large estimates. The standard deviation does also here increase with increasing bottom slope along with the increasing expected values. The MGAU05 and the OHG16 distributions generated larger standard deviation than the other wave distributions, but at the same time they do also predict larger expected values.

Figure 5.6 shows the expected value (circles) and standard deviation (bars) for the wave rundown calculated from the long-term wave distributions for each runup model at four different bottom slopes. The estimates are also here normalised by the expected value of the significant wave height in Table 5.3. The expected values in Figure 5.6 do not change much with different distributions, but it is observed that the MGAU05 and the OHG16 distributions predict a more negative wave rundown with the Bld model at steep bottom slopes. The Sc model does also here, like with the wind distributions, generate estimates with little spread with varying bottom slope. The standard deviation is largest for the MGAU05 and the OHG16 distributions that showed the largest expected values, and a larger spread in the expected values is also observed for these two distributions. The Bld model predicts positive wave rundown for the most gentle slopes, indicating wave rundown above SWL, and the wave rundown becomes more negative with increasing bottom slope.



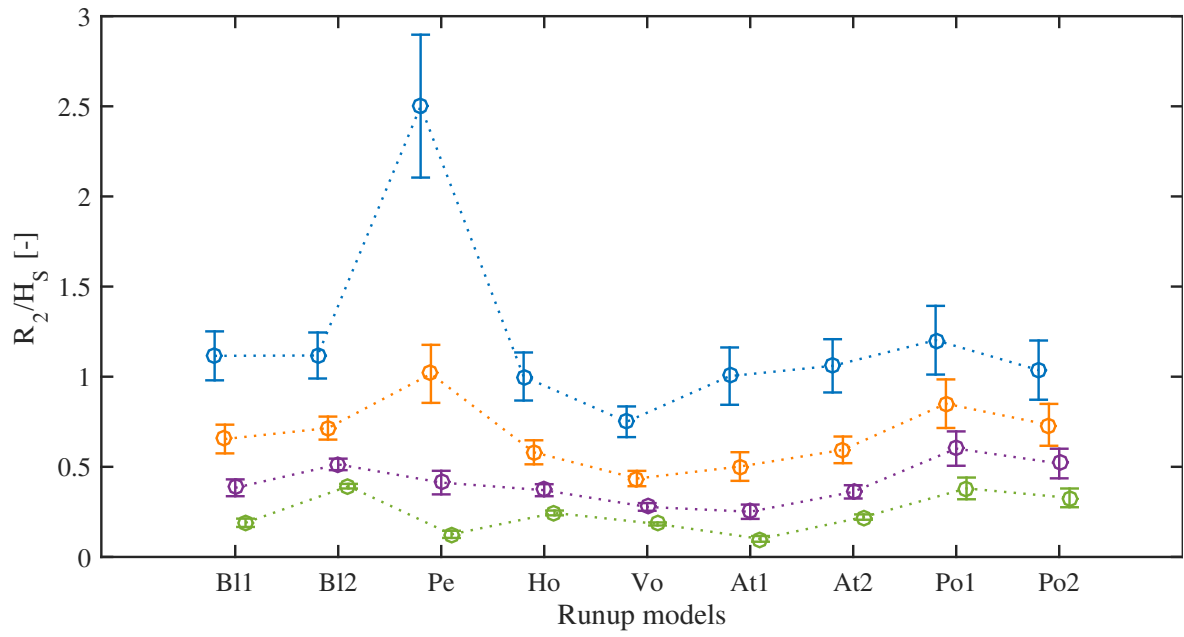
(a) MGAU05



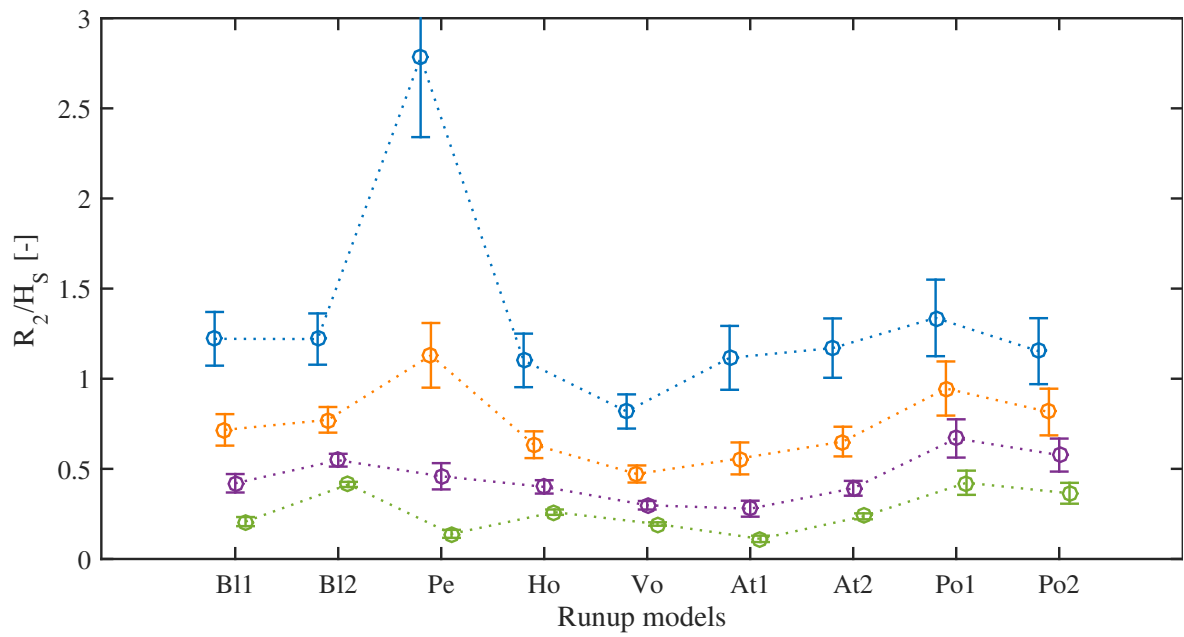
(b) OHG16

● 1/5 ● 1/10 ● 1/20 ● 1/50

Figure 5.5: Expected value (circle) with standard deviation (bars) for wave runup normalised by significant wave height at four different bottom slopes



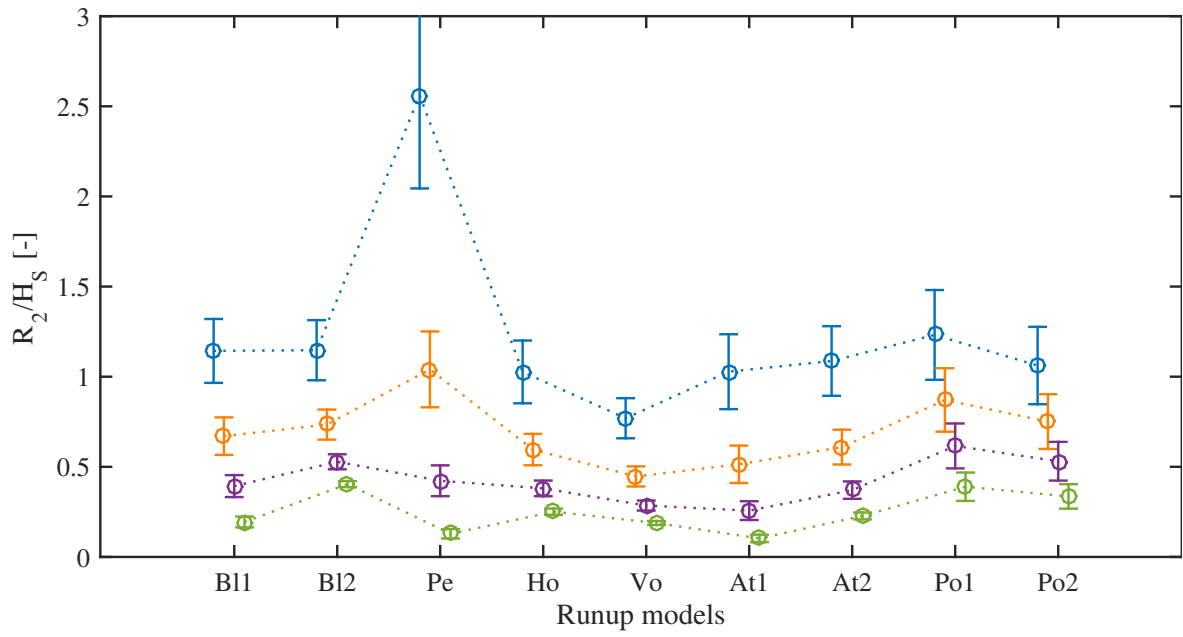
(c) BGG07 (1)



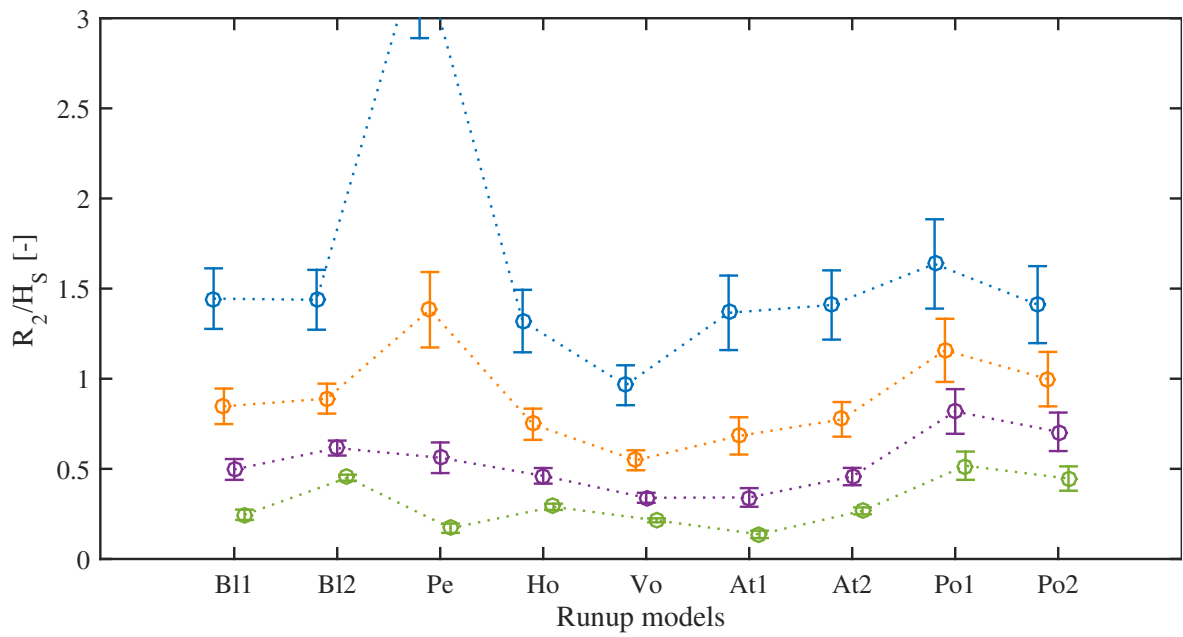
(d) BGG07 (2)

● ··· 1/5
 ● ··· 1/10
 ● ··· 1/20
 ● ··· 1/50

Figure 5.5: (Continued)



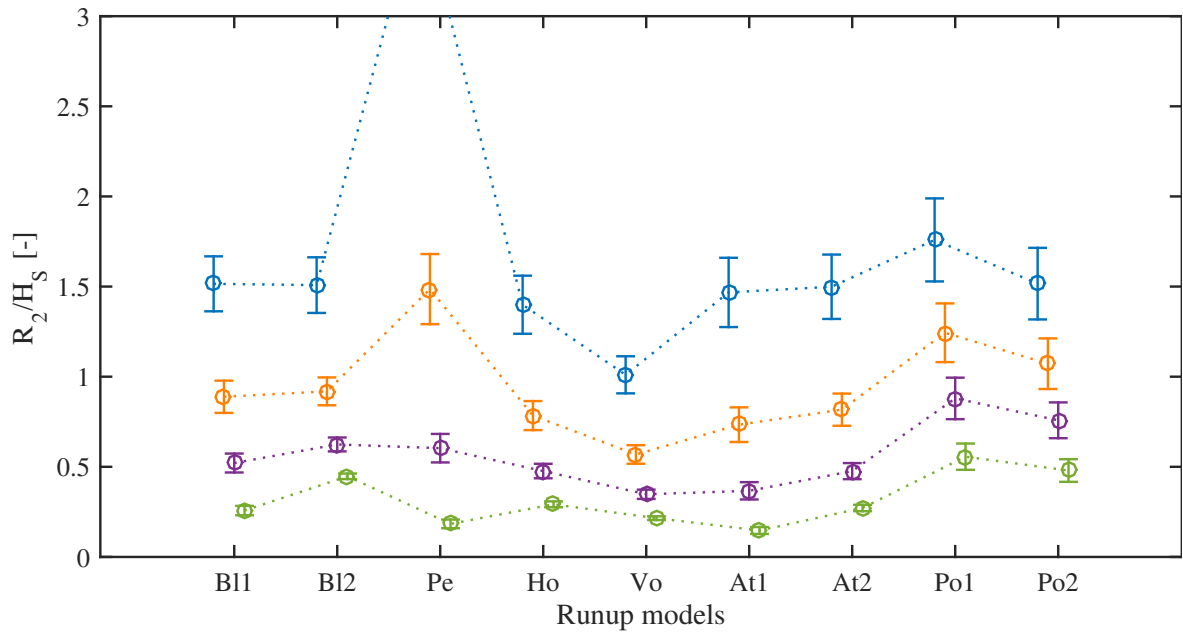
(e) BGG07 (3)



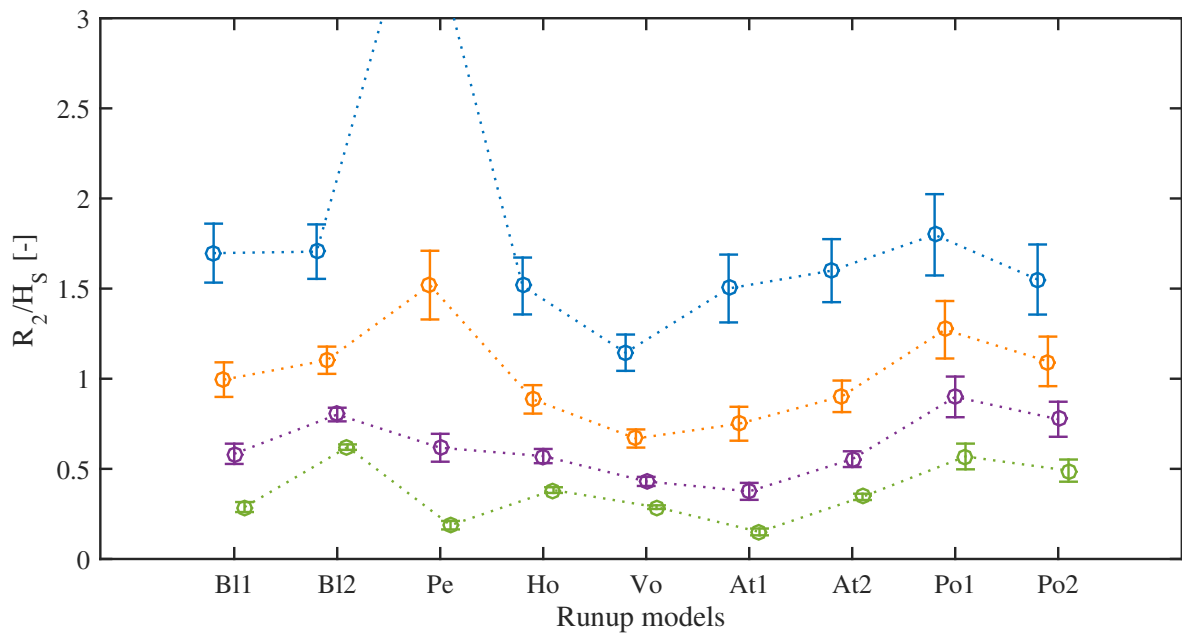
(f) BGG07 (4)

● ··· 1/5
 ● ··· 1/10
 ● ··· 1/20
 ● ··· 1/50

Figure 5.5: (Continued)



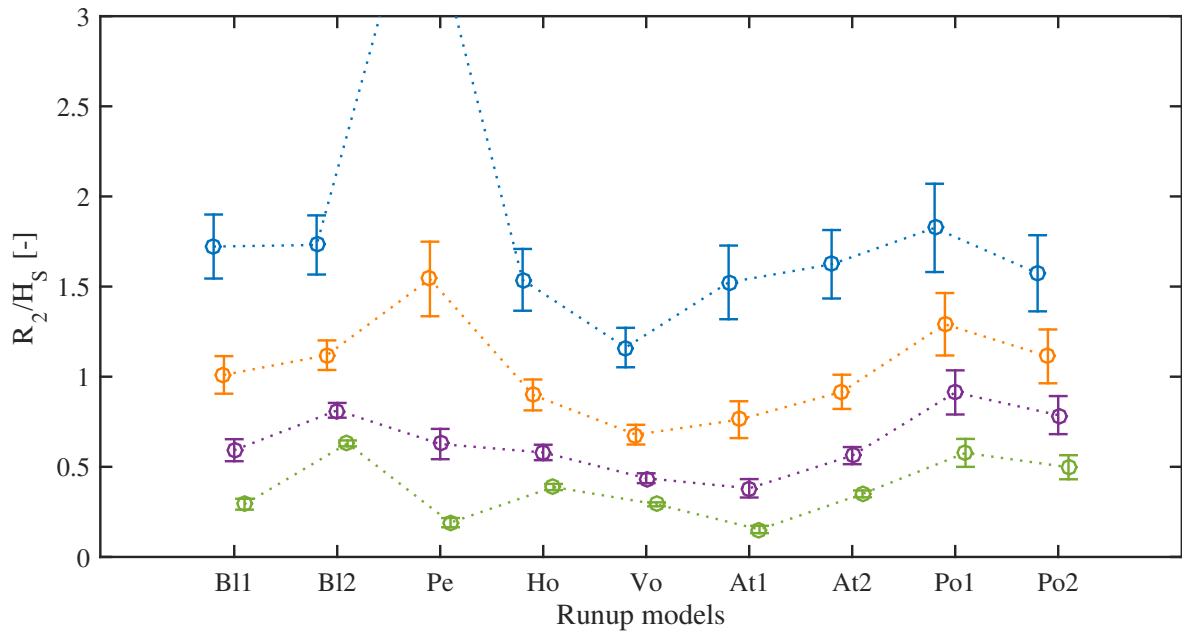
(g) BGG7 (5)



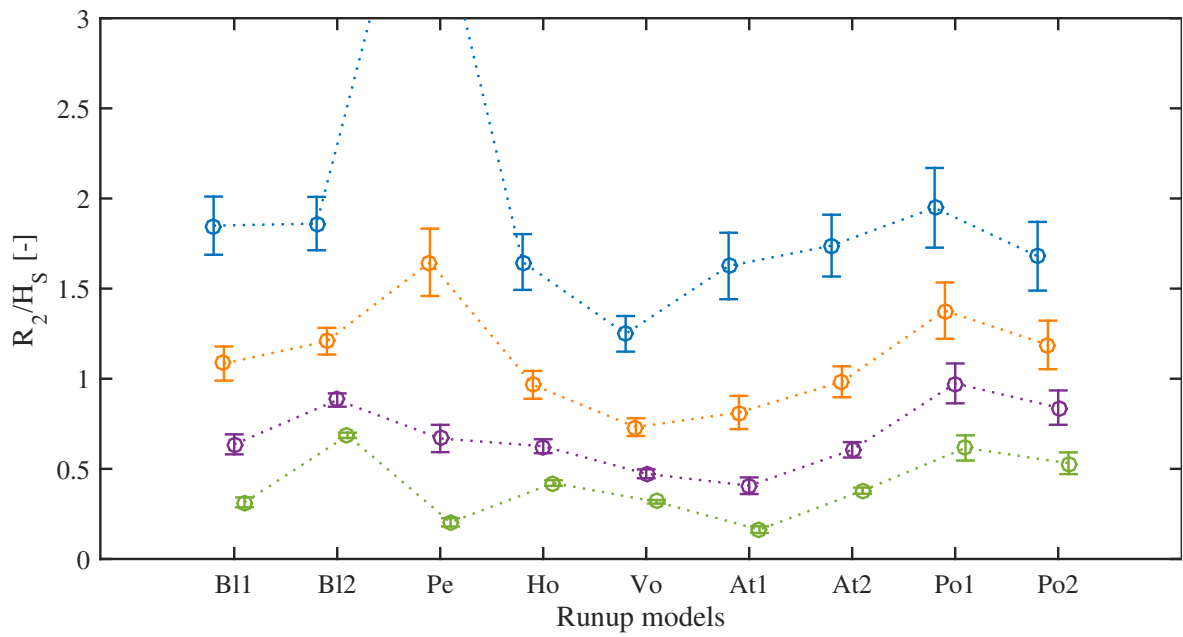
(h) MBG90 (1)

⋯○⋯ 1/5
 ⋯○⋯ 1/10
 ⋯○⋯ 1/20
 ⋯○⋯ 1/50

Figure 5.5: (Continued)



(i) MBG90 (2)



(j) MBG90 (3)

● 1/5
 ● 1/10
 ● 1/20
 ● 1/50

Figure 5.5: (Continued)

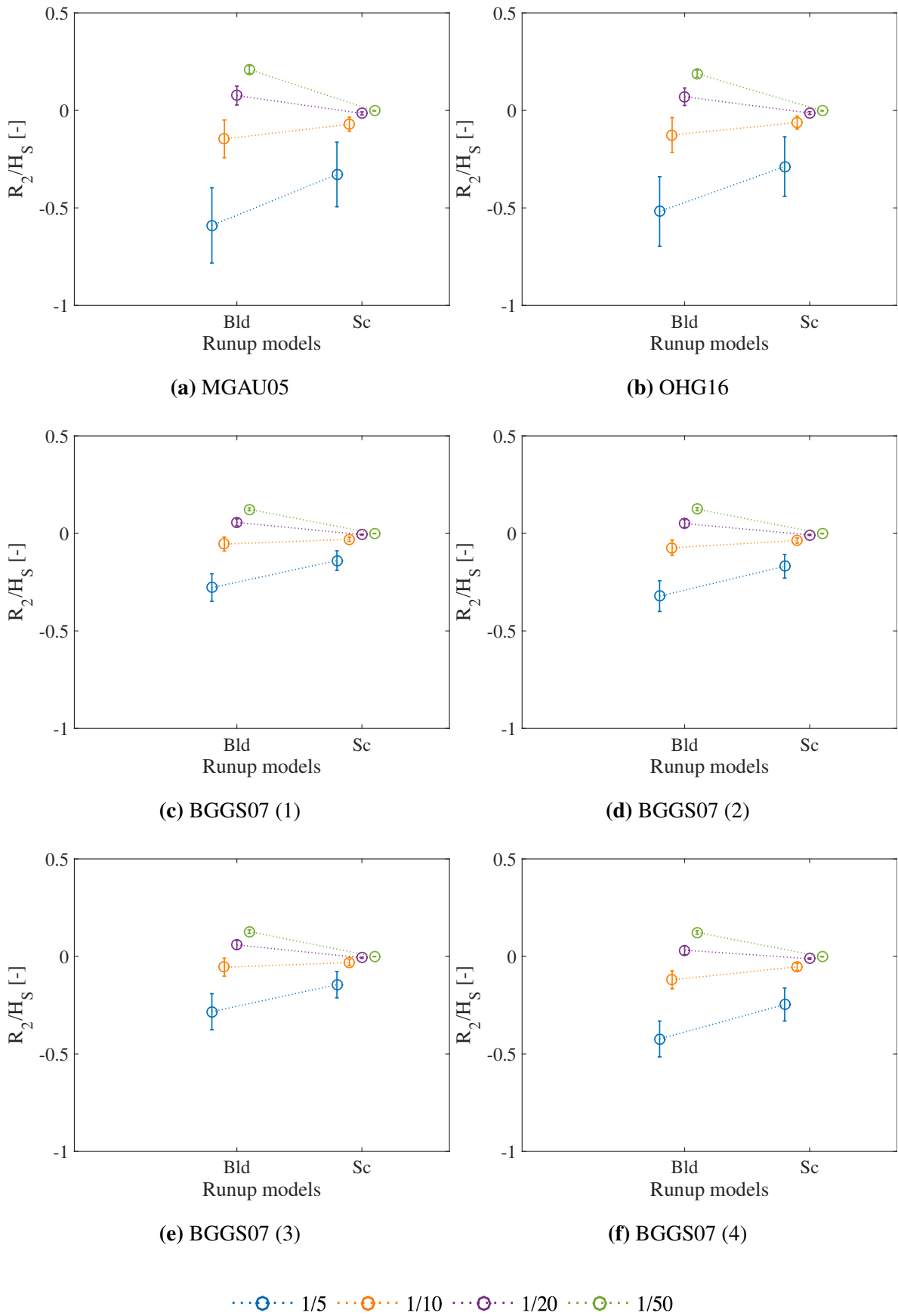
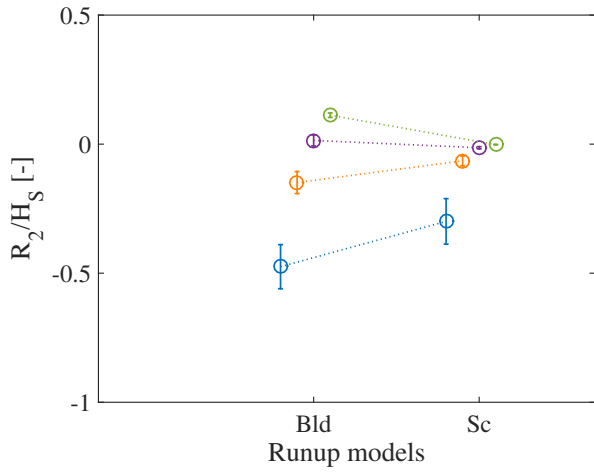
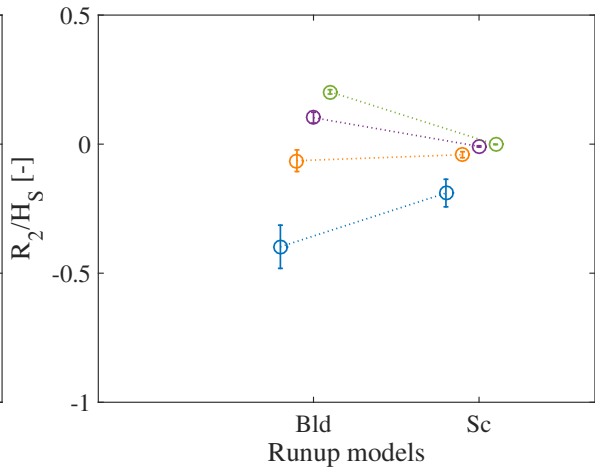


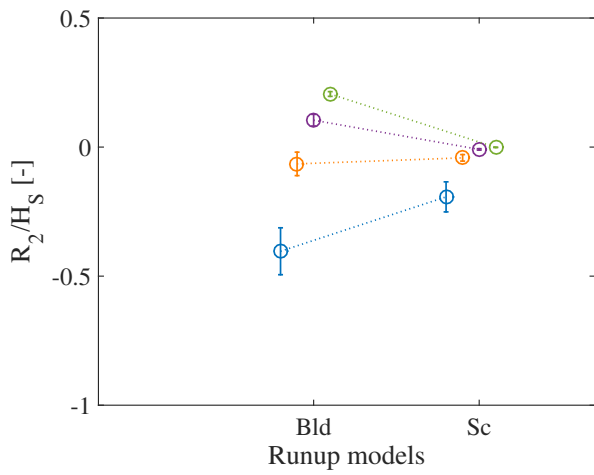
Figure 5.6: Expected value (circle) with standard deviation (bars) for wave rundown for four different bottom slopes



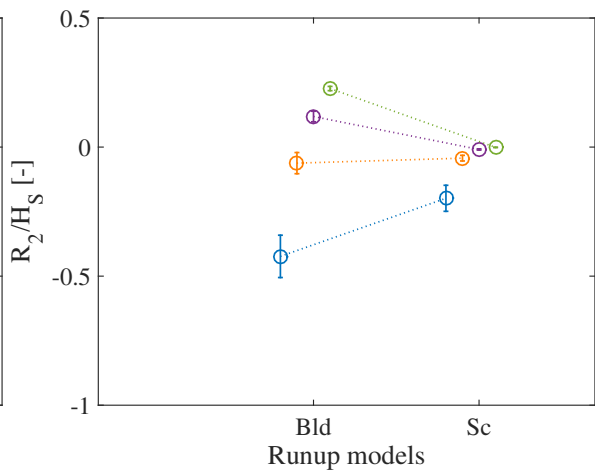
(g) BGG07 (5)



(h) MBG90 (1)



(i) MBG90 (2)



(j) MBG90 (3)

···○··· 1/5 ···○··· 1/10 ···○··· 1/20 ···○··· 1/50

Figure 5.6: (Continued)

5.2.2 Comparison of Results

Table 5.4 shows the wave runup and wave rundown values from the long-term wave distributions for 3m significant wave height and bottom slope 1/10. This table shows that it is generally little difference between the distributions for a given runup model. Yet, it is observed that all BGGs07 distributions gave results more similar to each other than the rest of the distributions. Similarly; the MBG90 distributions generated results close in value, and also the MGAU05 and the OHG16 distribution generated results quite similar to each other.

Table 5.4: Wave runup and wave rundown R_2 in metres for $H_S = 3\text{m}$

Runup model	Distributions				
	MGAU05	OHG16	BGGs07 (1)	BGGs07 (2)	BGGs07 (3)
B11	2.68	2.65	2.45	2.59	2.44
B12	2.87	2.85	2.68	2.79	2.67
B1d	-0.31	-0.30	-0.21	-0.27	-0.20
Sc	-0.15	-0.15	-0.11	-0.13	-0.11
Pe	4.28	4.23	3.81	4.08	3.79
Ho	2.37	2.35	2.18	2.29	2.17
Vo	1.75	1.74	1.63	1.70	1.62
At1	2.11	2.09	1.88	2.01	1.87
At2	2.44	2.42	2.23	2.35	2.22
Po1	3.58	3.54	3.19	3.42	3.17
Po2	3.08	3.05	2.75	2.94	2.73

Table 5.4: *(Continued)*

Runup	Distributions				
	BGGS07 (4)	BGGS07 (5)	MBG90 (1)	MBG90 (2)	MBG90 (3)
Bl1	2.90	3.15	2.33	2.33	2.28
Bl2	3.05	3.26	2.58	2.58	2.54
Bld	-0.41	-0.53	-0.15	-0.15	-0.13
Sc	-0.18	-0.23	-0.10	-0.10	-0.09
Pe	4.74	5.28	3.55	3.55	3.47
Ho	2.56	2.78	2.07	2.07	2.04
Vo	1.88	2.02	1.56	1.56	1.54
At1	2.34	2.61	1.76	1.76	1.71
At2	2.66	2.90	2.11	2.11	2.07
Po1	3.97	4.42	2.98	2.97	2.90
Po2	3.42	3.81	2.56	2.56	2.50

5.3 Extreme Value Estimates

5.3.1 Based on Long-Term Wind Distributions

For consistency and simplicity it would be preferable to assume that a 10 min average can be used for all the long-term wind distributions for calculation of extreme values. However, since the JMH02 distribution is based on 1 hour mean wind speed, in contrast to 10 min for the others, it is strictly 1 hour that should be used for the extreme value calculations for this distribution.

Choosing a 1 hour mean instead of a 10 min mean results in a different number of individual U_{10} averages during T_{return} years in Eq. (2.45), and consequently also another value of $U_{10,max}$. A mean of 1 hour leads to $N = 8760T_{return}$, while a mean of 10 min leads to $N = 52560T_{return}$. Recall from Eq. (2.46) that $U_{10,max} = \beta (\ln N)^{1/\alpha}$. Thus, the $U_{10,max}$ values will not be the same, even though the parameters for the distribution are equal. Values for $U_{10,max}$ calculated from both 1 hour and 10 min means are shown in Table 5.5.

Table 5.5: Mean wind speed for the JMH02 distribution for 1 hour and 10 minute averages

Return period (years)	$U_{10,max}$ (m/s)	
	1 hour	10 min
1	30.7	34.1
10	35.0	38.1
100	39.0	41.9
1000	42.7	45.4
10000	46.2	48.8

As described in Section 3.2.3, $R_{2,max}$ can be written as a function of $U_{10,max}^2$ or $U_{10,max}^3$, depending on the runup model. A difference in N will thus cause a difference in $R_{2,max}$ in line with Eq. (3.17) and (3.18). Calculating $U_{10,max}$ from 10 min mean resulted in a maximum of 11% higher $U_{10,max}$ values compared with calculations with 1 hour means. This would lead to an even larger difference in the $R_{2,max}$ values because $R_{2,max}$ and $U_{10,max}$ are connected with an exponent larger than one.

Due to the significant influence of the average length on the results, it was decided to use 1

hour means for the JMH02 distribution in the calculations. The other three wind distributions were based on 10 min averages.

Table 5.6 shows the extreme mean wind speed $U_{10,max}$ along with the corresponding sea state parameters $H_{S,max}$ and $T_{P,max}$ for five different return periods.

Table 5.6: Extreme mean wind speed and corresponding sea state parameters from the long-term wind distributions for five different return periods

(a) JMH02				(b) MR16 (1)			
Return period (years)	$U_{10,max}$ (m/s)	$H_{S,max}$ (m)	$T_{P,max}$ (s)	Return period (years)	$U_{10,max}$ (m/s)	$H_{S,max}$ (m)	$T_{P,max}$ (s)
1	30.7	17.2	19.6	1	20.1	7.4	12.9
10	35.0	22.5	22.4	10	21.8	8.7	14.0
100	39.0	27.9	25.0	100	23.4	10.0	15.0
1000	42.7	33.4	27.3	1000	24.8	11.3	15.9
10000	46.2	39.2	29.6	10000	26.2	12.6	16.8

(c) MR15 (2)				(d) BG15			
Return period (years)	$U_{10,max}$ (m/s)	$H_{S,max}$ (m)	$T_{P,max}$ (s)	Return period (years)	$U_{10,max}$ (m/s)	$H_{S,max}$ (m)	$T_{P,max}$ (s)
1	29.0	15.4	18.6	1	9.1	1.5	5.8
10	31.3	18.0	20.1	10	9.2	1.6	5.9
100	33.5	20.5	21.4	100	9.3	1.6	6.0
1000	35.4	23.0	22.7	1000	9.5	1.6	6.1
10000	37.2	25.4	23.8	10000	9.5	1.7	6.1

For each long-term wind distribution, the extreme wave runup $R_{2,max}$ was calculated based on $U_{10,max}$. Table 5.7 show the estimates of $R_{2,max}$ normalised with the corresponding $H_{S,max}$ value in Table 5.6. Estimates were calculated for five different return periods with each of the runup models for bottom slope 1/10. The wave runup and wave rundown values are presented in

increasing order, so that the wave rundown values are the two uppermost rows in the tables. Values are given relative to SWL so that negative values indicate wave runup or wave rundown below SWL. Results with dimensions can be found in Appendix B.3.

From Table 5.7 it is observed that the order of runup models is the same for the JMH02, MR15 (1) and MR15 (2) distributions. Estimates above one are observed for the runup models Pe, Po2 and Po1 for the JMH02, MR15 (1) and MR15 (2) distributions, indicating larger predicted wave runup than the offshore significant wave height. For the BG15 distribution, only the Pe model predicts normalised wave runup larger than one. The other runup models predict normalised wave runup in the range 0.39-0.86, which correspond to smaller wave runup than the offshore significant wave height. Regarding the wave rundown estimates, the Bld and Sc models give negative estimates indicating wave rundown below SWL. Only estimates from the runup models Vo, Po1 and Po2 change size with the wind distributions due to cancellation in the general equation for R_2 in Eq. (3.1) for the other runup models when this equation is normalised with H_S found from the Phillips spectrum.

Table 5.7: Wave runup and wave rundown for five different return periods for the wind distribution normalised by significant wave height for bottom slope 1/10. Values are given relative to SWL, so that negative values indicate wave runup or wave rundown below SWL

(a) JMH02						(b) MR15 (1)					
Runup	Return period (years)					Runup	Return period (years)				
	1	10	100	1000	10 000		1	10	100	1000	10 000
model	1	10	100	1000	10 000	model	1	10	100	1000	10 000
Bld	-0.050	-0.050	-0.050	-0.050	-0.050	Bld	-0.050	-0.050	-0.050	-0.050	-0.050
Sc	-0.031	-0.031	-0.031	-0.031	-0.031	Sc	-0.031	-0.031	-0.031	-0.031	-0.031
Vo	0.40	0.39	0.39	0.38	0.38	Vo	0.43	0.42	0.42	0.41	0.41
At1	0.58	0.58	0.58	0.58	0.58	At1	0.58	0.58	0.58	0.58	0.58
Ho	0.69	0.69	0.69	0.69	0.69	Ho	0.69	0.69	0.69	0.69	0.69
At2	0.70	0.70	0.70	0.70	0.70	At2	0.70	0.70	0.70	0.70	0.70
B11	0.78	0.78	0.78	0.78	0.78	B11	0.78	0.78	0.78	0.78	0.78
B12	0.86	0.86	0.86	0.86	0.86	B12	0.86	0.86	0.86	0.86	0.86
Pe	1.18	1.18	1.18	1.18	1.18	Pe	1.18	1.18	1.18	1.18	1.18
Po2	2.05	2.34	2.61	2.85	3.09	Po2	1.34	1.46	1.56	1.66	1.75
Po1	2.15	2.46	2.74	3.00	3.24	Po1	1.41	1.53	1.64	1.74	1.84

Table 5.7: (Continued)

		(c) MR15 (2)					(d) BG15					
Runup	model	Return period (years)					Runup	Return period (years)				
		1	10	100	1000	10 000		1	10	100	1000	10 000
Bld	Bld	-0.050	-0.050	-0.050	-0.050	-0.050	Bld	-0.050	-0.050	-0.050	-0.050	-0.050
Sc	Sc	-0.031	-0.031	-0.031	-0.031	-0.031	Sc	-0.031	-0.031	-0.031	-0.031	-0.031
Vo	Vo	0.40	0.40	0.39	0.39	0.39	At1	0.58	0.58	0.58	0.58	0.58
At1	At1	0.58	0.58	0.58	0.58	0.58	Po2	0.61	0.62	0.62	0.63	0.64
Ho	Ho	0.69	0.69	0.69	0.69	0.69	Po1	0.64	0.65	0.66	0.66	0.67
At2	At2	0.70	0.70	0.70	0.70	0.70	Vo	0.67	0.66	0.65	0.65	0.64
B11	B11	0.78	0.78	0.78	0.78	0.78	Ho	0.69	0.69	0.69	0.69	0.69
B12	B12	0.86	0.86	0.86	0.86	0.86	At2	0.70	0.70	0.70	0.70	0.70
Pe	Pe	1.18	1.18	1.18	1.18	1.18	B11	0.78	0.78	0.78	0.78	0.78
Po2	Po2	1.94	2.09	2.24	2.37	2.49	B12	0.86	0.86	0.86	0.86	0.86
Po1	Po1	2.03	2.20	2.35	2.48	2.61	Pe	1.18	1.18	1.18	1.18	1.18

5.3.2 Based on Long-Term Wave Distributions

Table 5.8 shows the extreme wave runup and wave rundown corresponding to five different return periods for bottom slope 1/10. The values are normalised with the corresponding significant wave height at the tangent point between the contour lines and the runup models in Appendix B.5. The runup models are presented in increasing order with respect to the size of their estimates.

The order of the runup models is the same for all the wave distributions, with exception of the Bld and Sc models in MGAU05, OHG16 and BGG07 (2). It is also the same as for the extreme values from the marginal JMH02, MR15 (1) and MR15 (2) wind distributions. Estimates above one are observed for the runup models Pe, Po2 and Po1, indicating that these models predict larger wave runup than the offshore significant wave height. The other runup models predicts normalised wave runup in the range 0.37-0.93, which correspond to smaller wave runup than the offshore significant wave height.

Regarding the wave rundown models, both the Bld and Sc models give negative estimates indicating rundown below SWL. It depends on the distribution, which runup model that estimate the largest absolute wave rundown.

Table 5.8: Wave runup and wave rundown corresponding to five different return periods for the wave distributions for bottom slope 1/10. Values are normalised with significant wave height for each model. Wave runup and wave rundown values are relative to SWL, so that negative values indicate wave runup or wave rundown below SWL

(a) MGAU05 distribution						(b) OHG16 distribution					
Runup model	Return period (years)					Runup model	Return period (years)				
	1	10	100	1000	10 000		1	10	100	1000	10 000
Sc	-0.436	-0.642	-1.082	-1.520	-2.087	Sc	-0.370	-0.521	-0.846	-1.147	-1.844
Bld	-0.351	-0.450	-0.498	-0.542	-0.712	Bld	-0.359	-0.395	-0.496	-0.634	-0.688
Vo	0.43	0.41	0.40	0.39	0.39	Vo	0.42	0.41	0.39	0.39	0.38
At1	0.62	0.59	0.58	0.57	0.57	At1	0.62	0.59	0.58	0.58	0.57
Ho	0.69	0.68	0.67	0.67	0.66	Ho	0.71	0.69	0.68	0.68	0.67
At2	0.71	0.70	0.69	0.68	0.68	At2	0.72	0.71	0.69	0.69	0.69
B11	0.78	0.77	0.76	0.75	0.75	B11	0.79	0.78	0.76	0.76	0.76
B12	0.85	0.84	0.84	0.83	0.83	B12	0.86	0.86	0.84	0.84	0.84
Pe	1.25	1.20	1.17	1.16	1.16	Pe	1.25	1.19	1.18	1.17	1.14
Po2	1.57	1.68	1.78	1.87	1.94	Po2	1.66	1.78	1.91	2.03	2.14
Po1	1.82	1.95	2.06	2.17	2.25	Po1	1.92	2.06	2.21	2.35	2.48

Table 5.8: (Continued)

(c) BGG07 (1) distribution						(d) BGG07 (2) distribution					
Runup model	Return period (years)					Runup model	Return period (years)				
	1	10	100	1000	10 000		1	10	100	1000	10 000
Bld	-0.135	-0.137	-0.151	-0.148	-0.160	Sc	-0.361	-0.586	-0.842	-1.241	-1.755
Sc	-0.047	-0.050	-0.054	-0.058	-0.062	Bld	-0.111	-0.104	-0.104	-0.104	-0.105
Vo	0.37	0.37	0.37	0.38	0.38	Vo	0.41	0.41	0.41	0.42	0.42
At1	0.54	0.56	0.57	0.58	0.59	At1	0.61	0.62	0.63	0.64	0.65
Ho	0.62	0.64	0.64	0.65	0.65	Ho	0.70	0.71	0.72	0.73	0.74
At2	0.64	0.65	0.65	0.68	0.68	At2	0.72	0.72	0.73	0.75	0.76
B11	0.71	0.71	0.72	0.75	0.75	B11	0.79	0.80	0.81	0.82	0.83
B12	0.79	0.79	0.80	0.80	0.81	B12	0.86	0.87	0.88	0.89	0.90
Pe	1.09	1.13	1.15	1.17	1.18	Pe	1.23	1.25	1.27	1.30	1.32
Po2	1.64	1.79	1.98	2.13	2.26	Po2	1.83	2.01	2.19	2.36	2.52
Po1	1.90	2.08	2.30	2.47	2.63	Po1	2.12	2.33	2.54	2.74	2.93

Table 5.8: (Continued)

		(e) BGG07 (3) distribution					(f) BGG07 (4) distribution					
Runup	model	Return period (years)					Runup	Return period (years)				
		1	10	100	1000	10 000		1	10	100	1000	10 000
Bld	Bld	-0.151	-0.159	-0.177	-0.180	-0.196	Bld	-0.208	-0.226	-0.243	-0.234	-0.247
Sc	Sc	-0.061	-0.068	-0.075	-0.083	-0.091	Sc	-0.108	-0.122	-0.135	-0.149	-0.163
Vo	Vo	0.42	0.44	0.44	0.45	0.46	Vo	0.44	0.43	0.44	0.44	0.43
At1	At1	0.64	0.66	0.71	0.73	0.75	At1	0.65	0.68	0.68	0.69	0.73
Ho	Ho	0.72	0.74	0.75	0.77	0.78	Ho	0.69	0.70	0.70	0.72	0.72
At2	At2	0.74	0.76	0.77	0.81	0.83	At2	0.72	0.72	0.74	0.74	0.77
B11	B11	0.81	0.83	0.85	0.87	0.92	B11	0.80	0.79	0.81	0.81	0.85
B12	B12	0.87	0.89	0.90	0.91	0.93	B12	0.84	0.83	0.82	0.84	0.84
Pe	Pe	1.30	1.34	1.43	1.48	1.53	Pe	1.32	1.38	1.38	1.39	1.48
Po2	Po2	2.03	2.30	2.61	2.86	3.11	Po2	1.70	1.81	1.96	2.06	2.15
Po1	Po1	2.36	2.66	3.03	3.32	3.60	Po1	1.97	2.10	2.28	2.39	2.50

Table 5.8: (Continued)

		(g) BGG07 (5) distribution					(h) MBG90 (1) distribution					
Runup	model	Return period (years)					Runup	Return period (years)				
		1	10	100	1000	10 000		1	10	100	1000	10 000
Bld	Bld	-0.180	-0.188	-0.180	-0.188	-0.197	Bld	-0.425	-0.072	-0.084	-0.095	-0.110
Sc	Sc	-0.077	-0.080	-0.084	-0.088	-0.084	Sc	-0.272	-0.404	-0.571	-0.779	-1.032
Vo	Vo	0.43	0.42	0.43	0.42	0.43	Vo	0.41	0.41	0.43	0.44	0.45
At1	At1	0.65	0.65	0.67	0.67	0.68	At1	0.58	0.60	0.63	0.66	0.69
Ho	Ho	0.71	0.72	0.72	0.72	0.73	Ho	0.68	0.70	0.72	0.74	0.77
At2	At2	0.75	0.74	0.74	0.74	0.77	At2	0.69	0.71	0.73	0.76	0.80
B11	B11	0.82	0.82	0.81	0.82	0.82	B11	0.76	0.78	0.81	0.84	0.87
B12	B12	0.87	0.86	0.87	0.87	0.87	B12	0.85	0.87	0.89	0.91	0.93
Pe	Pe	1.32	1.31	1.36	1.37	1.38	Pe	1.17	1.22	1.27	1.33	1.40
Po2	Po2	2.00	2.17	2.34	2.57	2.74	Po2	1.51	1.74	1.98	2.22	2.47
Po1	Po1	2.32	2.52	2.72	2.98	3.18	Po1	1.76	2.02	2.29	2.57	2.86

Table 5.8: (Continued)

		(i) MBG90 (2) distribution					(j) MBG90 (3) distribution					
Runup	model	Return period (years)					Runup	Return period (years)				
		1	10	100	1000	10 000		1	10	100	1000	10 000
Bld	Bld	-0.202	-0.260	-0.286	-0.310	-0.411	Bld	-0.346	-0.426	-0.060	-0.068	-0.073
Sc	Sc	-0.027	-0.028	-0.388	-0.511	-0.660	Sc	-0.291	-0.442	-0.640	-0.890	-1.201
Vo	Vo	0.39	0.38	0.38	0.38	0.39	Vo	0.40	0.39	0.40	0.40	0.41
At1	At1	0.53	0.54	0.55	0.56	0.57	At1	0.55	0.56	0.57	0.59	0.61
Ho	Ho	0.65	0.65	0.66	0.67	0.67	Ho	0.66	0.67	0.68	0.69	0.71
At2	At2	0.65	0.66	0.67	0.68	0.69	At2	0.67	0.68	0.69	0.71	0.72
B11	B11	0.72	0.73	0.74	0.75	0.76	B11	0.74	0.75	0.76	0.78	0.80
B12	B12	0.81	0.82	0.82	0.83	0.84	B12	0.82	0.83	0.84	0.85	0.88
Pe	Pe	1.08	1.09	1.11	1.13	1.15	Pe	1.11	1.13	1.16	1.19	1.24
Po2	Po2	1.44	1.60	1.75	1.90	2.04	Po2	1.44	1.63	1.81	2.00	2.18
Po1	Po1	1.67	1.85	2.03	2.20	2.37	Po1	1.67	1.89	2.10	2.31	2.53

5.3.3 Comparison of Extreme Values

Figure 5.7 shows the normalised wave runup and wave rundown estimated from both wind and wave distributions with different runup models for 1 year return period and bottom slope 1/10. The runup models are in increasing order with respect to the values that they predict for most of the distributions.

From Figure 5.7 it is observed that the runup models Po1 and Po2 give estimates of the normalised wave runup with large spread between the distributions. The Pe model does also generate larger spread than the general trend. The runup models At1, Ho, At2, B11 and B12, however, give very similar values with a maximum normalised spread of 0.12. For the Vo runup model, the BG15 distribution stands out from the other distributions, but the value is closer to the estimates from the other models. For the Bld and Sc models it is observed a larger spread compared with the At1, Ho, At2, B11 and B12 models, and the wave rundown is not in increasing order for all the distributions. The wind distributions give estimates with larger spread than the wave distributions.

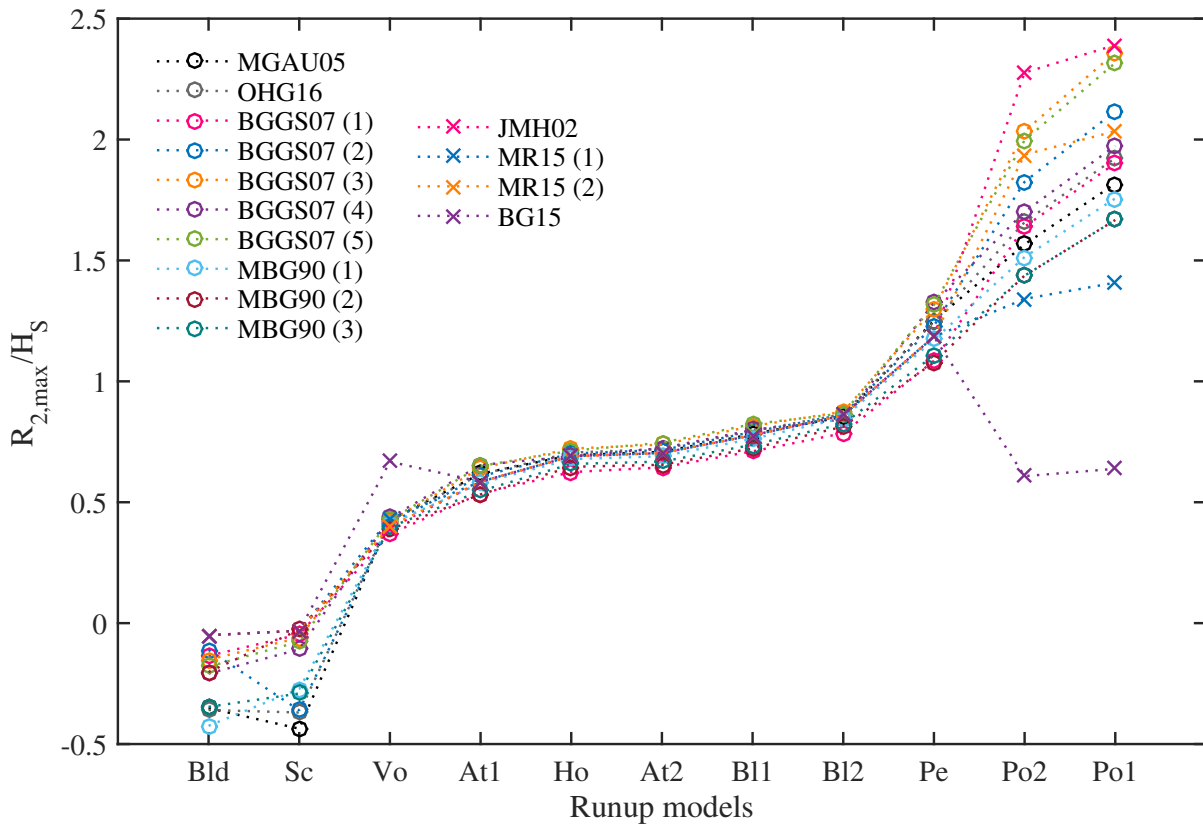


Figure 5.7: Extreme values of wave runup and wave rundown normalised with significant wave height. Values are calculated from both long-term wind and wave distributions for bottom slope 1/10 and a return period of 1 year

5.3.4 Range of Validity

The validity of the runup models for the extreme values was investigated by comparing the runup models range of validity in Table 3.2 with the sea state parameters for the extreme wave runup and wave rundown conditions in Table 5.6 for the long-term wind distributions, and in Appendix B.5 for the long-term wave distributions. It was only a few combinations of distributions and runup models that met the criterias for the models. A checkmark symbol is only used when all the available criterias were met. A validity range was suggested by the authors that presented the Pe and Sc runup models, and this range is considered here. For the other models, the range considered are the conditions that the experiments contained.

Table 5.9: Validity of runup models for the extreme values of 1 year return period and bottom slope 1/10 for wind and wave distributions. ✓ indicates that the runup model is valid for the sea state parameters from the corresponding distribution.

Wind and wave distributions	Runup and rundown models							
	B11, B12	Bld	Sc	Pe	Ho	Vo	At	Po1, Po2
MGAU05		✓	✓					
OHG16		✓	✓					
BGGS07 (1)			✓	✓				
BGGS07 (2)			✓					
BGGS07 (3)			✓					
BGGS07 (4)			✓					
BGGS07 (5)			✓					
MBG90 (1)		✓	✓	✓				
MBG90 (2)			✓	✓				
MBG90 (3)		✓	✓	✓				
JMH02			✓	✓				
MR15 (1)			✓	✓				
MR15 (2)			✓	✓				
BG15			✓	✓	✓	✓	✓	

The data from which the Pe model is based on does only include measurements with more gentle bottom slope than 1/10. Yet, this model is described as valid for several distributions in Table 5.9 because the authors of de la Pena et al. (2014) suggested that the runup model is valid for $\xi_P < 0.6$, and these distributions have ξ_P within this limit for their extreme values.

Chapter 6

Discussion

6.1 Wave Runup and Wave Rundown Based on Wind and Wave Statistics

Results based on wind distributions showed that the normalised expected values had approximately the same trend, with exception of the Pe model at steep slopes. Since this model is developed for dissipative slopes through experiments with bottom slopes 1/50, 1/30, and 1/20, it is not reliable for very steep slopes, and this could explain the deviation from the other runup models. By considering the standard deviation in addition to the expected values it was observed that most of the results cover approximately the same region of values. Also, the conditional BG15 distribution generated results with significantly lower standard deviation than the other marginal wind distributions.

In the comparison of the results for the expected value calculated from the stochastic and deterministic approach in Table 5.2, it was observed that the ratios between the results were all smaller than one for all combinations of distributions and runup models. Also, the stochastic approach contains more information about the wave spectrum and is therefore considered the more complete approach, and this indicates that the deterministic approach underestimates the expected values for wave runup and wave rundown. Thus the stochastic approach should be used whenever possible.

Results based on wave distributions did also show that the wave distributions in general had

the same trend, and that the Pe model stood out from the other runup models at steep slopes. When including the standard deviation, the results did also here overlap to a certain extent.

Because all the BGG07 distributions are developed from data collected in the same ocean area, it would be natural to assume that they lead to quite similar wave runup and wave rundown. From Figure 2.7 it was observed that the probability density functions for the distributions are not that similar, so some differences were expected. Table 5.4 shows that all BGG07 distributions gave quite similar results. The MGAU05 and OHG16 distributions did also give quite similar results, even though they are not from the same ocean region. Both the Barents Sea and the Northern North Sea are, however, known for their harsh environments; and Figure 2.7 shows that their pdfs are very similar. It was also observed from Figure 2.7 that the pdfs of all the three MBG90 distributions are quite similar in shape, but the kurtosis varies, and they generated very similar results.

6.2 Extreme Value Estimates

By comparing the results for the sea state parameters for the extreme value estimates with the range of the runup models in Table 3.2, it was observed that most of the runup models are strictly not valid for the extreme values, as outlined in Table 5.9.

In the comparison of results in Figure 5.7 it was observed that the runup models At1, Ho, At2, B11 and B12 predicted extreme values with small spread; both between the different distribution, and between the runup models. It was also observed that the extreme value calculated by the Vo runup model from the BG15 long-term wind distribution stands out from the rest of the estimates calculated by this model. This distribution is the only one that is strictly valid for this runup model, and this estimate was also more in line with estimates from the other models.

The Pe runup model predicted wave runup estimates with larger values than the just mentioned models. However, from the criteria of validity for the models it was observed that this model was more frequently valid than other models, but it should be noted that this model is not based on the bottom slope used in the calculation of extreme values. Note, though, that the distributions that are valid gave lower estimates, thus closer to the results with small spread.

For the Po1 and Po2 models, where the spread between the distributions was large, none of the

distributions are strictly valid. Recall though, that these models are intended for gravel beaches that are often very steep, and a direct comparison with other models developed from sandy beaches would hence not be fair.

The normalised extreme values did not change much with increasing return period. However, the significant wave height increased significantly with increasing return period, resulting in large wave runup and wave rundown, especially for the Po1 and Po2 models, see Appendix B.5. Also, the extreme mean wind speed in Table 5.5 induced large wave runup values, see Appendix B.3.

Extreme values calculated from the BG15 long-term wind distribution are valid for several of the runup models due to the given significant wave height that limits the extreme sea state values. For this distribution it is only the Bl and Po models that are not valid.

It could seem like the models are more in agreement when the models are extrapolated to larger waves than to other bottom slopes from which they were based on. The model Pe, Po1, and Po2 were developed from quite narrow range of conditions, and this could explain why they differ that much from the other models.

6.3 Error Sources and Uncertainties

The data for the wind distributions were collected over a period of maximum 26 years. Thus, calculations of values with return periods of 100, 1000 and 10 000 years require use of the extrapolated part in the tail of their pdfs. So, one should keep in mind that the results for these return periods are not necessarily based on actual records of such extreme values; and it follows that uncertainty is connected with these values because of the uncertainty in the tails of the distributions.

The same uncertainty issue addresses the wave distributions. Even though the records of the wave data are of greater extent, with a maximum length of 57 years, it is still considered a short period when dealing with 1000 and 10 000 years return periods. Nevertheless, the wave runup and wave rundown can be calculated directly from the wave distributions, while sea state parameters must be calculated through the Phillips spectrum when the wind distributions are applied. This spectrum does not necessarily represent the distributions well, resulting in

increased uncertainty. Other wave spectra could also have been used, and they might give a more realistic transition from wind to wave conditions.

Also for the runup models, extrapolation is required in order to use the models beyond their original range resulting in further increase in the uncertainty. Furthermore, possible error sources could be associated with the measuring of data both in wave runup experiments, and in wind and wave data measurements. Also, fitting of models to the data could cause errors and uncertainty, in addition to the already addressed issues.

Behind the final estimates of wave runup and wave rundown it does therefore lie a great deal of possible errors and uncertainties, and the values are therefore not to be considered as accurate. However, they do indicate the magnitude of the wave runup and wave rundown.

6.4 Evaluation of Results

Both large storm surge and wave runup are likely to occur simultaneously during storm conditions. Combined with high tide, and in particular spring high tide, the total sea level could be dramatic. At a particular location, the tide could influence the wave runup and wave rundown because the changing water depth could affect the amount of energy being dissipated by wave breaking, and the location at which the waves break could change, causing the wave runup and wave rundown to change. At flat beaches, the dissipation is larger than at steep beaches, and the wave runup will therefore be smaller. The results indicate the same trend, which is a direct result of the formulations of the runup models.

Most of the runup models used herein are developed from studies on beaches. They could also be applied on structures, but since the surface and the bathymetry usually are different, it is not expected to give very reliable results. Restrictions on bottom slopes for the application of the runup models are of course still important, and since structures usually have steep slopes, there are not many of the runup models herein that can be relied on for such estimates. If such estimates are performed after all, the models Po1 and Po2 would be the most relevant models for wave runup because they are intended for steep bottom slopes, and the Sc model would be the most relevant model for wave rundown because it is based on experiments on a structure.

Even though the wind and wave conditions found for the extreme conditions could occur on

a long term perspective, it is not necessarily likely that the wave runup and wave rundown predicted by the runup models are representative for these wind and wave conditions because the runup models are used beyond their range. Some of the runup models generated very large extreme wave runup estimates. This is not that evident in the normalised results, but when wind speed and sea state parameters become large, the wave runup becomes severe because the normalised values are multiplied with the significant wave height. It is the Pe model, but in particular the Po1 and Po2 models, that predict the largest wave runup for the longest return periods, see Appendix B.5. These models predicted a wave runup up to 100 metres, which would flood large areas of land; but again, application of the runup models to these sea states is way beyond their range, and the reliability is therefore poor.

Chapter 7

Conclusions and Recommendations

Overall the estimates of wave runup and wave rundown are associated with a large amount of uncertainty. However, when considering the normalised results with their respective standard deviation, quite similar results are found for the models that are based on approximately the same conditions. The method presented in this thesis is convenient due to its simplicity, but it should only be used for early estimates due to large uncertainties related to the results. It was observed that the Pe, Po1, and Po2 models led to results that deviated significantly from the results obtained by the other runup models. These three runup models were developed from a limited selection of conditions, which can explain their deviation, and they should therefore only be applied to the conditions that they were based on.

In order to improve the method it is recommended to investigate the effect of changing the wave spectrum that is used to find sea state parameters from the wind statistics. A Phillips spectrum was used here, but it is also possible to express a Pierson-Moskowitz spectrum in terms of the mean wind speed, and applying this spectrum to the wind distributions in the same manner as for the Phillips spectrum. A Pierson-Moskowitz spectrum does also contain low frequencies, while the Phillips spectrum only covers frequencies from the peak frequency and above. Since the Phillips spectrum includes the peak frequency, it represents most of the energy in the sea state, and it is therefore not expected that the results would have been greatly affected.

The method can be implemented in a computer program that requires only a few input parameters in order to give an estimate of the wave runup and wave rundown. The output of such a program could be extreme values relevant for early estimates of design parameters. This pro-

gram should take the range of the runup models into account, providing an indication of which runup model being the most reliable for the current condition. It is important though, to only consider the method to provide estimates, rather than accurate values, indicating that further and more detailed analysis must be carried out at a later stage in the design process.

References

- Atkinson, A. L., Power, H. E., Moura, T., Hammond, T., Callaghan, D. P. & Baldock, T. E. (2017), 'Assessment of runup predictions by empirical models on non-truncated beaches on the south-east australian coast', *Coastal Engineering Journal* **119**, 15–31.
- Bitner-Gregersen, E. (2015), 'Joint met-ocean description for design and operations of marine structures', *Applied Ocean Research* **51**, 279–292.
- Bitner-Gregersen, E. M. & Guedes Soares, C. (2007), 'Uncertainty of average wave steepness prediction from global wave databases', *Guedes Soares C, Das PK (eds) Advancements in marine structures* pp. 3–10.
- Blenkinsopp, C., Matias, A., Howe, D., Castelle, B., Marieu, V. & Turner, I. (2016), 'Wave runup and overwash on a prototype-scale sand barrier', *Coastal Engineering Journal* **113**, 88–103.
- Bury, K. V. (1975), *Statistical Models in Applied Science*, John Wiley & Sons.
- de la Pena, J. M., Sánchez-González, J. F. & Díaz-Sánchez, R. (2014), 'Wave runup in a sand bed physical model', *J. Waterway, Port, Coastal, Ocean Eng.* **140**(4), 04014015.
- Dean, R. G. & Dalrymple, R. A. (1984), *Water Wave Mechanics for Engineers and Scientists*, Prentice-Hall, Inc.
- DNV-RP-C205 (2014), *Environmental Conditions and Environmental Loads*, DNV GL AS.
- Haver, S. (1980), Analysis of uncertainties related to the stochastic modelling of ocean waves, PhD thesis, The Norwegian Institute of Technology, Trondheim. An optional note.
- Hedges, T. S. & Mase, H. (2004), 'Modified hunt's equation incorporating wave setup', *Journal of Waterways, Port, Coastal and Ocean Engineering* **C-ASCE 130**, 109–113.

- Holman, R. A. (1987), 'Extreme value statistics for wave run-up on a natural beach', *Coastal Engineering Journal* **9**, 527–544.
- Holthuijsen, L. H. (2007), *Waves in Oceanic and Coastal Waters*, Cambridge University Press.
- Johannessen, K., Meling, T. & Haver, S. (2002), 'Joint distribution for wind and waves in the northern north sea', *International Journal of Offshore and Polar Engineering* **12**(1), ISSN 1053–5381.
- Mao, W. & Rychlik, I. (2016), 'Estimation of weibull distribution for wind speeds along ship routes', *J. Engineering for the Maritime Environment* pp. 1–17.
- Mase, H. (1989), 'Random wave runup height on gentle slope', *Journal of Waterways, Port, Coastal and Ocean Engineering* **115**, 649–661.
- Masselink, G., Ruju, A., Conley, D., Turner, I., Ruessink, G., Matias, A., Thompson, C., Castelle, B., Puelo, J., Citerone, V. & Wolters, G. (2016), 'Large-scale barrier dynamics experiment ii (bardex ii): Experimental design, instrumentation, test program, and data set', *Coastal Engineering Journal* **113**, 3–18.
- Mathisen, J. & Bitner-Gregersen, E. (1990), 'Joint distributions for significant wave height and wave zero-up-crossing period', *Applied Ocean Research* **12**(2), 93–103.
- Moan, T., Gao, Z. & Ayala-Uraga, E. (2005), 'Uncertainty of wave-induced response of marine structures due to long-term variation of extratropical wave conditions', *Marine Structures* **18**(4), 359–382.
- Myrhaug, D. (2012), 'Kompendium UK-2012-100 TMR4230 Oceanography Current', Akademika forlag.
- Myrhaug, D. (2015), 'Estimation of wave runup on shorelines based on long-term variation of wave conditions', *J.Ocean Eng. Mar. Energy* **14**, 193–197.
- Myrhaug, D. (2017), 'Stokes drift estimation for sea states based on long-term variation of wind statistics', *Coastal Engineering Journal* **59**(2).
- Myrhaug, D. & Fouques, S. (2010), 'A joint distribution of significant wave height and characteristic surf parameter', *Coastal Engineering Journal* **57**, 948–952.

- Myrhaug, D. & Kjeldsen, S. P. (1987), 'Prediction of occurrences of steep and high waves in deep water', *Journal of Waterway, Port, Coastal, and Ocean Engineering* **113**(2), 122–138.
- Myrhaug, D. & Leira, B. (2017), 'Application of wave runup and wave rundown formulae based on long-term variation of wave conditions', *Coastal Engineering Journal* **120**, 75–77. (in press).
- Myrhaug, D. & Lian, W. (2009), 'Kompendium TMR4182 Marine Dynamics Irregular Waves', Kompendieforlaget.
- Nielsen, P. (2009), *Coastal and Estuarine Processes*, Vol. 29 of *Advances Series on Ocean Engineering*, World Scientific Publishing Co. Pte. Ltd.
- Orimolade, A. P., Haver, S. & Gudmestad, O. T. (2016), 'Estimation of extreme significant wave heights and the associated uncertainties: A case study using nora10 hindcast data for the barents sea', *Marine Structures* **49**, 1–17.
- Pedersen, T. D. (2014), personal communication.
- Poate, T. G., McCall, R. T. & Masselink, G. (2016), 'A new parameterisation for runup on gravel beaches', *Coastal Engineering Journal* **117**, 176–190.
- Pugh, D. (2004), *Changing Sea Levels Effects of Tides, Weather and Climate*, Cambridge University Press.
- Schüttrumpf, H., Bergmann, H. & Dette, H. H. (1994), The concept of residence time for the description of wave run-up, wave set-up and wave run-down, in 'Proceedings of 24th Conference on Coastal Engineering, Kobe, Japan, 1994', pp. 553–564.
- Vousdoukas, M. I. & Wziatek, D. (2012), 'Coastal vulnerability assessment based on video wave run-up observations at a mesotidal, steep-sloped beach', *Ocean Dynamics* **62**, 123–137.

Appendix A

Calculations

A.1 Expressing R_2 in Terms of U_{10}

In order to express R_2 in terms of U_{10} , ξ_P is first rewritten on the form in Eq. (A.1).

$$\xi_P = m \left(\frac{H_S}{\frac{g}{2\pi} T_P^2} \right)^{-1/2} = m \sqrt{\frac{g}{2\pi} \frac{T_P}{\sqrt{H_S}}} \quad (\text{A.1})$$

For the first general equation in Eq. (3.1), the expression for R_2 is used as a starting point for the derivation, and the relations $T_P = \frac{2\pi}{g} U_{10}$ and $H_S = \frac{2\sqrt{\alpha}}{g} U_{10}^2$ are inserted. The derivation is given in Eq. (A.2).

$$\begin{aligned}
R_2 &= (a + b\xi_P^c)H_S + d \\
&= aH_S + b\xi_P^c H_S + d \\
&= aH_S + b \left(m\sqrt{\frac{g}{2\pi}} \frac{T_P}{\sqrt{H_S}} \right)^c H_S + d \\
&= a \left(\frac{2\sqrt{\hat{\alpha}}}{g} U_{10}^2 \right) + b \left(m\sqrt{\frac{g}{2\pi}} \frac{\frac{2\pi}{g} U_{10}}{\sqrt{\frac{2\sqrt{\hat{\alpha}}}{g} U_{10}^2}} \right)^c \left(\frac{2\sqrt{\hat{\alpha}}}{g} U_{10}^2 \right) + d \\
&= a \frac{2\sqrt{\hat{\alpha}}}{g} U_{10}^2 + b \left(m\sqrt{\frac{g}{2\pi}} \frac{2\pi}{g} \right)^c \left(\frac{2\sqrt{\hat{\alpha}}}{g} \right)^{1-\frac{c}{2}} U_{10}^{c+2(1-\frac{c}{2})} + d \\
&= a \frac{2\sqrt{\hat{\alpha}}}{g} U_{10}^2 + b \left(m\sqrt{\frac{2\pi}{g}} \right)^c \left(\frac{2\sqrt{\hat{\alpha}}}{g} \right)^{1-\frac{c}{2}} U_{10}^2 + d \\
&= \left[a \frac{2\sqrt{\hat{\alpha}}}{g} + bm^c \left(\frac{2\pi}{g} \right)^{\frac{c}{2}} \left(\frac{2\sqrt{\hat{\alpha}}}{g} \right)^{1-\frac{c}{2}} \right] U_{10}^2 + d
\end{aligned} \tag{A.2}$$

For the second general equation in Eq. (3.2), an expression in terms of U_{10} is found for each of the two runup models that this equation represents. The relations $T_P = \frac{2\pi}{g} U_{10}$ or $T_Z = T_{m02} = 2\pi\sqrt{\frac{m_0}{m_2}} = \frac{\sqrt{2}\pi}{g} U_{10}$, and $H_S = \frac{2\sqrt{\hat{\alpha}}}{g} U_{10}^2$ are inserted into the equations, resulting in the expressions in Eq. (A.3) and Eq. (A.4).

$$R_2 = 0.49m^{0.5} \frac{2\pi\sqrt{2\hat{\alpha}}}{g^2} U_{10}^3 \tag{A.3}$$

$$R_2 = 0.33m^{0.5} \frac{4\pi\sqrt{\hat{\alpha}}}{g^2} U_{10}^3 \tag{A.4}$$

A.2 Change of Variables from (H_S, T) to (H_S, R_2)

A log-normal conditional distribution is given in Eq. (A.5) for T given H_S .

$$f(T|H_S) = \frac{1}{\sqrt{2\pi}\sigma_T T} \exp\left[-\frac{(\ln T - \mu_T)^2}{2\sigma_T^2}\right] \quad (\text{A.5})$$

In order to do a change of variables from (H_S, T) to (H_S, R_2) a relation between R_2 and T must be obtained. As a starting point the general expression for R_2 in Eq. (A.6) and the definition of the surf parameter in Eq. (A.7) are used. The relation between T and T_P is defined as $T_P = \hat{c}T$, where $\hat{c} = 1$ for $T = T_P$, and $\hat{c} = 1.28$ for $T = T_Z$.

$$R_2 = (a + b\xi_P^c)H_S + d \quad (\text{A.6})$$

$$\xi_P = m \left(\frac{H_S}{\frac{g}{2\pi} T_P^2} \right)^{-1/2} \quad (\text{A.7})$$

A relation between R_2 and T can then be found by inserting Eq. (A.7) into Eq. (A.6) and replacing T_P with $\hat{c}T$ as shown in Eq. (A.8).

$$\begin{aligned} R_2 &= aH_S + bH_S \xi_P^c + d = aH_S + bH_S m^c \left(\frac{H_S}{\frac{g}{2\pi} (\hat{c}T)^2} \right)^{-c/2} + d \\ &= aH_S + bH_S m^c \left(\frac{g}{2\pi} \right)^{c/2} H_S^{-c/2} \hat{c}^c T^c + d \\ &= aH_S + b m^c \hat{c}^c \left(\frac{g}{2\pi} \right)^{c/2} H_S^{1-c/2} T^c + d \end{aligned} \quad (\text{A.8})$$

Further, $R = R_2 - aH_S - d$ is defined for mathematical help. An expression for T as a function of R can be found by rearranging Eq. (A.8), and the results is shown in Eq. (A.9).

$$T = \left[\frac{R_2 - aH_S - d}{b m^c \hat{c}^c \left(\frac{g}{2\pi} \right)^{c/2} H_S^{1-c/2}} \right]^{1/c} = \left[\frac{R}{b m^c \hat{c}^c \left(\frac{g}{2\pi} \right)^{c/2} H_S^{1-c/2}} \right]^{1/c} \quad (\text{A.9})$$

The relation between the conditional pdf for T given H_S , and the conditional pdf for R given H_S are given in Eq. (A.10), where $|\partial T / \partial R|$ is the Jacobian in Eq. (A.11).

$$f(R|H_S) = f(T|H_S) \left| \frac{\partial T}{\partial R} \right| \quad (\text{A.10})$$

$$\left| \frac{\partial T}{\partial R} \right| = \frac{1}{c} \left[\frac{R}{bm^c \left(\frac{g}{2\pi}\right)^{c/2} \hat{c}^c H_S^{1-c/2}} \right]^{1/c-1} \frac{1}{bm^c \left(\frac{g}{2\pi}\right)^{c/2} \hat{c}^c H_S^{1-c/2}} \quad (\text{A.11})$$

The conditional pdf for R given H_S can then be found by inserting the expression for T as a function of R in Eq. (A.9) into $f(T|H_S)$ in Eq. (A.10) and inserting the relation in Eq. (A.11) for the Jacobian.

$$\begin{aligned} f(R|H_S) &= \frac{1}{\sqrt{2\pi}\sigma_T} \left[\frac{R}{bm^c \hat{c}^c \left(\frac{g}{2\pi}\right)^{c/2} H_S^{1-c/2}} \right]^{-1/c} \cdot \exp \left[-\frac{\left(\ln \left[\frac{R}{bm^c \hat{c}^c \left(\frac{g}{2\pi}\right)^{c/2} H_S^{1-c/2}} \right]^{1/c} - \mu_T \right)^2}{2\sigma_T^2} \right] \\ &= \frac{1}{\sqrt{2\pi}\sigma_T R} \left[\frac{R}{bm^c \left(\frac{g}{2\pi}\right)^{c/2} \hat{c}^c H_S^{1-c/2}} \right]^{1/c-1} \frac{1}{bm^c \left(\frac{g}{2\pi}\right)^{c/2} \hat{c}^c H_S^{1-c/2}} \\ &= \frac{1}{\sqrt{2\pi}\sigma_T R} \exp \left[-\frac{\left(\frac{1}{c} \ln R - \frac{1}{c} \ln \left(bm^c \hat{c}^c \left(\frac{g}{2\pi}\right)^{c/2} H_S^{1-c/2} \right) - \mu_T \right)^2}{2\sigma_T^2} \right] \\ &= \frac{1}{\sqrt{2\pi}\sigma_T R} \exp \left[-\frac{\left(\ln R - \left(\ln \left(bm^c \hat{c}^c \left(\frac{g}{2\pi}\right)^{c/2} H_S^{1-c/2} \right) + c\mu_T \right) \right)^2}{2c^2\sigma_T^2} \right] \\ &= \frac{1}{\sqrt{2\pi}\sigma_R R} \exp \left[-\frac{(\ln R - \mu_R)^2}{2\sigma_R^2} \right] \end{aligned} \quad (\text{A.12})$$

From Eq. (A.12) it can be concluded that $f(R|H_S)$ is log-normal distributed by recognising μ_R and σ_R^2 in Eq. (A.13) and Eq. (A.14) as the the mean value and variance of $\ln R$.

$$\mu_R = c\mu_T + \ln \left(bm^c \hat{c}^c \left(\frac{g}{2\pi}\right)^{c/2} H_S^{1-c/2} \right) \quad (\text{A.13})$$

$$\sigma_R^2 = c^2\sigma_T^2 \quad (\text{A.14})$$

Similarly, for the general equation in Eq. (3.2), a change of variable can be performed by considering the expression for R_2 given in Eq. (A.15).

$$R_2 = Cm^{0.5} \hat{c}TH_S \quad (\text{A.15})$$

By rewriting Eq. (A.15) an expression for T in Eq. (A.16) can be defined and the Jacobian can be calculated as given in Eq. (A.17).

$$T = \frac{R_2}{Cm^{0.5} \hat{c}H_S} \quad (\text{A.16})$$

$$\left| \frac{\partial T}{\partial R_2} \right| = \frac{1}{Cm^{0.5} \hat{c}H_S} \quad (\text{A.17})$$

The conditional pdf for R_2 given H_S can then be found by inserting the expression for T as a function of R_2 in Eq. (A.15) into $f(T|H_S)$ in Eq. (A.10), and inserting the relation in Eq. (A.17) for the Jacobian. The result is shown in Eq. (A.18).

$$\begin{aligned} f(R_2|H_S) &= \frac{1}{\sqrt{2\pi}\sigma_T} \frac{Cm^{0.5} \hat{c}H_S}{R_2} \exp \left[-\frac{\left(\ln \left(\frac{R_2}{Cm^{0.5} \hat{c}H_S} \right) - \mu_T \right)^2}{2\sigma_T^2} \right] \frac{1}{Cm^{0.5} \hat{c}H_S} \\ &= \frac{1}{\sqrt{2\pi}\sigma_T R_2} \exp \left[-\frac{(\ln R_2 - \ln(Cm^{0.5} \hat{c}H_S) - \mu_T)^2}{2\sigma_T^2} \right] \\ &= \frac{1}{\sqrt{2\pi}\sigma_T R_2} \exp \left[-\frac{(\ln R_2 - (\ln(Cm^{0.5} \hat{c}H_S) + \mu_T))^2}{2\sigma_T^2} \right] \\ &= \frac{1}{\sqrt{2\pi}\sigma_{R_2} R_2} \cdot \exp \left[-\frac{(\ln R_2 - \mu_{R_2})^2}{2\sigma_{R_2}^2} \right] \end{aligned} \quad (\text{A.18})$$

From Eq. (A.18) it can be concluded that $f(R|H_S)$ is log-normal distributed by recognising μ_{R_2} and $\sigma_{R_2}^2$ in Eq. (A.19) and Eq. (A.20) as the the mean value and variance of $\ln R_2$.

$$\mu_{R_2} = \mu_T + \ln(Cm^{0.5} \hat{c}H_S) \quad (\text{A.19})$$

$$\sigma_{R_2}^2 = \sigma_T^2 \quad (\text{A.20})$$

Appendix B

Results

The values in this chapter are given with the following dimensions: U_{10} (m/s), H_S (m), T_P (s), ξ_P (-), and R_2 (m).

B.1 Based on Wind Distributions

Table B.1: R_2 from JMH02 wind distribution. Values are given in metres as expected value \pm standard deviation

Runup model	Bottom slope			
	1/5	1/10	1/20	1/50
Bl1	1.87 ± 2.20	1.10 ± 1.29	0.64 ± 0.76	0.32 ± 0.37
Bl2	1.88 ± 2.21	1.21 ± 1.43	0.88 ± 1.04	0.68 ± 0.80
Bld	-0.44 ± 0.51	-0.07 ± 0.08	0.11 ± 0.13	0.22 ± 0.26
Sc	-0.20 ± 0.24	-0.04 ± 0.05	-0.01 ± 0.01	0.00 ± 0.00
Pe	4.12 ± 4.85	1.67 ± 1.97	0.68 ± 0.80	0.21 ± 0.24
Ho	1.67 ± 1.96	0.98 ± 1.15	0.63 ± 0.74	0.42 ± 0.50
Vo	1.50 ± 1.23	0.97 ± 0.62	0.71 ± 0.31	0.55 ± 0.12
At1	1.65 ± 1.94	0.83 ± 0.97	0.41 ± 0.49	0.17 ± 0.19
At2	1.76 ± 2.07	0.99 ± 1.17	0.61 ± 0.72	0.38 ± 0.45
Po1	1.76 ± 3.31	1.25 ± 2.34	0.88 ± 1.65	0.56 ± 1.05
Po2	1.68 ± 3.15	1.19 ± 2.23	0.84 ± 1.58	0.53 ± 1.00

Table B.2: R_2 from MR15 (1) wind distribution. Values are given in metres as expected value \pm standard deviation

Runup model	Bottom slope			
	1/5	1/10	1/20	1/50
B11	1.17 ± 1.02	0.69 ± 0.60	0.40 ± 0.35	0.20 ± 0.17
B12	1.17 ± 1.02	0.76 ± 0.66	0.55 ± 0.48	0.43 ± 0.37
Bld	-0.27 ± 0.24	-0.04 ± 0.04	0.07 ± 0.06	0.14 ± 0.12
Sc	-0.13 ± 0.11	-0.03 ± 0.02	-0.01 ± 0.01	0.00 ± 0.00
Pe	2.57 ± 2.24	1.05 ± 0.91	0.42 ± 0.37	0.13 ± 0.11
Ho	1.04 ± 0.91	0.61 ± 0.53	0.39 ± 0.34	0.26 ± 0.23
Vo	1.11 ± 0.57	0.78 ± 0.29	0.61 ± 0.14	0.52 ± 0.06
At1	1.03 ± 0.90	0.52 ± 0.45	0.26 ± 0.23	0.10 ± 0.09
At2	1.10 ± 0.96	0.62 ± 0.54	0.38 ± 0.33	0.24 ± 0.21
Po1	0.77 ± 1.01	0.54 ± 0.71	0.38 ± 0.51	0.24 ± 0.32
Po2	0.73 ± 0.96	0.52 ± 0.68	0.36 ± 0.48	0.23 ± 0.30

Table B.3: R_2 from MR15 (2) wind distribution. Values are given in metres as expected value \pm standard deviation

Runup model	Bottom slope			
	1/5	1/10	1/20	1/50
B11	2.74 ± 2.24	1.61 ± 1.32	0.94 ± 0.77	0.47 ± 0.38
B12	2.75 ± 2.25	1.78 ± 1.46	1.29 ± 1.06	1.00 ± 0.82
Bld	-0.64 ± 0.52	-0.10 ± 0.08	0.17 ± 0.14	0.33 ± 0.27
Sc	-0.30 ± 0.24	-0.06 ± 0.05	-0.01 ± 0.01	0.00 ± 0.00
Pe	6.04 ± 4.94	2.45 ± 2.01	1.00 ± 0.81	0.30 ± 0.25
Ho	2.45 ± 2.00	1.43 ± 1.17	0.92 ± 0.75	0.62 ± 0.50
Vo	1.99 ± 1.26	1.22 ± 0.63	0.83 ± 0.31	0.60 ± 0.13
At1	2.42 ± 1.98	1.21 ± 0.99	0.61 ± 0.50	0.24 ± 0.20
At2	2.58 ± 2.11	1.46 ± 1.19	0.89 ± 0.73	0.56 ± 0.46
Po1	2.69 ± 3.30	1.90 ± 2.34	1.35 ± 1.65	0.85 ± 1.04
Po2	2.56 ± 3.15	1.81 ± 2.23	1.28 ± 1.57	0.81 ± 1.00

Table B.4: R_2 from BG15 wind distribution for $H_S = 3\text{m}$. Values are given in metres as expected value \pm standard deviation

Runup model	Bottom slope			
	1/5	1/10	1/20	1/50
B11	1.29 ± 0.24	0.76 ± 0.14	0.44 ± 0.08	0.22 ± 0.04
B12	1.29 ± 0.24	0.84 ± 0.15	0.61 ± 0.11	0.47 ± 0.09
Bld	-0.30 ± 0.06	-0.05 ± 0.01	0.08 ± 0.01	0.15 ± 0.03
Sc	-0.14 ± 0.03	-0.03 ± 0.01	-0.01 ± 0.00	0.00 ± 0.00
Pe	2.84 ± 0.52	1.15 ± 0.21	0.47 ± 0.09	0.14 ± 0.03
Ho	1.15 ± 0.21	0.67 ± 0.12	0.43 ± 0.08	0.29 ± 0.05
Vo	1.17 ± 0.13	0.81 ± 0.07	0.63 ± 0.03	0.52 ± 0.01
At1	1.14 ± 0.21	0.57 ± 0.10	0.28 ± 0.05	0.11 ± 0.02
At2	1.21 ± 0.22	0.69 ± 0.12	0.42 ± 0.08	0.26 ± 0.05
Po1	0.71 ± 0.19	0.50 ± 0.13	0.36 ± 0.09	0.23 ± 0.06
Po2	0.68 ± 0.18	0.48 ± 0.13	0.34 ± 0.09	0.21 ± 0.06

B.2 Based on Wave Distributions

Table B.5: R_2 from MGAU05 wave distribution for $H_S = 3\text{m}$. Values are given in metres as expected value \pm standard deviation

Runup model	Bottom slope			
	1/5	1/10	1/20	1/50
Bl1	4.56 ± 0.76	2.68 ± 0.45	1.57 ± 0.26	0.78 ± 0.13
Bl2	4.56 ± 0.74	2.87 ± 0.37	2.02 ± 0.18	1.51 ± 0.07
Bld	-1.25 ± 0.41	-0.31 ± 0.20	0.16 ± 0.10	0.44 ± 0.04
Sc	-0.69 ± 0.35	-0.15 ± 0.08	-0.03 ± 0.02	-0.00 ± 0.00
Pe	10.53 ± 2.29	4.28 ± 0.93	1.74 ± 0.38	0.53 ± 0.11
Ho	4.14 ± 0.77	2.37 ± 0.38	1.49 ± 0.19	0.95 ± 0.08
Vo	3.06 ± 0.49	1.75 ± 0.25	1.10 ± 0.12	0.71 ± 0.05
At1	4.22 ± 0.92	2.11 ± 0.46	1.06 ± 0.23	0.42 ± 0.09
At2	4.40 ± 0.85	2.44 ± 0.43	1.46 ± 0.21	0.87 ± 0.09
Po1	5.06 ± 1.10	3.58 ± 0.78	2.53 ± 0.55	1.60 ± 0.35
Po2	4.36 ± 0.95	3.08 ± 0.67	2.18 ± 0.47	1.38 ± 0.30

Table B.6: R_2 from OHG16 wave distribution for $H_S = 3\text{m}$. Values are given in metres as expected value \pm standard deviation

Runup model	Bottom slope			
	1/5	1/10	1/20	1/50
B11	4.52 ± 0.79	2.65 ± 0.46	1.56 ± 0.27	0.77 ± 0.13
B12	4.52 ± 0.76	2.85 ± 0.38	2.01 ± 0.19	1.51 ± 0.08
Bld	-1.23 ± 0.42	-0.30 ± 0.21	0.17 ± 0.11	0.44 ± 0.04
Sc	-0.68 ± 0.36	-0.15 ± 0.08	-0.03 ± 0.02	-0.00 ± 0.00
Pe	10.41 ± 2.37	4.23 ± 0.96	1.72 ± 0.39	0.52 ± 0.12
Ho	4.10 ± 0.80	2.35 ± 0.40	1.48 ± 0.20	0.95 ± 0.08
Vo	3.03 ± 0.51	1.74 ± 0.25	1.10 ± 0.13	0.71 ± 0.05
At1	4.18 ± 0.95	2.09 ± 0.48	1.04 ± 0.24	0.42 ± 0.10
At2	4.36 ± 0.88	2.42 ± 0.44	1.45 ± 0.22	0.87 ± 0.09
Po1	5.00 ± 1.14	3.54 ± 0.81	2.50 ± 0.57	1.58 ± 0.36
Po2	4.31 ± 0.98	3.05 ± 0.69	2.16 ± 0.49	1.36 ± 0.31

Table B.7: R_2 from BGG07 (1) wave distribution for $H_S = 3\text{m}$. Values are given in metres as expected value \pm standard deviation

Runup model	Bottom slope			
	1/5	1/10	1/20	1/50
B11	4.18 ± 0.51	2.45 ± 0.30	1.44 ± 0.18	0.71 ± 0.09
B12	4.19 ± 0.48	2.68 ± 0.24	1.93 ± 0.12	1.47 ± 0.05
Bld	-1.04 ± 0.26	-0.21 ± 0.13	0.21 ± 0.07	0.46 ± 0.03
Sc	-0.52 ± 0.19	-0.11 ± 0.04	-0.02 ± 0.01	-0.00 ± 0.00
Pe	9.38 ± 1.49	3.81 ± 0.60	1.55 ± 0.25	0.47 ± 0.07
Ho	3.75 ± 0.50	2.18 ± 0.25	1.39 ± 0.12	0.92 ± 0.05
Vo	2.81 ± 0.32	1.63 ± 0.16	1.04 ± 0.08	0.69 ± 0.03
At1	3.76 ± 0.60	1.88 ± 0.30	0.94 ± 0.15	0.38 ± 0.06
At2	3.98 ± 0.55	2.23 ± 0.28	1.35 ± 0.14	0.83 ± 0.06
Po1	4.51 ± 0.71	3.19 ± 0.51	2.25 ± 0.36	1.43 ± 0.23
Po2	3.89 ± 0.62	2.75 ± 0.44	1.94 ± 0.31	1.23 ± 0.19

Table B.8: R_2 from BGG07 (2) wave distribution for $H_S = 3\text{m}$. Values are given in metres as expected value \pm standard deviation

Runup model	Bottom slope			
	1/5	1/10	1/20	1/50
B11	4.41 ± 0.54	2.59 ± 0.32	1.52 ± 0.18	0.75 ± 0.09
B12	4.41 ± 0.51	2.79 ± 0.26	1.98 ± 0.13	1.49 ± 0.05
Bld	-1.16 ± 0.28	-0.27 ± 0.14	0.18 ± 0.07	0.45 ± 0.03
Sc	-0.61 ± 0.22	-0.13 ± 0.05	-0.03 ± 0.01	-0.00 ± 0.00
Pe	10.05 ± 1.59	4.08 ± 0.65	1.66 ± 0.26	0.50 ± 0.08
Ho	3.98 ± 0.54	2.29 ± 0.27	1.44 ± 0.13	0.94 ± 0.05
Vo	2.96 ± 0.34	1.70 ± 0.17	1.08 ± 0.09	0.70 ± 0.03
At1	4.03 ± 0.64	2.01 ± 0.32	1.01 ± 0.16	0.40 ± 0.06
At2	4.22 ± 0.59	2.35 ± 0.30	1.42 ± 0.15	0.85 ± 0.06
Po1	4.83 ± 0.77	3.42 ± 0.54	2.41 ± 0.38	1.53 ± 0.24
Po2	4.16 ± 0.66	2.94 ± 0.47	2.08 ± 0.33	1.32 ± 0.21

Table B.9: R_2 from BGG07 (3) wave distribution for $H_S = 3\text{m}$. Values are given in metres as expected value \pm standard deviation

Runup model	Bottom slope			
	1/5	1/10	1/20	1/50
B11	4.16 ± 0.64	2.44 ± 0.38	1.43 ± 0.22	0.71 ± 0.11
B12	4.17 ± 0.61	2.67 ± 0.30	1.92 ± 0.15	1.47 ± 0.06
Bld	-1.03 ± 0.34	-0.20 ± 0.17	0.21 ± 0.08	0.46 ± 0.03
Sc	-0.53 ± 0.24	-0.11 ± 0.05	-0.02 ± 0.01	-0.00 ± 0.00
Pe	9.32 ± 1.88	3.79 ± 0.77	1.54 ± 0.31	0.47 ± 0.09
Ho	3.74 ± 0.63	2.17 ± 0.32	1.38 ± 0.16	0.91 ± 0.06
Vo	2.80 ± 0.40	1.62 ± 0.20	1.04 ± 0.10	0.68 ± 0.04
At1	3.74 ± 0.76	1.87 ± 0.38	0.93 ± 0.19	0.37 ± 0.08
At2	3.96 ± 0.70	2.22 ± 0.35	1.35 ± 0.18	0.83 ± 0.07
Po1	4.48 ± 0.91	3.17 ± 0.64	2.24 ± 0.45	1.42 ± 0.29
Po2	3.86 ± 0.78	2.73 ± 0.55	1.93 ± 0.39	1.22 ± 0.25

Table B.10: R_2 from BGG07 (4) wave distribution for $H_S = 3\text{m}$. Values are given in metres as expected value \pm standard deviation

Runup model	Bottom slope			
	1/5	1/10	1/20	1/50
B11	4.95 ± 0.58	2.90 ± 0.34	1.70 ± 0.20	0.84 ± 0.10
B12	4.93 ± 0.57	3.05 ± 0.28	2.11 ± 0.14	1.55 ± 0.06
Bld	-1.45 ± 0.31	-0.41 ± 0.16	0.11 ± 0.08	0.42 ± 0.03
Sc	-0.85 ± 0.29	-0.18 ± 0.06	-0.04 ± 0.01	-0.01 ± 0.00
Pe	11.67 ± 1.77	4.74 ± 0.72	1.93 ± 0.29	0.59 ± 0.09
Ho	4.53 ± 0.59	2.56 ± 0.30	1.58 ± 0.15	0.99 ± 0.06
Vo	3.30 ± 0.38	1.88 ± 0.19	1.16 ± 0.09	0.74 ± 0.04
At1	4.68 ± 0.71	2.34 ± 0.35	1.17 ± 0.18	0.47 ± 0.07
At2	4.83 ± 0.66	2.66 ± 0.33	1.57 ± 0.16	0.92 ± 0.07
Po1	5.61 ± 0.85	3.97 ± 0.60	2.81 ± 0.42	1.77 ± 0.27
Po2	4.84 ± 0.73	3.42 ± 0.52	2.42 ± 0.37	1.53 ± 0.23

Table B.11: R_2 from BGG07 (5) wave distribution for $H_S = 3\text{m}$. Values are given in metres as expected value \pm standard deviation

Runup model	Bottom slope			
	1/5	1/10	1/20	1/50
B11	5.38 ± 0.54	3.15 ± 0.32	1.85 ± 0.19	0.91 ± 0.09
B12	5.35 ± 0.55	3.26 ± 0.27	2.22 ± 0.14	1.59 ± 0.05
Bld	-1.69 ± 0.30	-0.53 ± 0.15	0.05 ± 0.08	0.40 ± 0.03
Sc	-1.06 ± 0.31	-0.23 ± 0.07	-0.05 ± 0.01	-0.01 ± 0.00
Pe	12.99 ± 1.70	5.28 ± 0.69	2.14 ± 0.28	0.65 ± 0.09
Ho	4.97 ± 0.57	2.78 ± 0.29	1.69 ± 0.14	1.04 ± 0.06
Vo	3.59 ± 0.37	2.02 ± 0.18	1.23 ± 0.09	0.76 ± 0.04
At1	5.21 ± 0.68	2.61 ± 0.34	1.30 ± 0.17	0.52 ± 0.07
At2	5.32 ± 0.63	2.90 ± 0.32	1.69 ± 0.16	0.96 ± 0.06
Po1	6.24 ± 0.82	4.42 ± 0.58	3.12 ± 0.41	1.97 ± 0.26
Po2	5.38 ± 0.70	3.81 ± 0.50	2.69 ± 0.35	1.70 ± 0.22

Table B.12: R_2 from MBG90 (1) wave distribution for $H_S = 3\text{m}$. Values are given in metres as expected value \pm standard deviation

Runup model	Bottom slope			
	1/5	1/10	1/20	1/50
B11	3.97 ± 0.38	2.33 ± 0.22	1.37 ± 0.13	0.67 ± 0.06
B12	3.99 ± 0.35	2.58 ± 0.18	1.87 ± 0.09	1.45 ± 0.04
Bld	-0.93 ± 0.20	-0.15 ± 0.10	0.24 ± 0.05	0.47 ± 0.02
Sc	-0.44 ± 0.12	-0.10 ± 0.03	-0.02 ± 0.01	-0.00 ± 0.00
Pe	8.75 ± 1.10	3.55 ± 0.45	1.44 ± 0.18	0.44 ± 0.06
Ho	3.54 ± 0.37	2.07 ± 0.18	1.34 ± 0.09	0.89 ± 0.04
Vo	2.68 ± 0.24	1.56 ± 0.12	1.01 ± 0.06	0.67 ± 0.02
At1	3.51 ± 0.44	1.76 ± 0.22	0.88 ± 0.11	0.35 ± 0.04
At2	3.74 ± 0.41	2.11 ± 0.20	1.30 ± 0.10	0.81 ± 0.04
Po1	4.21 ± 0.53	2.98 ± 0.37	2.10 ± 0.26	1.33 ± 0.17
Po2	3.63 ± 0.45	2.56 ± 0.32	1.81 ± 0.23	1.15 ± 0.14

Table B.13: R_2 from MBG90 (2) wave distribution for $H_S = 3\text{m}$. Values are given in metres as expected value \pm standard deviation

Runup model	Bottom slope			
	1/5	1/10	1/20	1/50
B11	3.97 ± 0.41	2.33 ± 0.24	1.36 ± 0.14	0.67 ± 0.07
B12	3.99 ± 0.38	2.58 ± 0.19	1.87 ± 0.09	1.45 ± 0.04
Bld	-0.93 ± 0.21	-0.15 ± 0.10	0.24 ± 0.05	0.47 ± 0.02
Sc	-0.44 ± 0.13	-0.10 ± 0.03	-0.02 ± 0.01	-0.00 ± 0.00
Pe	8.75 ± 1.17	3.55 ± 0.48	1.44 ± 0.19	0.44 ± 0.06
Ho	3.54 ± 0.39	2.07 ± 0.20	1.34 ± 0.10	0.89 ± 0.04
Vo	2.68 ± 0.25	1.56 ± 0.13	1.01 ± 0.06	0.67 ± 0.03
At1	3.51 ± 0.47	1.76 ± 0.24	0.88 ± 0.12	0.35 ± 0.05
At2	3.74 ± 0.44	2.11 ± 0.22	1.30 ± 0.11	0.81 ± 0.04
Po1	4.21 ± 0.56	2.97 ± 0.40	2.10 ± 0.28	1.33 ± 0.18
Po2	3.63 ± 0.49	2.56 ± 0.34	1.81 ± 0.24	1.15 ± 0.15

Table B.14: R_2 from MBG90 (3) wave distribution for $H_S = 3\text{m}$. Values are given in metres as expected value \pm standard deviation

Runup model	Bottom slope			
	1/5	1/10	1/20	1/50
B11	3.90 ± 0.34	2.28 ± 0.20	1.34 ± 0.12	0.66 ± 0.06
B12	3.92 ± 0.31	2.54 ± 0.16	1.86 ± 0.08	1.44 ± 0.03
Bld	-0.89 ± 0.17	-0.13 ± 0.09	0.25 ± 0.04	0.48 ± 0.02
Sc	-0.42 ± 0.11	-0.09 ± 0.02	-0.02 ± 0.00	-0.00 ± 0.00
Pe	8.54 ± 0.97	3.47 ± 0.39	1.41 ± 0.16	0.43 ± 0.05
Ho	3.47 ± 0.33	2.04 ± 0.16	1.32 ± 0.08	0.89 ± 0.03
Vo	2.63 ± 0.21	1.54 ± 0.10	1.00 ± 0.05	0.67 ± 0.02
At1	3.42 ± 0.39	1.71 ± 0.19	0.86 ± 0.10	0.34 ± 0.04
At2	3.66 ± 0.36	2.07 ± 0.18	1.28 ± 0.09	0.80 ± 0.04
Po1	4.10 ± 0.47	2.90 ± 0.33	2.05 ± 0.23	1.30 ± 0.15
Po2	3.54 ± 0.40	2.50 ± 0.28	1.77 ± 0.20	1.12 ± 0.13

B.3 Extreme Values from Wind Distributions

Table B.15: JMH02

(a) Runup model B11						(b) Runup model B12					
Year	U_{10}	H_S	T_P	ξ_P	R_2	Year	U_{10}	H_S	T_P	ξ_P	R_2
1	30.7	17.2	19.6	0.59	13.4	1	30.7	17.2	19.6	0.59	14.8
10	35.0	22.5	22.4	0.59	17.5	10	35.0	22.5	22.4	0.59	19.3
100	39.0	27.9	25.0	0.59	21.7	100	39.0	27.9	25.0	0.59	24.0
1000	42.7	33.4	27.3	0.59	26.0	1000	42.7	33.4	27.3	0.59	28.8
10000	46.2	39.2	29.6	0.59	30.4	10000	46.2	39.2	29.6	0.59	33.7

(c) Runup model B1d						(d) Runup model Sc					
Year	U_{10}	H_S	T_P	ξ_P	R_2	Year	U_{10}	H_S	T_P	ξ_P	R_2
1	30.7	17.2	19.6	0.59	-0.861	1	30.7	17.2	19.6	0.59	-0.539
10	35.0	22.5	22.4	0.59	-1.123	10	35.0	22.5	22.4	0.59	-0.702
100	39.0	27.9	25.0	0.59	-1.393	100	39.0	27.9	25.0	0.59	-0.871
1000	42.7	33.4	27.3	0.59	-1.671	1000	42.7	33.4	27.3	0.59	-1.045
10000	46.2	39.2	29.6	0.59	-1.956	10000	46.2	39.2	29.6	0.59	-1.224

(e) Runup model Pe						(f) Runup model Ho					
Year	U_{10}	H_S	T_P	ξ_P	R_2	Year	U_{10}	H_S	T_P	ξ_P	R_2
1	30.7	17.2	19.6	0.59	20.4	1	30.7	17.2	19.6	0.59	11.9
10	35.0	22.5	22.4	0.59	26.6	10	35.0	22.5	22.4	0.59	15.5
100	39.0	27.9	25.0	0.59	33.0	100	39.0	27.9	25.0	0.59	19.2
1000	42.7	33.4	27.3	0.59	39.6	1000	42.7	33.4	27.3	0.59	23.1
10000	46.2	39.2	29.6	0.59	46.4	10000	46.2	39.2	29.6	0.59	27.0

Table B.15: (Continued)

(g) Runup model Vo						(h) Runup model At1					
Year	U_{10}	H_S	T_P	ξ_P	R_2	Year	U_{10}	H_S	T_P	ξ_P	R_2
1	30.7	17.2	19.6	0.59	6.8	1	30.7	17.2	19.6	0.59	10.1
10	35.0	22.5	22.4	0.59	8.8	10	35.0	22.5	22.4	0.59	13.1
100	39.0	27.9	25.0	0.59	10.8	100	39.0	27.9	25.0	0.59	16.3
1000	42.7	33.4	27.3	0.59	12.9	1000	42.7	33.4	27.3	0.59	19.6
10000	46.2	39.2	29.6	0.59	15.0	10000	46.2	39.2	29.6	0.59	22.9

(i) Runup model At2						(j) Runup model Po1					
Year	U_{10}	H_S	T_P	ξ_P	R_2	Year	U_{10}	H_S	T_P	ξ_P	R_2
1	30.7	17.2	19.6	0.59	12.1	1	30.7	17.2	19.6	0.59	37.1
10	35.0	22.5	22.4	0.59	15.8	10	35.0	22.5	22.4	0.59	55.2
100	39.0	27.9	25.0	0.59	19.6	100	39.0	27.9	25.0	0.59	76.3
1000	42.7	33.4	27.3	0.59	23.5	1000	42.7	33.4	27.3	0.59	100.2
10000	46.2	39.2	29.6	0.59	27.5	10000	46.2	39.2	29.6	0.59	126.9

(k) Runup model Po2					
Year	U_{10}	H_S	T_P	ξ_P	R_2
1	30.7	17.2	19.6	0.59	35.3
10	35.0	22.5	22.4	0.59	52.6
100	39.0	27.9	25.0	0.59	72.6
1000	42.7	33.4	27.3	0.59	95.4
10000	46.2	39.2	29.6	0.59	120.9

Table B.16: MR15 (1)

(a) Runup model B11						(b) Runup model B12					
Year	U_{10}	H_S	T_P	ξ_P	R_2	Year	U_{10}	H_S	T_P	ξ_P	R_2
1	20.1	7.4	12.9	0.59	5.7	1	20.1	7.4	12.9	0.59	6.3
10	21.8	8.7	14.0	0.59	6.8	10	21.8	8.7	14.0	0.59	7.5
100	23.4	10.0	15.0	0.59	7.8	100	23.4	10.0	15.0	0.59	8.6
1000	24.8	11.3	15.9	0.59	8.8	1000	24.8	11.3	15.9	0.59	9.7
10000	26.2	12.6	16.8	0.59	9.8	10000	26.2	12.6	16.8	0.59	10.8

(c) Runup model B1d						(d) Runup model Sc					
Year	U_{10}	H_S	T_P	ξ_P	R_2	Year	U_{10}	H_S	T_P	ξ_P	R_2
1	20.1	7.4	12.9	0.59	-0.369	1	20.1	7.4	12.9	0.59	-0.231
10	21.8	8.7	14.0	0.59	-0.436	10	21.8	8.7	14.0	0.59	-0.273
100	23.4	10.0	15.0	0.59	-0.502	100	23.4	10.0	15.0	0.59	-0.314
1000	24.8	11.3	15.9	0.59	-0.566	1000	24.8	11.3	15.9	0.59	-0.354
10000	26.2	12.6	16.8	0.59	-0.629	10000	26.2	12.6	16.8	0.59	-0.394

(e) Runup model Pe						(f) Runup model Ho					
Year	U_{10}	H_S	T_P	ξ_P	R_2	Year	U_{10}	H_S	T_P	ξ_P	R_2
1	20.1	7.4	12.9	0.59	8.7	1	20.1	7.4	12.9	0.59	5.1
10	21.8	8.7	14.0	0.59	10.3	10	21.8	8.7	14.0	0.59	6.0
100	23.4	10.0	15.0	0.59	11.9	100	23.4	10.0	15.0	0.59	6.9
1000	24.8	11.3	15.9	0.59	13.4	1000	24.8	11.3	15.9	0.59	7.8
10000	26.2	12.6	16.8	0.59	14.9	10000	26.2	12.6	16.8	0.59	8.7

Table B.16: (Continued)

(g) Runup model Vo						(h) Runup model At1					
Year	U_{10}	H_S	T_P	ξ_P	R_2	Year	U_{10}	H_S	T_P	ξ_P	R_2
1	20.1	7.4	12.9	0.59	3.2	1	20.1	7.4	12.9	0.59	4.3
10	21.8	8.7	14.0	0.59	3.7	10	21.8	8.7	14.0	0.59	5.1
100	23.4	10.0	15.0	0.59	4.2	100	23.4	10.0	15.0	0.59	5.9
1000	24.8	11.3	15.9	0.59	4.7	1000	24.8	11.3	15.9	0.59	6.6
10000	26.2	12.6	16.8	0.59	5.1	10000	26.2	12.6	16.8	0.59	7.4

(i) Runup model At2						(j) Runup model Po1					
Year	U_{10}	H_S	T_P	ξ_P	R_2	Year	U_{10}	H_S	T_P	ξ_P	R_2
1	20.1	7.4	12.9	0.59	5.2	1	20.1	7.4	12.9	0.59	10.4
10	21.8	8.7	14.0	0.59	6.1	10	21.8	8.7	14.0	0.59	13.4
100	23.4	10.0	15.0	0.59	7.1	100	23.4	10.0	15.0	0.59	16.5
1000	24.8	11.3	15.9	0.59	8.0	1000	24.8	11.3	15.9	0.59	19.8
10000	26.2	12.6	16.8	0.59	8.9	10000	26.2	12.6	16.8	0.59	23.2

(k) Runup model Po2					
Year	U_{10}	H_S	T_P	ξ_P	R_2
1	20.1	7.4	12.9	0.59	9.9
10	21.8	8.7	14.0	0.59	12.7
100	23.4	10.0	15.0	0.59	15.7
1000	24.8	11.3	15.9	0.59	18.8
10000	26.2	12.6	16.8	0.59	22.1

Table B.17: MR15 (2)

(a) Runup model B11						(b) Runup model B12					
Year	U_{10}	H_S	T_P	ξ_P	R_2	Year	U_{10}	H_S	T_P	ξ_P	R_2
1	29.0	15.4	18.6	0.59	12.0	1	29.0	15.4	18.6	0.59	13.3
10	31.3	18.0	20.1	0.59	14.0	10	31.3	18.0	20.1	0.59	15.5
100	33.5	20.5	21.4	0.59	16.0	100	33.5	20.5	21.4	0.59	17.7
1000	35.4	23.0	22.7	0.59	17.9	1000	35.4	23.0	22.7	0.59	19.8
10000	37.2	25.4	23.8	0.59	19.7	10000	37.2	25.4	23.8	0.59	21.8

(c) Runup model B1d						(d) Runup model Sc					
Year	U_{10}	H_S	T_P	ξ_P	R_2	Year	U_{10}	H_S	T_P	ξ_P	R_2
1	29.0	15.4	18.6	0.59	-0.770	1	29.0	15.4	18.6	0.59	-0.482
10	31.3	18.0	20.1	0.59	-0.901	10	31.3	18.0	20.1	0.59	-0.563
100	33.5	20.5	21.4	0.59	-1.027	100	33.5	20.5	21.4	0.59	-0.642
1000	35.4	23.0	22.7	0.59	-1.149	1000	35.4	23.0	22.7	0.59	-0.719
10000	37.2	25.4	23.8	0.59	-1.269	10000	37.2	25.4	23.8	0.59	-0.794

(e) Runup model Pe						(f) Runup model Ho					
Year	U_{10}	H_S	T_P	ξ_P	R_2	Year	U_{10}	H_S	T_P	ξ_P	R_2
1	29.0	15.4	18.6	0.59	18.3	1	29.0	15.4	18.6	0.59	10.6
10	31.3	18.0	20.1	0.59	21.4	10	31.3	18.0	20.1	0.59	12.4
100	33.5	20.5	21.4	0.59	24.3	100	33.5	20.5	21.4	0.59	14.2
1000	35.4	23.0	22.7	0.59	27.2	1000	35.4	23.0	22.7	0.59	15.9
10000	37.2	25.4	23.8	0.59	30.1	10000	37.2	25.4	23.8	0.59	17.5

Table B.17: (Continued)

(g) Runup model Vo						(h) Runup model At1					
Year	U_{10}	H_S	T_P	ξ_P	R_2	Year	U_{10}	H_S	T_P	ξ_P	R_2
1	29.0	15.4	18.6	0.59	6.2	1	29.0	15.4	18.6	0.59	9.0
10	31.3	18.0	20.1	0.59	7.1	10	31.3	18.0	20.1	0.59	10.5
100	33.5	20.5	21.4	0.59	8.1	100	33.5	20.5	21.4	0.59	12.0
1000	35.4	23.0	22.7	0.59	9.0	1000	35.4	23.0	22.7	0.59	13.5
10000	37.2	25.4	23.8	0.59	9.9	10000	37.2	25.4	23.8	0.59	14.9

(i) Runup model At2						(j) Runup model Po1					
Year	U_{10}	H_S	T_P	ξ_P	R_2	Year	U_{10}	H_S	T_P	ξ_P	R_2
1	29.0	15.4	18.6	0.59	10.8	1	29.0	15.4	18.6	0.59	31.4
10	31.3	18.0	20.1	0.59	12.7	10	31.3	18.0	20.1	0.59	39.6
100	33.5	20.5	21.4	0.59	14.5	100	33.5	20.5	21.4	0.59	48.3
1000	35.4	23.0	22.7	0.59	16.2	1000	35.4	23.0	22.7	0.59	57.2
10000	37.2	25.4	23.8	0.59	17.9	10000	37.2	25.4	23.8	0.59	66.3

(k) Runup model Po2					
Year	U_{10}	H_S	T_P	ξ_P	R_2
1	29.0	15.4	18.6	0.59	29.9
10	31.3	18.0	20.1	0.59	37.8
100	33.5	20.5	21.4	0.59	46.0
1000	35.4	23.0	22.7	0.59	54.4
10000	37.2	25.4	23.8	0.59	63.1

Table B.18: BG15

(a) Runup model B11						(b) Runup model B12					
Year	U_{10}	H_S	T_P	ξ_P	R_2	Year	U_{10}	H_S	T_P	ξ_P	R_2
1	9.1	1.5	5.8	0.59	1.2	1	9.1	1.5	5.8	0.59	1.3
10	9.2	1.6	5.9	0.59	1.2	10	9.2	1.6	5.9	0.59	1.3
100	9.3	1.6	6.0	0.59	1.2	100	9.3	1.6	6.0	0.59	1.4
1000	9.5	1.6	6.1	0.59	1.3	1000	9.5	1.6	6.1	0.59	1.4
10000	9.5	1.7	6.1	0.59	1.3	10000	9.5	1.7	6.1	0.59	1.4

(c) Runup model B1d						(d) Runup model Sc					
Year	U_{10}	H_S	T_P	ξ_P	R_2	Year	U_{10}	H_S	T_P	ξ_P	R_2
1	9.1	1.5	5.8	0.59	-0.076	1	9.1	1.5	5.8	0.59	-0.047
10	9.2	1.6	5.9	0.59	-0.078	10	9.2	1.6	5.9	0.59	-0.049
100	9.3	1.6	6.0	0.59	-0.080	100	9.3	1.6	6.0	0.59	-0.050
1000	9.5	1.6	6.1	0.59	-0.082	1000	9.5	1.6	6.1	0.59	-0.051
10000	9.5	1.7	6.1	0.59	-0.083	10000	9.5	1.7	6.1	0.59	-0.052

(e) Runup model Pe						(f) Runup model Ho					
Year	U_{10}	H_S	T_P	ξ_P	R_2	Year	U_{10}	H_S	T_P	ξ_P	R_2
1	9.1	1.5	5.8	0.59	1.8	1	9.1	1.5	5.8	0.59	1.0
10	9.2	1.6	5.9	0.59	1.9	10	9.2	1.6	5.9	0.59	1.1
100	9.3	1.6	6.0	0.59	1.9	100	9.3	1.6	6.0	0.59	1.1
1000	9.5	1.6	6.1	0.59	1.9	1000	9.5	1.6	6.1	0.59	1.1
10000	9.5	1.7	6.1	0.59	2.0	10000	9.5	1.7	6.1	0.59	1.2

Table B.18: (Continued)

(g) Runup model Vo						(h) Runup model At1					
Year	U_{10}	H_S	T_P	ξ_P	R_2	Year	U_{10}	H_S	T_P	ξ_P	R_2
1	9.1	1.5	5.8	0.59	1.0	1	9.1	1.5	5.8	0.59	0.9
10	9.2	1.6	5.9	0.59	1.0	10	9.2	1.6	5.9	0.59	0.9
100	9.3	1.6	6.0	0.59	1.0	100	9.3	1.6	6.0	0.59	0.9
1000	9.5	1.6	6.1	0.59	1.1	1000	9.5	1.6	6.1	0.59	1.0
10000	9.5	1.7	6.1	0.59	1.1	10000	9.5	1.7	6.1	0.59	1.0

(i) Runup model At2						(j) Runup model Po1					
Year	U_{10}	H_S	T_P	ξ_P	R_2	Year	U_{10}	H_S	T_P	ξ_P	R_2
1	9.1	1.5	5.8	0.59	1.1	1	9.1	1.5	5.8	0.59	1.0
10	9.2	1.6	5.9	0.59	1.1	10	9.2	1.6	5.9	0.59	1.0
100	9.3	1.6	6.0	0.59	1.1	100	9.3	1.6	6.0	0.59	1.1
1000	9.5	1.6	6.1	0.59	1.2	1000	9.5	1.6	6.1	0.59	1.1
10000	9.5	1.7	6.1	0.59	1.2	10000	9.5	1.7	6.1	0.59	1.1

(k) Runup model Po2					
Year	U_{10}	H_S	T_P	ξ_P	R_2
1	9.1	1.5	5.8	0.59	0.9
10	9.2	1.6	5.9	0.59	1.0
100	9.3	1.6	6.0	0.59	1.0
1000	9.5	1.6	6.1	0.59	1.0
10000	9.5	1.7	6.1	0.59	1.1

B.4 Contour Lines with Runup Models

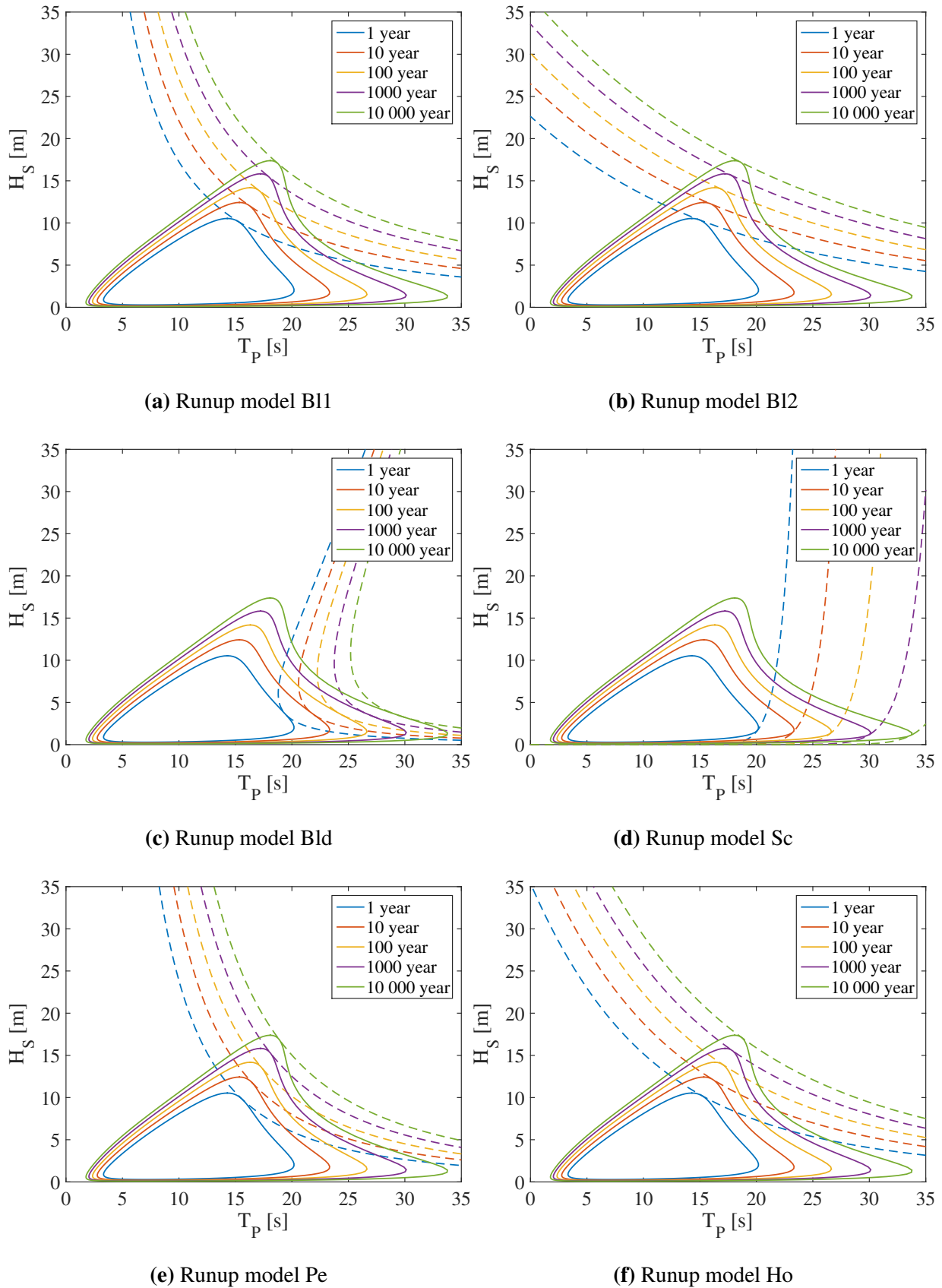
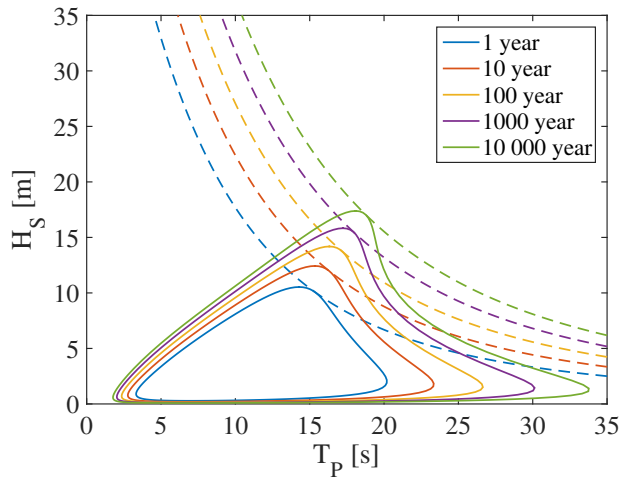
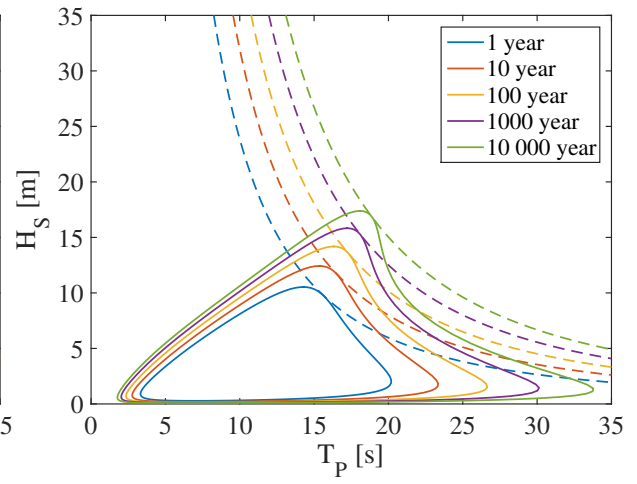


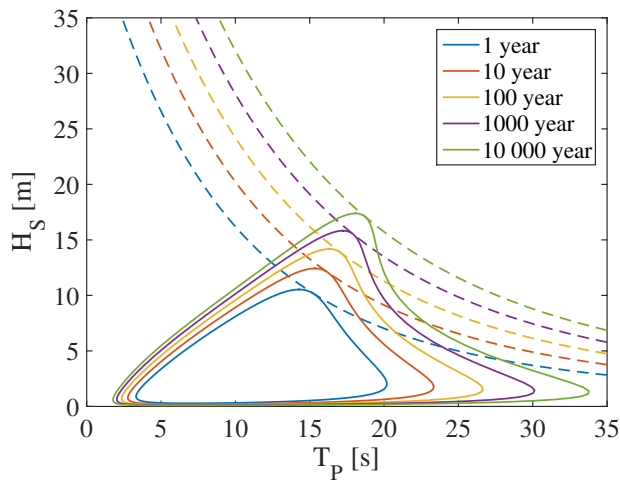
Figure B.1: MGAU05



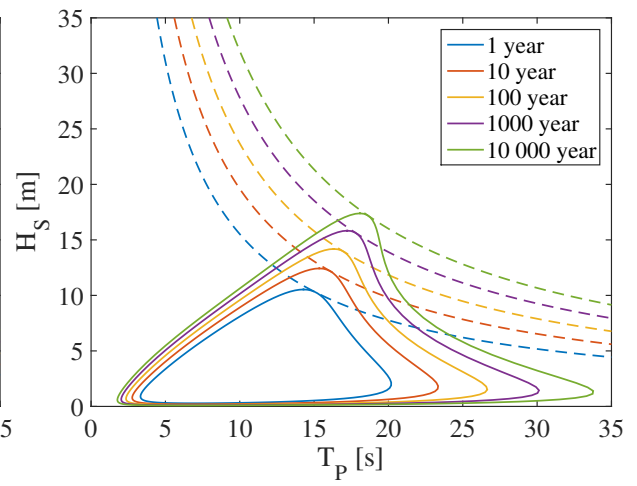
(g) Runup model Vo



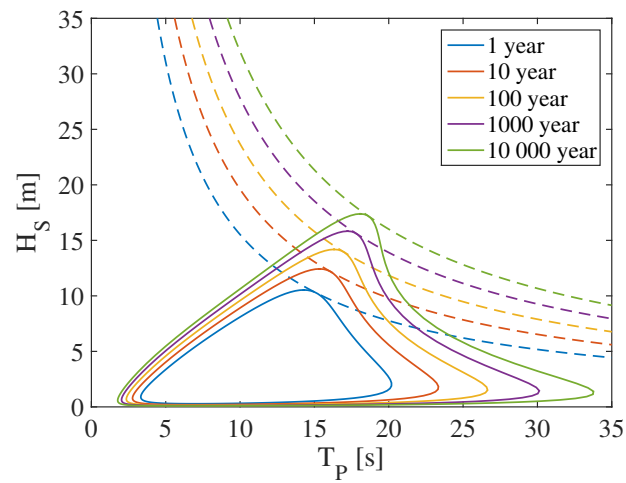
(h) Runup model At1



(i) Runup model At2

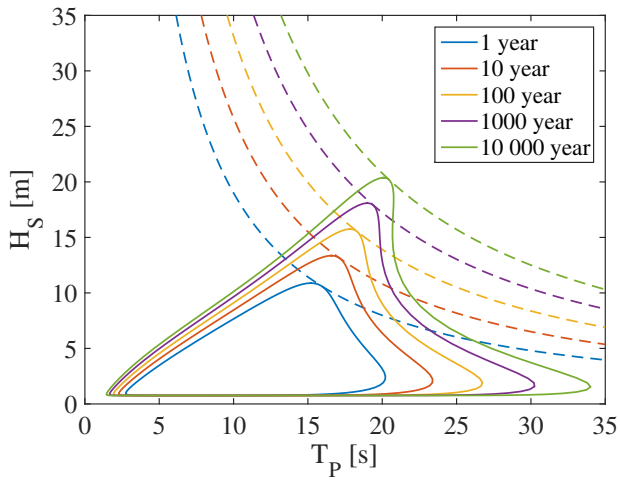


(j) Runup model Po1

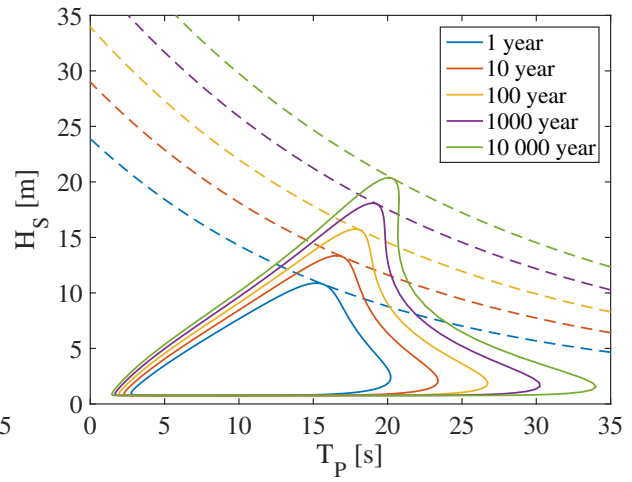


(k) Runup model Po2

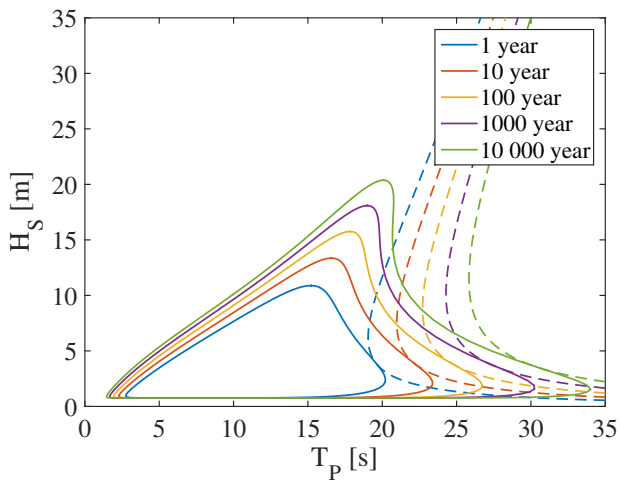
Figure B.1: (Continued)



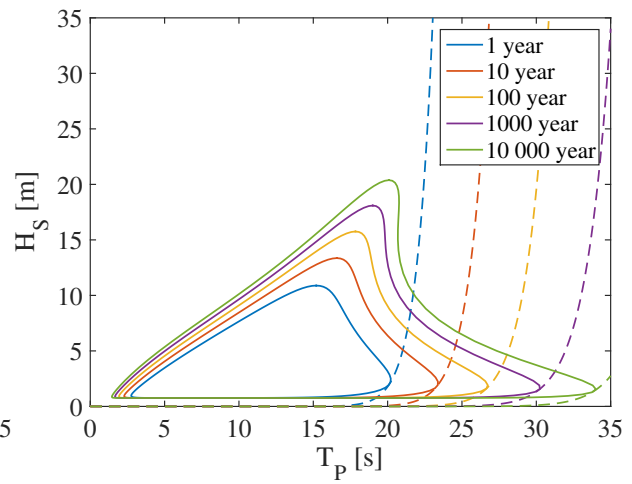
(a) Runup model B11



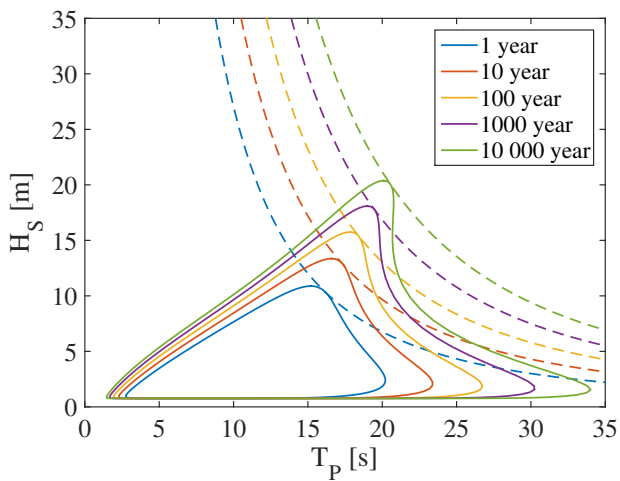
(b) Runup model B12



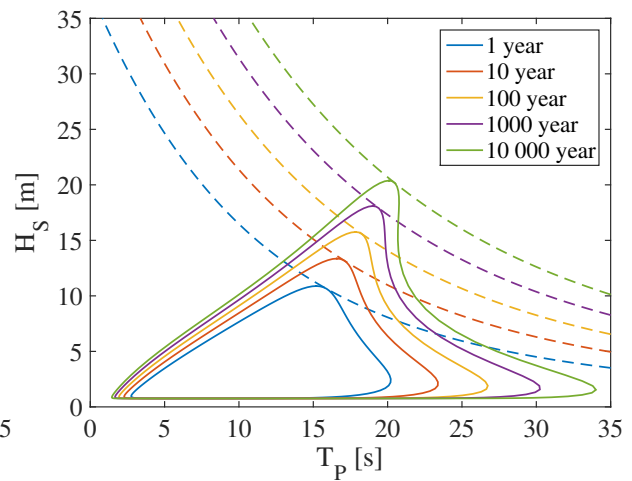
(c) Runup model B1d



(d) Runup model Sc

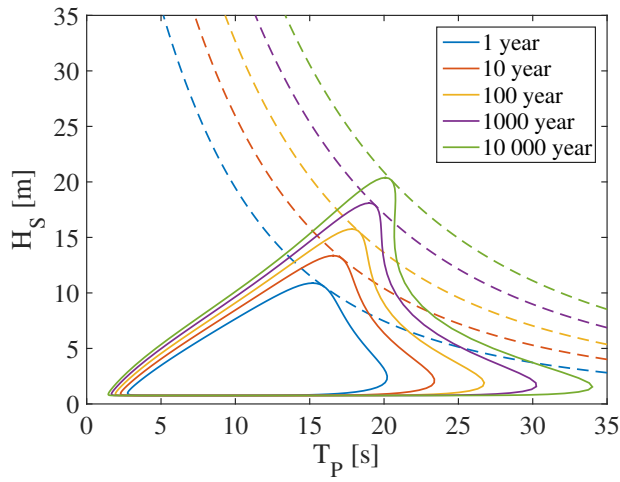


(e) Runup model Pe

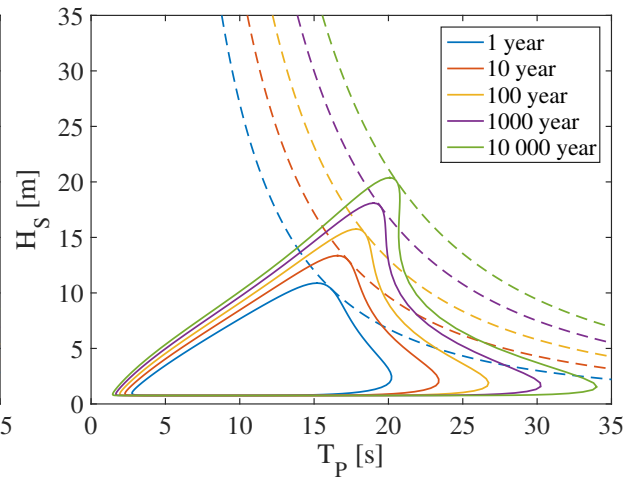


(f) Runup model Ho

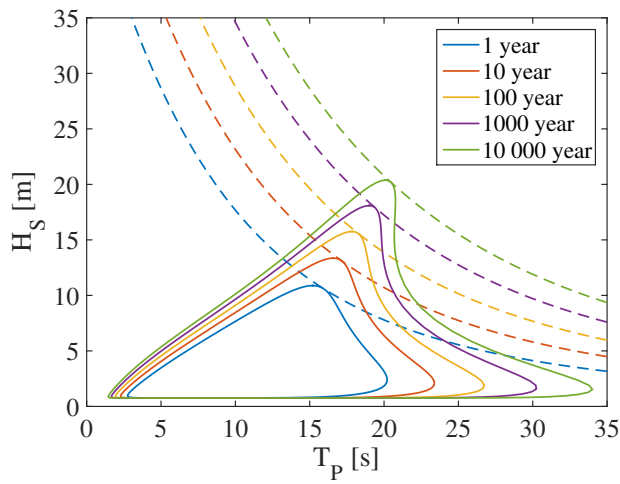
Figure B.2: OHG16



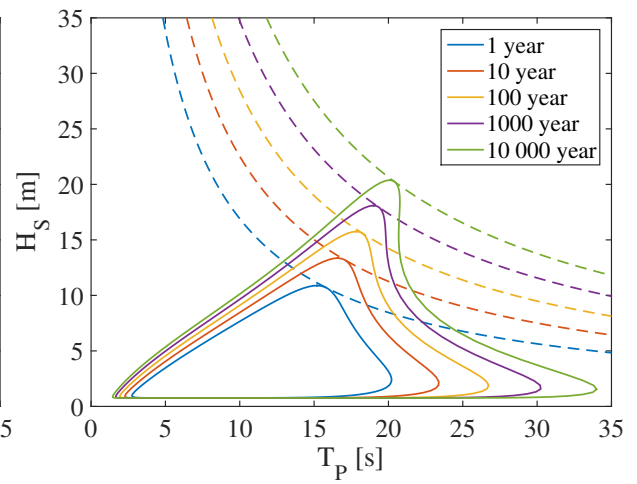
(g) Runup model Vo



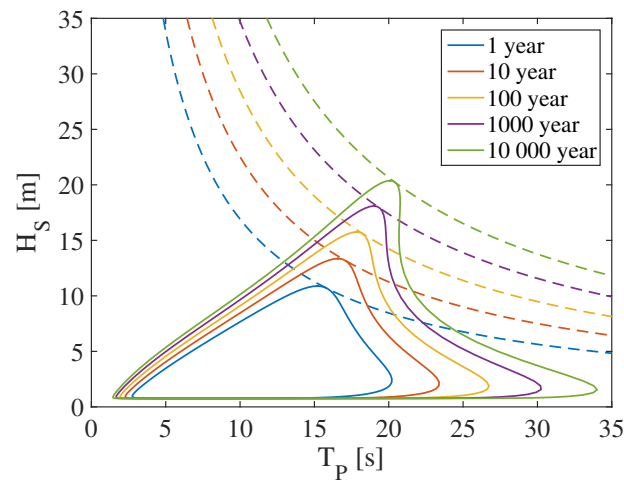
(h) Runup model At1



(i) Runup model At2

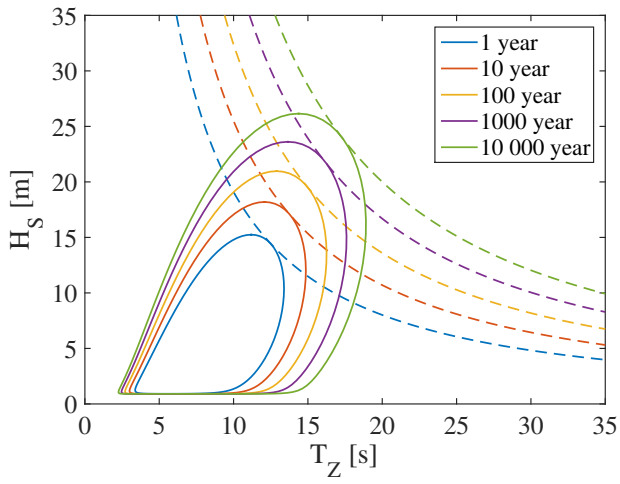


(j) Runup model Po1

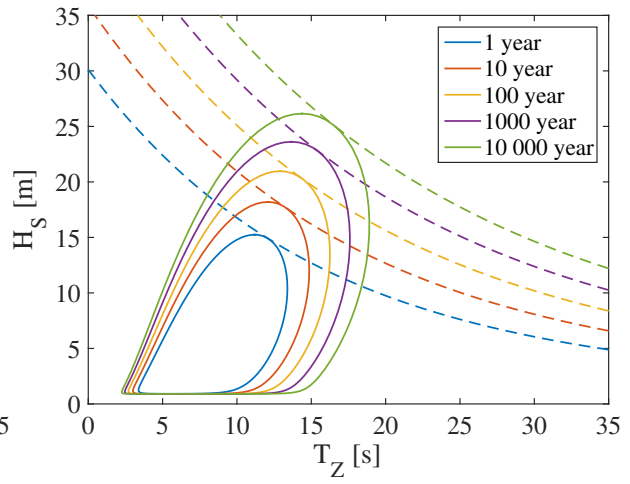


(k) Runup model Po2

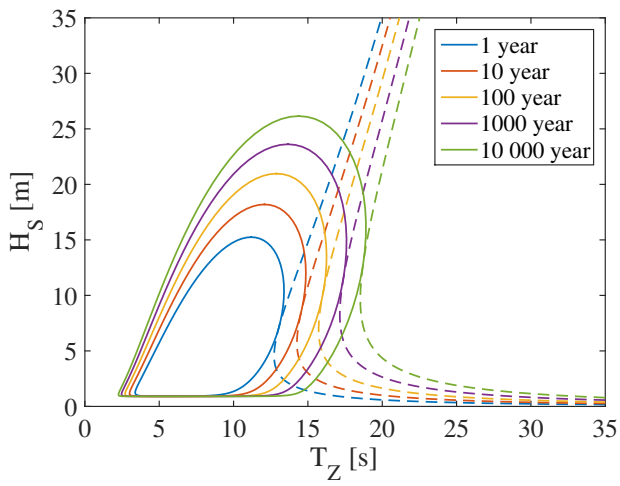
Figure B.2: (Continued)



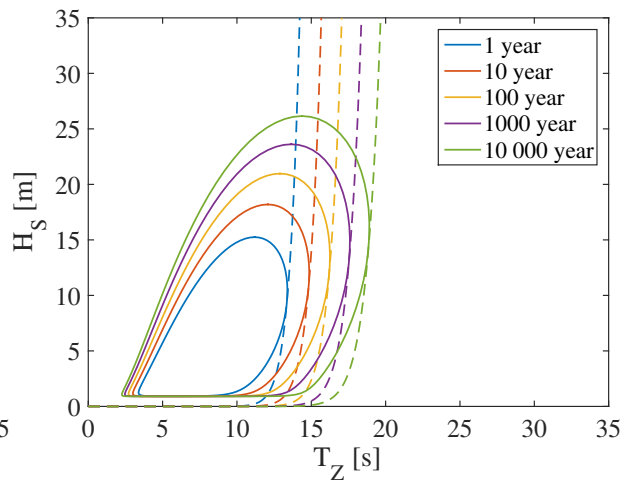
(a) Runup model B11



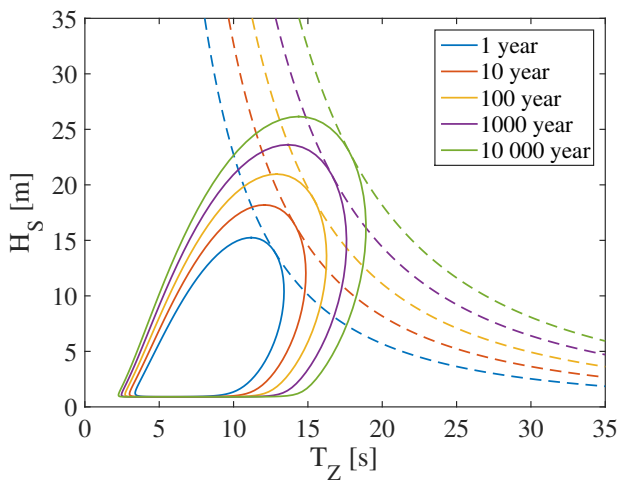
(b) Runup model B12



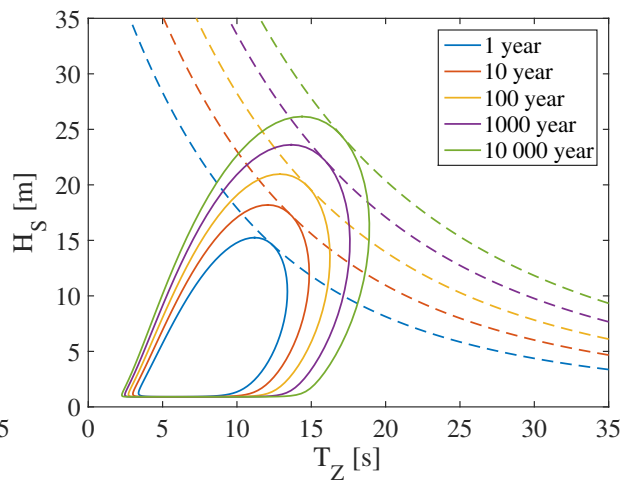
(c) Runup model B1d



(d) Runup model Sc

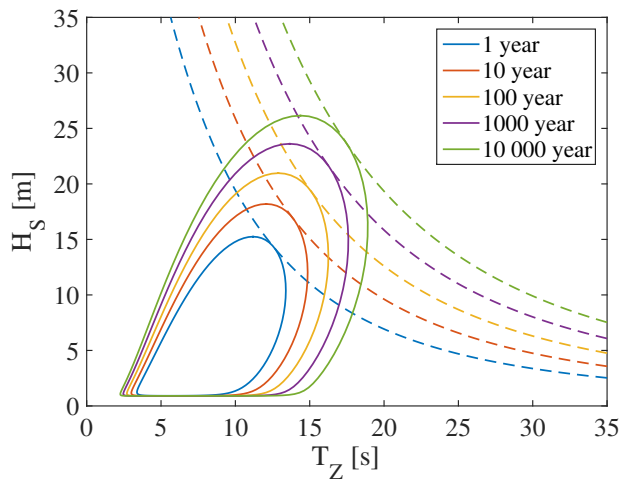


(e) Runup model Pe

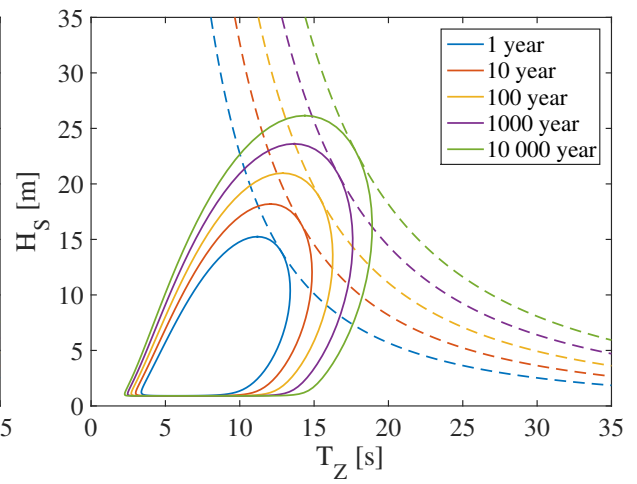


(f) Runup model Ho

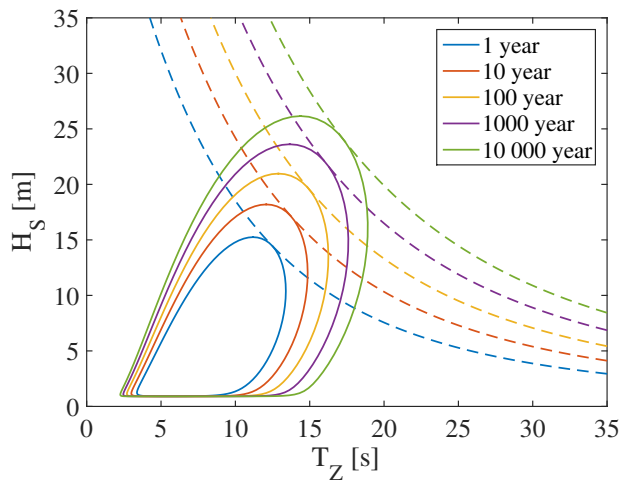
Figure B.3: BGS07 (1)



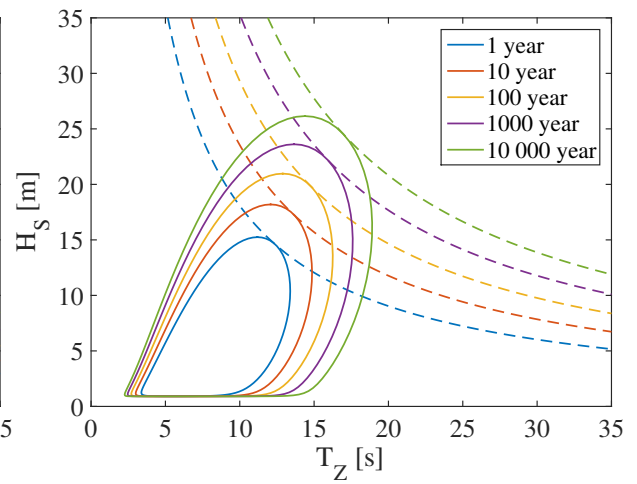
(g) Runup model Vo



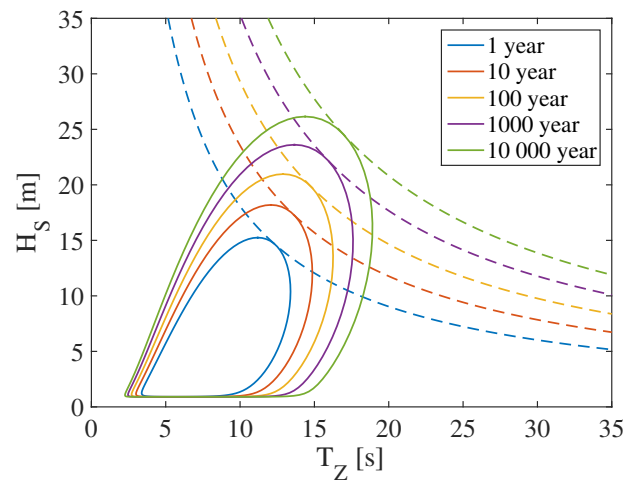
(h) Runup model At1



(i) Runup model At2

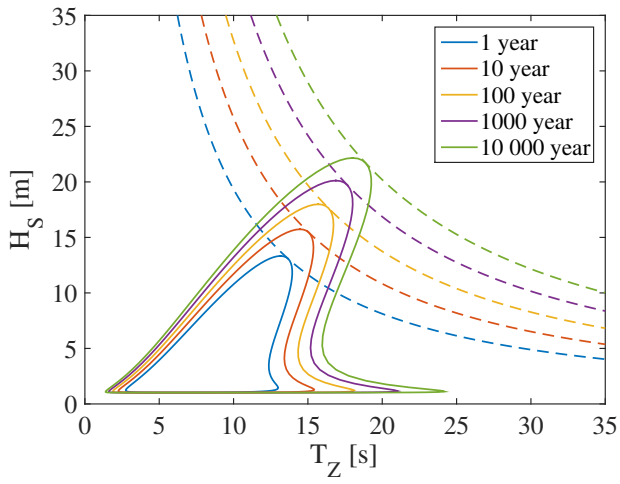


(j) Runup model Po1

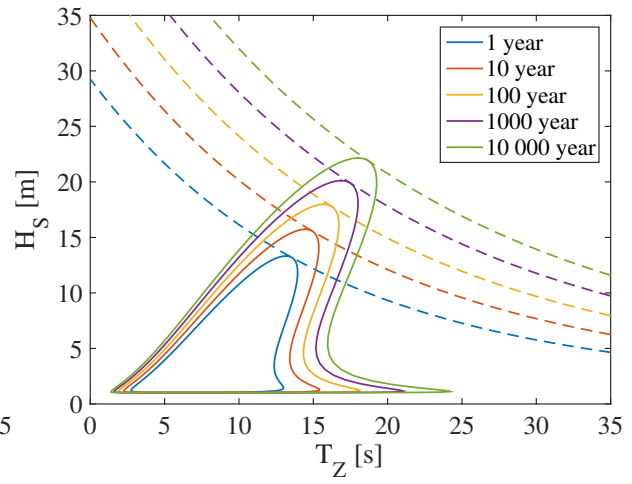


(k) Runup model Po2

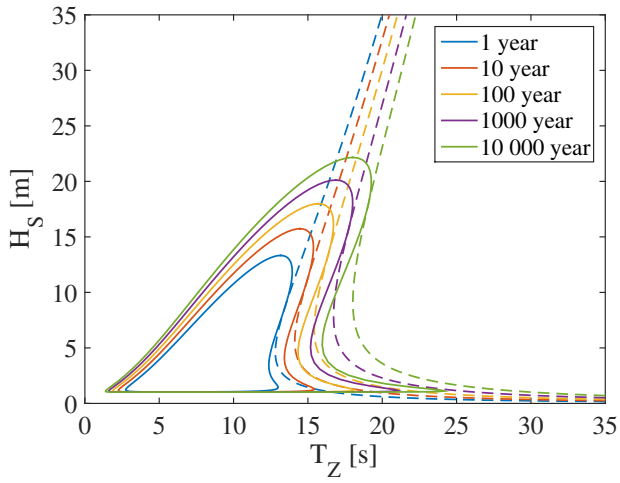
Figure B.3: (Continued)



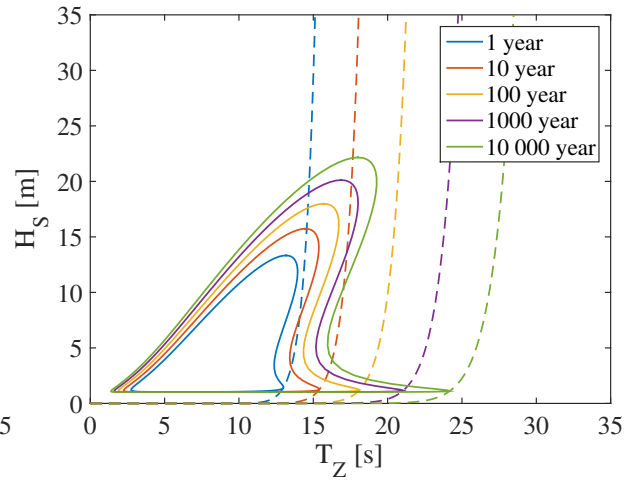
(a) Runup model B11



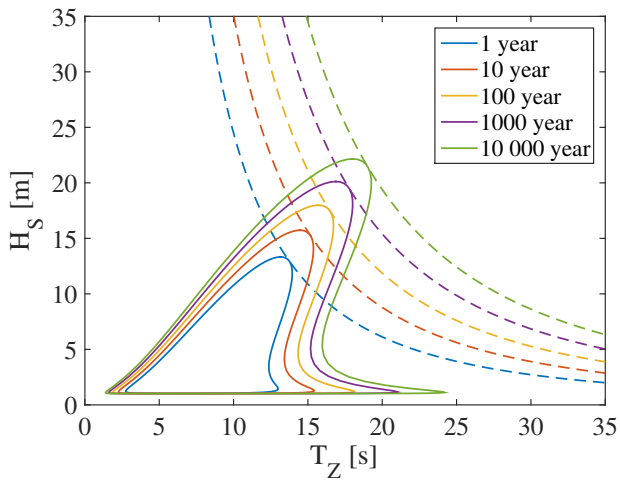
(b) Runup model B12



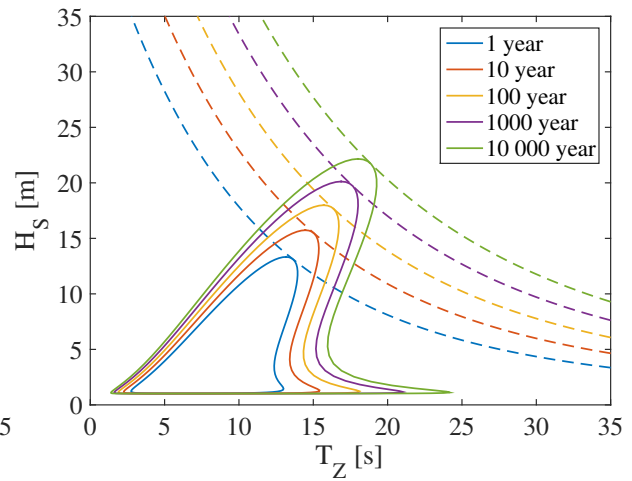
(c) Runup model B1d



(d) Runup model Sc

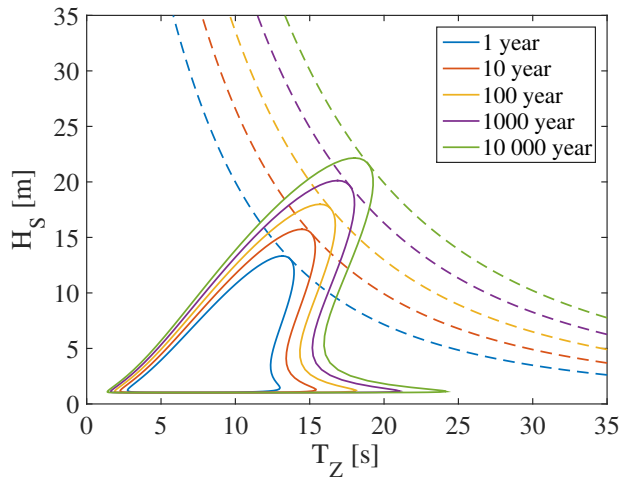


(e) Runup model Pe

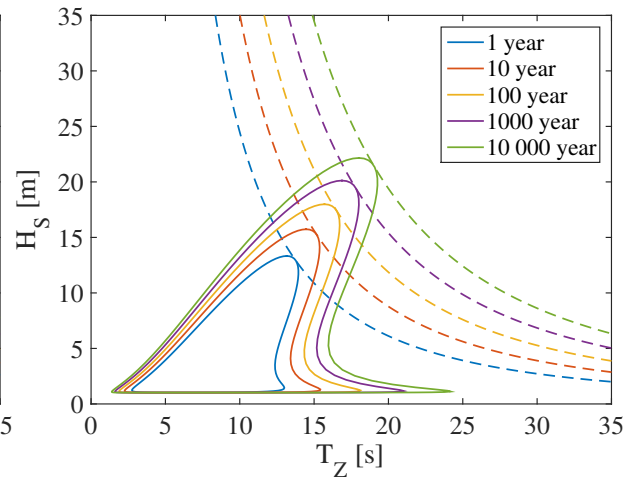


(f) Runup model Ho

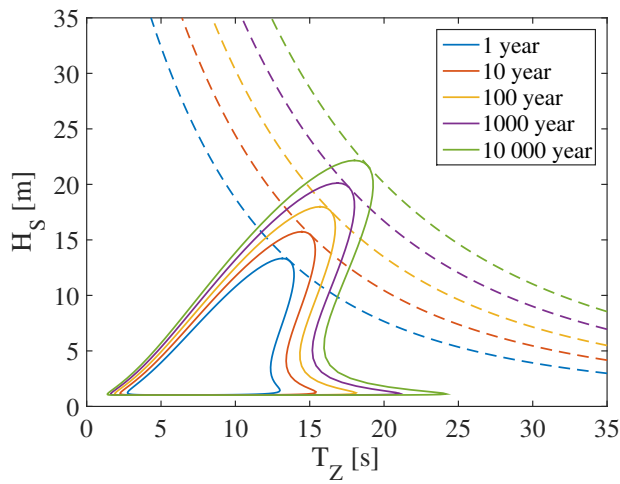
Figure B.4: BGS07 (2)



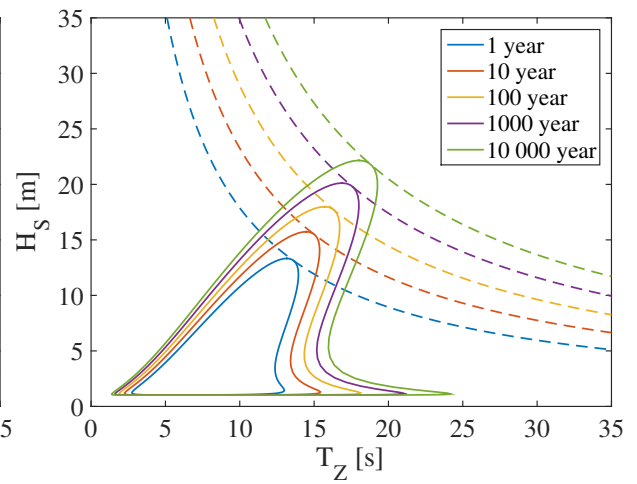
(g) Runup model Vo



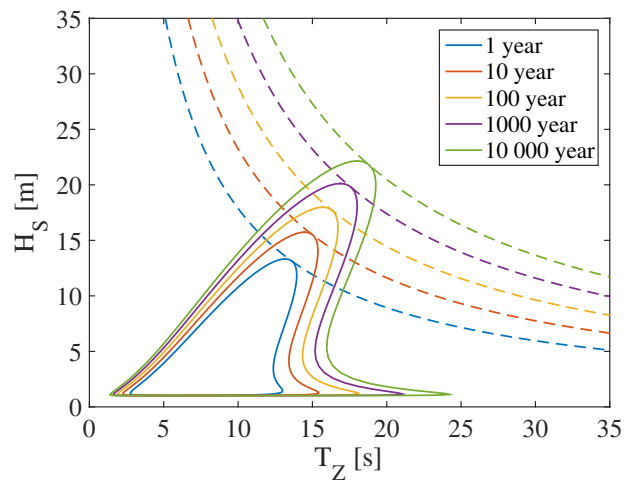
(h) Runup model At1



(i) Runup model At2

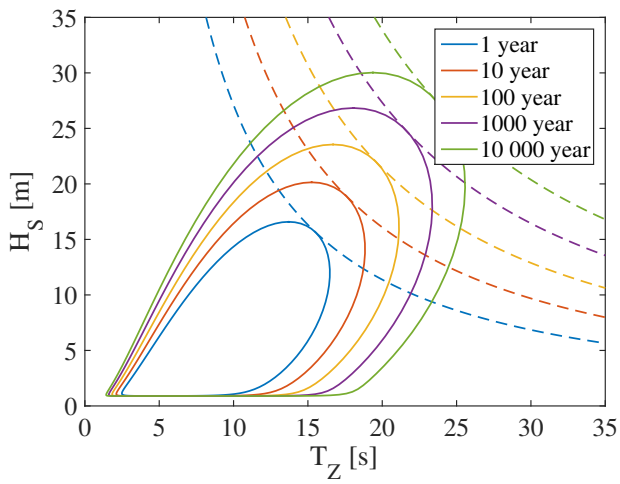


(j) Runup model Po1

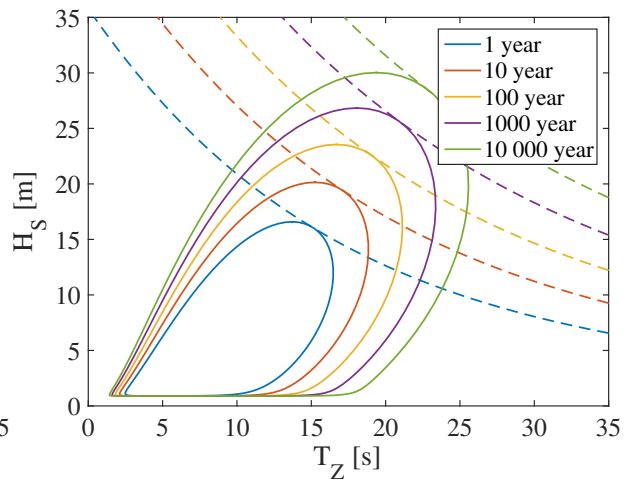


(k) Runup model Po2

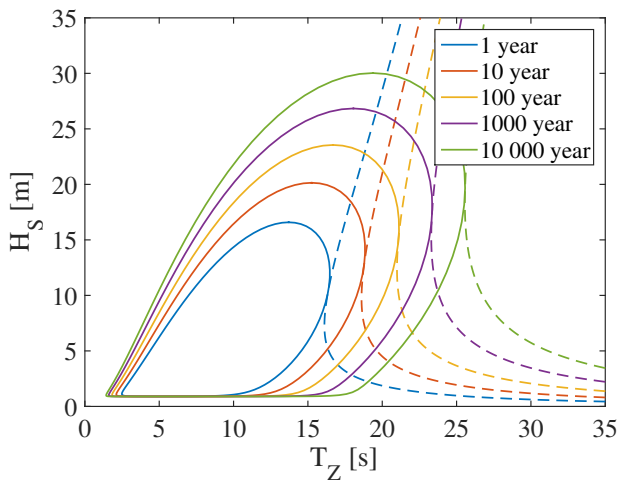
Figure B.4: (Continued)



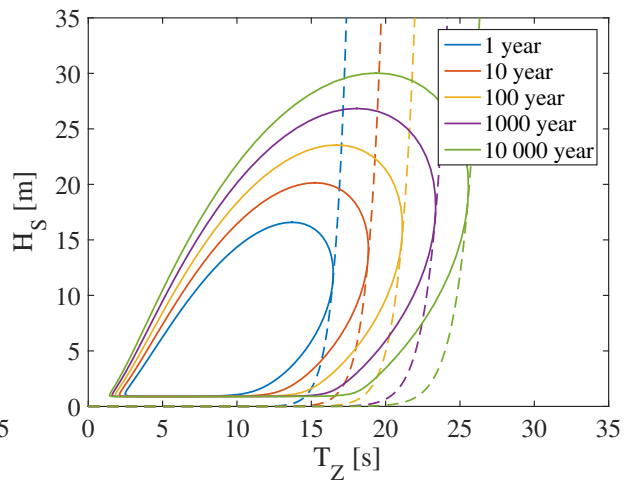
(a) Runup model B11



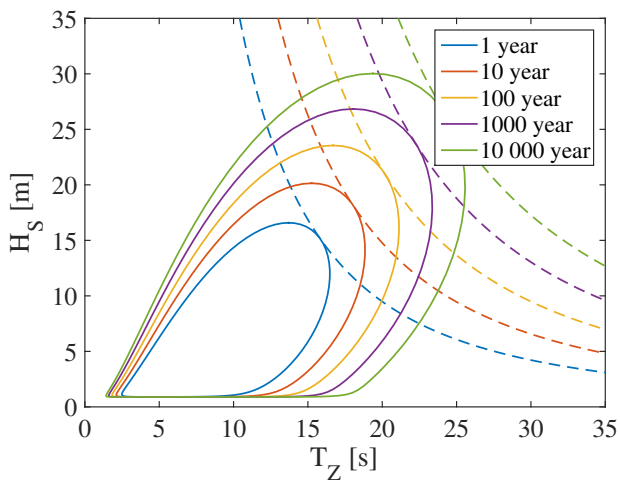
(b) Runup model B12



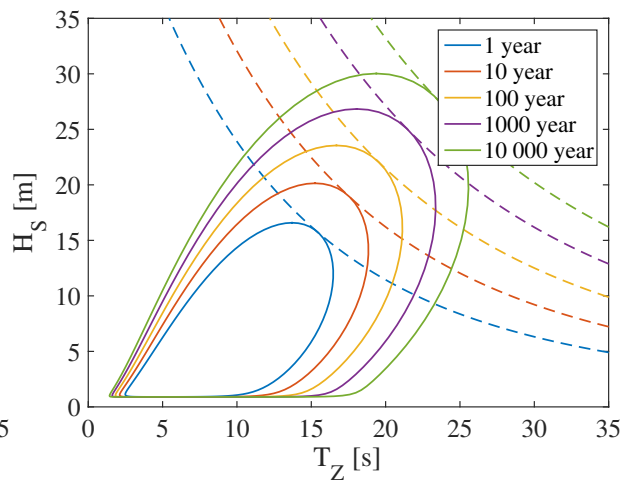
(c) Runup model B1d



(d) Runup model Sc

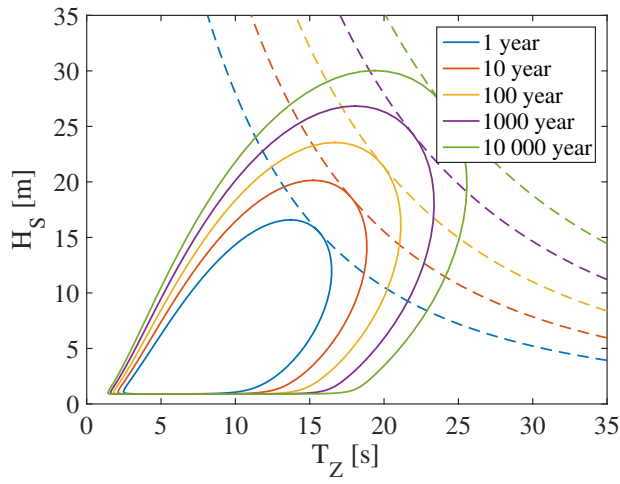


(e) Runup model Pe

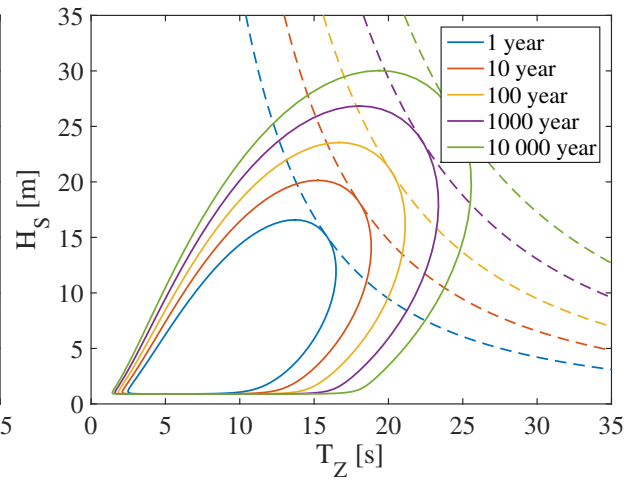


(f) Runup model Ho

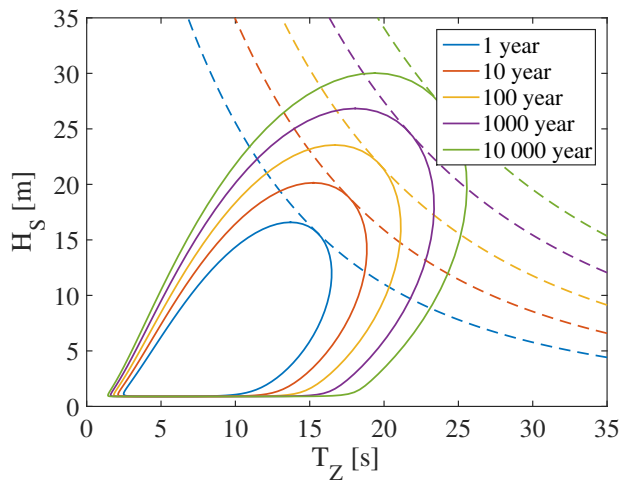
Figure B.5: BGS07 (3)



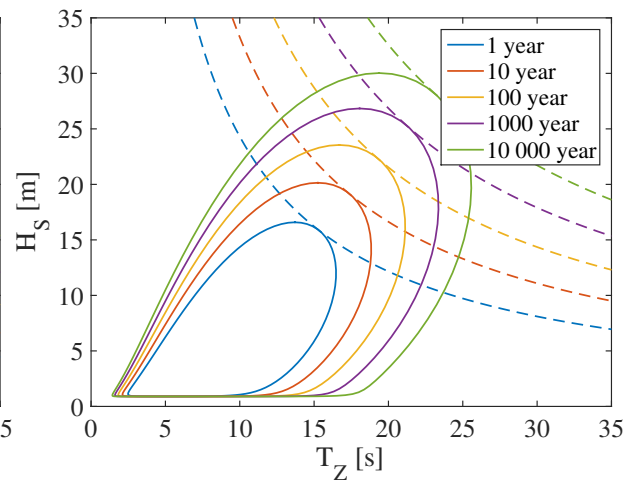
(g) Runup model Vo



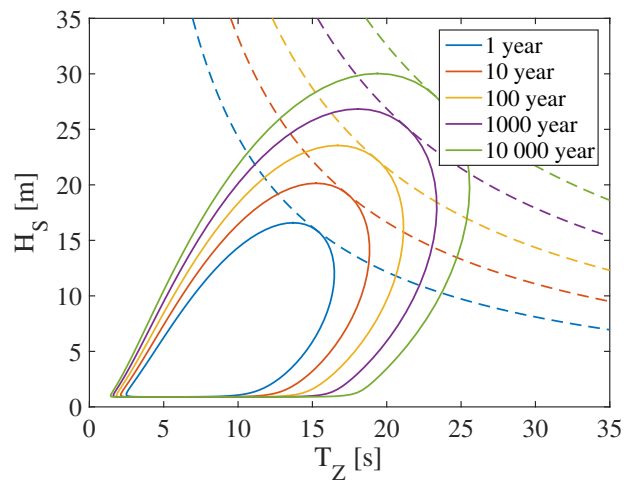
(h) Runup model At1



(i) Runup model At2

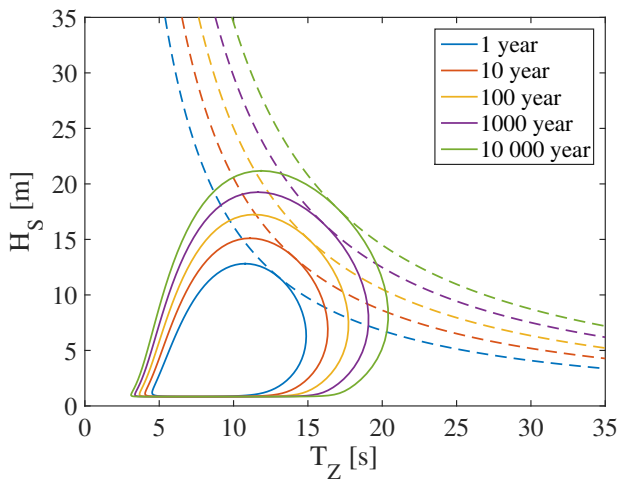


(j) Runup model Po1

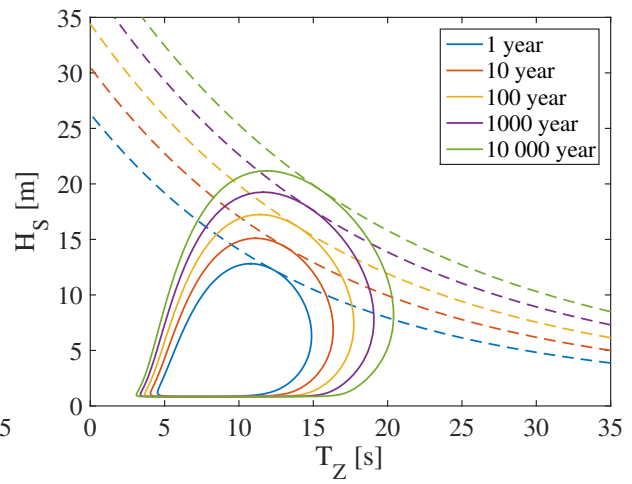


(k) Runup model Po2

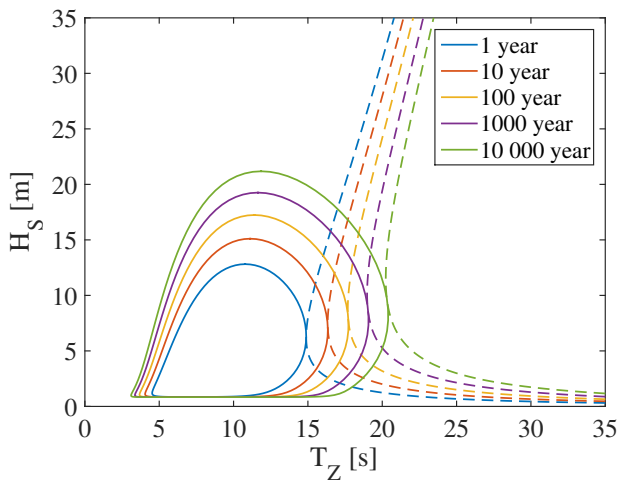
Figure B.5: (Continued)



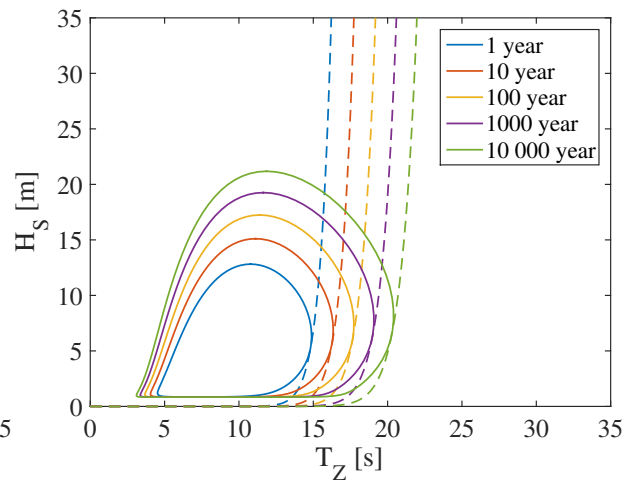
(a) Runup model B11



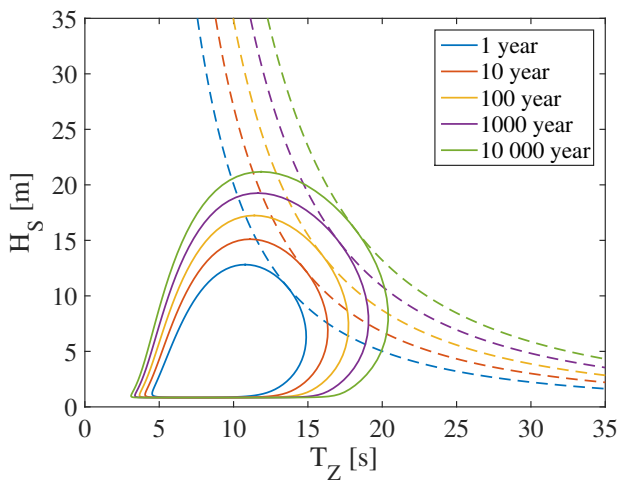
(b) Runup model B12



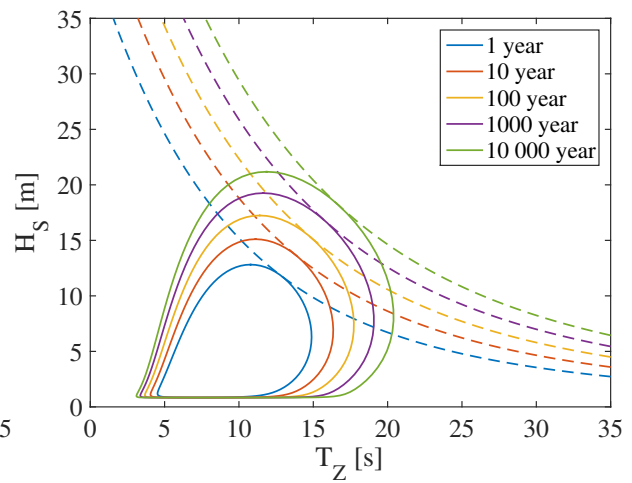
(c) Runup model B1d



(d) Runup model Sc

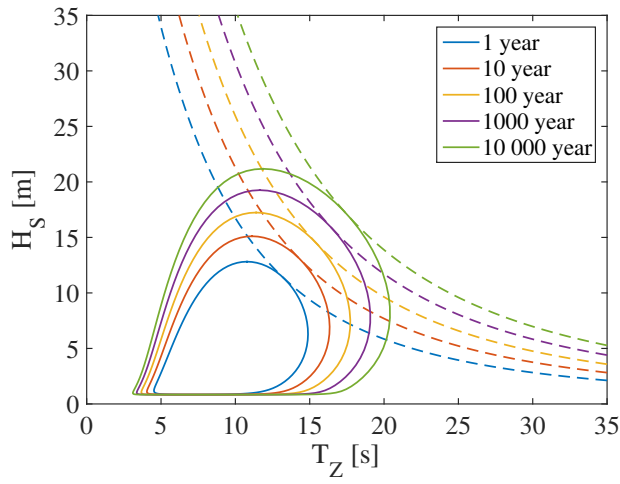


(e) Runup model Pe

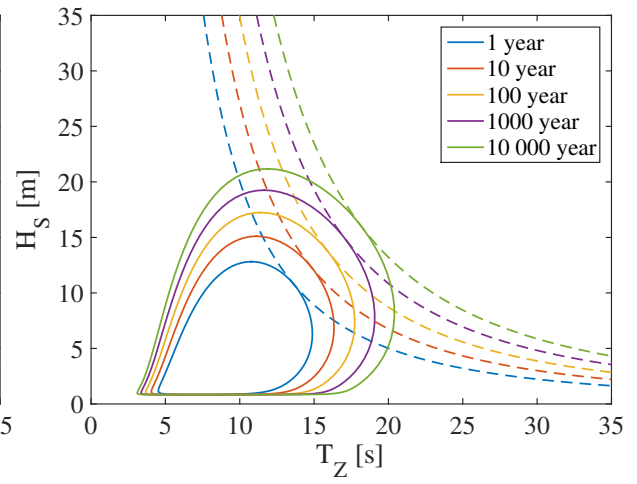


(f) Runup model Ho

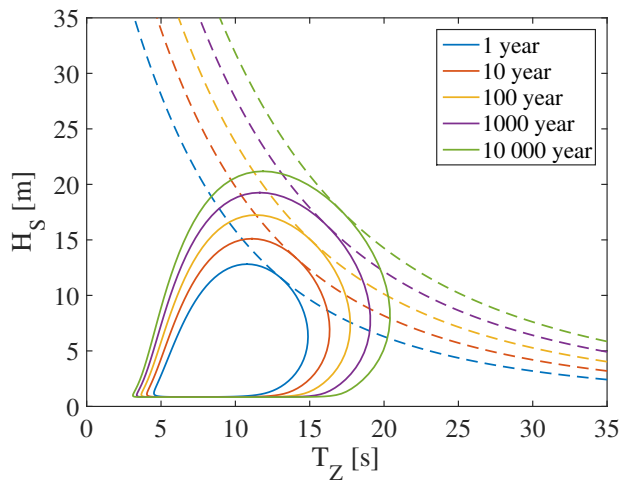
Figure B.6: BGS07 (4)



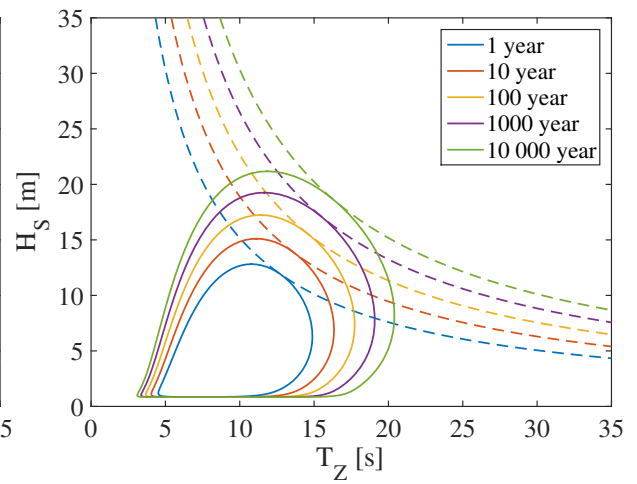
(g) Runup model Vo



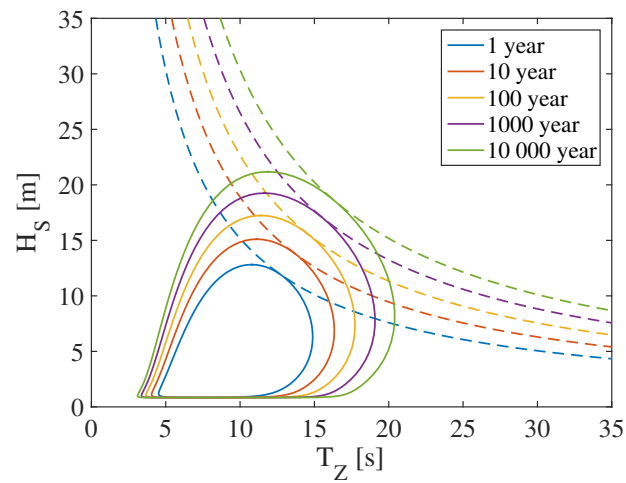
(h) Runup model At1



(i) Runup model At2

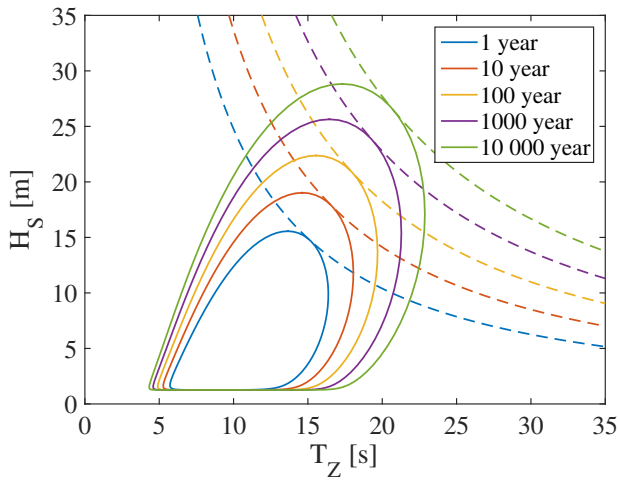


(j) Runup model Po1

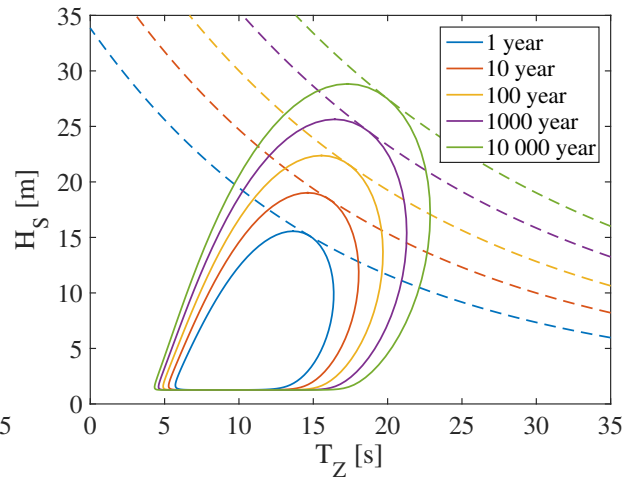


(k) Runup model Po2

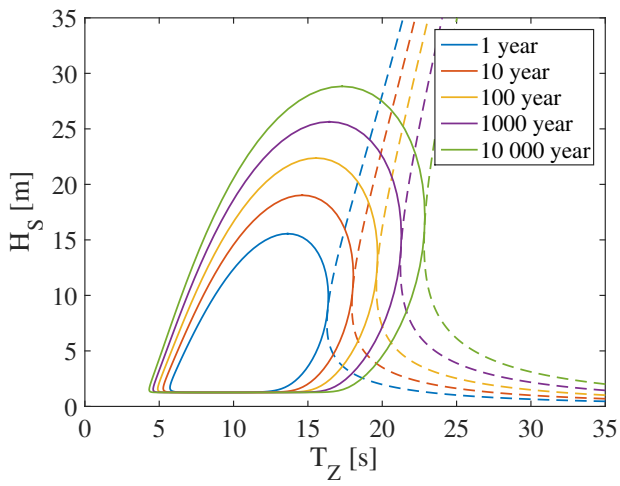
Figure B.6: (Continued)



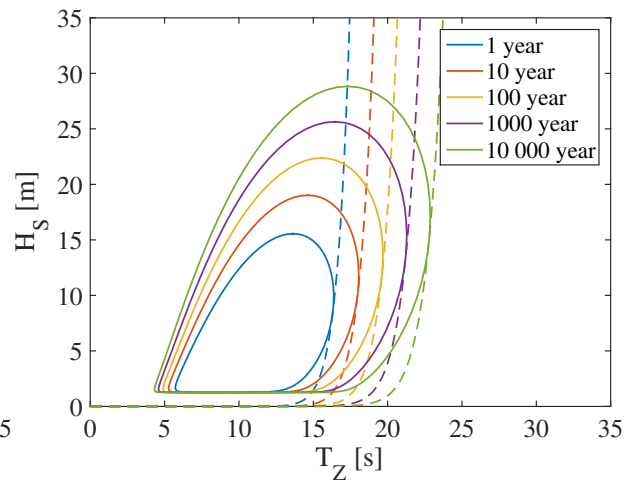
(a) Runup model B11



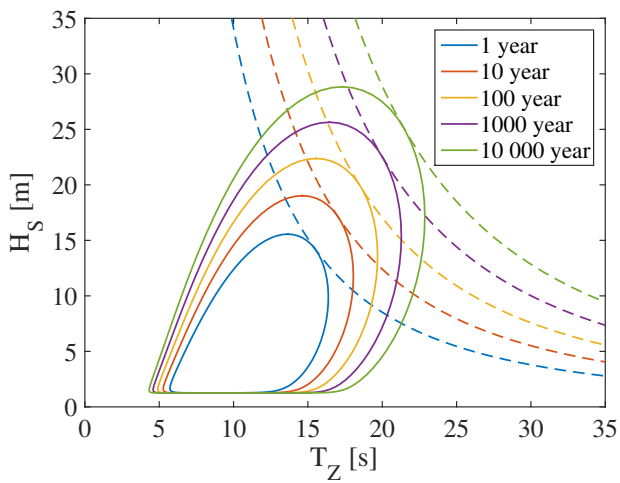
(b) Runup model B12



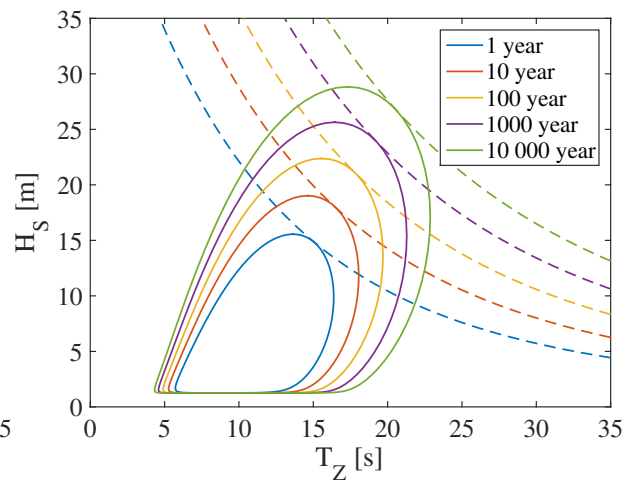
(c) Runup model B1d



(d) Runup model Sc

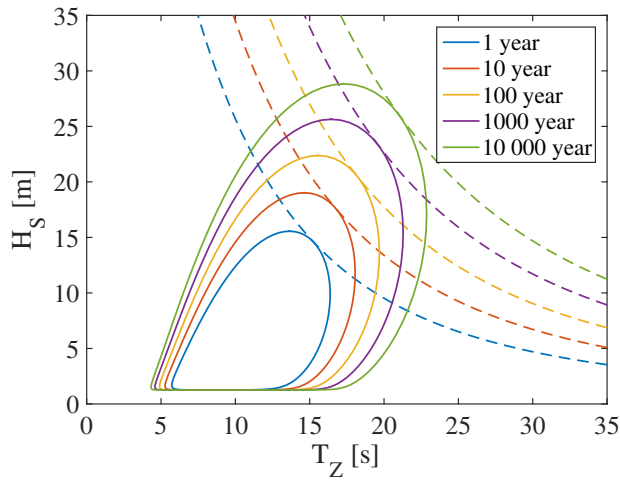


(e) Runup model Pe

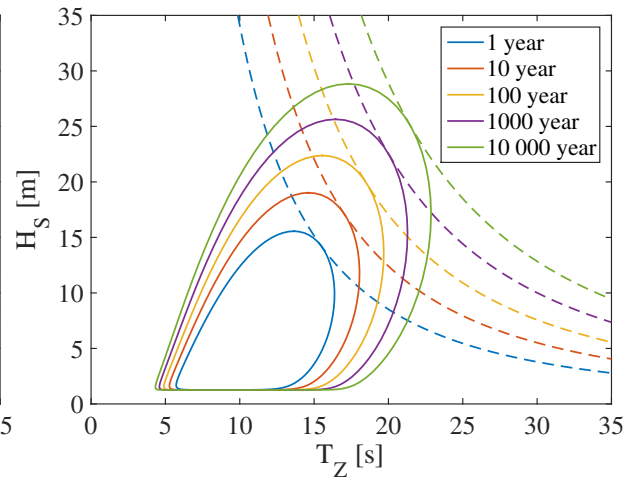


(f) Runup model Ho

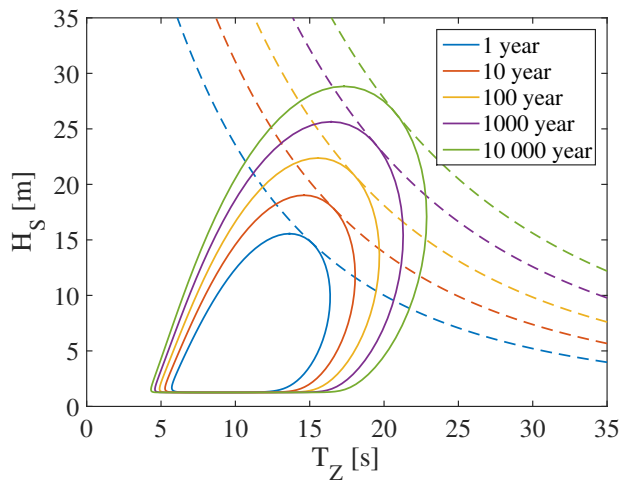
Figure B.7: BGS07 (5)



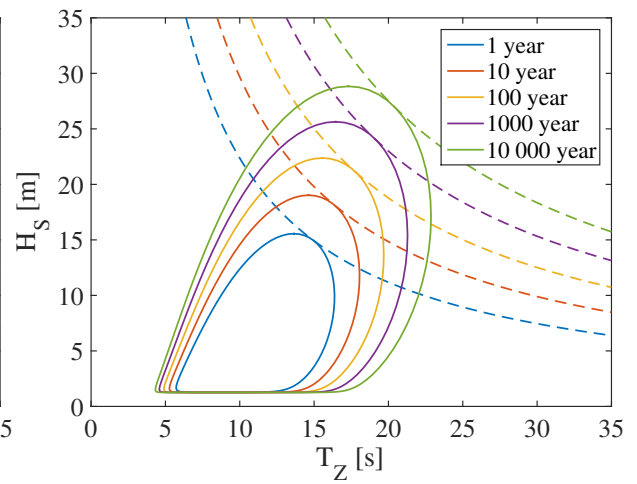
(g) Runup model Vo



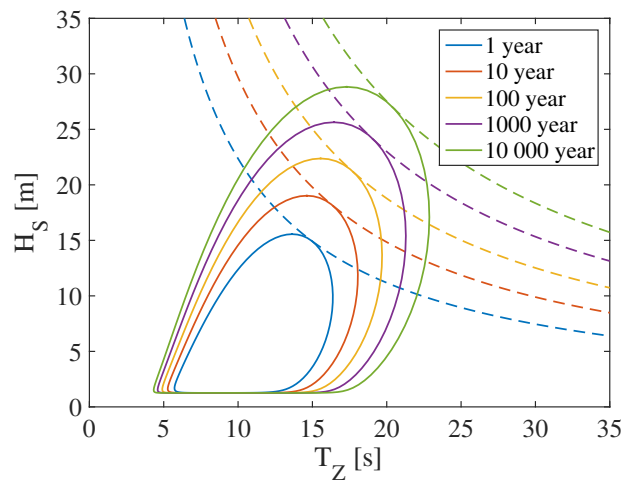
(h) Runup model At1



(i) Runup model At2

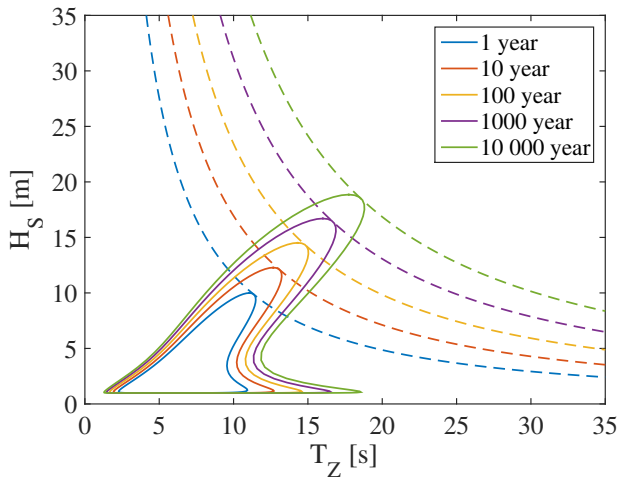


(j) Runup model Po1

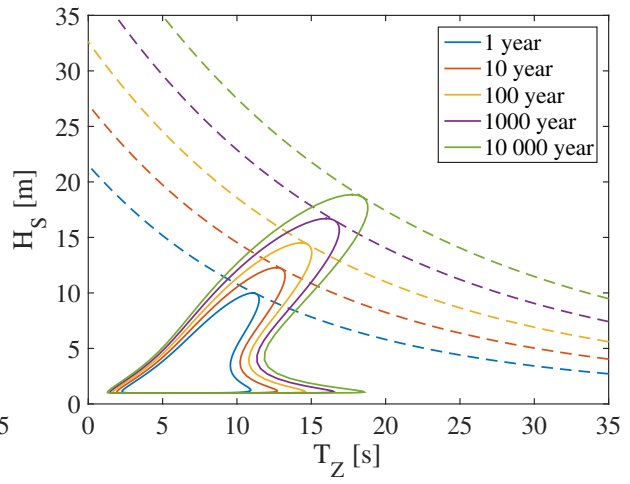


(k) Runup model Po2

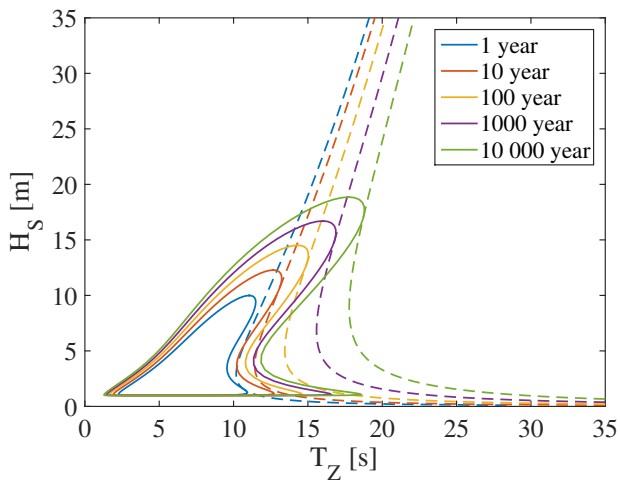
Figure B.7: (Continued)



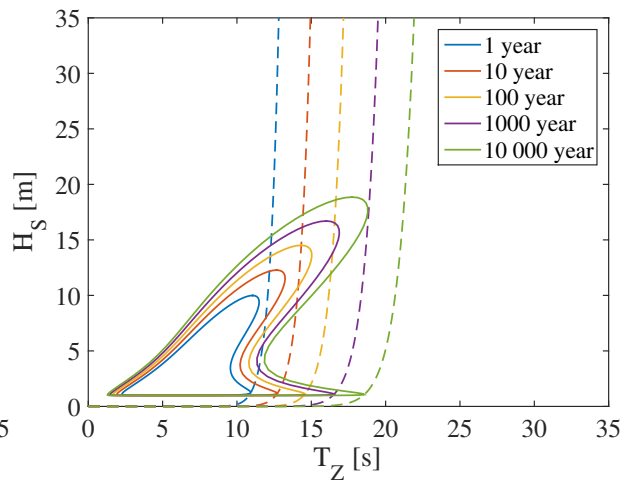
(a) Runup model B11



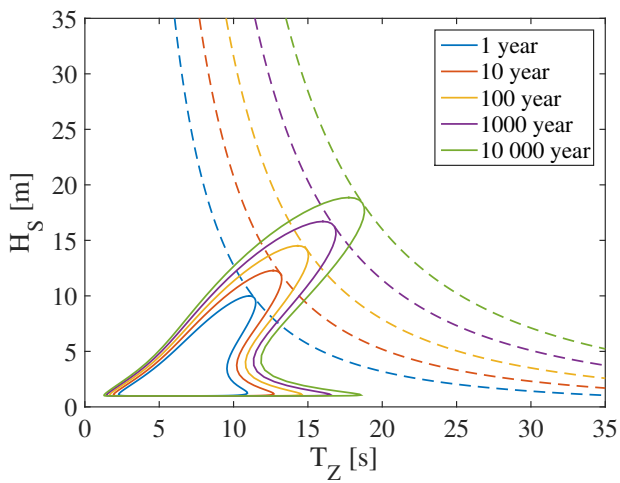
(b) Runup model B12



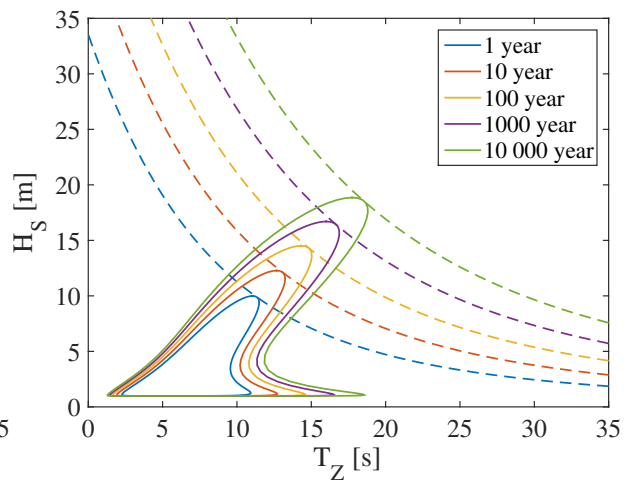
(c) Runup model B1d



(d) Runup model Sc

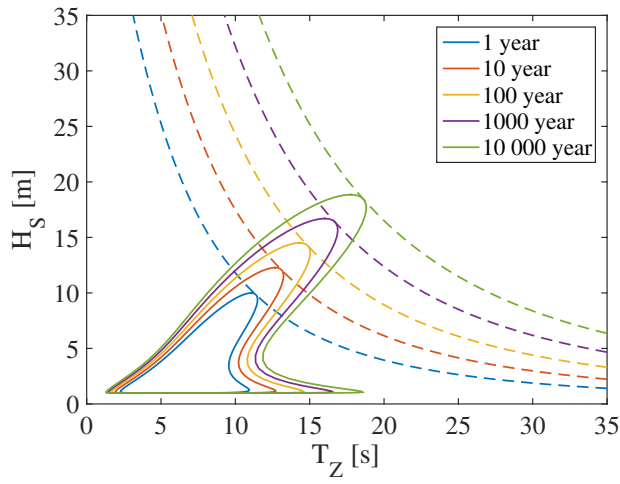


(e) Runup model Pe

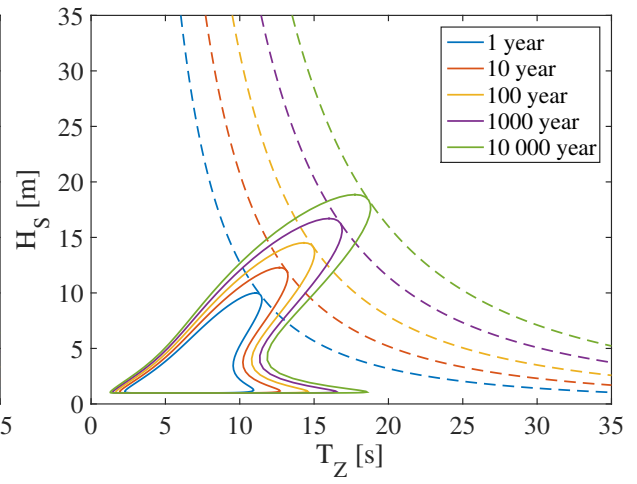


(f) Runup model Ho

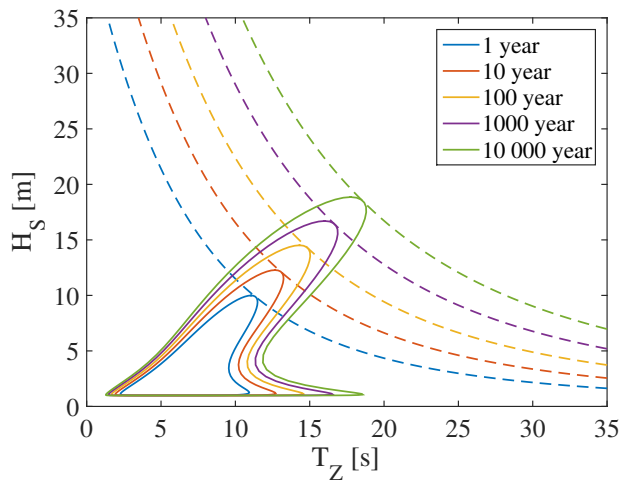
Figure B.8: MBG90 (1)



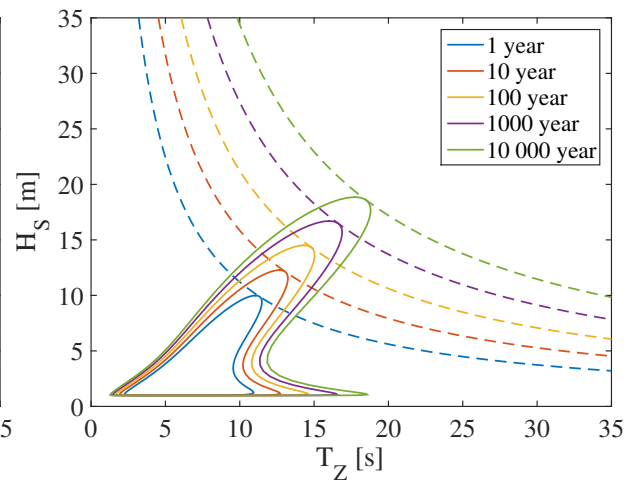
(g) Runup model Vo



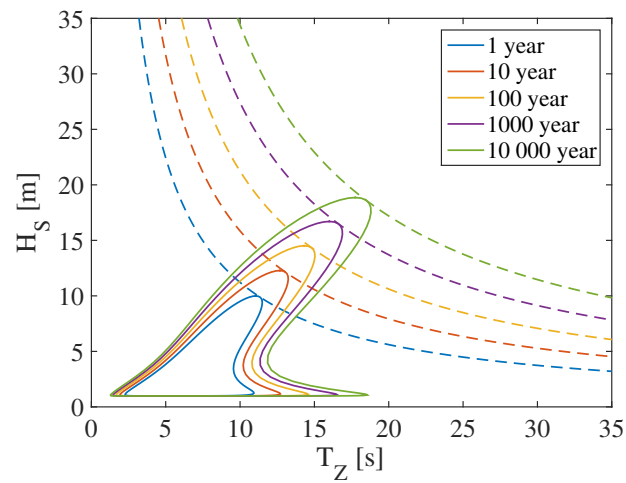
(h) Runup model At1



(i) Runup model At2

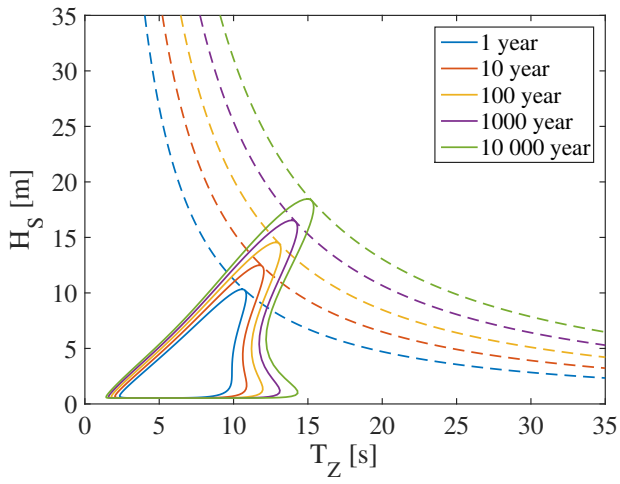


(j) Runup model Po1

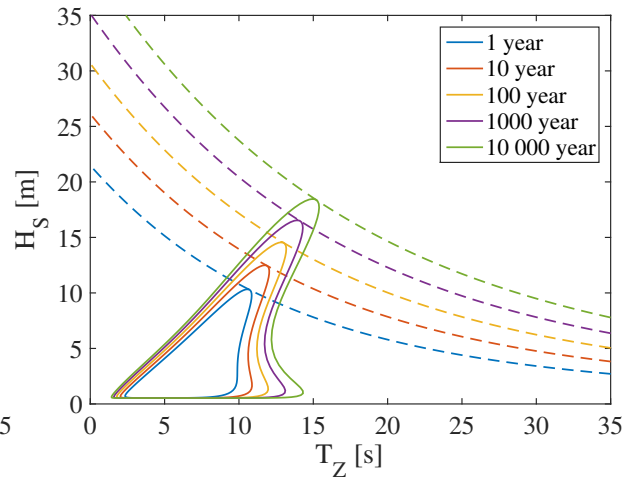


(k) Runup model Po2

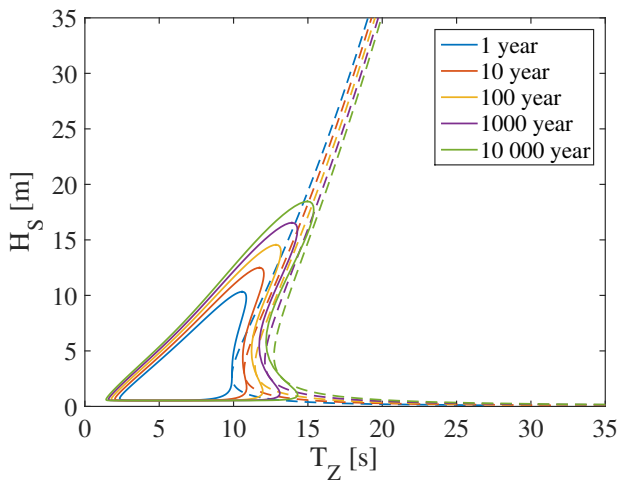
Figure B.8: (Continued)



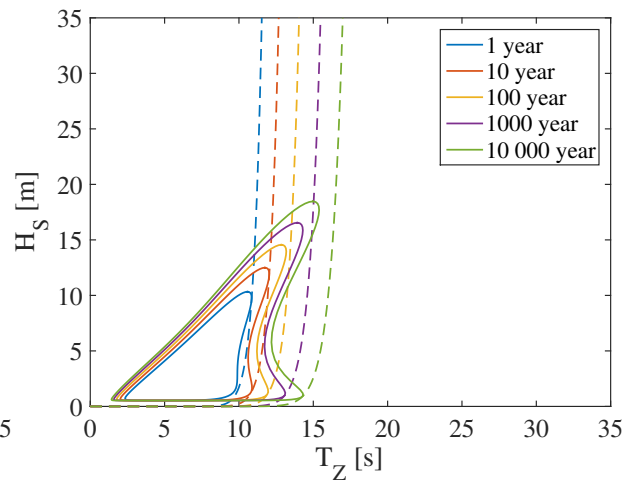
(a) Runup model B11



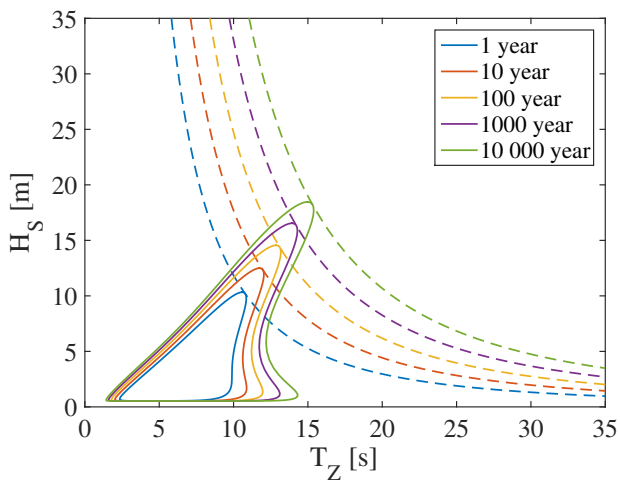
(b) Runup model B12



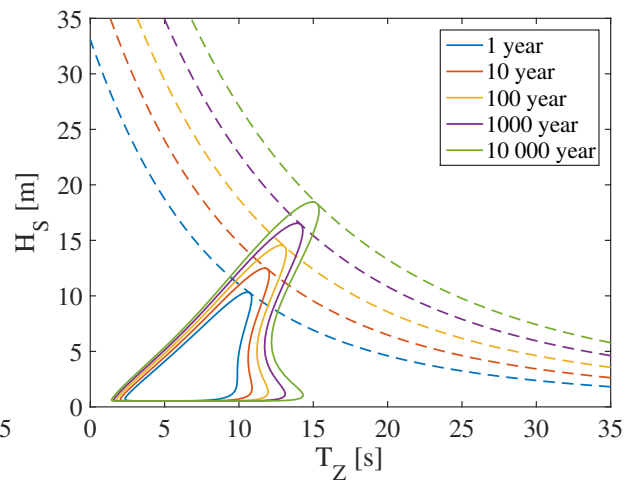
(c) Runup model B1d



(d) Runup model Sc

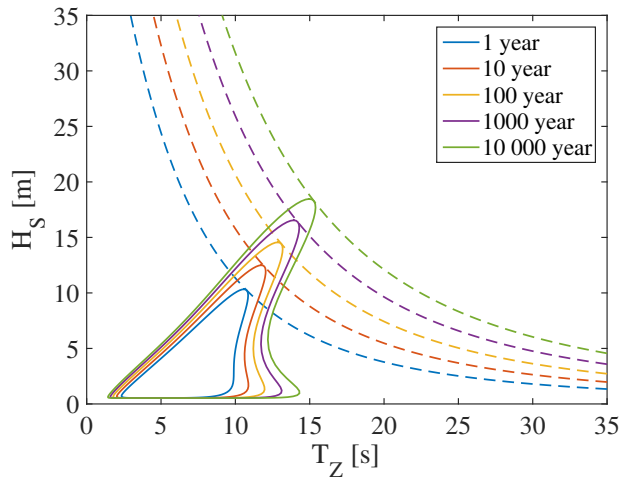


(e) Runup model Pe

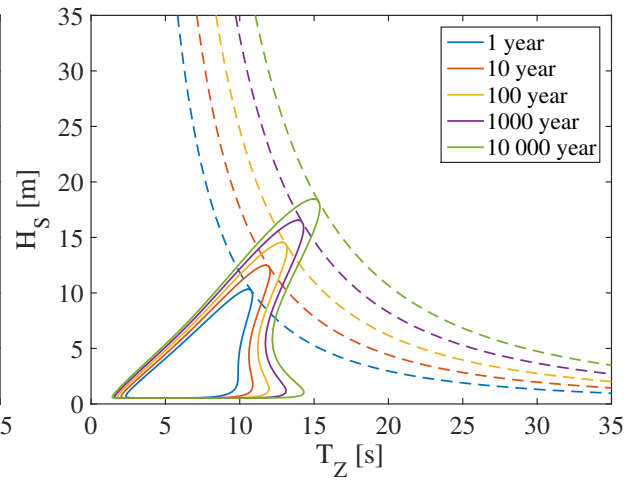


(f) Runup model Ho

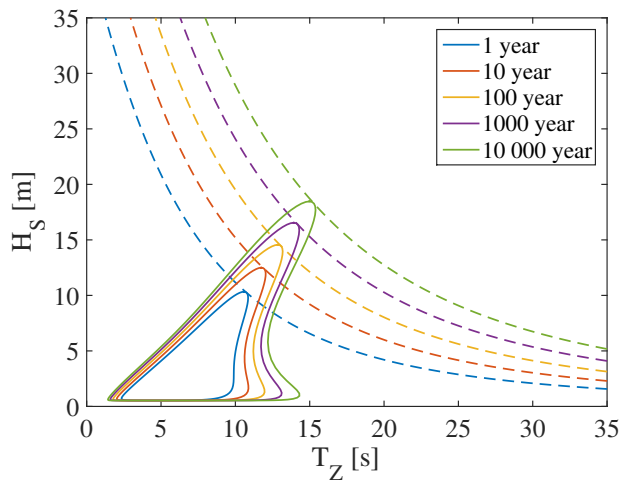
Figure B.9: MBG90 (2)



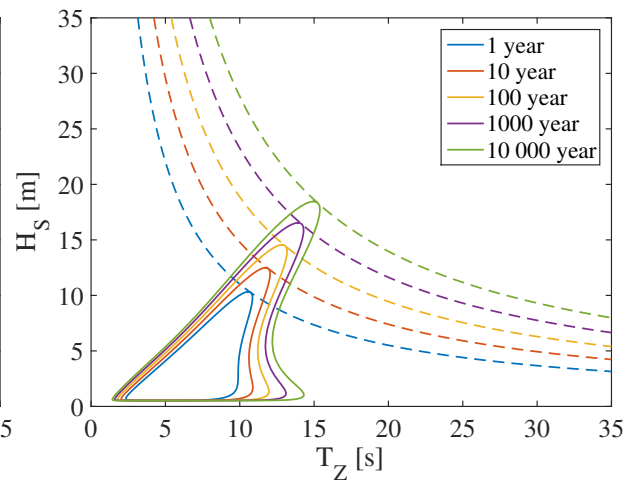
(g) Runup model Vo



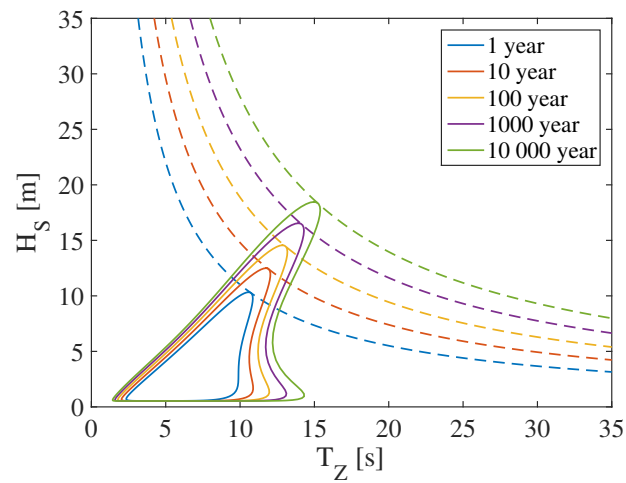
(h) Runup model At1



(i) Runup model At2

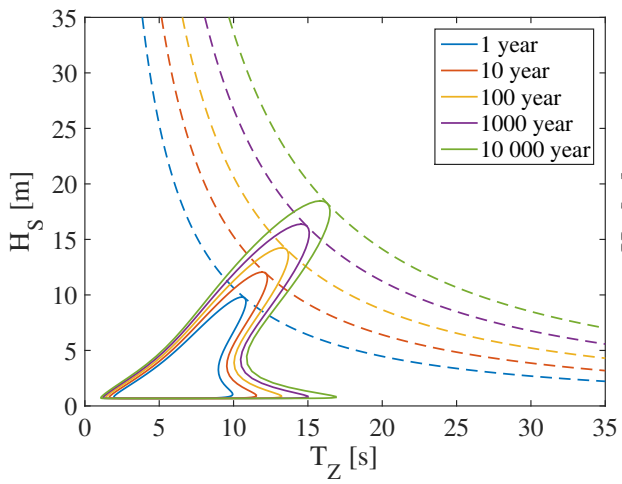


(j) Runup model Po1

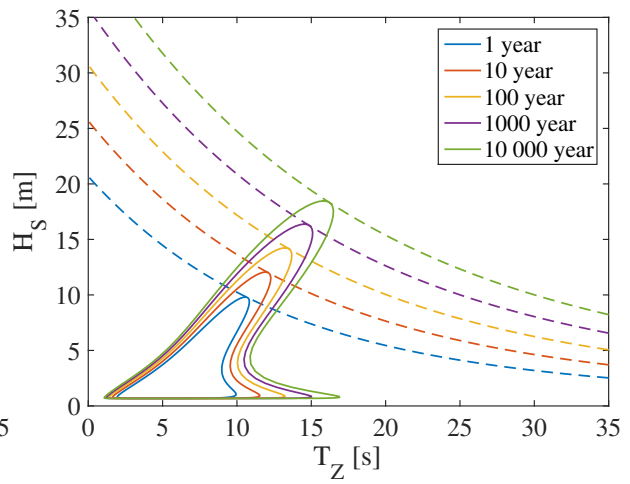


(k) Runup model Po2

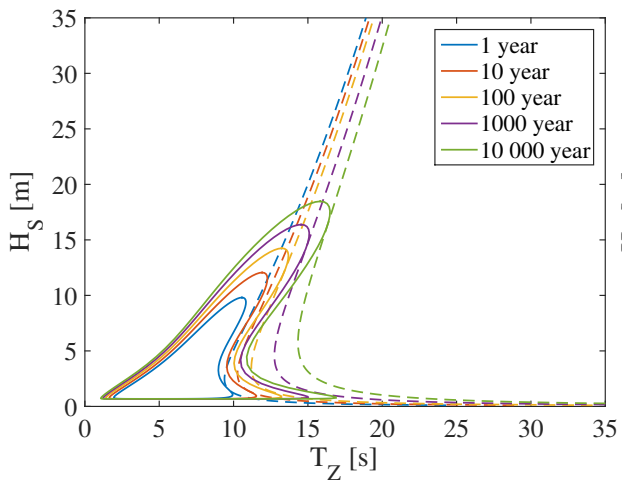
Figure B.9: (Continued)



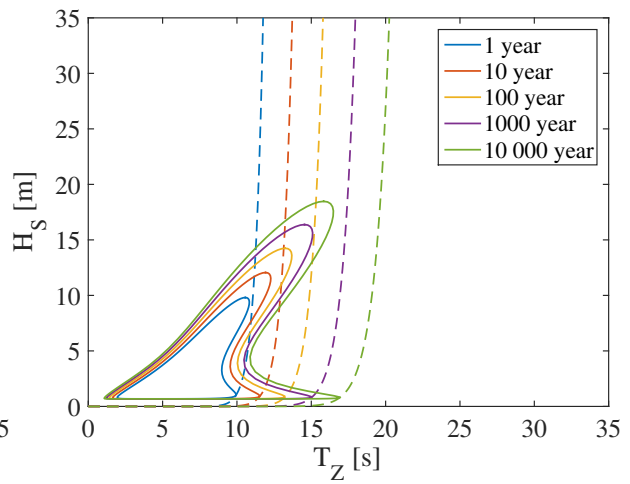
(a) Runup model B11



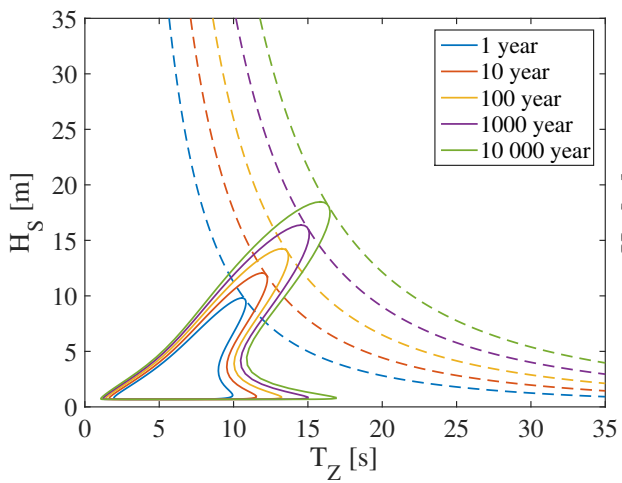
(b) Runup model B12



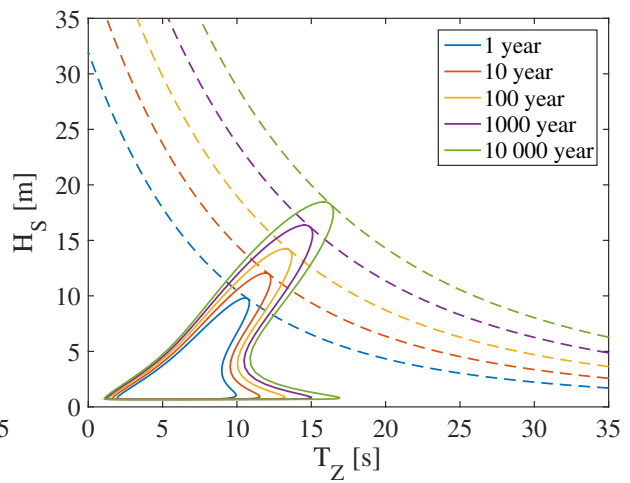
(c) Runup model B1d



(d) Runup model Sc

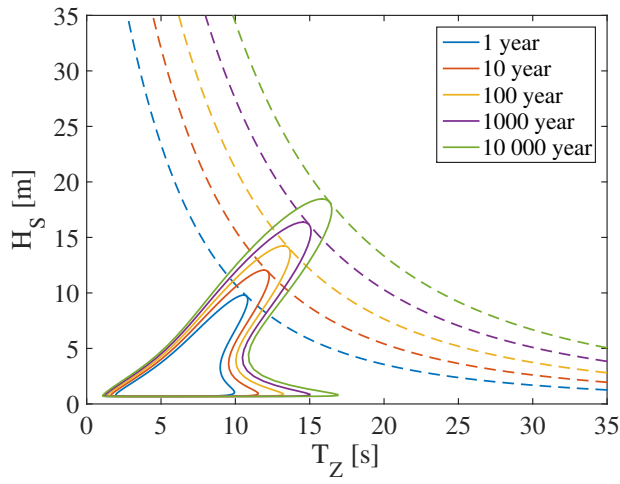


(e) Runup model Pe

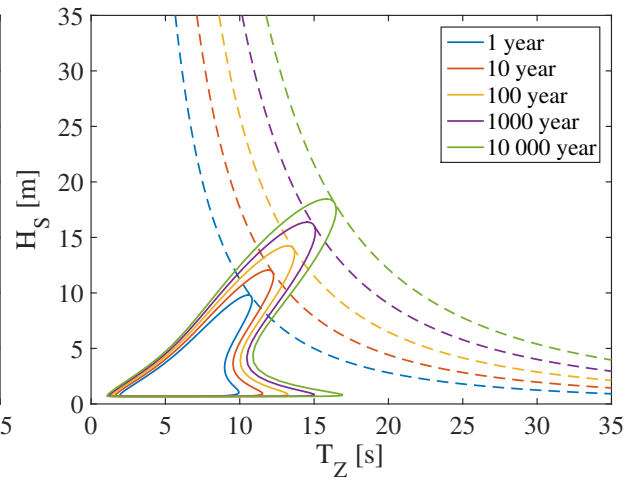


(f) Runup model Ho

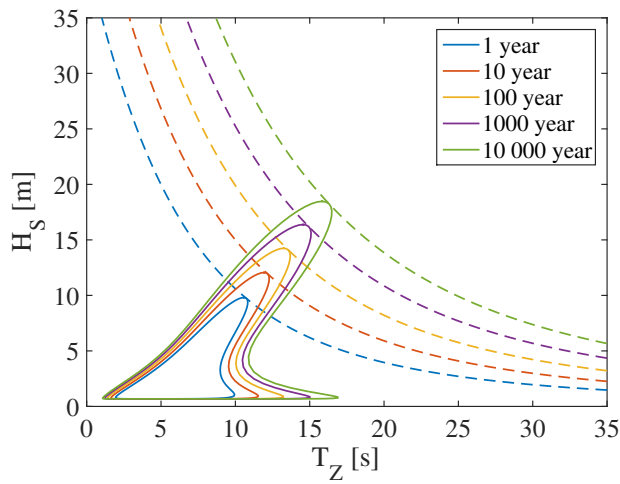
Figure B.10: MBG90 (3)



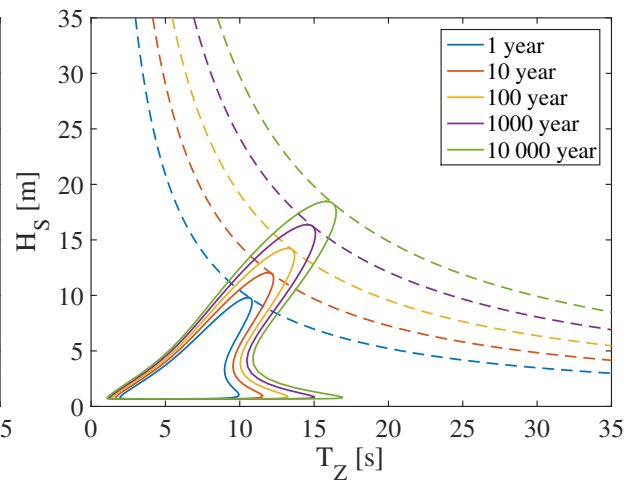
(g) Runup model Vo



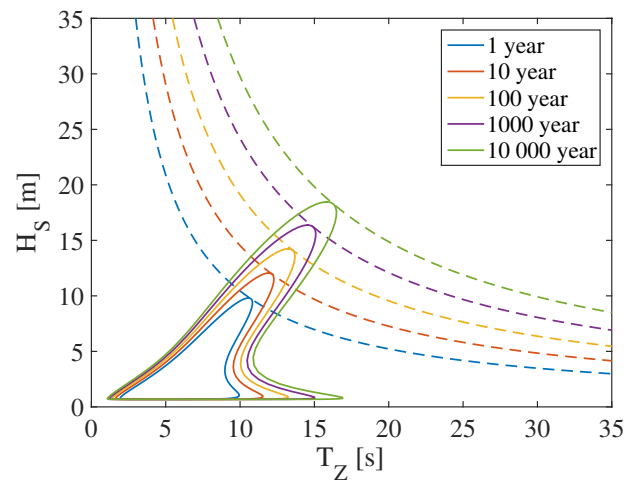
(h) Runup model At1



(i) Runup model At2



(j) Runup model Po1



(k) Runup model Po2

Figure B.10: (Continued)

B.5 Extreme Values from Wave Distributions

Table B.19: MGAU05

(a) Runup model B11					(b) Runup model B12				
Year	H_S	T_P	ξ_P	R_2	Year	H_S	T_P	ξ_P	R_2
1	10.2	15.2	0.60	8.0	1	10.3	15.0	0.58	8.8
10	12.0	16.3	0.59	9.3	10	12.3	15.9	0.56	10.3
100	13.9	17.0	0.57	10.5	100	14.1	16.8	0.56	11.7
1000	15.5	17.9	0.57	11.7	1000	15.7	17.7	0.56	13.1
10000	17.0	18.8	0.57	12.8	10000	17.2	18.6	0.56	14.4

(c) Runup model B1d					(d) Runup model Sc				
Year	H_S	T_P	ξ_P	R_2	Year	H_S	T_P	ξ_P	R_2
1	3.6	19.4	1.28	-1.271	1	1.7	20.1	1.95	-0.724
10	3.4	22.1	1.50	-1.526	10	1.6	23.3	2.32	-1.012
100	3.6	24.4	1.61	-1.781	100	1.3	26.5	2.94	-1.375
1000	3.7	26.5	1.71	-2.030	1000	1.2	30.0	3.43	-1.823
10000	3.2	30.0	2.10	-2.285	10000	1.1	33.7	3.95	-2.372

(e) Runup model Pe					(f) Runup model Ho				
Year	H_S	T_P	ξ_P	R_2	Year	H_S	T_P	ξ_P	R_2
1	9.8	15.6	0.62	12.2	1	10.2	15.2	0.60	7.1
10	11.8	16.5	0.60	14.2	10	12.2	16.1	0.58	8.3
100	13.7	17.2	0.58	16.0	100	13.9	17.0	0.57	9.4
1000	15.3	18.1	0.58	17.7	1000	15.5	17.9	0.57	10.4
10000	16.8	18.9	0.58	19.4	10000	17.2	18.6	0.56	11.4

Table B.19: (Continued)

(g) Runup model Vo					(h) Runup model At1				
Year	H_S	T_P	ξ_P	R_2	Year	H_S	T_P	ξ_P	R_2
1	10.0	15.4	0.61	4.3	1	9.8	15.6	0.62	6.0
10	12.0	16.3	0.59	4.9	10	11.8	16.5	0.60	7.0
100	13.7	17.2	0.58	5.5	100	13.7	17.2	0.58	7.9
1000	15.5	17.9	0.57	6.0	1000	15.3	18.1	0.58	8.8
10000	17.0	18.8	0.57	6.6	10000	16.8	18.9	0.58	9.6

(i) Runup model At2					(j) Runup model Po1				
Year	H_S	T_P	ξ_P	R_2	Year	H_S	T_P	ξ_P	R_2
1	10.2	15.2	0.60	7.2	1	10.3	15.0	0.58	18.8
10	12.0	16.3	0.59	8.4	10	12.2	16.1	0.58	23.7
100	13.9	17.0	0.57	9.5	100	13.9	17.0	0.57	28.7
1000	15.5	17.9	0.57	10.6	1000	15.5	17.9	0.57	33.7
10000	17.0	18.8	0.57	11.6	10000	17.2	18.6	0.56	38.8

(k) Runup model Po2				
Year	H_S	T_P	ξ_P	R_2
1	10.3	15.0	0.58	16.2
10	12.2	16.1	0.58	20.5
100	13.9	17.0	0.57	24.7
1000	15.5	17.9	0.57	29.0
10000	17.2	18.6	0.56	33.4

Table B.20: OHG16

(a) Runup model B11					(b) Runup model B12				
Year	H_S	T_P	ξ_P	R_2	Year	H_S	T_P	ξ_P	R_2
1	10.6	15.9	0.61	8.5	1	10.8	15.7	0.60	9.3
10	13.0	17.2	0.60	10.2	10	13.2	17.0	0.59	11.3
100	15.6	18.3	0.58	11.9	100	15.7	18.1	0.57	13.2
1000	17.9	19.4	0.57	13.6	1000	18.0	19.2	0.57	15.1
10000	20.1	20.5	0.57	15.2	10000	20.3	20.3	0.56	17.0

(c) Runup model B1d					(d) Runup model Sc				
Year	H_S	T_P	ξ_P	R_2	Year	H_S	T_P	ξ_P	R_2
1	3.6	19.7	1.29	-1.306	1	1.9	20.1	1.81	-0.712
10	4.0	22.0	1.38	-1.583	10	1.9	23.4	2.11	-0.998
100	3.7	24.8	1.60	-1.856	100	1.6	26.6	2.63	-1.358
1000	3.3	28.1	1.92	-2.123	1000	1.6	30.2	3.02	-1.800
10000	3.5	30.5	2.04	-2.401	10000	1.3	33.7	3.74	-2.345

(e) Runup model Pe					(f) Runup model Ho				
Year	H_S	T_P	ξ_P	R_2	Year	H_S	T_P	ξ_P	R_2
1	10.5	16.1	0.62	13.0	1	10.6	15.9	0.61	7.5
10	13.0	17.2	0.60	15.6	10	13.2	17.0	0.59	9.1
100	15.4	18.4	0.59	18.1	100	15.6	18.3	0.58	10.6
1000	17.6	19.6	0.58	20.6	1000	17.9	19.4	0.57	12.1
10000	20.1	20.5	0.57	23.1	10000	20.1	20.5	0.57	13.6

Table B.20: (Continued)

(g) Runup model Vo					(h) Runup model At1				
Year	H_S	T_P	ξ_P	R_2	Year	H_S	T_P	ξ_P	R_2
1	10.6	15.9	0.61	4.5	1	10.5	16.1	0.62	6.4
10	13.0	17.2	0.60	5.3	10	13.0	17.2	0.60	7.7
100	15.6	18.3	0.58	6.1	100	15.4	18.4	0.59	8.9
1000	17.9	19.4	0.57	6.9	1000	17.6	19.6	0.58	10.2
10000	20.1	20.5	0.57	7.7	10000	20.1	20.5	0.57	11.4

(i) Runup model At2					(j) Runup model Po1				
Year	H_S	T_P	ξ_P	R_2	Year	H_S	T_P	ξ_P	R_2
1	10.6	15.9	0.61	7.7	1	10.6	15.9	0.61	20.5
10	13.0	17.2	0.60	9.2	10	13.2	17.0	0.59	27.3
100	15.6	18.3	0.58	10.8	100	15.6	18.3	0.58	34.5
1000	17.9	19.4	0.57	12.3	1000	17.9	19.4	0.57	42.0
10000	20.1	20.5	0.57	13.8	10000	20.1	20.5	0.57	50.0

(k) Runup model Po2				
Year	H_S	T_P	ξ_P	R_2
1	10.6	15.9	0.61	17.6
10	13.2	17.0	0.59	23.5
100	15.6	18.3	0.58	29.7
1000	17.9	19.4	0.57	36.2
10000	20.1	20.5	0.57	43.1

Table B.21: BGG07 (1)

(a) Runup model B11					(b) Runup model B12				
Year	H_S	T_Z	ξ_P	R_2	Year	H_S	T_P	ξ_P	R_2
1	14.4	12.5	0.53	10.3	1	15.0	12.0	0.50	11.7
10	17.2	13.7	0.53	12.3	10	17.8	13.1	0.50	14.0
100	19.7	14.8	0.53	14.2	100	20.2	14.5	0.52	16.2
1000	21.6	16.3	0.56	16.1	1000	22.7	15.5	0.52	18.3
10000	23.9	17.4	0.57	18.0	10000	25.1	16.5	0.53	20.3

(c) Runup model B1d					(d) Runup model Sc				
Year	H_S	T_P	ξ_P	R_2	Year	H_S	T_P	ξ_P	R_2
1	7.1	13.0	0.78	-0.955	1	9.1	13.3	0.71	-0.423
10	8.7	14.6	0.79	-1.200	10	10.4	14.8	0.73	-0.525
100	9.7	15.9	0.82	-1.458	100	11.7	16.2	0.76	-0.632
1000	11.7	17.4	0.81	-1.733	1000	12.8	17.5	0.78	-0.746
10000	12.7	18.7	0.84	-2.023	10000	14.0	18.8	0.81	-0.866

(e) Runup model Pe					(f) Runup model Ho				
Year	H_S	T_P	ξ_P	R_2	Year	H_S	T_P	ξ_P	R_2
1	14.1	12.7	0.54	15.3	1	14.7	12.3	0.51	9.2
10	16.2	14.2	0.56	18.3	10	17.2	13.7	0.53	11.0
100	18.6	15.4	0.57	21.3	100	19.7	14.8	0.53	12.7
1000	20.9	16.6	0.58	24.3	1000	22.2	15.9	0.54	14.4
10000	23.1	17.7	0.59	27.3	10000	24.5	17.0	0.55	16.1

Table B.21: (Continued)

(g) Runup model Vo					(h) Runup model At1				
Year	H_S	T_P	ξ_P	R_2	Year	H_S	T_P	ξ_P	R_2
1	14.4	12.5	0.53	5.3	1	14.1	12.7	0.54	7.6
10	16.7	14.0	0.55	6.3	10	16.2	14.2	0.56	9.1
100	19.2	15.2	0.55	7.2	100	18.6	15.4	0.57	10.5
1000	21.6	16.3	0.56	8.1	1000	20.9	16.6	0.58	12.0
10000	23.9	17.4	0.57	9.0	10000	23.1	17.7	0.59	13.5

(i) Runup model At2					(j) Runup model Po1				
Year	H_S	T_P	ξ_P	R_2	Year	H_S	T_P	ξ_P	R_2
1	14.4	12.5	0.53	9.3	1	14.7	12.3	0.51	28.0
10	17.2	13.7	0.53	11.1	10	17.5	13.4	0.51	36.5
100	19.7	14.8	0.53	12.9	100	19.7	14.8	0.53	45.4
1000	21.6	16.3	0.56	14.6	1000	22.2	15.9	0.54	54.8
10000	23.9	17.4	0.57	16.3	10000	24.5	17.0	0.55	64.5

(k) Runup model Po2				
Year	H_S	T_P	ξ_P	R_2
1	14.7	12.3	0.51	24.1
10	17.5	13.4	0.51	31.4
100	19.7	14.8	0.53	39.1
1000	22.2	15.9	0.54	47.2
10000	24.5	17.0	0.55	55.6

Table B.22: BGG07 (2)

(a) Runup model B11					(b) Runup model B12				
Year	H_S	T_P	ξ_P	R_2	Year	H_S	T_P	ξ_P	R_2
1	13.1	13.7	0.60	10.3	1	13.2	13.5	0.59	11.4
10	15.4	15.1	0.61	12.3	10	15.6	14.9	0.60	13.6
100	17.6	16.4	0.62	14.3	100	17.8	16.2	0.61	15.7
1000	19.7	17.7	0.64	16.2	1000	19.9	17.4	0.63	17.7
10000	21.7	18.9	0.65	18.1	10000	21.9	18.7	0.64	19.7

(c) Runup model B1d					(d) Runup model Sc				
Year	H_S	T_P	ξ_P	R_2	Year	H_S	T_P	ξ_P	R_2
1	8.8	13.5	0.73	-0.967	1	1.3	13.0	1.79	-0.485
10	11.4	15.0	0.71	-1.175	10	1.2	15.4	2.23	-0.717
100	13.5	16.4	0.71	-1.403	100	1.2	18.1	2.62	-1.028
1000	15.8	17.8	0.71	-1.650	1000	1.2	21.0	3.13	-1.440
10000	18.2	19.1	0.72	-1.915	10000	1.1	24.2	3.66	-1.963

(e) Runup model Pe					(f) Runup model Ho				
Year	H_S	T_P	ξ_P	R_2	Year	H_S	T_P	ξ_P	R_2
1	12.9	13.8	0.61	15.9	1	13.1	13.7	0.60	9.2
10	15.2	15.2	0.62	19.0	10	15.4	15.1	0.61	10.9
100	17.3	16.5	0.64	22.1	100	17.6	16.4	0.62	12.7
1000	19.4	17.8	0.65	25.2	1000	19.7	17.7	0.64	14.3
10000	21.3	19.1	0.66	28.2	10000	21.7	18.9	0.65	16.0

Table B.22: (Continued)

(g) Runup model Vo					(h) Runup model At1				
Year	H_S	T_P	ξ_P	R_2	Year	H_S	T_P	ξ_P	R_2
1	13.1	13.7	0.60	5.4	1	12.9	13.8	0.61	7.8
10	15.4	15.1	0.61	6.4	10	15.2	15.2	0.62	9.4
100	17.6	16.4	0.62	7.3	100	17.3	16.5	0.64	10.9
1000	19.7	17.7	0.64	8.2	1000	19.4	17.8	0.65	12.4
10000	21.7	18.9	0.65	9.2	10000	21.3	19.1	0.66	13.9

(i) Runup model At2					(j) Runup model Po1				
Year	H_S	T_P	ξ_P	R_2	Year	H_S	T_P	ξ_P	R_2
1	13.1	13.7	0.60	9.4	1	13.1	13.7	0.60	27.7
10	15.4	15.1	0.61	11.2	10	15.4	15.1	0.61	36.0
100	17.6	16.4	0.62	12.9	100	17.6	16.4	0.62	44.8
1000	19.7	17.7	0.64	14.7	1000	19.7	17.7	0.64	53.9
10000	21.7	18.9	0.65	16.4	10000	21.7	18.9	0.65	63.5

(k) Runup model Po2				
Year	H_S	T_P	ξ_P	R_2
1	13.1	13.7	0.60	23.9
10	15.4	15.1	0.61	31.1
100	17.6	16.4	0.62	38.6
1000	19.7	17.7	0.64	46.5
10000	21.7	18.9	0.65	54.7

Table B.23: BGG07 (3)

(a) Runup model B11					(b) Runup model B12				
Year	H_S	T_P	ξ_P	R_2	Year	H_S	T_P	ξ_P	R_2
1	15.6	15.5	0.63	12.7	1	16.0	15.2	0.61	14.0
10	18.9	17.6	0.65	15.7	10	19.3	17.2	0.63	17.2
100	22.0	19.5	0.67	18.8	100	22.6	19.1	0.64	20.3
1000	25.1	21.4	0.68	21.8	1000	25.7	20.9	0.66	23.5
10000	27.2	23.9	0.73	24.9	10000	28.7	22.6	0.67	26.6

(c) Runup model B1d					(d) Runup model Sc				
Year	H_S	T_P	ξ_P	R_2	Year	H_S	T_P	ξ_P	R_2
1	10.1	16.3	0.82	-1.530	1	10.9	16.4	0.80	-0.658
10	12.8	18.8	0.84	-2.041	10	12.8	18.8	0.84	-0.870
100	14.7	21.1	0.88	-2.598	100	14.7	21.1	0.88	-1.105
1000	17.8	23.4	0.89	-3.200	1000	16.4	23.3	0.92	-1.365
10000	19.7	25.6	0.92	-3.851	10000	18.2	25.5	0.96	-1.650

(e) Runup model Pe					(f) Runup model Ho				
Year	H_S	T_P	ξ_P	R_2	Year	H_S	T_P	ξ_P	R_2
1	15.2	15.8	0.65	19.8	1	15.6	15.5	0.63	11.3
10	18.4	17.9	0.67	24.6	10	18.9	17.6	0.65	13.9
100	20.7	20.3	0.72	29.6	100	22.0	19.5	0.67	16.6
1000	23.5	22.4	0.74	34.7	1000	25.1	21.4	0.68	19.3
10000	26.2	24.4	0.76	40.0	10000	28.0	23.3	0.70	21.9

Table B.23: (Continued)

(g) Runup model Vo					(h) Runup model At1				
Year	H_S	T_P	ξ_P	R_2	Year	H_S	T_P	ξ_P	R_2
1	15.6	15.5	0.63	6.6	1	15.2	15.8	0.65	9.8
10	18.4	17.9	0.67	8.0	10	18.4	17.9	0.67	12.2
100	21.4	20.0	0.69	9.5	100	20.7	20.3	0.72	14.6
1000	24.3	21.9	0.71	11.0	1000	23.5	22.4	0.74	17.2
10000	27.2	23.9	0.73	12.6	10000	26.2	24.4	0.76	19.7

(i) Runup model At2					(j) Runup model Po1				
Year	H_S	T_P	ξ_P	R_2	Year	H_S	T_P	ξ_P	R_2
1	15.6	15.5	0.63	11.5	1	16.0	15.2	0.61	37.7
10	18.9	17.6	0.65	14.3	10	19.3	17.2	0.63	51.5
100	22.0	19.5	0.67	17.0	100	22.0	19.5	0.67	66.7
1000	24.3	21.9	0.71	19.8	1000	25.1	21.4	0.68	83.2
10000	27.2	23.9	0.73	22.6	10000	28.0	23.3	0.70	100.9

(k) Runup model Po2				
Year	H_S	T_P	ξ_P	R_2
1	16.0	15.2	0.61	32.5
10	19.3	17.2	0.63	44.4
100	22.0	19.5	0.67	57.5
1000	25.1	21.4	0.68	71.7
10000	28.0	23.3	0.70	87.0

Table B.24: BGG07 (4)

(a) Runup model B11					(b) Runup model B12				
Year	H_S	T_P	ξ_P	R_2	Year	H_S	T_P	ξ_P	R_2
1	11.6	13.0	0.61	9.3	1	12.2	12.4	0.57	10.3
10	13.6	13.9	0.60	10.7	10	14.3	13.1	0.56	11.9
100	14.9	15.1	0.63	12.1	100	16.3	13.8	0.55	13.4
1000	16.6	15.9	0.63	13.5	1000	17.7	14.9	0.57	14.9
10000	17.4	17.3	0.66	14.8	10000	19.4	15.5	0.56	16.3

(c) Runup model B1d					(d) Runup model Sc				
Year	H_S	T_P	ξ_P	R_2	Year	H_S	T_P	ξ_P	R_2
1	6.3	14.9	0.95	-1.306	1	5.2	14.8	1.04	-0.565
10	7.0	16.3	0.99	-1.572	10	5.7	16.3	1.09	-0.689
100	7.6	17.7	1.03	-1.843	100	6.1	17.7	1.15	-0.820
1000	9.1	19.0	1.01	-2.124	1000	6.4	19.0	1.20	-0.959
10000	9.8	20.3	1.04	-2.414	10000	6.8	20.3	1.25	-1.107

(e) Runup model Pe					(f) Runup model Ho				
Year	H_S	T_P	ξ_P	R_2	Year	H_S	T_P	ξ_P	R_2
1	10.8	13.6	0.66	14.4	1	11.9	12.7	0.59	8.2
10	12.1	14.9	0.69	16.7	10	13.6	13.9	0.60	9.5
100	13.7	16.0	0.69	18.9	100	15.4	14.7	0.60	10.7
1000	15.2	16.9	0.69	21.1	1000	16.6	15.9	0.63	11.9
10000	15.7	18.3	0.74	23.3	10000	18.2	16.7	0.63	13.1

Table B.24: (Continued)

(g) Runup model Vo					(h) Runup model At1				
Year	H_S	T_P	ξ_P	R_2	Year	H_S	T_P	ξ_P	R_2
1	11.2	13.3	0.64	4.9	1	10.8	13.6	0.66	7.1
10	13.1	14.3	0.63	5.6	10	12.1	14.9	0.69	8.2
100	14.3	15.6	0.66	6.3	100	13.7	16.0	0.69	9.3
1000	15.9	16.4	0.66	6.9	1000	15.2	16.9	0.69	10.4
10000	17.4	17.3	0.66	7.6	10000	15.7	18.3	0.74	11.5

(i) Runup model At2					(j) Runup model Po1				
Year	H_S	T_P	ξ_P	R_2	Year	H_S	T_P	ξ_P	R_2
1	11.6	13.0	0.61	8.4	1	11.9	12.7	0.59	23.5
10	13.6	13.9	0.60	9.7	10	14.0	13.5	0.58	29.3
100	14.9	15.1	0.63	11.0	100	15.4	14.7	0.60	35.1
1000	16.6	15.9	0.63	12.2	1000	17.2	15.4	0.60	41.0
10000	17.4	17.3	0.66	13.4	10000	18.8	16.1	0.59	47.0

(k) Runup model Po2				
Year	H_S	T_P	ξ_P	R_2
1	11.9	12.7	0.59	20.3
10	14.0	13.5	0.58	25.2
100	15.4	14.7	0.60	30.3
1000	17.2	15.4	0.60	35.4
10000	18.8	16.1	0.59	40.5

Table B.25: BGG07 (5)

(a) Runup model B11					(b) Runup model B12				
Year	H_S	T_P	ξ_P	R_2	Year	H_S	T_P	ξ_P	R_2
1	14.6	15.2	0.64	12.0	1	15.2	14.7	0.60	13.2
10	17.8	16.6	0.63	14.5	10	18.6	15.9	0.59	16.0
100	20.9	18.0	0.63	17.0	100	21.4	17.5	0.61	18.7
1000	23.9	19.3	0.63	19.5	1000	24.5	18.8	0.61	21.4
10000	26.8	20.5	0.63	22.0	10000	27.5	20.0	0.61	24.0

(c) Runup model B1d					(d) Runup model Sc				
Year	H_S	T_P	ξ_P	R_2	Year	H_S	T_P	ξ_P	R_2
1	8.7	16.3	0.89	-1.563	1	8.7	16.3	0.89	-0.665
10	10.1	18.0	0.90	-1.902	10	10.1	18.0	0.90	-0.810
100	12.6	19.7	0.89	-2.266	100	11.5	19.6	0.92	-0.966
1000	14.1	21.3	0.90	-2.655	1000	12.8	21.2	0.95	-1.132
10000	15.6	22.8	0.92	-3.069	10000	15.6	22.8	0.92	-1.311

(e) Runup model Pe					(f) Runup model Ho				
Year	H_S	T_P	ξ_P	R_2	Year	H_S	T_P	ξ_P	R_2
1	14.2	15.5	0.66	18.7	1	15.0	15.0	0.62	10.7
10	17.3	16.9	0.65	22.6	10	17.8	16.6	0.63	12.9
100	19.5	18.7	0.68	26.5	100	20.9	18.0	0.63	15.1
1000	22.3	20.1	0.68	30.4	1000	23.9	19.3	0.63	17.3
10000	25.0	21.5	0.69	34.5	10000	26.8	20.5	0.63	19.5

Table B.25: (Continued)

(g) Runup model Vo					(h) Runup model At1				
Year	H_S	T_P	ξ_P	R_2	Year	H_S	T_P	ξ_P	R_2
1	14.6	15.2	0.64	6.2	1	14.2	15.5	0.66	9.2
10	17.8	16.6	0.63	7.4	10	17.3	16.9	0.65	11.2
100	20.3	18.3	0.65	8.6	100	19.5	18.7	0.68	13.1
1000	23.1	19.7	0.66	9.8	1000	22.3	20.1	0.68	15.0
10000	26.0	21.1	0.66	11.0	10000	25.0	21.5	0.69	17.0

(i) Runup model At2					(j) Runup model Po1				
Year	H_S	T_P	ξ_P	R_2	Year	H_S	T_P	ξ_P	R_2
1	14.6	15.2	0.64	10.9	1	15.0	15.0	0.62	34.7
10	17.8	16.6	0.63	13.2	10	18.2	16.3	0.61	46.0
100	20.9	18.0	0.63	15.4	100	21.4	17.5	0.61	58.2
1000	23.9	19.3	0.63	17.7	1000	23.9	19.3	0.63	71.3
10000	26.0	21.1	0.66	19.9	10000	26.8	20.5	0.63	85.3

(k) Runup model Po2				
Year	H_S	T_P	ξ_P	R_2
1	15.0	15.0	0.62	29.9
10	18.2	16.3	0.61	39.6
100	21.4	17.5	0.61	50.2
1000	23.9	19.3	0.63	61.4
10000	26.8	20.5	0.63	73.5

Table B.26: MBG90 (1)

(a) Runup model B11					(b) Runup model B12				
Year	H_S	T_P	ξ_P	R_2	Year	H_S	T_P	ξ_P	R_2
1	9.9	11.3	0.58	7.5	1	9.9	11.3	0.58	8.4
10	12.1	13.0	0.60	9.5	10	12.1	13.0	0.60	10.5
100	14.4	14.8	0.62	11.6	100	14.4	14.8	0.62	12.7
1000	16.5	16.6	0.65	13.9	1000	16.5	16.6	0.65	15.0
10000	18.6	18.5	0.68	16.2	10000	18.6	18.5	0.68	17.4

(c) Runup model B1d					(d) Runup model Sc				
Year	H_S	T_P	ξ_P	R_2	Year	H_S	T_P	ξ_P	R_2
1	1.4	10.8	1.44	-0.611	1	1.2	10.9	1.57	-0.336
10	10.7	13.1	0.64	-0.770	10	1.2	12.7	1.88	-0.472
100	12.6	14.9	0.67	-1.066	100	1.1	14.6	2.20	-0.641
1000	15.0	16.8	0.69	-1.431	1000	1.1	16.5	2.53	-0.849
10000	16.9	18.7	0.73	-1.864	10000	1.1	18.6	2.88	-1.100

(e) Runup model Pe					(f) Runup model Ho				
Year	H_S	T_P	ξ_P	R_2	Year	H_S	T_P	ξ_P	R_2
1	9.8	11.4	0.58	11.4	1	9.9	11.3	0.58	6.7
10	12.0	13.2	0.61	14.6	10	12.1	13.0	0.60	8.5
100	14.1	14.9	0.64	18.0	100	14.4	14.8	0.62	10.3
1000	16.3	16.8	0.67	21.7	1000	16.5	16.6	0.65	12.3
10000	18.4	18.7	0.70	25.7	10000	18.6	18.5	0.68	14.3

Table B.26: (Continued)

(g) Runup model Vo					(h) Runup model At1				
Year	H_S	T_P	ξ_P	R_2	Year	H_S	T_P	ξ_P	R_2
1	9.9	11.3	0.58	4.0	1	9.8	11.4	0.58	5.7
10	12.1	13.0	0.60	5.0	10	12.0	13.2	0.61	7.2
100	14.1	14.9	0.64	6.0	100	14.1	14.9	0.64	8.9
1000	16.3	16.8	0.67	7.1	1000	16.3	16.8	0.67	10.7
10000	18.4	18.7	0.70	8.3	10000	18.4	18.7	0.70	12.7

(i) Runup model At2					(j) Runup model Po1				
Year	H_S	T_P	ξ_P	R_2	Year	H_S	T_P	ξ_P	R_2
1	9.9	11.3	0.58	6.8	1	9.9	11.3	0.58	17.4
10	12.1	13.0	0.60	8.6	10	12.1	13.0	0.60	24.6
100	14.4	14.8	0.62	10.5	100	14.4	14.8	0.62	32.9
1000	16.5	16.6	0.65	12.6	1000	16.5	16.6	0.65	42.5
10000	18.4	18.7	0.70	14.7	10000	18.6	18.5	0.68	53.3

(k) Runup model Po2				
Year	H_S	T_P	ξ_P	R_2
1	9.9	11.3	0.58	15.0
10	12.1	13.0	0.60	21.2
100	14.4	14.8	0.62	28.4
1000	16.5	16.6	0.65	36.6
10000	18.6	18.5	0.68	45.9

Table B.27: MBG90 (2)

(a) Runup model B11					(b) Runup model B12				
Year	H_S	T_P	ξ_P	R_2	Year	H_S	T_P	ξ_P	R_2
1	10.2	10.8	0.54	7.4	1	10.3	10.7	0.53	8.4
10	12.4	12.0	0.54	9.0	10	12.5	11.9	0.54	10.2
100	14.4	13.1	0.55	10.6	100	14.5	13.0	0.55	12.0
1000	16.4	14.2	0.56	12.2	1000	16.5	14.1	0.55	13.7
10000	18.3	15.3	0.57	13.8	10000	18.4	15.2	0.56	15.5

(c) Runup model B1d					(d) Runup model Sc				
Year	H_S	T_P	ξ_P	R_2	Year	H_S	T_P	ξ_P	R_2
1	2.9	9.9	0.94	-0.577	1	9.7	10.9	0.56	-0.267
10	2.6	10.8	1.07	-0.677	10	11.7	12.0	0.56	-0.328
100	2.7	11.6	1.13	-0.772	100	1.1	11.9	1.85	-0.412
1000	2.8	12.3	1.18	-0.864	1000	1.0	13.1	2.09	-0.511
10000	2.3	13.4	1.41	-0.954	10000	0.9	14.3	2.35	-0.626

(e) Runup model Pe					(f) Runup model Ho				
Year	H_S	T_P	ξ_P	R_2	Year	H_S	T_P	ξ_P	R_2
1	10.2	10.8	0.54	11.0	1	10.2	10.8	0.54	6.6
10	12.4	12.0	0.54	13.5	10	12.4	12.0	0.54	8.1
100	14.4	13.1	0.55	15.9	100	14.4	13.1	0.55	9.5
1000	16.4	14.2	0.56	18.4	1000	16.4	14.2	0.56	10.9
10000	18.3	15.3	0.57	21.0	10000	18.3	15.3	0.57	12.3

Table B.27: (Continued)

(g) Runup model Vo					(h) Runup model At1				
Year	H_S	T_P	ξ_P	R_2	Year	H_S	T_P	ξ_P	R_2
1	10.2	10.8	0.54	4.0	1	10.2	10.8	0.54	5.5
10	12.4	12.0	0.54	4.7	10	12.4	12.0	0.54	6.7
100	14.4	13.1	0.55	5.5	100	14.4	13.1	0.55	7.9
1000	16.4	14.2	0.56	6.3	1000	16.4	14.2	0.56	9.1
10000	18.3	15.3	0.57	7.0	10000	18.3	15.3	0.57	10.3

(i) Runup model At2					(j) Runup model Po1				
Year	H_S	T_P	ξ_P	R_2	Year	H_S	T_P	ξ_P	R_2
1	10.2	10.8	0.54	6.7	1	10.2	10.8	0.54	17.1
10	12.4	12.0	0.54	8.2	10	12.4	12.0	0.54	22.9
100	14.4	13.1	0.55	9.6	100	14.4	13.1	0.55	29.2
1000	16.4	14.2	0.56	11.1	1000	16.4	14.2	0.56	36.0
10000	18.3	15.3	0.57	12.5	10000	18.3	15.3	0.57	43.3

(k) Runup model Po2				
Year	H_S	T_P	ξ_P	R_2
1	10.2	10.8	0.54	14.7
10	12.4	12.0	0.54	19.8
100	14.4	13.1	0.55	25.2
1000	16.4	14.2	0.56	31.1
10000	18.3	15.3	0.57	37.3

Table B.28: MBG90 (3)

(a) Runup model B11					(b) Runup model B12				
Year	H_S	T_P	ξ_P	R_2	Year	H_S	T_P	ξ_P	R_2
1	9.7	10.8	0.55	7.2	1	9.8	10.7	0.55	8.1
10	11.9	12.2	0.56	8.9	10	12.0	12.1	0.56	10.0
100	14.1	13.6	0.58	10.8	100	14.2	13.4	0.57	12.0
1000	16.2	14.9	0.59	12.6	1000	16.3	14.8	0.58	14.0
10000	18.3	16.3	0.61	14.5	10000	18.3	16.3	0.61	16.0

(c) Runup model B1d					(d) Runup model Sc				
Year	H_S	T_P	ξ_P	R_2	Year	H_S	T_P	ξ_P	R_2
1	1.5	9.7	1.26	-0.520	1	1.0	9.9	1.62	-0.278
10	1.5	10.9	1.45	-0.622	10	0.9	11.5	1.96	-0.391
100	12.4	13.5	0.61	-0.739	100	0.8	13.2	2.32	-0.533
1000	14.2	14.9	0.63	-0.958	1000	0.8	15.0	2.69	-0.709
10000	16.6	16.4	0.64	-1.211	10000	0.8	16.9	3.08	-0.924

(e) Runup model Pe					(f) Runup model Ho				
Year	H_S	T_P	ξ_P	R_2	Year	H_S	T_P	ξ_P	R_2
1	9.7	10.8	0.55	10.7	1	9.7	10.8	0.55	6.4
10	11.9	12.2	0.56	13.5	10	11.9	12.2	0.56	8.0
100	14.1	13.6	0.58	16.3	100	14.1	13.6	0.58	9.6
1000	16.2	14.9	0.59	19.3	1000	16.2	14.9	0.59	11.2
10000	18.0	16.4	0.62	22.3	10000	18.3	16.3	0.61	12.9

Table B.28: (Continued)

(g) Runup model Vo					(h) Runup model At1				
Year	H_S	T_P	ξ_P	R_2	Year	H_S	T_P	ξ_P	R_2
1	9.7	10.8	0.55	3.9	1	9.7	10.8	0.55	5.3
10	11.9	12.2	0.56	4.7	10	11.9	12.2	0.56	6.7
100	14.1	13.6	0.58	5.6	100	14.1	13.6	0.58	8.1
1000	16.2	14.9	0.59	6.5	1000	16.2	14.9	0.59	9.5
10000	18.3	16.3	0.61	7.4	10000	18.0	16.4	0.62	11.0

(i) Runup model At2					(j) Runup model Po1				
Year	H_S	T_P	ξ_P	R_2	Year	H_S	T_P	ξ_P	R_2
1	9.7	10.8	0.55	6.5	1	9.7	10.8	0.55	16.2
10	11.9	12.2	0.56	8.1	10	11.9	12.2	0.56	22.5
100	14.1	13.6	0.58	9.7	100	14.1	13.6	0.58	29.6
1000	16.2	14.9	0.59	11.4	1000	16.2	14.9	0.59	37.5
10000	18.3	16.3	0.61	13.2	10000	18.3	16.3	0.61	46.1

(k) Runup model Po2				
Year	H_S	T_P	ξ_P	R_2
1	9.7	10.8	0.55	14.0
10	11.9	12.2	0.56	19.4
100	14.1	13.6	0.58	25.5
1000	16.2	14.9	0.59	32.3
10000	18.3	16.3	0.61	39.7

Appendix C

MATLAB Codes

C.1 Wave Runup and Wave Rundown Based on Wind Statistics

```
close all
%% INFORMATION
% This script calculates expected value and standard deviation of wave
% runup and wave rundown based on wind distributions.
% Results can be found in the variable "Results", where the matrixes are
% ordered so that each row represent one bottom slope in the vector md,
% and each column represent one equation

%% PARAMETERS

% Input
alpha.hat=0.0081;           % Phillips constant
g=9.81;                    % Acceleration of gravity
neq = 11;                  % number of equations
nm=7;                      % number of slopes in calculation
nd = 4;                   % number of distributions
md = [1/5 1/7 1/10 1/15 ... % bottom slopes
      1/20 1/30 1/50];

% Declarations
Results = struct([]);      % Structure for saving results
ER2=zeros(nm,neq);       % expected value of R2
VarR2=zeros(nm,neq);    % variance of R2
ER2det=zeros(nm,neq);   % deterministic expected value of R2

% Colours for plot
colours = [
    0         0         0;   % black
    0.402     0.402     0.402; % grey
    0         0         0;   % black
    0.402     0.402     0.402; % grey
```



```

1.000      0      0.500;    % pink
0          0.447  0.741;    % blue
1.000     0.500      0;    % orange
0.494     0.184  0.556;    % purple
0.466     0.674  0.188;    % green
0.301     0.745  0.933;    % light blue
0.635     0.078  0.184];   % red

% Strings for plots and saving results
markers = {'-', '-', '--', '--', '-', '-', '-', '-', '-', '-', '-', '-'};
distr = {'JMH02', 'MR15_1040', 'MR15_2060', 'BG15'};
distr_name = {'JMH02', 'MR15 (1)', 'MR15 (2)', 'BG15'};

%% CALCULATIONS
for i = 1:nd
    % Parameters distributions
    if i == 1      % JMH01
        alpha=1.708;
        beta=8.426;
    elseif i ==2  % MR15 (1)
        alpha=2.30;
        beta=7.11;
    elseif i ==3  % MR15 (2)
        alpha=2.46;
        beta=10.99;
    else          % BG15
        hs=3;
        alpha=1.250+5.600*hs^(.660);
        beta=0.050+5.514*hs^(.280);
    end

    %% Moments of the distributions
    W=zeros(1,6);
    for mo=1:6
        W(mo)= beta^mo * gamma(1+mo/alpha);
    end

    %% Statistical values

    for mn = 1:nm
        m = md(mn);
        K=4*m^(0.3);

        % General equation 1
        a=[0 0.39 -0.21 0 0 0.2 0.58*m 0 0.16];
        b=[1.165 0.795 0.44 0.1 K 0.83 0.53 0.99 0.92];
        c=[0.77 1 1 2.21 1 1 1 1 1];
        d=[0 0 0 0 0 0 0.45 0 0];
        for eq = 1:(neq-2)
            C = a(eq)*2*sqrt(alpha_hat)/g + b(eq)*m^(c(eq))*...
                (2*pi/g)^(c(eq)/2)*(2*sqrt(alpha_hat)/g)^(1-c(eq)/2);
            ER2(mn,eq) = C*W(2)+d(eq);
            VarR2(mn,eq) = C^2*(W(4)-(W(2))^2);
            ER2det(mn,eq) = C*(W(1))^2+d(eq);
        end

        % General equation 2

```

```

C1 = 0.49*m^(.5)*2*pi*sqrt(2*alpha_hat)/(g^2);
C2 = 0.33*m^(.5)*4*pi*sqrt(alpha_hat)/(g^2);
ER2(mn,10) = C1*W(3);
ER2(mn,11) = C2*W(3);
VarR2(mn,10) = C1^2*(W(6)-(W(3))^2);
VarR2(mn,11) = C2^2*(W(6)-(W(3))^2);
ER2det(mn,10) = C1*(W(1))^3;
ER2det(mn,11) = C2*(W(1))^3;

end

StdR2=sqrt(VarR2);

%% Other calculations

% EXPECTED MEAN WIND AND SIGNIFICANT WAVE HEIGHT
EU10 = W(1); % Expected mean wind speed
EHS=2*sqrt(alpha_hat)/g*EU10^2; % Expected significant wave height
xiPd=pi^.5/alpha_hat^(1/4)*EU10;
xiP=md.*xiPd; % Surf parameter

% DIMENSIONLESS RUNUP
ER2D= ER2/EHS; % divided by Hs
ER2DD(1,:) = ER2(1,:)./xiP(1); % divided by surf parameter
ER2DD(2,:) = ER2(2,:)./xiP(2); % divided by surf parameter
ER2DD(3,:) = ER2(3,:)./xiP(3); % divided by surf parameter
ER2DD(4,:) = ER2(4,:)./xiP(4); % divided by surf parameter
ER2DD(5,:) = ER2(5,:)./xiP(5); % divided by surf parameter

% RATIO BETWEEN DET. AND STOCH. METHOD
ER2comp=ER2det./ER2;

% VECTORS WITH RUNUP ONLY
ER_up=zeros(nm,neq-2);
STD_up=zeros(nm,neq-2);
ER_up(:,1:2)=ER2(:,1:2);
STD_up(:,1:2)=StdR2(:,1:2);
ER_up(:,3:9)=ER2(:,5:11);
STD_up(:,3:9)=StdR2(:,5:11);

%CALCULATING ERRORBAR
error_min = zeros(nm,neq-2);
for mn = 1:nm
    for eq = 1:neq-2
        if ER_up(mn,eq) < STD_up(mn,eq)
            error_min(mn,eq) = ER_up(mn,eq);
        else
            error_min(mn,eq) = STD_up(mn,eq);
        end
    end
end
end

% CREATING FILE FOR TABLES
ResTab = zeros(neq,8);
mnd=1;
for mn = [1 3 5 7]
    ResTab(:,mnd) = ER2(mn,:);
    ResTab(:,mnd+1) = StdR2(mn,:);
end

```

```

        mnd = mnd+2;
end

%CHANGING SIGN ON RUNDOWN
ER2(:, 3) = ER2(:, 3)*(-1);
ER2(:, 4) = ER2(:, 4)*(-1);
kd=1;
for k = 1:4
    ResTab(3, kd)=ResTab(3, kd)*(-1);
    ResTab(4, kd)=ResTab(4, kd)*(-1);
    kd=kd+2;
end

% VECTORS WITH RUNDOWN ONLY
ER_down=zeros(nm, 2);
STD_down=zeros(nm, 2);
ER_down(:, 1:2)=ER2(:, 3:4);
STD_down(:, 1:2)=StdR2(:, 3:4);

%% SAVING RESULTS
Results(i).Distributions = distr_name(i);
Results(i).ExpU10 = EU10;
Results(i).ExpHs = EHS;
Results(i).SurfParameter = xiP.';
Results(i).ExpectedValue=ER2;
Results(i).StandardDeviation=StdR2;
Results(i).ExpRunup = ER_up;
Results(i).StdRunup = STD_up;
Results(i).MinRunup = error_min;
Results(i).ExpRundown = ER_down;
Results(i).StdRundown = STD_down;
Results(i).MinRundown = STD_down;

end

```

C.2 Wave Runup and Wave Rundown Based on Wave Statistics

```

close all
%% INFORMATION
% This script calculates expected value and standard deviation of wave
% runup and wave rundown based on wave distributions.
% Results can be found in the variable "Results", where the matrixes are
% ordered so that each row represent one bottom slope in the vector md,
% and each column represent one equation

%% PARAMETERS

% Input
g=9.81; %Acceleration of gravity
Hs=3; %Significant wave height
nd=10; %number of distributions
neq=11; %number of equations for R2
nm=7; %number of bottom slopes
hs_shift = 3.25; % shifting point combined distribution
md = [1/5 1/7 1/10 1/15 ...

```

```

    1/20 1/30 1/50];           % bottom slopes
marginal = ...
    [1 2 3 3 3 3 3 4 4 4];    % type of distribution
                                % 1:MGAU05 2:OHG16 3:BGG07 4:MBG90
c_hat = [1 1 1.28 1.28 1.28 ...
    1.28 1.28 1.28 1.28 1.28]; % coefficient: 1 for T=Tp, 1.28 for T=Tz

% Declaration
ER2=zeros(length(md),neq);    % expected value of R2
STDR2=zeros(length(md),neq);  % standard deviation of R2
EHS = zeros(1,nd);           % Expected value of Hs
ER_up=zeros(nm,neq-2);       % expected value runup
STD_up=zeros(nm,neq-2);      % standard deviation runup
ER_down=zeros(nm,2);         % expected value rudown
STD_down=zeros(nm,2);        % standard deviation rundown
Results = struct([]);        % structure for results
ResTab = zeros(neq,nm*2);    % matrix for storing results

% Colours for plot
colours = [
    0          0          0;    % black
    0.402     0.402     0.402; % grey
    0          0          0;    % black
    0.402     0.402     0.402; % grey
    1.000     0          0.500; % pink
    0          0.447     0.741; % blue
    1.000     0.500     0;      % orange
    0.494     0.184     0.556; % purple
    0.466     0.674     0.188; % green
    0.301     0.745     0.933; % light blue
    0.635     0.078     0.184]; % red

% Strings for plots and saving results
model = {'Bl1', 'Bl2', 'Bld', 'Sc', 'Pe', 'Ho', 'Vo', 'At1', 'At2', 'Po1', 'Po2'};
markers = {'-', '-', '---', '---', '-', '-', '-', '-', '-', '-', '-'};
distr = {'MGAU05', 'NORA10', 'BGG07_1', 'BGG07_2', 'BGG07_3'...
    , 'BGG07_4', 'BGG07_5', 'MBG90_1', 'MBG90_2', 'MBG90_3'};
distr.name = {'MGAU05', 'NORA10', 'BGG07 (1)', 'BGG07 (2)', 'BGG07 (3)'...
    , 'BGG07 (4)', 'BGG07 (5)', 'MBG90 (1)', 'MBG90 (2)', 'MBG90 (3)'};

%% Parameters distributions

% Parameters for conditional distribution of Hs and T
a1=[1.780 0.74 1.350 1.365 0.790 0.835 1.952 1.240 1.090 0.933];
a2=[0.288 1.20 0.366 0.375 0.805 1.139 0.168 0.337 0.479 0.578];
a3=[0.474 0.21 0.392 0.453 0.292 0.119 0.499 0.538 0.417 0.395];
b1=[0.001 0.001 0.020 0.033 0.055 0.140 0.070 0.0728 0.0407 0.0550];
b2=[0.097 0.113 0.165 0.285 0.195 0.030 0.066 0.383 0.221 0.336];
b3=[-0.255 -0.275 -0.166 -0.752 -0.269 -0.958 -0.081 -0.665 -0.289 -0.585];

%Parameters for marginal distribution of Hs
s = [0.801 1.690 3.104 2.848 2.939 2.857 2.420 1.410 1.910 1.500];
r = [1.531 1.160 1.357 1.419 1.240 1.449 1.169 1.120 1.270 1.150];
t = [2.713 0.760 0.906 1.021 0.896 0.838 1.258 0.987 0.532 0.679];
k = [0.371^0.5 0 0 0 0 0 0 0 0 0];

%% CALCULATIONS

```

```

for i = 1:nd %distributions
mnd=1;
for mn = 1:nm %bottom slope
%% Parameters equations
m = md(mn);
K=4*m^(0.3);

%Parameters for general equation 1
a=[0 0.39 -0.21 0 0 0.2 0.58*m 0 0.16];
b=[1.165 0.795 0.44 0.1 K 0.83 0.53 0.99 0.92];
c=[0.77 1 1 2.21 1 1 1 1 1];
d=[0 0 0 0 0 0 0 0.45 0 0];

%Parameters for general equation 2
C = [0 0 0 0 0 0 0 0 0 0.49/1.28 0.33];

%% Statistical values

for j = 1:neq %equations
meanT = a1(i)+a2(i)*Hs^a3(i);
if marginal(i) == 1 || marginal(i) == 2
varT = b1(i)+b2(i)*exp(b3(i)*Hs);
elseif marginal(i) == 3
varT = (b1(i)+b2(i)*Hs^(b3(i)))^2;
elseif marginal(i) == 4
varT = (b1(i)+b2(i)*exp(b3(i)*Hs))^2;
end
if j <= neq-2 %General equation 1
meanR = c(j)*meanT+log(b(j)*m^(c(j))*c_hat(i)^(c(j))...
*(g/(2*pi))^(c(j)/2)*Hs^(1-c(j)/2));
varR = c(j)^2*varT;
ER = exp(meanR+0.5*varR);
STDR = ((exp(varR)-1)*exp(2*meanR+varR))^0.5;
ER2(mn,j) = ER + a(j)*Hs+d(j);
STDR2(mn,j) = STDR;
elseif j > neq-2 %General equation 2
meanR = meanT +log(C(j)*m^.5*c_hat(i)*Hs);
varR = varT;
ER2(mn,j) = exp(meanR+0.5*varR);
STDR2(mn,j) = ((exp(varR)-1)*exp(2*meanR+varR))^0.5;
end
end

ResTab(:,mnd) = ER2(mn,:);
ResTab(:,mnd+1) = STDR2(mn,:);
mnd = mnd+2;

end

%CHANGING SIGN ON RUNDOWN
ER2(:,3) = ER2(:,3)*(-1);
ER2(:,4) = ER2(:,4)*(-1);
kd=1;
for k = 1:nm
ResTab(3,kd)=ResTab(3,kd)*(-1);
ResTab(4,kd)=ResTab(4,kd)*(-1);
kd=kd+2;

```

```

end

%% EXPECTED VALUE OF HS
if marginal(i) == 1
    EHS(i) = exp(s(i)+0.5*k(i)^2)*normcdf((log(hs_shift)-(s(i)...
        +k(i)^2))/k(i))+ t(i)*gammainc(1+1/r(i), (hs_shift/t(i))^r(i));
else
    EHS(i) = t(i) + s(i)*gamma(1+1/r(i));
end

%% OTHER CALCULATIONS

% VECTORS WITH RUNUP ONLY
ER_up(:,1:2)=ER2(:,1:2);
STD_up(:,1:2)=STDR2(:,1:2);
ER_up(:,3:9)=ER2(:,5:11);
STD_up(:,3:9)=STDR2(:,5:11);

% VECTORS WITH RUNDOWN ONLY
ER_down(:,1:2)=ER2(:,3:4);
STD_down(:,1:2)=STDR2(:,3:4);

%CALCULATING ERRORBARS
error_min = zeros(nm,neq-2);
for mn = 1:nm
    for eq = 1:neq-2
        if ER_up(mn,eq) < STD_up(mn,eq)
            error_min(mn,eq) = ER_up(mn,eq);
        else
            error_min(mn,eq) = STD_up(mn,eq);
        end
    end
end
end

%% SAVING RESULTS

% Saving results in struct
Results(i).Distribution = distr_name(i);
Results(i).ExpectedValues = ER2;
Results(i).StandardDeviation = STDR2;
Results(i).ExpValueRunup = ER_up;
Results(i).StdRunup = STD_up;
Results(i).MinRunup = error_min;
Results(i).ExpValueRundown = ER_down;
Results(i).StdRundown = STD_down;
Results(i).MinRundown = STD_down;

end

```

C.3 Extreme Value Estimates Based on Wind Statistics

```

close all
%% INFORMATION
% This script calculates the extreme values from wind statistics

```

```

%% PARAMETERS

% Input
alpha_hat=0.0081; % Phillips constant
g=9.81; % Acceleration of gravity
neq = 11; % number of equations
nm=7; % number of slopes in calculation
m = 0.1; % bottom slope
RP = [1 10 100 1000 10000]; % return periods
K=4*m^(0.3);

% Declaration
U_max = zeros(1,length(RP));
Hs_max = zeros(1,length(RP));
Tp_max = zeros(1,length(RP));
Tz_max = zeros(1,length(RP));
R2_max = zeros(neq,length(RP));
xi_max = zeros(1,length(RP));

% Strings for plots and saving results
model = {'B11', 'B12', 'B1d', 'Sc', 'Pe', 'Ho', 'Vo', 'At1', 'At2', 'Po1', 'Po2'};
period = {'1', '10', '100', '1000', '10000'};
distr = {'JMH02', 'MR15_1040', 'MR15_2060', 'BG15'};
model_char = [1 1 1 1 1 1 1 1 1 1 2 3];

%% Parameters equations

%Parameters for general equation 1
a=[0 0.39 0.21 0 0 0.2 0.58*m 0 0.16];
b=[1.165 0.795 -0.44 -0.1 K 0.83 0.53 0.99 0.92];
c=[0.77 1 1 2.21 1 1 1 1 1];
d=[0 0 0 0 0 0 0.45 0 0];

for nd = 1:4 %DISTRIBUTION

    %% DISTRIBUTION PARAMETERS
    if nd == 1 % JMH01
        alpha=1.708;
        beta=8.426;
    elseif nd ==2 % MR15 10W40N
        alpha=2.30;
        beta=7.11;
    elseif nd ==3 % MR15 20W60N
        alpha=2.46;
        beta=10.99;
    else % BG15
        hs=3;
        alpha=1.250+5.600*hs^(.660);
        beta=0.050+5.514*hs^(.280);
    end

    %% CALCULATION OF EXTREME VALUES

    for ieq = 1:neq %RUNUP MODEL
        for irp = 1:length(RP) %RETURN PERIOD
            rp = RP(irp);
            if nd == 1 % JMH01

```

```

        N = 365*24*60/60*rp;
else
        N = 365*24*60/10*rp;
end
U_max(irp) = beta*(log(N))^(1/alpha);
Tp_max(irp) = 2*pi/g*U_max(irp);
Hs_max(irp) = 2*sqrt(alpha_hat)/g*U_max(irp)^2;
Tz_max(irp) = sqrt(2)*pi/g*U_max(irp);
xi_max(irp) = m*sqrt(g/(2*pi))*Tp_max(irp)^2/Hs_max(irp));

if model_char(ieq) == 1           %General equation abcd
    R2_max(ieq,irp) = (a(ieq)+b(ieq)*xi_max(irp)^(ieq))...
        *Hs_max(irp)+d(ieq);
elseif model_char(ieq) == 2      %Po1
    R2_max(ieq,irp) = 0.49*m^.5*Tz_max(irp)*Hs_max(irp);
elseif model_char(ieq) == 3     %Po2
    R2_max(ieq,irp) = 0.33*m^.5*Tp_max(irp)*Hs_max(irp);
end
end
end
%% Writing results to file for tables in the report

%Extreme sea state values
FileName = ['ExtremeValuesSeastate-' distr{nd} '.txt'];
FilePath = ...
    '/Users/tonjesunde/Documents/MATLAB/Masteroppgave/Tables_Extreme_dimless_1hour';

fid = fopen(fullfile(FilePath,FileName),'w');
for irp = 1:length(RP)
    fprintf(fid,'% -5d & % -5.1f & % -5.1f & % -5.1f \\\ \ \ \ \ \n',...
        RP(irp),U_max(irp),Hs_max(irp),Tp_max(irp));
end
fclose(fid);

%Extreme runup values
Model = (1:neq).';
R2_max1 = R2_max(:,1)/Hs_max(1);
R2_max10 = R2_max(:,2)/Hs_max(2);
R2_max100 = R2_max(:,3)/Hs_max(3);
R2_max1000 = R2_max(:,4)/Hs_max(4);
R2_max10000 = R2_max(:,5)/Hs_max(5);
Sep = {'&'; '&'; '&'; '&'; '&'; '&'; '&'; '&'; '&'; '&'; '&'; '&'; '&'; '&'};
EndSep = {'\ \ \'; '\ \ \'; '\ \ \'; '\ \ \'; '\ \ \'; '\ \ \'; '\ \ \'}...
    ; '\ \ \'; '\ \ \'; '\ \ \'; '\ \ \'; '\ \ \'};
R2tab = [Model R2_max1 R2_max10 R2_max100 R2_max1000 R2_max10000];
R2sort = sortrows(R2tab,2);

FileName = ['ExtremeValuesRunup-' distr{nd} '.txt'];
FilePath = ...
    '/Users/tonjesunde/Documents/MATLAB/Masteroppgave/Tables_Extreme_dimless_1hour';
fid = fopen(fullfile(FilePath,FileName),'w');
for ieq = 1:neq
    if ieq == 1 || ieq == 2
        fprintf(fid,...
            '% -5s & % -5.3f & % -5.3f & % -5.3f & % -5.3f & % -5.3f \\\ \ \ \ \ \n'...
            ,model{R2sort(ieq)}, R2sort(ieq,2), R2sort(ieq,3),...
            R2sort(ieq,4), R2sort(ieq,5), R2sort(ieq,6));
    else

```



```

        fprintf(fid,...
            '-5s & %-5.2f & %-5.2f & %-5.2f & %-5.2f & %-5.2f \\\n'...
            ,model{R2sort(ieq)}, R2sort(ieq,2), R2sort(ieq,3),...
            R2sort(ieq,4), R2sort(ieq,5), R2sort(ieq,6));
    end
end
fclose(fid);
end

```

C.4 Extreme Value Estimates Based on Wave Statistics

```

%% INFORMATION
% This script calculates the extreme values from wave statistics

%% PARAMETERS

% Input
neq = 11; % number of equations
m = 0.1; % bottom slope
g=9.81; % acceleration of gravity
sp =100; % number of sampling points
RP = [1 10 100 1000 10000]; % return periods
Axis = [0 35 0 35]; % axis contour line plots
x = Axis(1):0.1:Axis(2); % x-values in plot
model_char = ...
    [1 2 2 1 1 2 2 1 2 3 4]; % type of runup model
                                % 1:a=0 2:c=1 3:Po1 4:Po2

% Declaration
Re = zeros(1,length(RP)); % handle for contour line plots
R2 = zeros(1,sp); % R2
T_max = zeros(neq,length(RP)); % extreme value wave period
H_max = zeros(neq,length(RP)); % extreme value Hs
R2_max = zeros(neq,length(RP)); % extreme value R2
xi_max = zeros(neq,length(RP)); % extreme value surf parameter
R2sort_compWave=struct([]); % R2 sorted by value

% Strings for plots and saving results
distr = {'MGAU05','NORA10','BGG07-1','BGG07-2','BGG07-3','BGG07-4'...
        , 'BGG07-5','MBG90-1','MBG90-2','MBG90-3'};
model = {'B11','B12','Bld','Sc','Pe','Ho','Vo','M1','M2','Po1','Po2'};
model_name = {'B11','B12','Bld','Sc','Pe','Ho','Vo','At1','At2','Po1','Po2'};
color = {'[0 0.4470 0.7410]','[0.8500 0.3250 0.0980]'...
        , '[0.9290 0.6940 0.1250]','[0.4940 0.1840 0.5560]'...
        , '[0.4660 0.6740 0.1880]'};

%Parameters for marginal distribution of Hs
s = [0.801 1.690 3.104 2.848 2.939 2.857 2.420 1.410 1.910 1.500];
r = [1.531 1.160 1.357 1.419 1.240 1.449 1.169 1.120 1.270 1.150];
t = [2.713 0.760 0.906 1.021 0.896 0.838 1.258 0.987 0.532 0.679];
k = [0.371^0.5 0 0 0 0 0 0 0 0 0];

%Parameters for conditional distribuiton of Tp given Hs
marginal = [3 1 2 2 2 2 2 4 4 4];
c_hat = [1 1 1.28 1.28 1.28 1.28 1.28 1.28 1.28 1.28];
a1=[1.780 0.74 1.350 1.365 0.790 0.835 1.952 1.240 1.090 0.933];

```

```

a2=[0.288 1.20 0.366 0.375 0.805 1.139 0.168 0.337 0.479 0.578];
a3=[0.474 0.21 0.392 0.453 0.292 0.119 0.499 0.538 0.417 0.395];
b1=[0.001 0.001 0.020 0.033 0.055 0.140 0.070 0.0728 0.0407 0.0550];
b2=[0.097 0.113 0.165 0.285 0.195 0.030 0.066 0.383 0.221 0.336];
b3=[-0.255 -0.275 -0.166 -0.752 -0.269 -0.958 -0.081 -0.665 -0.289 -0.585];

```

```

%Parameters for general equation 1

```

```

a=[0 0.39 0.21 0 0 0.2 0.58*m 0 0.16];
b=[1.165 0.795 -0.44 -0.1 4*m^(0.3) 0.83 0.53 0.99 0.92];
c=[0.77 1 1 2.21 1 1 1 1 1];
d=[0 0 0 0 0 0 0.45 0 0];

```

```

%Parameters for general equation 2

```

```

C = [0 0 0 0 0 0 0 0 0 0.49/1.28 0.33];

```

```

%% CALCULATIONS

```

```

for nd = 1:10          %distributions
    close all;
    for ieq = 1:neq    %runup model
        for rp = 1:length(RP) %return period
            %% Contour lines

            %Creating values for imaginary plane
            q = 1/(2920*RP(rp));
            beta = -norminv(q,0,1);
            theta = linspace(0,2*pi,sp);
            u1 = beta*cos(theta);
            u2 = beta*sin(theta);

            %Transforming back to physical plane
            F = normcdf(u1,0,1);

            if marginal(nd) == 1          %OHG16
                H = t(nd)+s(nd)*(-log(1-F)).^(1/r(nd));
                meanT = a1(nd)+a2(nd)*H.^a3(nd);
                stdT = sqrt(b1(nd)+b2(nd)*exp(b3(nd)*H));
                T = exp(stdT.*u2+meanT);

            elseif marginal(nd) == 2      %BGG07
                H = t(nd)+s(nd)*(-log(1-F)).^(1/r(nd));
                meanT = a1(nd)+a2(nd)*H.^a3(nd);
                stdT = b1(nd)+b2(nd)*H.^b3(nd);
                T = exp(stdT.*u2+meanT);

            elseif marginal(nd) == 3      %MGAU05
                H = t(nd)*(-log(1-F)).^(1/r(nd)); % Hs > 3.25m
                for j=1:sp
                    if H(j) <= 3.25 % Hs<= 3.25m
                        H(j) = exp(s(nd)+u1(j)*k(nd));
                    end
                end
                meanT = a1(nd)+a2(nd)*H.^a3(nd);
                stdT = sqrt(b1(nd)+b2(nd)*exp(b3(nd)*H));
                T = exp(stdT.*u2+meanT);

            else % MBG90
                H = t(nd)+s(nd)*(-log(1-F)).^(1/r(nd));
                meanT = a1(nd)+a2(nd)*H.^a3(nd);

```

```

        stdT = b1(nd)+b2(nd)*exp(b3(nd)*H);
        T = exp(stdT.*u2+meanT);
end

%% Plotting contour lines

figI = figure(nd*20+ieq);
Re(rp) = plot(T,H, 'LineWidth',1.5, 'Color',color{rp});
hold on
if nd == 1 || nd == 2
    xlabel('T-P [s]')
else
    xlabel('T-Z [s]')
end
ylabel('H-S [m]')
set(gca, 'FontSize',22, 'Fontname', 'Times New Roman')
axis(Axis)

%% Maximum values for runup along contour lines

for j = 1:sp
    if model_char(ieq) == 1           %a=0
        R2(j) = b(ieq)*(m*c_hat(nd))^c(ieq)*(g/(2*pi))^c(ieq)/2)...
            *H(j)^(1-c(ieq)/2)*T(j)^c(ieq)+d(ieq);
    elseif model_char(ieq) == 2      %c=1
        R2(j) = a(ieq)*H(j)+b(ieq)*m*c_hat(nd)...
            *sqrt(g/(2*pi)*H(j))*T(j)+d(ieq);
    else                               %Po
        R2(j) = C(ieq)*m^.5*c_hat(nd)*T(j)*H(j);
    end
end

if ieq == 3 || ieq == 4
    maxd=find(R2==min(R2));
else
    maxd=find(R2==max(R2));
end

T_max(ieq,rp) = T(maxd); %Tp or Tz
H_max(ieq,rp) = H(maxd);
R2_max(ieq,rp) = R2(maxd);
xi_max(ieq,rp) = m*sqrt(g/(2*pi))*c_hat(nd)*...
    T_max(ieq,rp)/sqrt(H_max(ieq,rp));

%% Plotting runup models for maximum runup

x = Axis(1):0.1:Axis(2);
y = Axis(3):0.1:Axis(4);

if model_char(ieq) == 1           %a=0
    H1 = ((R2(maxd)-d(ieq))./(b(ieq)*(m*c_hat(nd))^c(ieq)...
        *(g/(2*pi))^c(ieq)/2).*x.^c(ieq)).^(2/(2-c(ieq)));

    figure(nd*20+ieq);
    plot(x,H1, '--', 'Color',color{rp}, 'linewidth',1.5);

elseif model_char(ieq) == 2      %c=1

```

```

T1 = (R2(maxd)-a(ieq).*y-d(ieq))./...
      (b(ieq)*m*c_hat(nd)*sqrt(g/(2*pi)).*sqrt(y));

figure(nd*20+ieq);
plot(T1,y,'--','Color',color{rp},'linewidth',1.5);

else %Po
H1 = R2(maxd)/(C(ieq)*m^.5*c_hat(nd))./x;

figure(nd*20+ieq);
plot(x,H1,'--','Color',color{rp},'linewidth',1.5);

end

end

legend(Re,'1 year','10 year','100 year','1000 year','10 000 year',...
'Location','NE')
hold off

%% Write extreme values to file for tables in report

FileName = ['ExtremeValues_' distr{nd} '_' model{ieq} '.txt'];
FilePath = ...
'/Users/tonjesunde/Documents/MATLAB/Masteroppgave/Tables_ExtremeValues';

fid = fopen(fullfile(FilePath,FileName),'w');
if ieq == 3 || ieq == 4
for rp = 1:length(RP)
fprintf(fid,'% -8d & % -10.1f & % -10.1f & % -10.2f & % -10.3f \\\ \n'...
, RP(rp), H_max(ieq,rp), T_max(ieq,rp), xi_max(ieq,rp), R2_max(ieq,rp));
end
else
for rp = 1:length(RP)
fprintf(fid,'% -8d & % -10.1f & % -10.1f & % -10.2f & % -10.1f \\\ \n'...
, RP(rp), H_max(ieq,rp), T_max(ieq,rp), xi_max(ieq,rp), R2_max(ieq,rp));
end
end
end
fclose(fid);

end

Model = (1:neq).';
R2dim = R2_max./H_max;
R2tab = [Model R2dim(:,1) R2dim(:,2) R2dim(:,3) R2dim(:,4) R2dim(:,5)];
R2sort = sortrows(R2tab,2);

FileName = ['ExtremeValues_' distr{nd} '.txt'];
FilePath = ...
'/Users/tonjesunde/Documents/MATLAB/Masteroppgave/Tables_Extreme_dimless';

fid = fopen(fullfile(FilePath,FileName),'w');
for ieq = 1:neq
if ieq == 1 || ieq == 2
fprintf(fid,'% -5s & % -5.3f & % -5.3f & % -5.3f & % -5.3f & % -5.3f \\\ \n'...
,model_name{R2sort(ieq)}, R2sort(ieq,2), R2sort(ieq,3), ...

```

```

        R2sort(ieq,4), R2sort(ieq,5), R2sort(ieq,6));
else
    fprintf(fid, '%-5s & %-5.2f & %-5.2f & %-5.2f & %-5.2f & %-5.2f \\\n'...
        , model_name{R2sort(ieq)}, R2sort(ieq,2), R2sort(ieq,3), ...
        R2sort(ieq,4), R2sort(ieq,5), R2sort(ieq,6));
end
end
fclose(fid);

R2sort_compWave(nd).Distribution = distr(nd);
R2sort_compWave(nd).R2sortWave = R2sort;

end

```